Chemistry–A European Journal

Supporting Information

Synthesis of New Donor-Substituted Biphenyls: Pre-ligands for Highly Luminescent (C^C^D) Gold(III) Pincer Complexes

Wolfram Feuerstein,[a] Christof Holzer,[b] Xin Gui,[c] Lilly Neumeier,[a] Wim Klopper,*[c] and Frank Breher*[a]

Content

S 1 Additional Synthetic Approaches to the (C^C^N) Preligand

S 1.1 Approach 1

Our first approach started with 2,6-dibromo(chloro)benzene (**s1**) which was STILLE-coupled[1] with 2-(tributylstannyl)pyridine to obtain **s2**. After coupling with 2-chlorophenylboronic acid the 2,2'-dichlorobiphenyl **s3** was obtained.

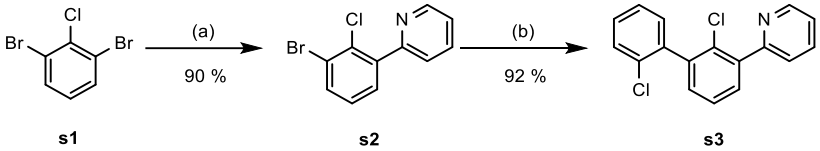

s1 **s2** **s3**

Scheme S 1. Preparation of dichloro-based preligand **s3**.Conditions: (a) 2-(tributylstannyl)pyridine, LiCl, [$Pd(PPh_3)_4$] (2 mol%), toluene, 115 °C, 15 h; (b) 2-chlorophenylboronic acid, K_3PO_4, XPhos Pd G3 (3 mol%),[2] THF/H_2O (1:1), 70 °C, 18 h.

However, aryl chlorides may only in exceptional cases be activated by elemental metals like magnesium or lithium.[3] Unfortunately, attempts to activate the C–Cl-bonds of **s3** with palladium catalysts[4] failed. Thus, **s3** is not a suitable preligand for the preparation of (C^C^N)-pincer ligands. By the way, we note that 2-(2,2'-dichloro-biphenyl-3-yl)pyridine is a central motif of natural product Chloptosin,[5] an apoptosis inducer.[6]

S 1.2 Approach 2

When we recognized diazotization-iodination of nitrophenyl aniline **20** (Scheme 4, main text) could not be achieved, we tried to borylate iodophenyl pyridine **19**.[7] The latter should then be coupled with diiodo benzene to obtain the iodophenyl substituted nitro benzene **s5**. However, palladium catalysed borylation of **19** failed and attempts to lithiate-borylate **19** by means of an *in-situ-quench*[8] only led to decomposition.[9]

Reduction of **19** gave the aniline **s6** which was subjected to MIYAURA-borylation[7a, 10] employing different catalysts and conditions, however, in all cases the boronic acid ester **s7** formed only in traces while most of the reactant **s6** was deiodinated.

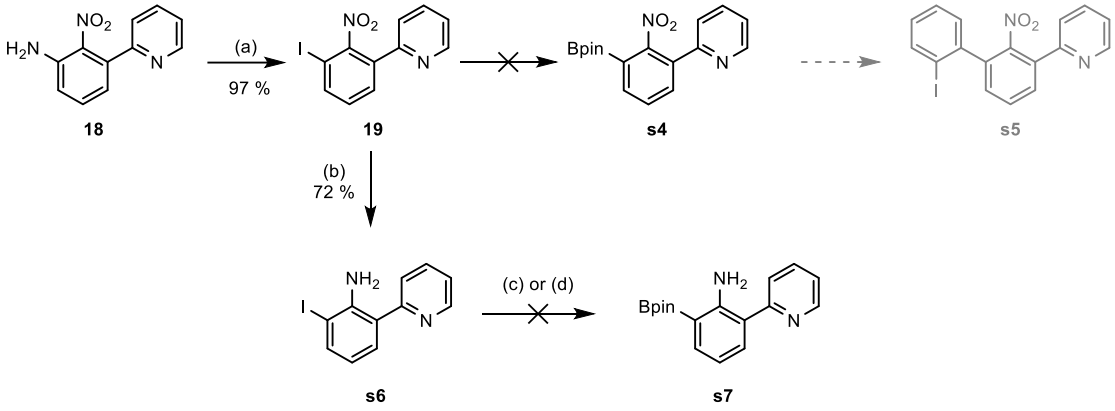

18 **19** **s4** **s5**

s6 **s7**

Scheme S 2. Attempts to introduce 2-iodophenyl at **19**. Conditions: (a) 1) HCl, $NaNO_2$, H_2O, 0 °C, 30 min 2) KI, 0 °C → rt, 12 h. (b) $SnCl_2$, EtOH, 70 °C, 1 h; (c) B_2pin_2, KOAc, 1,4-dioxane, 80 → 100 °C, 2 → 24 h, cat. [(dppf)$PdCl_2$] *or* cat. $Pd(OAc)_2$/XPhos[10a] *or* cat. $Pd(OAc)_2$/SPhos;[10b] (d) HBpin, cat. [(dppf)$PdCl_2$], Et_3N, 1,4-dioxane, 80 °C.

We also prepared the bromo nitro benzene **s8** which was not suitable for preparation of boronic acid ester **s7** neither (Scheme S 3).

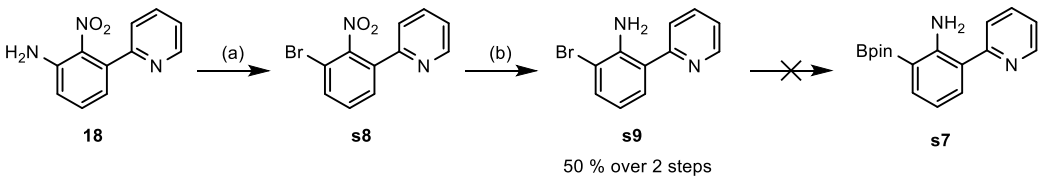

18 **s8** **s9** **s7**

50 % over 2 steps

Scheme S 3. Conditions: (a) 1) HBr, $NaNO_2$, MeCN/H_2O (2:1), –20 °C, 30 min 2) CuBr, –20 ° C → rt, 16 h; (b) $SnCl_2$, EtOH, 70 °C, 1 h.

Then we tried to succeed by coupling of **19** with 2-bromophenyl boronic acid **s10** (Scheme S 4). Unfortunately, coupling product **s11** could not be isolated in pure form. Thus, we directly reduced **s11** to obtain the aniline **s12**. Only traces beside from unidentified by-

products formed. Aniline **s12** could have been a suitable precursor for the preparation of the dihalobiphenyl **s13**. Due to the simpler procedures of the triazene based route (Scheme 5 and 6, main text) the attempts based on nitro-aromatics were discarded.

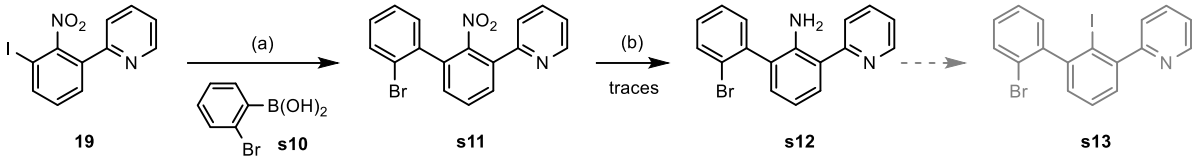

Scheme S 4. Attempts to transform nitro benzene **19** to the desired (C^C^N)-preligand. Conditions: (a) K_3PO_4, XPhos Pd G3 (3 mol%),[2] 1,4-dioxane/H_2O (4:1), 70 °C, 24 h, directly used in the next step; (b) Fe, HOAc/EtOH, reflux, 4 h.

S 1.3 Approach 3

After preparation of triazene **24** we faced the challenge to activate its Br–C-bond and introduce a 2-iodophenyl ring (Scheme 6, main text). Thus, we followed an alternative approach by coupling of **24** with 2-(aminophenyl)boronic acid (**s14**) to obtain the aniline **s15**. Single crystals of triazene **s15** suitable for X-Ray diffraction analysis were obtained by layering a concentrated solution in toluene with *n*-pentane (Scheme S 5 right).

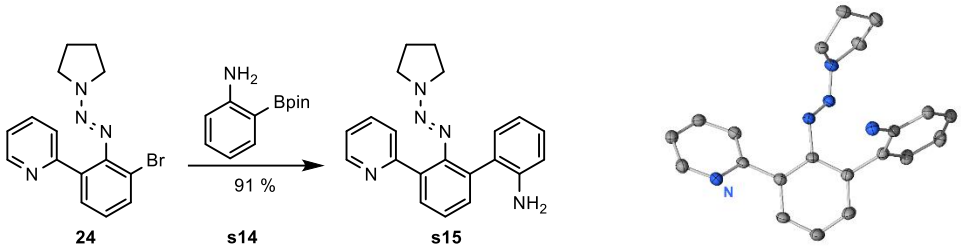

Scheme S 5. Preparation of **s15**. Conditions: XPhos Pd G3 (3 mol%),[2] K_3PO_4, 1,4-dioxane/H_2O (4:1), 80 °C, 24 h. Right: Solid state molecular structure of **s15**. Thermal ellipsoids are set at 30 % probability. Hydrogen atoms are omitted for clarity.

We then aimed to liberate the respective diazonium salt of **s15** to substitute the triazene group by iodide. Although the cyclization of neighbouring amines upon diazotization is described in the literature,[11] we suspended **s15** to acidic conditions. As expected, the cyclized cinnoline **s16** formed (Scheme S 6).

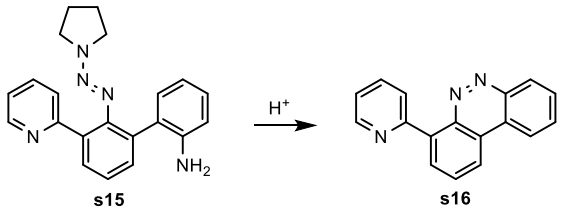

Scheme S 6. Formation of benzo[c]cinnoline **s16** upon treatment of **s15** with acid. Conditions: HCl, $NaNO_2$, H_2O, 0 °C, 30 min 2) KI, 0 °C → RT, 12 h.

Attempts to obtain the diiodide **26** via Fmoc protection, iodination, deprotection and diazotization-iodination failed, since the protected amine **s17** cyclizes to a protected carbazole under acidic conditions, which upon deprotection yields **s18**. Even if it turned out that aminophenyl substituted triazene **s15** was not suitable for the preparation of diiodobiphenyl **26**, it is interesting to note that ring-size control is achievable by introduction of the Fmoc protecting group: Unprotected aniline **s15** forms the cinnoline **s16** while Fmoc protected aniline **s17** yields carbazole **s18**.

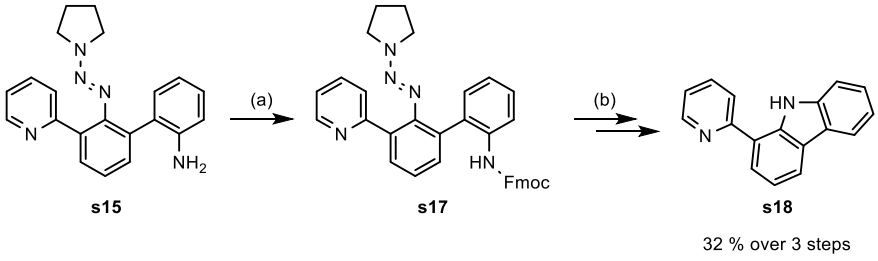

Scheme S 7. Protection of **s15** with Fmoc-Cl and subsequent attempt to substitute the triazene group of **s17** by iodide. Conditions: (a) Na_2CO_3, Fmoc-Cl, 1,4-dioxane/H_2O (1:1), 0 °C → RT, 4 h; (b) 1) HCl, KI, 0 °C → RT, 12 h *or* NaI, TMS-I, MeCN, 60 °C, 1h 2) DMF/piperidine (5:1), 30 min.

S 2 Further Reactions of Dihalobiphenyl 31 not Reported in the Main Text

S 2.1 Triazine formation

Upon diazotization-iodination the aniline **30** forms the iodo biphenyl **31** (Scheme 7, main text). However, if the conditions for this reaction are not strongly acidic, instead of **31** the triazine **s19** is formed (Scheme S 8).

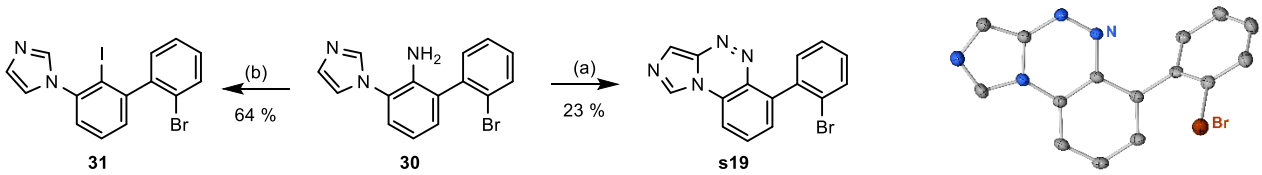

Scheme S 8. Formation of triazine **s19** under modestly acidic conditions and of iodo biphenyl **31** under strongly acidic conditions:: (a) 1) HCl, $NaNO_2$, MeCN, –15 °C → 0 °C, 30 min; (b) 1) 6 M HCl, $NaNO_2$, 0 °C, 30 min 2) KI, 0 °C → rt, 3 h. Right: Molecular structure of **s19** in the solid state. Thermal ellipsoids are set at 30 % probability. Hydrogen atoms are omitted for clarity.

Comparable pyrrolo triazines[12] and imidazole triazines[13] were reported in the literature. [13]Pozharskii *et al.*[14] investigated the pH dependence of intramolecular cyclizations of diazotized 2-(*1H*-imidazol-1-yl)anilines. Based on their findings, we succeeded in the diazotization-iodination of **30** by thoroughly grinding the reactants and suspending them in a 1:1 mixture of water and concentrated hydrochloric acid. Thus, the iodo biphenyl **31** was obtained in acceptable yields of 64 %.

S 2.2 Au(I) NHC complex

Dihalobiphenyl **31** was quaternized using methyl iodide to obtain the imidazolium salt **s20** (Scheme S 9). The latter was reacted with [(THT)AuCl] in the presence of K_2CO_3 to obtain Au(I) complex **s21** in 60 % yield.

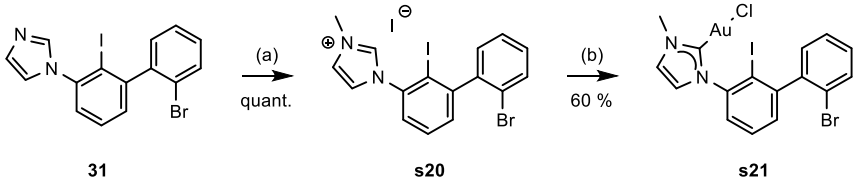

Scheme S 9. Synthesis of Au(I) complex **s21**. Conditions: (a) MeI, THF, 3 d; (b) [(THT)AuCl], K_2CO_3, MeCN, rt, 24 h.

Crystals suitable for X-ray diffraction were obtained from CH_2Cl_2/*n*-hexane (Figure S 1). Unfortunately, the data set obtained was of poor quality and discussion of bond parameters would be meaningless, however, the identity of **s21** could clearly be proven by NMR, MS and CHN analysis.

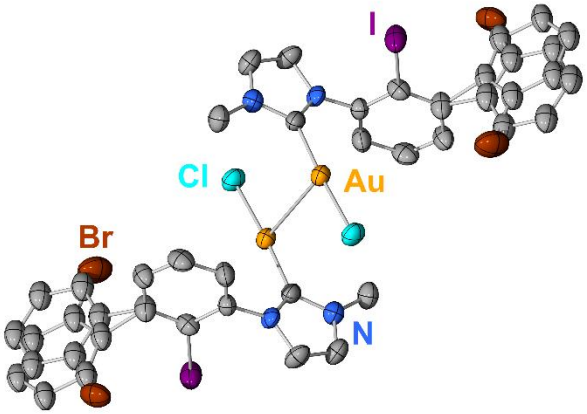

Figure S 1. Molecular structure of **s21** in the solid state. Thermal ellipsoids are set at 30 % probability. Hydrogen atoms are omitted for clarity. Both molecules of the unit cell are depicted to show aurophilic interactions ($d_{Au\text{-}Au}$ = 331 pm).[15] The bromo phenyl group is disordered. The crystal quality is not sufficient for the discussion of bond parameters.

Following work of Bourissou and co-workers[16] who described oxidative addition of Au(I) into the C−I-bond of a 8-(iodonaphthyl)phosphane with formation of the respective cyclometalated [(C^P)Au(III)] complex, we tried to enforce C−I bond activation

of **s21**. However, we did not observe any cyclometallation, even if we substituted the chloride of **s21** by iodide. These results were not too surprising since Echavarren and co-workers[17] found for similar reactions to be thermodynamically allowed, but kinetically hindered. Obviously, the naphthyl backbone employed in the group of Bourissou lowers the kinetic barrier for oxidative addition due to its steric rigidity.[18]

S 3 Computational Details

S 3.1 General Computational Procedures and Geometry Optimizations

All geometries have been optimized using the PBE0[19], CAM-B3LYP[20], and TPSSh[21] functional in conjunction with the def2-TZVP[22] basis set for the all atoms. For Au we used an effective core potential (ECP) with 60 electrons described by the core potential (ECP60MWB[23]). In all calculations an integration grid of size 3a ("gridsize 3a" in TURBOMOLE jargon) or better was employed for evaluating the DFT exchange-correlation potential. Further, the Coulomb part was approximated using the "resolution-of-the-identity" (RI) method in conjunction with the appropriate def2 auxiliar basis sets ("jbas" in ground state calculations, "cbas" in excited state calculations).[24] Ground state energies were converged to 10^{-8} Hartree (scfconv 8) and the geometry optimization was considered converged when the change in energy and cartesian gradients reached thresholds of 10^{-6} and 10^{-4} Hartree, respectively. At each converged geometry, listed in Section S 7, analytical second derivatives were evaluated and showed no (ground state) or exactly one (transition states) imaginary frequency conforming the geometries to be stationary. Transition state searches were started from a geometry confined within C_s symmetry and after initial convergence the symmetry restrained was removed and the transition state was allowed to relax fully. Stable transition states with coplanar π systems could only be located for alkynylide complexes **34** and **39**. In TD-DFT and BSE calculations the eigenvectors were considered as converged when a residual norm of 10^{-5} Hartree or lower was reached. All calculations were performed using the TURBOMOLE package[25].

S 3.2 Excited state TD-DFT spectra of the S_0 geometry

For the ground state geometry TD-DFT/def2-TZVP excitation spectra were calculated using the same method as described in Section S 3.1. Overall, the predicted spectra agree very well with the experimentally measured spectra depicted in Figure 2 (main text) for TD-TPSSh (Figure S 2) and TD-PBE0 (Figure S 3). A redshift of approximately 0.3 eV is observed for TD-TPSSh, being well within the accuracy range of TD-DFT. Furthermore, the shift is linear within TD-TPSSh and all spectral features are well represented. The prolonged tail of the absorption spectra of the [(C^C^N)Au^{III}] complexes **34** and **35** is dominated by a HOMO-LUMO excitation at 2.95 eV which is shifted by 0.5 eV in case of the [(C^C^C')Au^{III}] complexes.

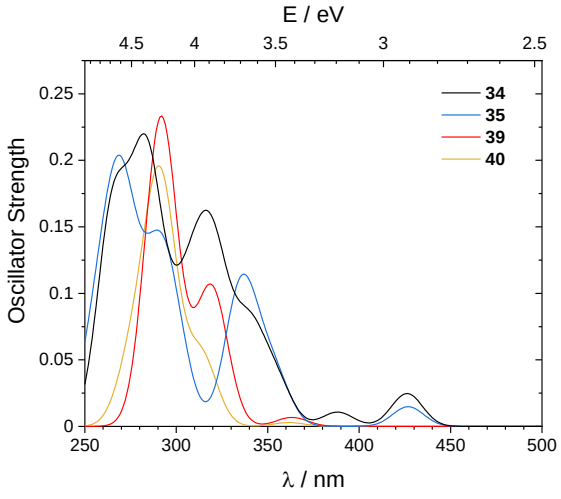

Figure S 2: Absorption spectra of complexes **34**, **35**, **39** and **40** calculated using TPSSh/def2-TZVP at the optimized ground state (S_0) geometries.

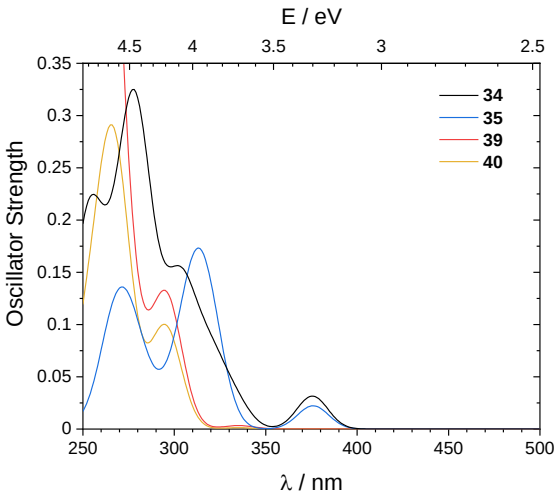

Figure S 3: Absorption spectra of complexes **34**, **35**, **39** and **40** calculated using PBE0/def2-TZVP at the optimized ground state (S_0) geometries.

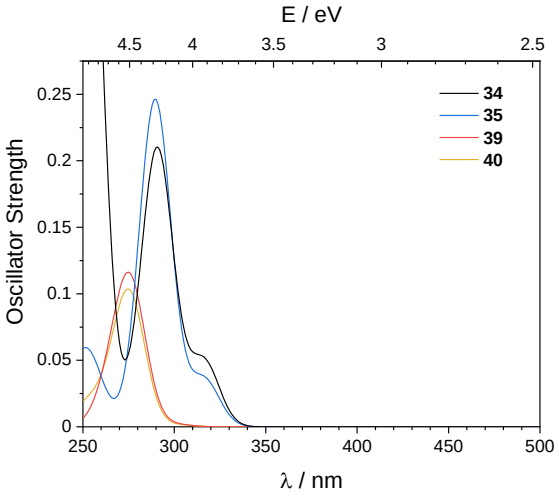

Figure S 4: Absorption spectra of complexes **34**, **35**, **39** and **40** calculated using CAM-B3LYP/def2-TZVP at the optimized ground state (S_0) geometries.

Spectra predicted using TD-CAM-B3LYP as shown in Figure S 4 are significantly too blue-shifted due to the rather high amount of Hartree-Fock exchange incorporated by the functional. Overall reproduction of the measured spectra is significantly worse for TD-CAM-B3LYP than for either TD-TPSSh or TD-PBE0 making it unsuitable for the class of compounds investigated within this work. While TD-TPSSh spectra are red-shifted compared to TD-PBE0 and the experimental spectra, they best describe the structure of the experimentally observed peaks. Therefore, all further investigations were performed using TD-TPSSh, but conclusions drawn from either TD-TPSSh or TD-PBE0 are expected to be very similar.

S 3.3 Two-component Excited state TD-DFT and GW/BSE at the T_1 geometry including spin-orbit coupling

To gain insight into the mechanism of phosphorescence we performed elaborate two-component (2c) TD-DFT and *GW*/BSE spectra including spin-orbit coupling.[26] To allow for additional flexibility the dhf-TZVPP-2c (Au, C, N, O, and F) and dhf-TZVP-2c (H) basis sets optimized for 2c quasi-relativistic calculations were used. Again, we will denote this combination as dhf-TZVP(P)-2c in further discussions. For Au, spin-orbit parameters were included in the ECP60MDF[27] core potential with 60 electrons described by the core potential. In G_0W_0 calculations HOMO and LUMO were corrected by G_0W_0, all further orbitals were shifted appropriately. The inclusion of more orbitals in the *GW* correction, or performing self-consistent iterations (ev*GW*) was prohibited by the steep increase in cost at the 2c level of theory.

As shown in Table S 1, TD-TPSSh nearly perfectly predicts the shift of the first triplet peak to the same energy, in close resemblance of experimental findings of nearly identical phosphorescence spectra for all complexes. Again, the spectra are redshifted similar to the predicted spectra at S_0 geometry. Predicted oscillator strengths f_{int}, and therefore lifetimes τ_{int} and transition probabilities of the singlet-triplet excitations, are however underestimated within the TD-DFT framework and are improved within the *GW*/BSE scheme. The latter yields good agreement with the experimentally observed lifetimes but fails to predict the position well. This can be related to deficiencies in the *GW* treatment that was applied only to HOMO and LUMO which will directly influence the position of the peaks but only has minor influences on the corresponding oscillator strengths and lifetimes. Therefore, GW/BSE oscillator strengths and lifetimes resemble the trend observed in Table 1 of the main manuscript roughly, though in terms of absolute values, differences of up to an order of magnitude remain. An NTO analysis (Figure S 5 and Figure S 6) reveals that both triplet excitations listed in Table S 1 and Table S 2 are pure

Table S 1. First triplet excitation energy T_1, and most intense triplet excitation T_{int} in the energetic range between states S_1 and T_1 for complexes **34**, **35**, **39**, and **40** at the optimized T_1 geometries. Additionally, oscillator strengths f and electric dipole radiative lifetime τ are given. All results obtained using two-component TD-TPSSh/dhf-TZVP(P)-2c. Excitation energies of triplets are given at their center of mass. The calculated splittings were below 0.01 eV and therefore not relevant. Oscillator strengths and lifetimes were taken from the most intense component.

TD-TPSSh/ dhf-TZVP(P)-2c	**[(C^C^N)Au^{III}CCPh] (34)**	**[(C^C^N)Au^{III}C$_6$F$_5$] (35)**	**[(C^C^C')Au^{III}CCPh] (39)**	**[(C^C^C')Au^{III}C$_6$F$_5$] (40)**
T_1 / eV (nm)	2.00 (620)	2.00 (620)	1.99 (623)	1.98 (626)
f_1 / a.u.	$3.891\cdot10^{-6}$	$2.115\cdot10^{-6}$	$9.467\cdot10^{-6}$	$5.572\cdot10^{-6}$
τ_1 / µs	1476	2725	615	1056
T_{int} / eV (nm)	2.37 (523)	2.39 (519)	2.85 (435)	2.85 (435)
f_{int} / a.u.	$3.961\cdot10^{-4}$	$2.069\cdot10^{-5}$	$6.041\cdot10^{-5}$	$4.440\cdot10^{-5}$
τ_{int} / µs	10.4	20.7	47.0	63.8

Table S 2. First triplet excitation energy T_1, and most intense triplet excitation T_{int} in the energetic range between S_1 and T_1 for complexes **34**, **35**, **39**, and **40** at the optimized T_1 geometries. Additionally, oscillator strengths f and electric dipole radiative lifetimes τ are given. All results obtained using two-component G_0W_0/BSE@TPSSh/dhf-TZVP(P)-2c. Excitation energies of triplets are given at their center of mass. The calculated splittings were below 0.01 eV and therefore not relevant. Oscillator strengths and lifetimes were taken from the most intense component.

G_0W_0/BSE@TPSSh/ dhf-TZVP(P)-2c	**[(C^C^N)Au^{III}CCPh] (34)**	**[(C^C^N)Au^{III}C$_6$F$_5$] (35)**	**[(C^C^C')Au^{III}CCPh] (39)**	**[(C^C^C')Au^{III}C$_6$F$_5$] (40)**
T_1 / eV (nm)	2.18 (569)	1.95 (636)	1.82 (681)	1.82 (681)
f_1 / a.u.	$2.585\cdot10^{-6}$	$3.864\cdot10^{-6}$	$8.04\cdot10^{-6}$	$4.964\cdot10^{-6}$
τ_1 / µs	2356	1259 µs	865 µs	1393 µs
T_{int} / eV (nm)	2.58 (481)	2.40 (517)	2.66 (466)	2.67 (464)
f_{int} / a.u.	$1.806\cdot10^{-4}$	$1.562\cdot10^{-6}$	$4.379\cdot10^{-4}$	$2.272\cdot10^{-3}$
τ_{int} / µs	18.3	25.6	7.4	1.4

Table S 3. First triplet excitation energy T_1, and most intense triplet excitation T_{int} in the energetic range between S_1 and T_1 for the coplanar structures of complexes **34** and **39** at the optimized transition state. Additionally, oscillator strength f and electric dipole radiative lifetime τ are given. All results obtained using two-component TD-TPSSh/dhf-TZVP(P)-2c. Excitation energies of triplets are given at their center of mass. The calculated splittings were below 0.01 eV and therefore not relevant. Oscillator strengths and lifetimes were taken from the most intense component.

TD-TPSSh/ dhf-TZVP(P)-2c	**[(C^C^N)Au^{III}CCPh] (34)**	**[(C^C^C')Au^{III}CCPh] (39)**
T_1 / eV (nm)	2.43 (510)	2.69 (461)
f_1 / a.u.	$4.001\cdot10^{-5}$	$4.497\cdot10^{-5}$
τ_1 / µs	97.6	70.6
T_{int} / eV (nm)	2.59 eV (479)	3.18 (390)
f_{int} / a.u.	$1.828\cdot10^{-2}$	$3.329\cdot10^{-3}$
τ_{int} / µs	0.19	0.68

intra-ligand (IL) excitations located at the pincer ligand. However, in case of the coplanar configurations of alkynylides **34** and **39**, the oscillator strengths are significantly higher and radiative lifetimes τ_1 and τ_{int} are shorter by one to two orders of magnitude. This mirrors the nonradiative relaxation pahways accompanied with the rotation of the phenylalkynylide ligand, thus, corroborating the assumptions from the main manuscript.

2c TD-TPSSh T_1	hole NTO	particle NTO
[(C^C^N)Au^{III}CCPh] (34)		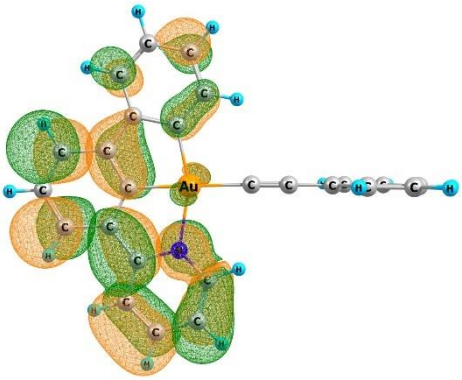
[(C^C^N)Au^{III}C$_6$F$_5$] (35)	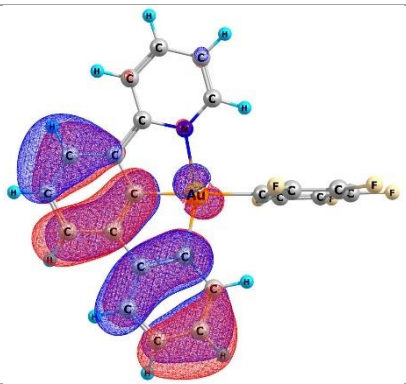	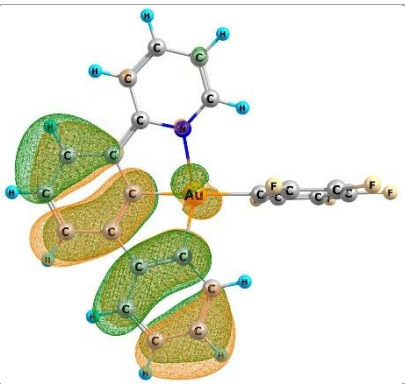
[(C^C^C')Au^{III}CCPh] (39)	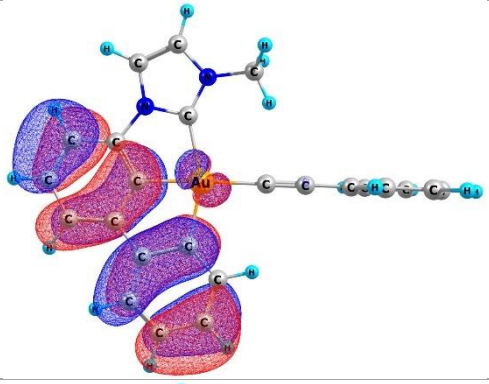	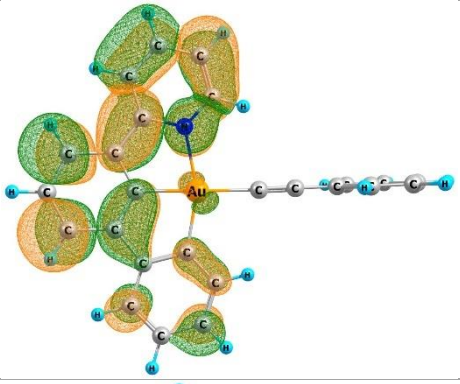
[(C^C^C')Au^{III}C$_6$F$_5$] (40)	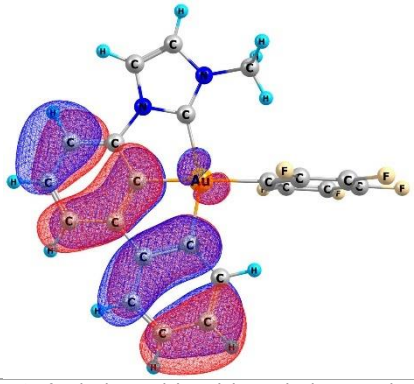	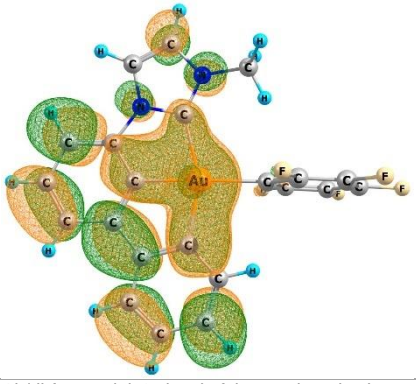

Figure S 5. Hole (left) and particle (right) NTOs for the lowest lying triplet excitation T_1 at the 2c TD-TPSSh/dhf-TZVP(P)-2c level of theory plotted using an isovalue of 0.02.

2c TD-TPSSh T_{int}	hole NTO	particle NTO
[(C^C^N)Au^{III}CCPh] (34)	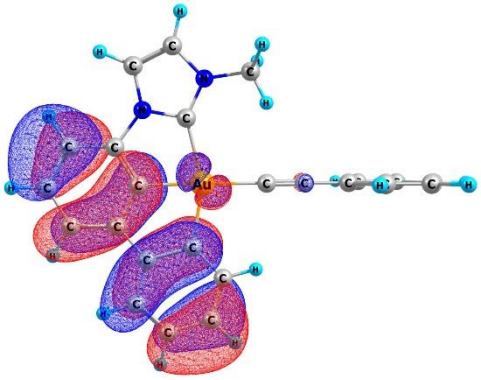	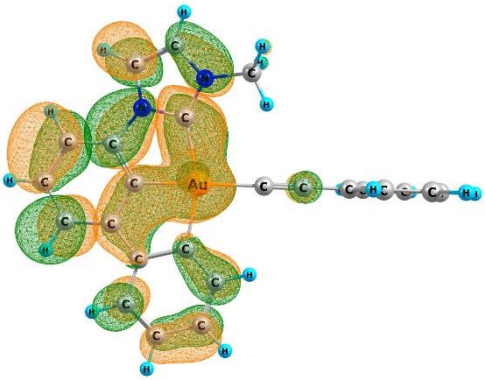
[(C^C^N)Au^{III}C$_6$F$_5$] (35)	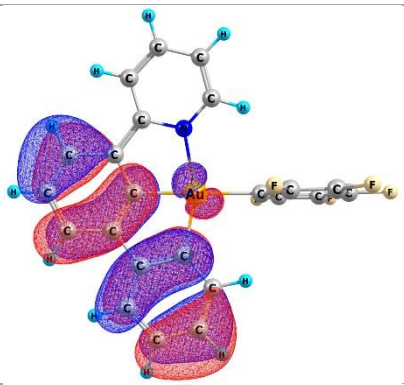	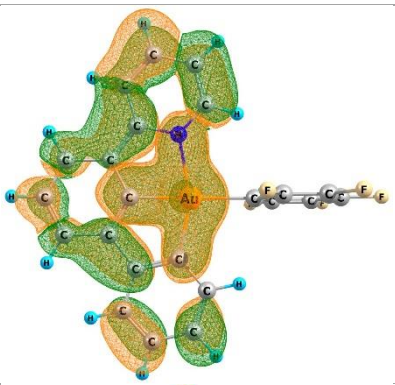
[(C^C^C')Au^{III}CCPh] (39)	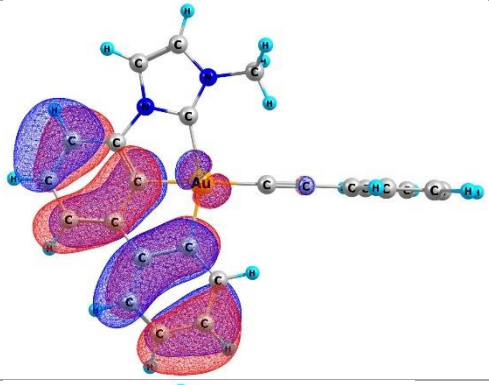	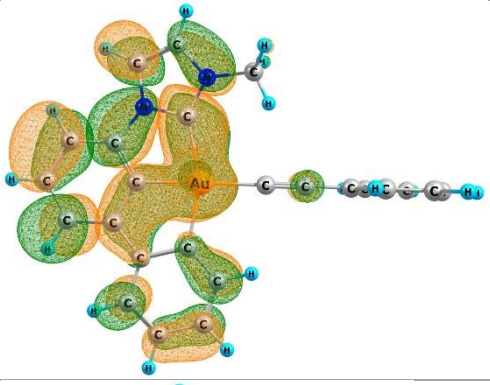
[(C^C^C')Au^{III}C$_6$F$_5$] (40)	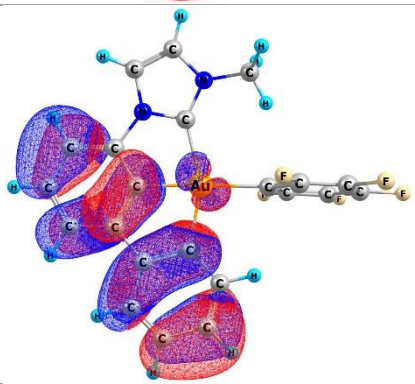	

Figure S 6. Hole (left) and particle (right) NTOs for the triplet excitation T_{int} with largest oscillator strength between T_1 and S_1 at the 2c TD-TPSSh/dhf-TZVP(P)-2c level of theory plotted using an isovalue of 0.02.

2c TD-TPSSh coplanar T_1	hole NTO	particle NTO
[(C^C^N)Au^{III}CCPh] (34)	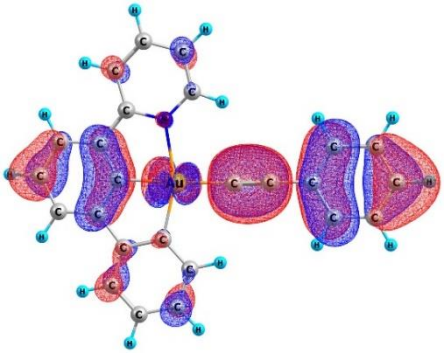	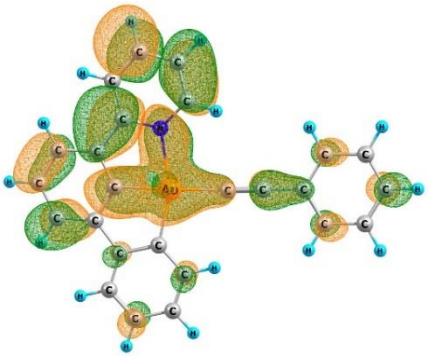
[(C^C^C')Au^{III}CCPh] (39)	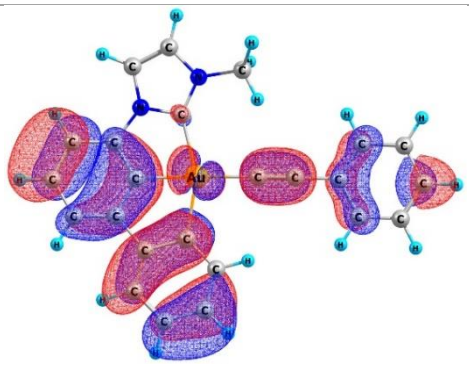	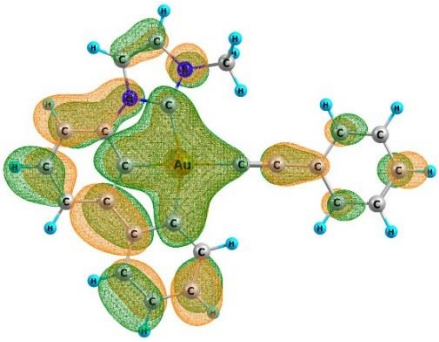

Figure S 7. Hole (left) and particle (right) NTOs for the lowest lying triplet excitation T_1 of the planar transition states of alkynylides **34** and **39** at the 2c TD-TPSSh/dhf-TZVP(P)-2c level of theory plotted using an isovalue of 0.02.

2c TD-TPSSh plan. str. T	hole NTO	particle NTO
[(C^C^N)Au^{III}CCPh] (34)	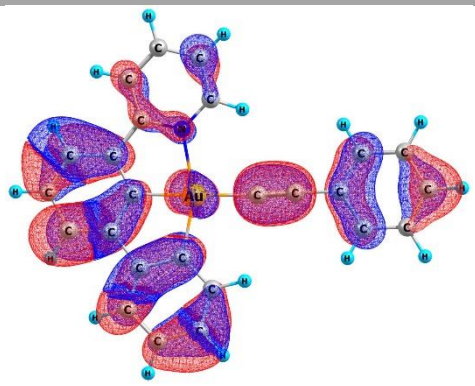	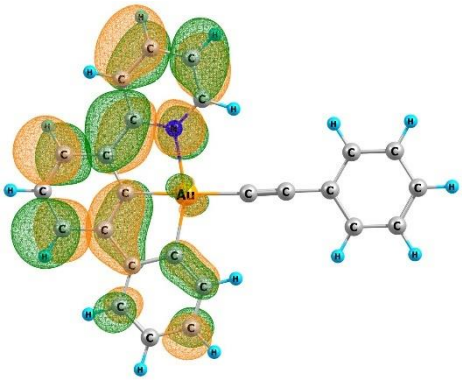
[(C^C^C')Au^{III}CCPh] (39)	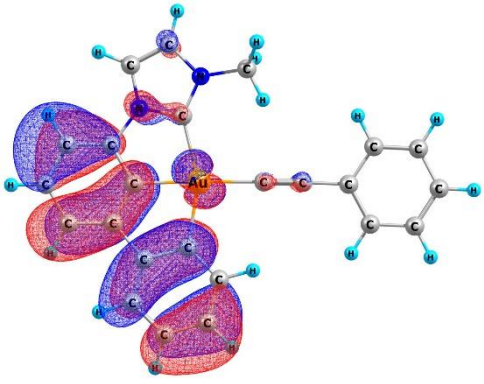	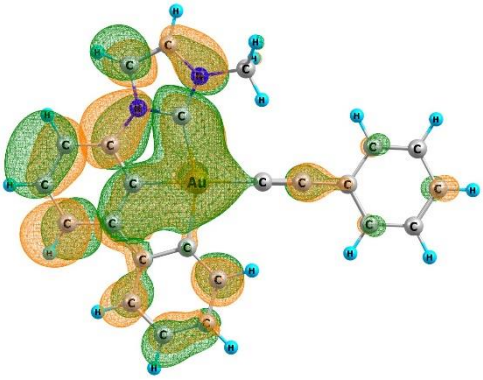

Figure S 8. Hole (left) and particle (right) NTOs for the triplet excitation T_{int} with largest oscillator strength between T_1 and S_1 of the planar transition states of the alkynylides **34** and **39** at the 2c TD-TPSSh/dhf-TZVP(P)-2c level of theory plotted using an isovalue of 0.02.

S 4 Experimental Details

S 4.1 General Synthetic and Workup Procedures

General Conditions A (GCA). Manipulations were performed under an dry and oxygen-free argon or nitrogen atmosphere using standard Schlenk techniques.[28]
THF, toluene, *n*-hexane, benzene, xylene (mixed isomers) and 1,4-dioxane were freshly distilled under argon or nitrogen from sodium/benzophenone. Acetonitrile, CCl_4 and triethylamine were distilled under argon or nitrogen from CaH_2. EtOH was distilled under argon from Magnesium wire. Et_2O, CH_2Cl_2 and *n*-pentane were purchased pre-dried and de-oxygenated and further purified by passing through alumina columns of an Innovative Technology® Solvent Purification System.
For NMR-measurements of air- or moisture sensitive compounds C_6D_6 and THF-d8 were vacuum transferred from potassium/benzophenone, CD_2Cl_2 and MeCN-d3 from CaH_2 into thoroughly dried glassware equipped with Young teflon valves.
Air sensitive compounds were stored and weighed in glove boxes (Braun MB150 G-I and Unilab system). Transfer of liquids and solutions was done by use of PP disposable syringes equipped with steel cannula which were purged with inert gas three times prior to use.

General Conditions B (GCB). Manipulations were performed open to air using HPLC-grade solvents.

General Workup A (GWA). The workup was performed under a dry and oxygen-free argon or nitrogen atmosphere using standard Schlenk[28] techniques and solvents purified as described for GCA.

General Workup B (GWB). The workup was done open to air using HPLC-grade solvents. Volatiles were removed in vacuo by using a rotary evaporator and drying the obtained residues under vacuum ($p < 10^{-3}$ mbar).

Starting Materials. If not stated otherwise, all starting materials were used as received. XPhos Pd G3[2], 1-(2,6-dibromophenylazo)pyrrolidine (**23**)[29], and $[(MeCN)AgC_6F_5]$[30] were prepared according to a literature procedure. Amberlyst 15® was dried by washing with EtOH and heating to 120 °C in high vacuum for 3 h.

Thin Layer Chromatography (TLC). Silica gel (SiO_2) coated aluminium plates (Merck, silica gel 60 Å, F254) were used for TLC, if not stated otherwise. They were analysed under UV-light at 254 nm and/or 365 nm and/or by dipping into staining solution and subsequently gentle warming with a heat-gun: aqueous $KMnO_4$ solution (3 g $KMnO_4$, 20 g K_2CO_3, 5 ml 5 % NaOH, 300 ml H_2O); *Seebach*-solution (2.5 % phosphomolybdic acid, 1.0 % cerium(IV)sulphate-tetrahydrate, 6.0 % conc. H_2SO_4, 90.5 % H_2O).
For TLC using Al_2O_3 or Silica-C18 as stationary phases, neutral alumina coated aluminium plates (Macherey-Nagel, Alox N 60 Å, F254), which were dried for 15 min at 150 °C prior to use, and reversed-phase C18 modified silica coated aluminium plates (Merck, RP-18(C18) 60 Å, F254), respectively, were used.

Column Chromatography. Chromatography was performed by the method of Still[31] using 60 Å silica gel (particle size 0.040 – 0.063 mm, 230 – 400 mesh ASTM, Sigma Aldrich) or neutral alumina 90 (particle size 0.063 – 0.200 mm, Carl Roth). If not stated otherwise, isocratic solvent mixtures are understood as volume/volume. Gradient runs are given in percentage of solvents and are indicated by an arrow with starting and end gradient (% % → % %).
Flash chromatography was performed on a CombiFlash Rf+ (Teledyne ISCO). Fraction collection was based on UV detection using suitable wavelengths. Interchim Puriflash cartridges (SiO_2, Al_2O_3 or RP-C18) were used. Analytes were dried on Celite® and transferred into an adapted pre-column. HPLC-grade solvents were used throughout.

S 4.2 Analytics and Instrumentation

NMR Spectroscopy. If not stated otherwise, solution NMR spectra were recorded at 300 K using Bruker Avance instruments operating at ^1H Larmor frequencies of 300 or 400 MHz; chemical shifts are given in parts per million (ppm) relative to TMS for ^{13}C and ^1H, to H_3PO_4 for ^{31}P, CCl_3F for ^{19}F, $NH_{3(l)}$ for ^{15}N and $SnMe_4$ for ^{119}Sn. ^1H spectra are referenced to residual ^1H solvent signals of the deuterated solvents, ^{13}C spectra to the respective solvent ^{13}C signal as internal standard.[32]
Coupling constants *J* are given in Hertz (Hz) as positive values regardless of their real individual signs. The multiplicity of the signals is indicated as s, d, t, q, m, dd, dt, td, or ddd for singlets, doublets, triplets, quartets, multiplets, doublets of doublets, doublets of triplets, triplets of doublets or doublet of doublets of doublets, respectively. The abbreviation br is given for broadened signals, brm for broadened multiplet. Other couplings than H-H (*J*) couplings are indicated by an index ($J_{nucleus1\text{-}nucleus2}$).
The assignments were confirmed, as necessary, with the use of 2D NMR correlation experiments (COSY = *Correlated Spectroscopy*; NOESY = *Nuclear Overhauser Enhancement Spectroscopy*; HSQC = *Heteronuclear Single Quantum Coherence*; HMBC = *Heteronuclear Multiple Quantum Correlation;* HMQC = *Heteronuclear Multiple Quantum Correlation Transfer*).
The multiplicity of ^{13}C-NMR-signals was determined by the use of DEPT 90- and DEPT 135-spectra (DEPT = Distortionless Enhancement by Polarization Transfer): DEPT: + = primary CH or tertiary CH_3 (positive DEPT-signal), – = secondary CH_2 (negative DEPT-signal), C_q = quaternary C-atoms (no DEPT-signal).[33] The spectra were analysed according to first order.
NMR samples were prepared in oven-dried 5 mm NMR tubes. Air or moisture sensitive compounds were prepared inside a glovebox using screw cap or Young valve NMR tubes or by vacuum transfer of the solvent to the samples and melting off the NMR tube.
Unless otherwise stated, standard Bruker software routines (TOPSPIN[34]) were used for the 1D and 2D NMR measurements.

IR Spectroscopy. IR spectra were recorded on a Bruker Alpha FT-IR spectrometer using the ATR technique (attenuated total reflection) on bulk material, and the data are quoted in wavenumbers (cm^{-1}).
The intensities of the absorption bands are indicated as follows: vs = very strong (0 – 10 % transmission (T)), s = strong (11 – 30 % T), m=medium (31 – 70 % T), w = weak (71 – 90 % T), vw = very weak (91 – 100 % T).

Mass Spectrometry. Mass spectra using different ionization methods were recorded using the following spectrometers:

Atomic pressure chemical ionization (APCI) - Advion Express LCMS

Electrospray Ionization Mass Spectrometry (ESI-MS) - Advion Express LCMS or Thermo Fisher Scientific Q Exactive (Orbitrap) mass spectrometer

Electron Ionization (EI) - Varian MAT 3830 (70 eV)

Fast Atom Bombardment (FAB) - Finnigan MAT 95

Air or moisture sensitive samples were melted off in glass capillaries under argon (EI) or were syringe-transferred using inert solvents (ESI-MS).
If detectable, the positive molecular ion peak $[M]^+$ or the protonated molecular ion peak $[M+H]^+$ as well as characteristic fragment peaks ($[M\text{-fragment}]^+$ and $[fragment]^+$) are given. For ESI-MS, if detectable, the negative molecular ion peak $[M]^-$ is given. Intensities are given relative to the base peak (100 %).

Elemental Analysis. Elemental analyses were recorded by the institutional technical laboratories of the Karlsruhe Institute of Technology (KIT).

Melting Points. Melting points were measured with a Thermo Fischer Scientific digital melting point apparatus of the IA9300 series and are not corrected. Pure samples of the compounds were added to a capillary tube under argon which was then sealed from air by fusemelting the glass end.

UV/Vis Spectroscopy. UV/Vis spectra were recorded on a Lambda 750 Spectrometer (Perkin Elmer) using fused silica cuvettes with 10 mm path length.

Photoluminescence Spectroscopy. Photoluminescence spectra were recorded on a Horiba Jobin Yvon Spex Fluorolog 3 (Horiba Jobin Yvon, Bensheim, Germany). It was equipped with a 450 W Xe lamp, double grating monochromators for excitation and emission, integrating sphere and photomultiplier detector (excitation source and detector in orthogonal arrangement).
Slit widths for excitation and detection were adjusted individually for each sample.
Solution samples were of 100 μmol/L concentration. At this concentration absorbance at the excitation wavelengths were for all samples below 0.05 with the cuvettes (fused silica) used.
Absolute quantum yields were determined as average of three independent measurements by means of an integrating sphere (error ± 2 %).
If not stated otherwise, OriginPro 2019b[35] was used for data evaluation.

S 4.3 Experimental Procedures

2-Nitro-2-(pyridine-2-yl)aniline (18)

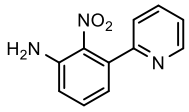

GCA, GWB. 3-Bromo-2-nitroaniline (2.17 g, 10.0 mmol, 1.00 eq.), LiCl (424 mg, 40.0 mmol, 4.00 eq.) and $Pd(PPh_3)_4$ (462 mg, 0.40 mmol, 0.04 eq.) were dissolved in 40 ml xylene (mixed isomers). 2-Tributylstannylpyridine (4.79 g, 13.0 mmol, 1.30 eq.) was added via syringe and the resulting mixture heated to reflux under continuous stirring. After 6 h TLC control indicated complete consumption of 3-bromo-2-nitroaniline. The mixture was cooled to room temperature and stirred with 7 M KF_{aq} for 30 min. The mixture was passed through a plug of Celite® which was extracted with EtOAc (3 x 50 ml). The aqueous layer was separated, and the combined organic layers washed with brine and dried over $MgSO_4$. After evaporating all solvent in vacuo, the residue was purified by flash column chromatography (SiO_2, cyclohexane/EtOAc 90 % / 10 % → 60 % / 40 %). 1.99 g (92 %) yellow solid were obtained.

$\mathbf{R_f}$ = 0.24 (SiO_2. cyclohexane/EtOAc = 3/1). **M.p.** = 121 °C. **^{1}H-NMR** (300 MHz, $CDCl_3$): δ = 8.59 (ddd, *J* = 4.9, 1.8, 1.0 Hz, 1 H), 7.75 (td, *J* = 7.7, 1.8 Hz, 1 H), 7.44 (dt, *J* = 7.9, 1.1 Hz, 1 H), 7.29 (dd, *J* = 8.4, 7.3 Hz, 1 H), 7.28 – 7.23 (m, 1 H), 6.82 (dd, *J* = 8.4, 1.3 Hz, 1 H), 6.79 (dd, *J* = 7.3, 1.3 Hz, 1 H), 5.25 (br, 2 H, N*H*$_2$). **^{13}C-NMR** (75 MHz, $CDCl_3$): δ = 157.1 (C_q), 149.4 (CH), 142.7 (C_q), 137.8 (C_q), 136.9 (CH), 134.8 (C_q), 132.7 (CH), 122.6 (CH), 122.4 (CH), 120.1 (CH), 118.6 (CH). **IR (ATR):** $\tilde{\nu}/cm^{-1}$ = 3461 (w), 3256 (vw), 3125 (vw), 3067 (vw), 1615 (s), 1590 (s), 1568 (s), 1503 (vs), 1468 (s), 1460 (s), 1443 (s), 1421 (m), 1371 (vw), 1344 (s), 1294 (vw), 1279 (m), 1248 (s), 1171 (w), 1151 (vw), 1127 (w), 1098 (vw), 1041 (w), 997 (w), 969 (vw), 919 (vw), 888 (vw), 849 (m), 796 (m), 782 (vs), 768 (vs), 753 (m), 744 (s), 704 (s), 664 (w), 627 (m), 585 (w), 553 (vw), 521 (w), 486 (vw), 461 (w), 421 (w), 404 (w), 380 (vw). **MS (EI, 70 eV)**, m/z (%): 215.1 (100 %) $[M]^+$, 198.1 (81 %) $[M–NH_3]^+$, 168.1 (64 %) $[M–HNO_2]^+$. **Elemental analysis** calculated (%) for $C_{11}H_9N_3O_2$: C 61.39, H 4.22, N 19.53, found: C 61.13, H 4.24, N 19.44.

2-(3-Iodo-2-nitrophenyl)pyridine (19)

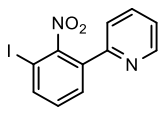

GCB, GWB. **18** (1.81 g, 8.41 mmol, 1.00 eq.) was dissolved in MeCN (10 ml) and conc. HCl_{aq} (3 ml) and cooled to –15 °C. $NaNO_2$ (697 mg, 10.10 mmol, 1.20 eq.) in water (3 ml) was added dropwise into the vigorously stirred solution. The mixture was stirred for 30 min at –15 °C after which KI (1.80 g, 16.87 mmol, 2.00 eq.) in water (3 ml) was added dropwise. Immediately, the mixture turned brown and a strong gas evolution occurred. Stirring was

continued overnight at room temperature. The mixture was diluted with water (20 ml) and K_2CO_3 was carefully added (strong gas evolution) until the pH of the mixture was > 8. The mixture was extracted with EtOAc (3 x 50 ml) and the combined organic extracts washed with conc. aqueous $Na_2S_2O_3$ and brine. After drying over $MgSO_4$ all volatiles were removed in vacuo and the residue purified by column chromatography (Al_2O_3, *n*-heptane/EtOAc = 10/1) to obtain a yellowish solid (2.65 g, 97 %). Crystals suitable for X-Ray diffraction analysis were obtained by recrystallizing from cyclohexane/EtOAc.

R_f = 0.23 (Al_2O_3. *n*-heptane/EtOAc = 10/1). **M.p.** = 147 °C (Z). **^{1}H-NMR** (300 MHz, $CDCl_3$): δ = 8.65 (ddd, *J* = 4.8, 1.8, 1.0 Hz, 1 H), 7.96 (dd, *J* = 7.9, 1.3 Hz, 1 H), 7.79 (td, *J* = 7.8, 1.8 Hz, 1 H), 7.65 (dd, *J* = 7.8, 1.3 Hz, 1 H), 7.50 (dt, *J* = 7.9, 1.0 Hz, 1 H), 7.32 (ddd, *J* = 7.6, 4.9, 1.1 Hz, 1 H), 7.28 (t, *J* = 7.9 Hz, 1 H). **^{13}C-NMR** (75 MHz, $CDCl_3$): δ = 153.6 (C_q), 149.9 (CH), 140.4 (CH), 137.2 (CH), 134.7 (C_q), 131.4 (CH), 130.4 (CH), 128.2 (C_q), 123.5 (CH), 122.4 (CH), 87.0 (C_q). **IR (ATR):** $\tilde{\nu}$/cm^{-1} = 3068 (vw), 2879 (vw), 2193 (vw), 2180 (vw), 2150 (vw), 2135 (vw), 2092 (vw), 2039 (vw), 2001 (vw), 1959 (vw), 1896 (vw), 1863 (vw), 1695 (vw), 1621 (vw), 1580 (m), 1558 (w), 1530 (vs), 1474 (w), 1449 (vw), 1433 (m), 1400 (vw), 1357 (m), 1304 (vw), 1286 (w), 1237 (vw), 1204 (vw), 1154 (w), 1094 (vw), 1054 (w), 1034 (vw), 994 (m), 898 (vw), 850 (m), 801 (w), 790 (w), 775 (vs), 750 (m), 710 (w), 691 (w), 649 (w), 623 (w), 582 (vw), 565 (w), 531 (w), 507 (vw), 475 (vw), 467 (vw), 453 (vw), 430 (vw), 409 (w), 400 (w), 389 (vw), 381 (vw). **MS (EI. 70 eV)**, m/z (%): 326.1 (32 %) $[M]^+$, 296.1 (62 %) $[M–NO]^+$, 280.0 (24 %) $[M–NO_2]^+$. **Elemental analysis** calculated (%) for $C_{11}H_9N_2O_2I$: C 40.52, H 2.164, N 8.59, found: C 41.05, H 2.15, N 8.38.

2'-Nitro-3'-(pyridin-2-yl)-[1,1'-biphenyl]-2-amine (20)

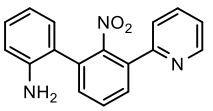

GCA, GWB. A Schlenk-tube was charged with **19** (1.23 g, 3.78 mmol, 1.00 Eq.), 2-aminophenylboronic acid pinacol ester (994 mg, 4.54 mmol, 1.20 eq.), XPhos Pd G3[2] (96 mg, 0.11 mmol, 0.03 eq.) and K_3PO_4 (1.61 g, 7.57 mmol, 2.00 eq.). 1,4-Dioxane (12 ml) and water (3 ml) were added. The resulting mixture was stirred at 70 °C. After 90 min all **s6** was consumed as indicated by TLC control. The mixture was cooled to room temperature and diluted with EtOAc (30 ml) and water (30 ml). The aqueous phase was separated, and the organic phase washed with 1 M $NaOH_{aq}$ and brine and finally dried over $MgSO_4$. After removing all volatiles, the brown residue was purified by column chromatography (SiO_2, cyclohexane/EtOAc = 1/1) to obtain 980 mg (89 %) of a yellow solid. Crystals suitable for X-ray diffraction analysis were obtained by crystallization from cyclohexane/EtOAc.

R_f = 0.27 (SiO_2. cyclohexane/EtOAc = 1/1). **M.p.** = 130 °C. **^{1}H-NMR** (300 MHz, $CDCl_3$): δ = 8.66 (ddd, *J* = 4.9, 1.8, 0.9 Hz, 1 H), 7.80 (td, *J* = 7.8, 1.8 Hz, 1 H), 7.69 (dd, *J* = 7.7, 1.7 Hz, 1 H), 7.63 (t, *J* = 7.6 Hz, 1 H), 7.57 (dt, *J* = 7.9, 1.1 Hz, 1 H), 7.50 (dd, *J* = 7.4, 1.7 Hz, 1 H), 7.32 (ddd, *J* = 7.6, 4.9, 1.1 Hz, 1 H), 7.20 (ddd, *J* = 8.1, 7.4, 1.6 Hz, 1 H), 7.01 (dd, *J* = 7.8, 1.5 Hz, 1 H), 6.84 – 6.73 (m, 2 H), 3.64 (br, 2 H, N*H*$_2$). **^{13}C-NMR** (75 MHz, $CDCl_3$): δ = 154.6 (C_q), 150.3 (C_q), 149.9 (CH), 144.2 (C_q), 137.3 (CH), 133.7 (C_q), 132.8 (C_q), 132.3 (CH), 130.7 (CH), 130.2 (CH), 130.0 (CH), 129.8 (CH), 123.3 (CH), 122.8 (CH), 121.8 (C_q), 118.7 (CH), 116.2 (CH). **IR (ATR):** $\tilde{\nu}$/cm^{-1} = 3422 (vw), 3332 (vw), 3212 (vw), 3028 (vw), 2922 (vw), 2852 (vw), 1992 (vw), 1965 (vw), 1912 (vw), 1630 (w), 1601 (vw), 1585 (m), 1566 (vw), 1540 (vs), 1498 (m), 1480 (w), 1461 (m), 1442 (w), 1374 (m), 1302 (w), 1292 (w), 1269 (vw), 1192 (vw), 1145 (vw), 1093 (vw), 1043 (vw), 1018 (vw), 993 (w), 968 (vw), 938 (vw), 926 (vw), 903 (vw), 852 (w), 822 (vw), 797 (vw), 780 (s), 749 (vs), 725 (w), 711 (vw), 663 (w), 626 (m), 613 (w), 593 (w), 558 (vw), 520 (w), 489 (s), 424 (vw), 401 (w). **MS (EI. 70 eV)**, m/z (%): 192.1 (20 %) $[M]^+$, 245.1 (100 %) $[M–NO_2]^+$. **Elemental analysis** calculated (%) for $C_{17}H_{13}N_3O_2$: C 70.09, H 4.500, N 14.42, found: C 70.30, H 4.78, N 14.33.

2-(3-Bromo-2-(pyrrolidin-1-yldiazenyl)phenyl)pyridine (24)

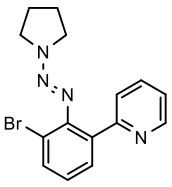

24 was synthesized according to a modified literature procedure.[29] GCA, GWB. In a round bottom flask, a solution of 1-(2,6-dibromophenylazo)pyrrolidine (**23**) (6.66 g, 20.00 mmol, 1.00 eq.) in THF (6 ml) was cooled to –40 °C by means of a cryostat. 16.9 ml of *i*PrMgCl-LiCl (1.30 M in THF, 3.20 g, 22.00 mmol, 1.10 eq.) were slowly added via syringe pump (~ 48 ml / h). After the addition was complete, the obtained dark red mixture was warmed to –15 °C and stirred at this temperature for 4 h. The completeness of the Br-Mg-exchange was checked via APCI-MS of quenched (MeOH-*d4*) reaction aliquots. Then, the reaction mixture was cooled to –20 °C and 24 ml $ZnBr_2$ (1.00 M in THF, 5.40 g, 24.00 mmol, 1.20 Eq.) were added via syringe pump (~ 48 ml / h). After addition, the mixture was stirred at 5 °C for 1 h and then cannula transferred to a round bottom flask equipped with a reflux condenser containing 2-bromopyridine (4.11 g, 26.00 mmol, 2.48 ml, 1.30 eq.) and $Pd(PPh_3)_4$ (2.31 g, 2.00 mmol, 0.10 eq.) in 40 ml THF. The obtained mixture was stirred under reflux for 16 h. After cooling to room temperature, the reaction was quenched with water (50 ml) and stirred for 30 min. Et_2O (100 ml) was added and the aqueous phase separated. The latter was extracted with Et_2O (3 x 100 ml) and the combined organic phases were washed with brine and dried over $MgSO_4$. After evaporating all solvents were removed and the dark red crude was purified by column chromatography (SiO_2, CH_2Cl_2/EtOAc = 10/1). 5.76 g (87 %) of a dark red oil were obtained.

R_f = 0.33 (SiO_2. CH_2Cl_2/EtOAc = 10/1). **M.p.** = oil. **^{1}H-NMR** (300 MHz, $CDCl_3$): δ = 8.60 (ddd, *J* = 4.9, 1.8, 1.0 Hz, 1 H), 7.62 (dd, *J* = 7.9, 1.4 Hz, 1 H), 7.59 – 7.51 (m, 2 H), 7.26 (dt, *J* = 8.0, 1.1 Hz, 1 H), 7.12 (ddd, *J* = 7.5, 4.9, 1.1 Hz, 1 H), 7.09 (t, *J* = 7.8 Hz, 1 H), 3.55 (t, *J* = 6.8 Hz, 4 H), 1.92 (br, 4 H). **^{13}C-NMR** (75 MHz, $CDCl_3$): δ = 158.5 (C_q), 149.2 (CH), 148.2 (C_q), 135.3(C_q), 135.1 (CH), 133.3 (CH), 130.2 (CH), 126.0 (CH), 125.5 (CH), 121.2 (CH), 118.4 (C_q), 50.9 (CH_2)[1], 46.7 (CH_2), 23.9 (2 CH_2). **IR (ATR):** $\tilde{\nu}$/cm^{-1} = 3058 (vw), 2972 (w), 2870 (w), 1585 (m), 1565 (w), 1550 (w), 1472 (w), 1449 (w), 1408 (vs), 1313 (vs), 1288 (s), 1256 (m), 1218 (m), 1192 (w), 1150 (m), 1106 (w), 1071 (w), 1059 (w), 1033 (w), 989 (w), 968 (vw), 934 (vw), 904 (vw), 849 (vw), 801 (w), 768 (vs), 745 (vs), 705 (w), 656 (s), 622 (w), 593 (w), 569 (w), 492 (vw), 438 (vw), 404 (w). **MS (ESI)**, m/z (%): 331.0 (28 %) $[M+H]^+$, 260.0 (25 %) $[M–Pyrrolidin]^+$, 232.0 (100 %) $[M–Pyrrolidin–N_2]^+$. **Elemental analysis** could not be done for oils.

[1] The NN-(*CH*$_2$)-atoms in α-position of the nitrogen atom of the pyrrolidine group exhibit different chemical shifts, probably due to hindered rotations around the N–N-axis (cf. Figure S **20** and Figure S 76).

2-(2'-Iodo-2-(pyrrolidin-1-yldiazenyl)-[1,1'-biphenyl]-3-yl)pyridine (25)

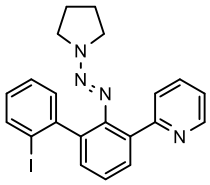

GCA, GWB. In a flame dried 500 ml round bottom flask, a solution of **24** (6.62 g, 20.00 mmol, 1.00 eq.) in THF (100 ml) was cooled to –98 °C (MeOH + $N_{2(l)}$). 13.13 ml 1.6 M *n*-BuLi (1.35g, 21.00 mmol, 1.05 eq.) were cooled in a dropping funnel to –78 °C (*i*-PrOH + $CO_{2(s)}$) and then added dropwise over a period of 30 min to the vigorously stirred solution of **24**. After the addition was complete, the obtained dark red mixture was stirred for 1 h at –98 °C. Then, $ZnBr_2$ (4.95 g, 22.00 mmol, 1.10 eq.) was dissolved in 50 ml THF and cooled to –78 °C inside a dropping funnel as well and then added dropwise over a period of 10 min to the vigorously stirred lithium organyl. The resulting mixture was warmed to –78 °C and stirred for another hour.

The cooling bath was removed and the resulting red mixture (zinc reagent) warmed to room temperature. In a second flame dried 500 ml round bottom flask 1,2-diiodobenzene (7.92 g, 24 mmol, 1.20 eq.) and $Pd(PPh_3)_4$ (1.16 g, 1.00 mmol, 0.05 eq.) were dissolved in THF (10 ml). The freshly prepared zinc reagent was cannula transferred to the iodine compound solution under vigorous stirring. Then, the resulting mixture was stirred under reflux overnight.

The clear red reaction mixture was quenched with water (200 ml). The aqueous phase was extracted with EtOAc (3 x 200 ml) and the combined organic phases washed with brine and dried over $MgSO_4$. Finally, all volatiles were removed in vacuo. The resulting brown foam was purified by flash column chromatography (SiO_2, *n*-heptane/EtOAc 100 % / 0 % → 20 % / 80 %) to obtain 4.91 g (54 %) of a white solid. Crystals suitable for X-Ray diffraction analysis are obtained by slow evaporation of a concentrated solution in hexanes. Yields are notably higher (> 70 %) on a smaller scale (< 5 mmol).

$\mathbf{R_f}$ = 0.37 (SiO_2. *n*-heptane/EtOAc = 1/1). **M.p.** = 120 – 121 °C. **^{1}H-NMR** (300 MHz, $CDCl_3$): δ = 8.66 (ddd, *J* = 4.9, 1.8, 1.0 Hz, 1 H), 7.87 – 7.80 (m, 1 H), 7.75 (dd, *J* = 7.7, 1.6 Hz, 1 H), 7.58 (ddd, *J* = 8.0, 7.1, 1.8 Hz, 1 H), 7.52 (ddd, *J* = 8.0, 1.5, 1.0, Hz, 1 H), 7.34 – 7.22 (m, 3 H), 7.18 (dd, *J* = 7.5, 1.6 Hz, 1 H), 7.13 (ddd, *J* = 6.8, 4.9, 1.5 Hz, 1 H), 6.92 (ddd, *J* = 7.9, 6.7, 2.4 Hz, 1 H), 3.63 – 3.00 (m, 4 H), 1.73 (p, *J* = 3.1 Hz, 4 H). **^{13}C-NMR** (75 MHz, $CDCl_3$): δ = 158.5 (C_q), 149.1 (CH), 147.2 (C_q), 146.7 (C_q), 138.3 (CH), 137.5 (C_q), 134.9 (CH), 134.3 (C_q), 131.5 (CH), 131.0 (CH), 130.6 (CH), 127.7 (CH), 127.2 (CH), 126.3 (CH), 124.7 (CH), 121.2 (CH), 100.8 (CH), 48.6 (2 CH_2)[2], 23.8 (2 CH_2). **IR (ATR):** $\tilde{\nu}$/cm^{-1} = 3051 (vw), 2971 (vw), 2868 (vw), 1735 (w), 1584 (m), 1561 (w), 1473 (w), 1452 (w), 1408 (vs), 1314 (vs), 1240 (w), 1209 (m), 1184 (vw), 1152 (w), 1127 (vw), 1107 (w), 1095 (vw), 1075 (vw), 1045 (w), 1021 (vw), 1009 (m), 989 (vw), 968 (vw), 937 (vw), 905 (vw), 849 (vw), 824 (vw), 812 (vw), 795 (vw), 775 (s), 751 (vs), 719 (m), 692 (w), 682 (w), 650 (w), 608 (m), 587 (vw), 563 (vw), 520 (w), 440 (w), 404 (w). **MS (ESI)**, m/z (%): 455.0 (100 %) $[M+H]^+$, 384.0 (11 %) $[M–Pyrrolidin]^+$, 356.0 (21 %) $[M–Pyrrolidin–N_2]^+$. **Elemental analysis** calculated (%) for $C_{21}H_{19}N_4I$: C 55.52, H 4.22, N 12.33, found: C 55.54, H 3.99, N 12.32.

(2,2'-Diiodo-[1,1'-biphenyl]-3-yl)pyridine (26)

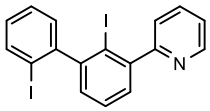

GCA, GWB. A Schlenk flask was charged with Amberlyst 15® (12.6 g), NaI (9.37g, 62.51 mmol, 5.00 eq.) and MeCN (100 ml) and heated to 70 °C. Under vigorous stirring a solution of **25** (5.70 g, 12.55 mmol, 1.00 eq.) in 1,2-dichloroethane was added dropwise on which the solution immediately turned dark brown and a strong gas evolution occurred. After the addition was complete the resulting slurry was stirred for 10 min at 70 °C and then cooled to room temperature and stirred overnight. Azo-test (stippling with 2-Naphthol + K_2CO_3) was negative and the reaction mixture diluted with EtOAc (50 ml) and filtered. The filtrate was washed with conc. $Na_2CO_{3(aq)}$ (50 ml) and brine. After drying over $MgSO_4$ all volatiles were removed in vacuo and the residue purified by column chromatography (SiO_2, *n*-heptane/EtOAc = 10/1) to obtain 4.43 g (73 %) of yellowish oil which contained EtOAc even after drying in vacuo for 48 h. However, after standing for three months at room temperature the oil solidified and drying in vacuo removed remaining solvent.

$\mathbf{R_f}$ = 0.32 (SiO_2. *n*-heptane/EtOAc = 10/1). **M.p.** = 118 °C. **^{1}H-NMR** (300 MHz, CD_2Cl_2): δ = 8.69 (ddd, *J* = 4.9, 1.8, 1.0 Hz, 1 H), 7.97 (ddd, *J* = 8.0, 1.2, 0.4 Hz, 1 H), 7.79 (ddd, *J* = 7.6, 1.8 Hz, 1 H), 7.56 – 7.45 (m, 1 H), 7.51 (t, *J* = 7.5 Hz, 1 H), 7.45 (dd, *J* = 7.5, 1.3 Hz, 1 H), 7.40 (dd, *J* = 7.6, 1.8 Hz, 1 H), 7.32 (ddd, *J* = 7.6, 4.9, 1.2 Hz, 1 H), 7.28 (ddd, *J* = 7.6, 1.7, 0.4 Hz, 1 H), 7.22 (dd, *J* = 7.5, 1.8 Hz, 1 H), 7.12 (ddd, *J* = 8.0, 7.4, 1.7 Hz, 1 H). **^{13}C-NMR** (75 MHz, $CDCl_3$): δ = 162.2 (C_q), 150.7 (C_q), 150.4 (C_q), 149.7 (CH), 147.2 (C_q), 139.4 (CH), 136.4 (CH), 130.7 (CH), 129.9 (CH), 129.9 (CH), 129.8 (CH), 128.7 (CH), 128.5 (CH), 125.1 (CH), 123.1 (CH), 102.8 (C_q, I*C*), 100.4 (C_q, I*C*). **IR (ATR):** $\tilde{\nu}$/cm^{-1} = 3047 (vw), 3006 (vw), 2922 (vw), 1946 (vw), 1882 (vw), 1733 (vw), 1585 (m), 1563 (m), 1472 (w), 1446 (m), 1425 (s), 1389 (m), 1316 (vw), 1280 (vw), 1249 (vw), 1180 (vw), 1148 (w), 1103 (vw), 1090 (vw), 1060 (vw), 1043 (w), 1016 (m), 1003 (s), 989 (m), 945 (vw), 908 (vw), 864 (vw), 802 (w), 777 (s), 748 (vs), 718 (vs), 656 (m), 647 (m), 620 (m), 607 (m), 566 (vw), 534 (m), 501 (vw), 441 (m), 402 (w). **MS (ESI)**, m/z (%): 483.9 (100 %) $[M+H]^+$. **Elemental analysis** calculated (%) for $C_{17}H_{11}NI_2$: C 42.27, H 2.30, N 2.90, found: C 42.61, H 2.62, N 3.44.

1-(3-Bromo-2-nitrophenyl)-*1H*-imidazole (28)

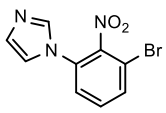

GCB, GWB. 1-Bromo-3-fluoro-2-nitrobenzene (**27**) (5.31 g, 24.13 mmol, 1.00 eq.) and imidazole (1.64 g, 24.13 mmol, 1.00 eq.) were dissolved in DMSO (25 ml). Under stirring, powdered NaOH (1.45 g, 36.20 mmol, 1.50 Eq.) was added in small portions on which the mixture noticeably warmed. The mixture was stirred for 2 h and then diluted with water (100 ml). The aqueous phase was extracted with EtOAc (3 x 100 ml). The combined organic phases were washed with brine, dried over $MgSO_4$ and evaporated to dryness to obtain a white solid (6.47 g, quantitative).

M.p. = 112 °C. **^{1}H-NMR** (300 MHz, $CDCl_3$): δ = 7.78 (dd, *J* = 8.1, 1.3 Hz, 1 H), 7.62 (t, *J* = 1.1 Hz, 1 H), 7.50 (t, *J* = 8.1 Hz, 1 H), 7.41 (dd, *J* = 8.0, 1.3 Hz, 1 H), 7.19 (dd, *J* = 1.4, 0.9 Hz, 1 H), 7.08 (t, *J* = 1.4 Hz, 1 H). **^{13}C-NMR** (75 MHz, $CDCl_3$): δ = 147.8 (C_q, *C*NO_2), 137.4 (CH), 134.0 (CH), 131.9 (CH), 130.9 (CH), 130.7 (C_q), 126.7 (CH), 120.3 (CH), 114.5 (C_q). **IR (ATR):** $\tilde{\nu}$/cm^{-1} = 3326 (vw), 3152 (vw), 3106 (vw), 3051 (vw), 3017 (vw), 2891 (vw), 2230 (vw), 2216 (vw), 2150 (vw), 2047 (vw), 2028 (vw), 1988 (vw), 1919 (vw), 1688 (w), 1637 (vw), 1591 (m), 1577 (w), 1530 (vs), 1502 (m), 1425 (vw), 1395 (vw), 1362 (m), 1303 (m), 1249 (m), 1200 (vw), 1185 (vw), 1142 (vw), 1110 (m), 1095 (w), 1056 (vs), 981 (m), 933 (vw), 905 (m), 874 (vw), 850 (m), 841 (m), 801 (m), 766 (w), 741 (vs), 696 (m), 656 (vs), 626 (w), 591 (vw), 571 (vw), 558 (vw), 539

[2] The NN-(CH_2)-atoms in α-position of the nitrogen atom of the pyrrolidine group exhibit significantly broadened signals probably due to hindered rotation around the *N*-*N*-axis and/or the ability of fast *E*/*Z*-isomerization of the N–N-double bond (Figure S 22).

(vw), 521 (vw), 492 (vw), 470 (vw), 432 (m), 401 (vw), 381 (vw). **MS (APCI)**, m/z (%): 268.0 (100 %) $[M+H]^+$. **Elemental analysis** calculated (%) for $C_9H_6N_3O_2Br$: C 40.32, H 2.26, N 15.68, found: C 39.99, H 2.40, N 15.44.

1-(2'-Bromo-2-nitro-[1,1'-biphenyl]-3-yl)-1H-imidazole (29)

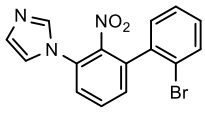

GCA, GWB. A Schlenk flask was charged with a stirring bar, **28** (6.17 g, 23.00 mmol, 1.00 eq.), 2-Bromophenyl boronic acid (5.08 g, 25.30 mmol, 1.10 eq.), $Pd(PPh_3)_4$ (1.33 g, 1.15 mmol, 0.05 eq.) and K_2CO_3 (6.99 g, 50.60 mmol, 2.20 eq.). THF (50 ml) and deoxygenated water (25 ml) were added and the resulting mixture stirred under reflux for 18 h. The mixture was cooled to room temperature and filtered through a plug of Celite®. The plug was extracted with EtOAc (2 x 50 ml) and the combined organic phases washed with brine and dried over $MgSO_4$. After evaporation of all volatiles an orange oil was isolated which may be used without further purification in the next step. Analytically pure samples are obtained by column chromatography (SiO_2, $\mathbf{R_f}$ = 0.26 (SiO_2. *n*-hexane/EtOAc = 2/1). **M.p.** = 147 °C. **^{1}H-NMR** (300 MHz, $CDCl_3$): δ = 7.72 – 7.61 (m, 3 H), 7.48 (d, *J* = 0.5 Hz, 1 H), 7.46 (s, 1 H), 7.38 – 7.24 (m, 3 H), 7.19 – 7.15 (m, 1 H), 7.12 (t, *J* = 1.4 Hz, 1 H). **^{13}C-NMR** (75 MHz, $CDCl_3$): δ = 146.2 (C_q, *C*NO_2), 137.5 (CH), 135.6 (C_q), 135.3 (C_q), 133.2 (CH), 132.1 (CH), 130.9 (CH), 130.8 (CH), 130.6 (CH), 130.5 (CH), 129.4 (C_q), 127.6 (CH), 127.2 (CH), 123.1 (C_q), 120.4 (CH). **IR (ATR):** $\tilde{\nu}$/cm^{-1} = 3147 (vw), 3121 (vw), 3062 (vw), 2219 (vw), 2199 (vw), 2180 (vw), 2148 (vw), 2116 (vw), 2061 (vw), 2026 (vw), 2005 (vw), 1989 (vw), 1908 (vw), 1734 (vw), 1605 (vw), 1577 (vw), 1564 (vw), 1532 (vs), 1510 (w), 1497 (m), 1480 (m), 1444 (vw), 1424 (w), 1373 (w), 1360 (m), 1310 (vw), 1298 (w), 1280 (vw), 1244 (w), 1190 (vw), 1164 (vw), 1144 (vw), 1105 (w), 1088 (vw), 1065 (m), 1036 (m), 1028 (m), 978 (vw), 955 (vw), 930 (vw), 901 (m), 870 (vw), 851 (m), 808 (m), 756 (vs), 746 (vs), 703 (w), 668 (w), 655 (s), 628 (m), 587 (vw), 544 (w), 478 (vw), 453 (m), 422 (vw), 405 (w), 389 (vw). **MS (APCI)**, m/z (%): 344.3 (100 %) $[M+H]^+$, 264.2 (15 %) $[M–Br]^+$. **Elemental analysis** calculated (%) for $C_{15}H_{10}N_3O_2Br$: C 52.35, H 2.93, N 12.21, found: C 52.27, H 2.83, N 12.5.

2'-Bromo-3-(1H-imidazol-1-yl)-[1,1'-biphenyl]-2-amine (30)

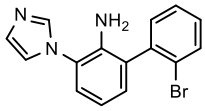

GCB, GWB. A round bottom flask was charged with **29** (7.60 g, 22.08 mmol, 1.00 eq.) and iron powder (6.17 g, 55.85 mmol, 5.00 eq.). EtOH (50 ml) and HOAc (50 ml) were added and the resulting mixture stirred under reflux for 3 h. After cooling to room temperature, the mixture was diluted with water (100 ml) and neutralized with conc. $K_2CO_{3(aq)}$ (ph ~ 8). The aqueous layer was extracted with CH_2Cl_2 (3 x 100 ml) and the combined organic phases washed with brine and dried over $MgSO_4$. After evaporating all volatiles, the crude yellow solid was purified by flash column chromatography (SiO_2, CH_2Cl_2/MeOH 100 % / 0 % → 90 % / 10 %) to obtain 6.59 g (95 %) of a yellow, microcrystalline solid. Yields are comparable when using crude **29** (85 − 93 % over three steps starting from 1-bromo-3-fluoro-2-nitrobenzene **27**).$\mathbf{R_f}$ = 0.29 (SiO_2. CH_2Cl_2/MeOH = 30/1). **M.p.** = 164 °C. **^{1}H-NMR** (300 MHz, $CDCl_3$): δ = 7.64 (dd, *J* = 8.1, 1.2 Hz, 1 H), 7.61 (s, 1 H), 7.34 (td, *J* = 7.4, 1.2 Hz, 1 H), 7.27 (dd, *J* = 7.6, 2.0 Hz, 1 H), 7.20 (td, *J* = 7.5, 2.1 Hz, 1 H), 7.16 (s, 1H), 7.08 (dd, *J* = 7.7, 1.6 Hz, 2 H), 7.03 (dd, *J* = 7.7, 1.5 Hz, 1 H), 6.79 (t, *J* = 7.7 Hz, 1 H), 3.49 (br, 2 H, N*H*$_2$). **^{13}C-NMR** (75 MHz, $CDCl_3$): δ = 139.7 (C_q), 138.8 (C_q), 137.8 (CH), 133.4 (CH), 131.7 (CH), 130.9 (CH), 130.1 (CH), 129.9 (CH), 128.3 (C_q), 128.1 (CH), 126.9 (CH), 124.1 (C_q), 123.5 (C_q), 120.3 (CH), 117.7 (CH). **IR (ATR):** $\tilde{\nu}$/cm^{-1} = 3471 (vw), 3318 (vw), 3195 (vw), 3129 (vw), 3106 (vw), 3052 (vw), 3020 (vw), 2230 (vw), 2205 (vw), 2184 (vw), 2154 (vw), 2044 (vw), 2009 (vw), 1989 (vw), 1960 (vw), 1932 (vw), 1732 (vw), 1689 (vw), 1625 (m), 1590 (w), 1533 (w), 1499 (s), 1469 (w), 1456 (m), 1433 (w), 1420 (w), 1396 (vw), 1364 (vw), 1329 (vw), 1305 (w), 1241 (w), 1219 (w), 1166 (vw), 1136 (vw), 1110 (w), 1061 (s), 1014 (w), 971 (vw), 926 (vw), 908 (w), 852 (vw), 814 (w), 792 (w), 759 (s), 741 (vs), 696 (w), 674 (w), 657 (s), 636 (w), 583 (vw), 556 (vw), 539 (w), 506 (vw), 493 (vw), 444 (w), 429 (w), 411 (vw), 401 (vw), 392 (vw), 383 (vw). **MS (APCI)**, m/z (%): 314.1 (100 %) $[M+H]^+$. **Elemental analysis** calculated (%) for $C_{15}H_{12}N_3Br$: C 57.34, H 3.85, N 13.37, found: C 57.10, H 3.74, N 13.56.

1-(2'-Bromo-2-iodo-[1,1'-biphenyl]-3-yl)-*1H*-imidazole (31)

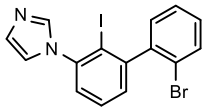

GCB, GWB. In a round bottom flask, thoroughly powdered **30** (5.59 g, 17.79 mmol, 1.00 eq.) was suspended in H_2O (45 ml) and conc. $HCl_{(aq)}$ (45 ml). Under vigorous stirring, a solution of $NaNO_2$ (1.47 g, 21.35 mmol, 1.20 eq.) was added dropwise at 0 °C. The resulting yellow, cloudy solution was stirred for 30 min at 0 °C (diazonium salt solution).

In a second flask, a solution of KI (5.91 g, 35.60 mmol, 2.00 eq.) in water (50 ml) was prepared and cooled to 0 °C. Under vigorous stirring by means of a KPG stirrer, the diazonium salt solution was cannula transferred to the KI solution. Gas evolution occurred and a brownish foam formed. Stirring was continued for 3 h at room temperature. The reaction was neutralized with conc. $K_2CO_{3(aq)}$ (pH ~ 8) and extracted with CH_2Cl_2 (3 x 50 ml). The combined organic extracts were washed with conc. $Na_2S_2O_{3(aq)}$, brine and dried over $MgSO_4$. After evaporating all volatiles, the residue was purified by column chromatography (SiO_2, *n*-hexane/EtOAc = 1/4) to obtain a yellow oil which solidified upon drying in high vacuum for several hours. Analytically pure samples are obtained by flash column chromatography (C18, water/MeCN 90 % / 10 % → 10 % / 90 %); 4.84 g (64 %).

$\mathbf{R_f}$ = 0.27 (SiO_2. *n*-hexane/EtOAc = 1/4), 0.35 (C18. water/MeCN = 3/1). **M.p.** = 146 °C (Z). **^{1}H-NMR** (300 MHz, $CDCl_3$): δ = 7.73 (ddd, *J* = 8.0, 1.3, 0.4 Hz, 1 H), 7.72 (t, *J* = 1.1 Hz, 1 H), 7.55 (dd, *J* = 7.9, 7.5 Hz, 1 H), 7.46 (td, *J* = 7.5, 1.3 Hz, 1 H), 7.41 – 7.28 (m, 3 H), 7.28 (ddd, *J* = 7.5, 1.8, 0.4 Hz, 1 H), 7.26 (t, *J* = 1.1 Hz, 1 H), 7.18 (t, *J* = 1.3 Hz, 1 H). **^{13}C-NMR** (75 MHz, $CDCl_3$): δ = 148.8 (C_q), 144.8 (C_q), 141.0 (C_q), 137.7 (CH), 132.8 (CH), 130.8 (CH), 130.4 (CH), 129.9 (CH), 129.5 (CH), 128.9 (CH), 127.5 (CH), 126.9 (CH), 123.2 (C_q), 120.8 (CH), 102.3 (C_q). **IR (ATR):** $\tilde{\nu}$/cm^{-1} = 3146 (vw), 3098 (vw), 3052 (vw), 2924 (vw), 2851 (vw), 2223 (vw), 2176 (vw), 2143 (vw), 2091 (vw), 2006 (vw), 1971 (vw), 1956 (vw), 1927 (vw), 1899 (vw), 1736 (vw), 1627 (vw), 1589 (vw), 1564 (vw), 1495 (s), 1479 (w), 1448 (w), 1433 (w), 1410 (w), 1360 (vw), 1312 (vw), 1277 (vw), 1240 (w), 1162 (vw), 1135 (vw), 1121 (vw), 1103 (w), 1084 (vw), 1060 (m), 1023 (m), 973 (vw), 944 (vw), 916 (vw), 903 (m), 868 (vw), 852 (vw), 825 (vw), 804 (m), 789 (vw), 756 (vs), 738 (m), 722 (s), 700 (w), 669 (w), 658 (vs), 637 (w), 620 (w), 561 (vw), 540 (vw), 506 (vw), 487 (vw), 465 (vw), 443 (w), 402 (vw), 390 (vw). **MS (APCI)**, m/z (%): 425.5 (100 %) $[M+H]^+$, 299.5 (24 %) $[M–I+2H]^+$. **Elemental analysis** calculated (%) for $C_{15}H_{10}N_2BrI$: C 42.39, H 2.37, N 6.59, found: C 42.73, H 2.34, N 6.47.

2-(5,5-Dimethyl-dibenzo[b,d]stannol-4-yl)pyridine (32)

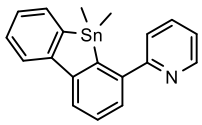

GCA, GWA. In a Schlenk tube, thoroughly powdered **26** (483.09 mg, 1.00 mmol, 1.00 eq.) was dissolved in Et_2O (10 ml) and cooled to –78 °C (*i*-PrOH + $CO_{2(s)}$). 1.7 M *t*-BuLi (256.2 mg, 4.00 mmol, 2.35 ml, 4.00 eq.) in hexanes was added dropwise and the formerly colorless mixture turned intensively yellow. After stirring for 2 h at –78 °C, a solution of Me_2SnCl_2 (241.7 mg, 1.10 mmol, 1.10 eq.) in Et_2O (10 ml) was added dropwise. The cooling bath was removed and the reaction mixture stirred overnight. All volatiles were removed, the residue taken up in toluene and filtered. The filtrate was evaporated in vacuo to obtain crude **32** (ca. 85 % yield) as a beige sticky solid. Since **32** slowly decomposes in the presence of moisture and air, in general, the crude was used without further purification in the next step.

However, the stannole **32** may be purified by rapid column chromatography (SiO_2, *n*-heptane/EtOAc = 15/1) with notable reduction of yields (white solid, 43 %).

$\mathbf{R_f}$ = 0.40 (SiO_2. *n*-Heptan/EtOAc = 15/1). **M.p.** = 127 − 128 °C. **^{1}H-NMR** (300 MHz, C_6D_6): δ = 8.12 – 7.96 (m, 3 H), 7.94 – 7.80 (m, 1 H), 7.76 – 7.61 (m, 1 H), 7.48 (dd, *J* = 8.1, 1.1 Hz, 1 H), 7.44 – 7.30 (m, 3 H), 7.03 (ddd, *J* = 8.0, 7.4, 1.8 Hz, 1 H), 6.54 (ddd, *J* = 7.4, 4.9, 1.0 Hz, 1 H), 0.51 (dd, $J_{119Sn\text{-}1H}$ = 63.4, $J_{117Sn\text{-}1H}$ = 60.6 Hz, 6 H, Sn(CH_3)$_2$). **^{1}H-NMR** (300 MHz, CD_2Cl_2): δ = 8.57 (ddd, *J* = 4.9, 1.8, 1.0 Hz, 1 H)[3], 8.13 – 8.03 (m, 2 H), 8.03 – 7.97 (m, 2 H), 7.85 (ddd, *J* = 8.1, 7.5, 1.8 Hz, 1 H), 7.75 (ddd, *J* = 6.7, 1.6, 0.6 Hz, 1 H), 7.56 (t, *J* = 7.7 Hz, 1 H), 7.37 (td, *J* = 7.5, 1.6 Hz, 1 H), 7.34 – 7.25 (m, 2 H), 0.47 (dd, $J_{119Sn\text{-}1H}$ = 64.3, $J_{117Sn\text{-}1H}$ = 61.4 Hz, 6 H, Sn(CH_3)$_2$). **^{13}C-NMR** (75 MHz, C_6D_6): δ = 155.1 (C_q), 149.4 (C_q), 148.5 (C_q), 147.3 (CH), 147.0 (C_q), 140.7 (C_q), 140.6 (C_q), 137.4 (CH), 136.6 (d, $J_{C\text{-}Sn}$ = 36.6 Hz, CH), 130.5 (d, $J_{C\text{-}Sn}$ = 8.3 Hz, CH), 128.6 (d, $J_{C\text{-}Sn}$ = 7.0 Hz, CH), 128.0 (d, $J_{C\text{-}Sn}$ = 30.2 Hz, CH), 123.6 (CH), 123.3 (d, $J_{C\text{-}Sn}$ = 20.3 Hz, CH), 122.8 (d, $J_{C\text{-}Sn}$ = 15.3 Hz, CH), 122.3 (CH), 119.3 (d, $J_{C\text{-}Sn}$ = 5.4 Hz, CH), –7.1 (d, $J_{119Sn\text{-}13C}$ = 448.5, $J_{117Sn\text{-}13C}$ = 428.5 Hz, Sn(CH_3)$_2$). **^{119}Sn NMR** (112 MHz, C_6D_6): δ = –78.9. **IR (ATR):** $\tilde{\nu}$/cm^{-1} = 3047 (vw), 2982 (vw), 2917 (vw), 1942 (vw), 1804 (vw), 1623 (vw), 1591 (w), 1577 (w), 1561 (w), 1476 (w), 1461 (vw), 1447 (w), 1428 (w), 1390 (vw), 1300 (vw), 1284 (vw), 1260 (vw), 1244 (vw), 1188 (vw), 1155 (vw), 1130 (vw), 1112 (vw), 1100 (vw), 1088 (vw), 1044 (vw), 1015 (vw), 998 (vw), 976 (vw), 940 (vw), 903 (vw), 882 (vw), 866 (vw), 814 (vw), 780 (vw), 753 (vs), 709 (m), 664 (w), 655 (w), 623 (m), 533 (s), 516 (s), 469 (m), 450 (vw), 415 (w), 401 (w). **MS (EI, 70 eV)**, m/z (%): 380.0 (43 %) $[M+H]^+$, 364.0 (100 %) $[M–CH_3]^+$, 349.0 (43 %) $[M−2CH_3]^+$. **Elemental analysis** calculated (%) for $C_{19}H_{17}NSn$: C 60.36, H 4.53, N 3.70, found: C 60.53, H 4.38, N 3.81.

[(C^C^N)Au(III)Cl] (33)

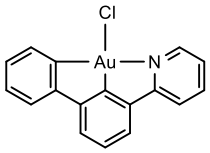

GCB, GWB. $KAuCl_4$ (755.7 mg, 2.00 mmol, 1.00 eq.) was suspended in MeCN (20 ml) and cooled to 0 °C. Under vigorous stirring, a solution of crude **32** (756.1 mg, 2.00 mmol, 1.00 eq.) in MeCN (20 ml) was added dropwise. The resulting mixture was warmed to room temperature on which the mixture turned dark and a colorless solid precipitated. Stirring was continued for 1 h. Then, the mixture was poured into 100 ml Et_2O under vigorous stirring. A voluminous colorless solid precipitated which was filtered off, washed with Et_2O (50 ml), taken up in CH_2Cl_2 and filtered. Solvent was removed under reduced pressure and the beige residue dried in vacuo to obtain 744 mg (81 %) **33**.

Upon evaporation of solutions of **33**, in any case, a mixture of colourless and yellow solid formed. That even happened if separated colorless solid was redissolved and the solvent again evaporated. The yellow solid turned out to be a sparingly soluble form of **33**, which may be analyzed NMR-spectroscopically in DMSO-*d6* at 100 °C.

Analytically pure samples may be obtained by column chromatography (SiO_2, 100 % CH_2Cl_2), however, the insoluble form will be lost reducing overall yields (62 %). Thus, in general crude **33** was used in the next steps without further purification.

33 is stable in solid form to ambient conditions for months, however, it slowly decomposes in solution when exposed to light. Crystals suitable for XRay-diffraction analysis are obtained by layering a concentrated solution of **33** in CH_2Cl_2 with *n*-hexane.

$\mathbf{R_f}$ = 0.69 (SiO_2. 100 % CH_2Cl_2). **M.p.** = 291 °C (Z). **^{1}H-NMR** (400 MHz, 373 K, DMSO-*d6*): δ = 9.00 (ddd, *J* = 5.7, 1.7, 0.9 Hz, 1 H), 8.31 – 8.20 (m, 2 H), 7.79 – 7.72 (m, 2 H), 7.66 (dd, *J* = 7.8, 1.1 Hz, 1 H), 7.47 (m, 2 H), 7.35 (t, *J* = 7.7 Hz, 1 H), 7.22 (td, *J* = 7.5, 1.3 Hz, 1 H), 7.06 (td, *J* = 7.6, 1.6 Hz, 1 H). **^{13}C-NMR** (101 MHz, 373 K, DMSO-*d6*): δ = 165.4 (C_q), 162.5 (C_q), 153.9 (C_q), 149.9 (C_q), 149.1 (C_q), 148.3 (CH), 142.4 (CH), 139.9 (C_q), 134.0 (CH), 128.7 (CH), 128.2 (CH), 127.8 (CH), 125.6 (CH), 123.6 (CH), 123.1 (CH), 122.7 (CH), 121.3 (CH). **IR (ATR):** $\tilde{\nu}$/cm^{-1} = 3054 (vw), 2958 (vw), 2921 (vw), 2851 (vw), 2207 (vw), 2188 (vw), 2136 (vw), 2052 (vw), 2013 (vw), 1995 (vw), 1921 (vw), 1636 (vw), 1606 (w), 1588 (w), 1557 (vw), 1489 (w), 1465 (w), 1432 (w), 1400 (w), 1318 (vw), 1287 (vw), 1259 (vw), 1242 (vw), 1157 (vw), 1134 (vw), 1118 (vw), 1090 (vw), 1044 (vw), 1014 (w), 945 (vw), 880 (vw), 802 (vw), 775 (vw), 749 (vs), 738 (vs), 661 (vw), 647 (w), 620 (w), 553 (vw), 535 (vw), 516 (vw), 495 (vw), 480 (w), 453 (vw), 427 (w), 408 (vw), 396 (vw), 387 (w). **MS (EI, 70 eV)**, m/z (%): 461.0 (14 %) $[M]^+$, 426.1 (100 %) $[M–Cl]^+$, 229.1 (81 %) $[M–Cl–Au]^+$. **Elemental analysis** calculated (%) for $C_{17}H_{11}NAuCl$: C 44.23, H 2.40, N 3.03, found (colourless form): C 44.03, H 2.336, N 3.07, found (yellow form): C 44.33, H 2.35, N 3.07.

[(C^C^N)Au(III)CCPh] (34)

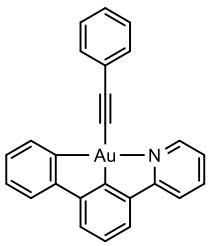

GCA, GWB. In a Schlenk tube, phenylacetylene (53 mg, 57 µl, 0.52 mmol, 1.20 eq.) was dissolved in Et_2O (10 ml). 1.6 M *n*-BuLi in *n*-hexane (30 mg, 0.473 mmol, 296 µl, 1.10 eq.) was added dropwise. After stirring for 5 min, the solution of lithium phenylacetylide was added to a stirred suspension of **33** (200 mg, 0.427 mmol, 1.00 eq.) in toluene (10 ml). The solid disappeared and the solution turned clear. After stirring for 1 h the volume was reduced (~ 2 ml) and *n*-pentane (20 ml) was added. A colorless solid formed which was filtered off and purified by flash chromatography (SiO_2, *n*-hexane/EtOAc 100 % / 0 % → 0 % / 100 %) to obtain 196 mg (86 %) of a white solid.

$\mathbf{R_f}$ = 0.17 (SiO_2. *n*-hexane/EtOAc = 1/1). **M.p.** = 224 °C (Z). **^{1}H-NMR** (300 MHz, CD_2Cl_2): δ = 9.19 (ddd, *J* = 5.4, 1.7, 0.8 Hz, 1 H), 8.01 (ddd, *J* = 8.1, 7.6, 1.8 Hz, 1 H), 7.98 (ddd, *J* = 7.6, 1.3, 0.4 Hz, 1 H), 7.83 (ddd, *J* = 8.2, 1.3, 0.8 Hz,

[3] In CD_2Cl_2, the signal of the proton in α-position to pyridine-N is significantly shifted to lower fields (δ = 8.57 ppm) compared to C_6D_6 (δ = 6.54 ppm). This may be due to coordination of the pyridine ring to the central Sn atom in the less polar solvent benzene generating a pentacoordinate tin center.

1 H), 7.59 – 7.52 (m, 2 H), 7.49 – 7.39 (m, 2 H), 7.41 – 7.20 (m, 6 H), 7.20 (td, *J* = 7.5, 1.3 Hz, 1 H), 7.03 (td, *J* = 7.5, 1.6 Hz, 1 H). **^{13}C-NMR** (75 MHz, CD_2Cl_2): δ = 175.6 (C_q), 167.1 (C_q), 156.9 (C_q), 152.0 (C_q), 151.8 (CH), 147.9 (C_q), 143.3 (C_q), 141.4 (CH), 137.8 (CH), 132.1 (2 CH), 130.0 (C_q), 128.7 (2 CH), 128.5 (CH), 128.2 (CH), 128.2 (CH), 127.3 (C_q), 127.0 (CH), 125.1 (CH), 123.2 (CH), 122.6 (CH), 122.6 (CH), 120.9 (CH), 106.7 (C_q). **IR (ATR):** $\tilde{\nu}$/cm^{-1} = 3051 (vw), 2125 (vw), 2022 (vw), 2003 (vw), 1953 (vw), 1916 (vw), 1606 (w), 1595 (w), 1581 (vw), 1569 (vw), 1556 (vw), 1486 (m), 1464 (w), 1431 (w), 1398 (w), 1312 (vw), 1286 (vw), 1265 (vw), 1242 (vw), 1212 (vw), 1174 (vw), 1160 (vw), 1117 (vw), 1101 (vw), 1088 (vw), 1068 (vw), 1044 (vw), 1017 (w), 1004 (vw), 967 (vw), 941 (vw), 912 (vw), 894 (vw), 874 (vw), 850 (vw), 814 (vw), 796 (w), 762 (m), 749 (vs), 734 (s), 692 (m), 649 (w), 621 (w), 553 (vw), 531 (w), 511 (vw), 483 (w), 466 (vw), 454 (vw), 431 (w), 410 (vw), 382 (vw). **UV/Vis** (CH_2Cl_2): λ_{max}/nm (ε/[dm^{3}mol^{-1}cm^{-1}]) = 298 (15200), 312 (13400), 327 (12500), 376 (1500). **Luminescence** (CH_2Cl_2): λ_{ex} = 365 nm, λ_{em} = 473 nm. **MS (EI, 70 eV)**, m/z (%): 527.1 (30 %) [M]$^+$, 426.1 (19 %) [M–CCPh]$^+$. **Elemental analysis** calculated (%)for $C_{25}H_{16}NAu$: C 56.94, H 3.06, N 2.66, found: C 56.88, H 3.20, N 2.69.

[(C^C^N)Au(III)C_6F_5] (35)

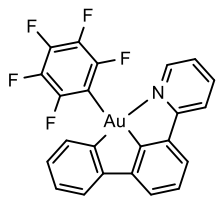

GCA, GWB. In a Schlenk tube, **33** (200 mg, 0.43 mmol, 1.00 eq.) was dissolved in CH_2Cl_2 (10 ml). Under vigorous stirring, a solution of [(MeCN)AgC_6F_5][30] (151 mg, 0.48 mmol, 1.10 Eq.) in CH_2Cl_2 (10 ml) was added upon which the formerly clear solution turned cloudy. The mixture was stirred overnight in the dark. Water (20 ml) was added and the organic phase separated. The aqueous phase was extracted with CH_2Cl_2 (2 x 20 ml) and the combined organic phases washed with brine and dried over $MgSO_4$. After evaporation of all volatiles, the residue was purified by flash column chromatography (SiO_2, *n*-hexane/EtOAc 100 % / 0 % → 0 % / 100 %) to obtain 221 mg (87 %) of a yellowish, microcrystalline solid. Crystals suitable for X-ray diffraction analysis were obtained by vapor diffusion of *n*-pentane into a concentrated solution in toluene.

M.p. = 231 − 233 °C. **^{1}H-NMR** (300 MHz, CD_2Cl_2): δ = 8.27 (d, *J* = 4.8 Hz, 1 H), 8.02 (ddd, *J* = 8.0, 7.6, 1.7 Hz, 1 H), 7.89 (dt, *J* = 8.1, 1.2 Hz, 1 H), 7.47 (dd, *J* = 7.7, 0.9 Hz, 1 H), 7.46 – 7.31 (m, 3 H), 7.36 – 7.24 (m, 1 H), 7.18 (td, *J* = 7.5, 1.3 Hz, 1 H), 7.01 (d, *J* = 6.9 Hz, 1 H), 6.90 (td, *J* = 7.5, 1.5 Hz, 1 H). **^{13}C-NMR** (126 MHz, CD_2Cl_2): δ = 176.6 (dt, J_{C-F} = 8.2, 2.5 Hz, C_q, (C^C^N)), 167.4 (C_q), 156.8 (C_q), 151.4 (C_q), 151.2 (CH), 148.6 – 146.4 (m, 2 CF), 147.2 (C_q), 142.7 (C_q), 141.7 (CH), 140.8 – 137.8 (m, CF), 138.7 (ddd, J_{C-F} = 253.0, 30.4, 12.8 Hz, 2 CF), 136.6 (CH), 136.5 (dd, J_{C-F} = 117.3, 2.0 Hz, C_q, C_5F_5CAu), 128.6 (CH), 128.5 (CH), 128.4 (CH), 125.2 (CH), 123.5 (CH), 122.9 (CH), 122.7 (CH), 121.3 (CH). **^{19}F-NMR** (282 MHz, CD_2Cl_2): δ = −114.65 – −122.99 (m, 2 F), −159.20 (t, *J* = 19.5 Hz, 1 F), −160.98 – −165.53 (m, 2 F). **IR (ATR):** $\tilde{\nu}$/cm^{-1} = 3031 (vw), 2055 (vw), 2014 (vw), 1990 (vw), 1950 (vw), 1634 (vw), 1606 (w), 1584 (vw), 1557 (vw), 1503 (m), 1488 (w), 1464 (vw), 1448 (s), 1434 (s), 1401 (vw), 1353 (vw), 1316 (vw), 1292 (vw), 1256 (w), 1177 (vw), 1160 (vw), 1118 (vw), 1100 (vw), 1089 (vw), 1058 (m), 1047 (m), 1015 (w), 950 (vs), 899 (vw), 885 (vw), 858 (vw), 807 (vw), 775 (m), 752 (vs), 740 (s), 670 (vw), 647 (w), 622 (w), 609 (vw), 537 (vw), 481 (w), 467 (vw), 452 (vw), 431 (vw), 408 (vw), 388 (vw). **UV/Vis** (CH_2Cl_2): λ_{max}/nm (ε/[dm^{3}mol^{-1}cm^{-1}]) = 278 (12700), 285 (11600), 295 (8700), 314 (10000), 326 (12900), 370 (1200). **Luminescence** (CH_2Cl_2): λ_{ex} = 360 nm, λ_{em} = 475 nm. **MS (APCI)**, m/z (%): 593.6 (100 %) [M+H]$^+$, 425.6 (100 %) [M–C_6F_5]$^+$. **Elemental analysis** calculated (%)for $C_{23}H_{11}NAuF_5$: C 46.56, H 1.87, N 2.36, found: C 46.12, H 1.83, N 2.55.

1-(5,5-Dimethyl-dibenzo[b,d]stannol-4-yl)-imidazole (36)

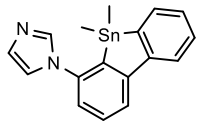

GCA, GWB. In a Schlenk tube **31** (425 mg, 1.00 mmol, 1.00 eq.) was dissolved in Et_2O (10 ml) and cooled to –78 °C. Under stirring 1.7 M *t*-BuLi (263 mg, 4.10 mmol, 2.41 ml, 4.10 eq.) in *n*-pentane was added over the course of 15 min by means of a syringe pump and the resulting yellow mixture stirred for 2 h at –78 °C. Then a solution of Me_2SnCl_2 in Et_2O (10 ml) was added dropwise. Immediately a white preticipate formed. The mixture was stirred for 1 h at –78 °C and then warmed to room temperature. Water (20 ml) was added and the organic phase separated. The aqueous phase was extracted with EtOAc (2 x 20 ml) and the combined organic phases washed with water, brine and dried over $MgSO_4$. All volatiles were removed and the resulting brownish oil treated with Et_2O several times, until a beige solid remained (ca. 380 mg). Unfortunately, we were not able to isolate pure samples of **36** by crystallization. In addition, **36** rapidly decomposes during chromatography (SiO_2, Al_2O_3, C18). Thus, the crude stannole was used without further purification. **36** slowly decomposed in the presence of moisture and air, thus it was stored under an inert atmosphere at –30 °C. A small amount of the corresponding methyl-*t*-butyl-

^{1}H-NMR (300 MHz, CD_2Cl_2): δ = 8.06 (t, *J* = 1.2 Hz, 1 H), 8.01 (ddt, *J* = 10.5, 7.7, 0.7 Hz, 2 H), 7.67 (ddd, *J* = 7.0, 1.5, 0.6 Hz, 1 H), 7.54 (t, *J* = 7.8 Hz, 1 H), 7.44 (ddd, *J* = 7.9, 7.4, 1.5 Hz, 1 H), 7.39 (t, *J* = 1.2 Hz, 1 H), 7.33 (ddd, *J* = 11.3, 7.4, 1.0 Hz, 2 H), 7.26 (t, *J* = 1.4 Hz, 1 H), 0.46 (dd, $J_{119Sn-1H}$ = 61.7, $J_{117Sn-1H}$ = 59.0 Hz, 6 H, *Sn*(CH_3)$_2$). **^{119}Sn NMR** (112 MHz, CD_2Cl_2): δ = –19.0. **MS (APCI)**, m/z (%): 368.8 (100 %) [M+H]$^+$, 410.8 (23 %) [M–CH_3+*t*-Bu+H]$^+$.

1-(5,5-Dimethyl-5H-dibenzo[b,d]stannol-4-yl)-3-methyl-1H-imidazol-3-ium trifluoromethanesulfonate (37)

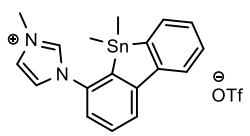

GCA, GWA. In a Schlenk tube crude **36** (380 mg, ca. 1.00 mmol, 1.00 eq.) was dissolved in CH_2Cl_2 (10 ml). MeOTf (180 mg, 1.10 mmol, 124 µl) was added and the resulting mixture stirred for 2 h. All volatiles were removed in vacuo and the resulting foam (~ 540 mg) stored under an inert atmosphere at –30 °C. **36** decomposes in solution during a couple of days. We were not able to obtain pure samples neither by crystallization nor chromatography due to stability reasons. **36** was directly used in the next step.

MS (ESI), m/z (%): 383.4 (100 %) [M]$^+$, 149.2 [OTf]$^-$.

[(C^C^C')AuCl] (38)

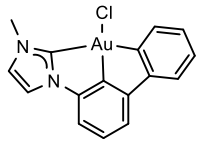

GCA, GWA. A Schlenk tube was charged with $KAuCl_4$ (378 mg, 1.00 mmol, 1.00 eq.) and K_2CO_3 (276 mg, 2.00 mmol, 2.00 eq.). The solids were dried for 30 min at 200 °C in high vacuum and then suspended in MeCN (10 ml). A solution of crude **37** (ca. 1 mmol) in MeCN (10 ml) was added dropwise under vigorous stirring on which the mixture turned dark. Stirring was continued for 2 h. After filtration, the filtrate was reduced in volume to approximately 5 ml and Et_2O (20 ml) was added. Upon shaking a voluminous white solid formed which settled upon standing. The supernatant solution was taken off and the residue washed with Et_2O (2 x 10 ml). After drying in vacuo, the crude brown solid (ca. 600 mg, contained various tin species as indicated by mass spectrometry) was directly used in the

next step. **38** is very sensitive against moisture and light. Attempts to crystallize samples failed due to decomposition in solution after two days.

MS (APCI), m/z (%): 465,3 (8 %) $[M+H]^+$; 429,3 (100 %) $[M-Cl]^+$.

[(C^C^C')]AuCCPh (39)

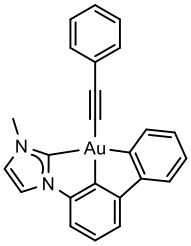

GCA, GWB. In a Schlenk tube, phenylacetylene (52.8 mg, 57 ml, 0.516 mmol, 1.20 eq.) in Et_2O (10 ml) was treated with 1.6 M *n*-BuLi in *n*-hexane (30 mg, 0.473 mmol, 296 µl, 1.10 eq.). After stirring for 5 min, the so obtained solution was added dropwise to a suspension of crude **38** (199 mg, 0.427 mmol, 1.00 eq.)[4] in toluene (10 ml). The mixture turned clear and stirring was continued for 3 h. Volatiles were removed and the brownish residue purified by flash column chromatography (SiO_2, *n*-hexane/EtOAc 50 % / 50 % → 0 % / 100 %) to obtain 97 mg colorless solid (43 % over four steps starting from **31**). Crystals suitable for X-Ray analysis were obtained by vapor diffusion of *n*-pentane into a concentrated solution in toluene.

$\mathbf{R_f}$ = 0.30 (SiO_2. *n*-hexane/EtOAc = 5/4). **M.p.** = 222 °C (Z). **^{1}H-NMR** (300 MHz, CD_2Cl_2): δ = 8.02 (dd, J = 7.0, 1.7 Hz, 1 H), 7.45 – 7.37 (m, 2 H), 7.31 (dd, J = 7.2, 1.7 Hz, 1 H), 7.28 – 6.99 (m, 8 H), 6.89 (d, J = 2.0 Hz, 1 H), 6.81 (dd, J = 7.5, 1.1 Hz, 1 H), 4.14 (s, 3 H, *C*H$_3$). **^{13}C-NMR** (75 MHz, CD_2Cl_2): δ = 180.6 (C_q, $C_{(Carben)}$), 157.8 (C_q), 157.1 (C_q), 155.8 (C_q), 155.0 (C_q), 144.1 (C_q), 137.9 (CH), 131.9 (2 CH), 128.7 (2 CH), 128.4 (2 CH), 127.9 (C_q), 127.4 (CH), 126.8 (CH), 122.6 (CH, $CH_{(NHC)}$), 122.2 (CH, $CH_{(NHC)}$), 119.3 (CH), 118.5 (C_q), 117.2 (CH), 110.4 (CH), 110.2 (C_q), 39.0 (CH_3). **IR (ATR)**: $\tilde{\nu}$/cm^{-1} = 3171 (vw), 3148 (vw), 3039 (vw), 2945 (vw), 2188 (vw), 2124 (vw), 1899 (vw), 1595 (w), 1575 (vw), 1557 (vw), 1525 (vw), 1480 (m), 1428 (m), 1352 (vw), 1307 (w), 1283 (vw), 1264 (vw), 1251 (vw), 1240 (vw), 1211 (vw), 1172 (vw), 1148 (vw), 1134 (vw), 1111 (vw), 1085 (vw), 1067 (vw), 1020 (vw), 983 (vw), 967 (vw), 944 (vw), 913 (vw), 874 (vw), 814 (vw), 794 (w), 762 (s), 750 (vs), 714 (vs), 691 (s), 668 (m), 633 (vw), 614 (w), 595 (vw), 565 (vw), 554 (vw), 529 (w), 509 (vw), 495 (vw), 480 (w), 432 (vw), 398 (vw). **UV/Vis** (CH_2Cl_2): λ_{max}/nm (ε/[dm^{3}mol^{-1}cm^{-1}]) = 284 (15100), 303 (11300), 314 (10200). **Luminescence** (CH_2Cl_2): λ_{ex} = 311 nm, λ_{em} = 471 nm. **MS (APCI)**, m/z (%): 531.3 (70 %) $[M+H]^+$, 429.2 (19 %) $[M-CCPh]^+$. **Elemental analysis** calculated (%) for $C_{24}H_{17}N_2Au$: C 54.35, H 3.23, N 5.28, found: C 53.72, H 3.21, N 5.48.

[(C^C^C')AuC$_6$F$_5$] (40)

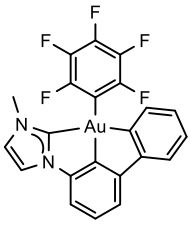

GCA, GWB. Crude **38** (200 mg, 0.43 mmol, 1.00 eq.)[4] was dissolved in CH_2Cl_2 (10 ml). Under vigorous stirring a solution of $(MeCN)AgC_6F_5$[30] (229 mg, 0.65 mmol, 1.50 Eq.) in CH_2Cl_2 (10 ml) was added upon which the formerly clear solution turned cloudy. The mixture was stirred overnight in the dark. Water (20 ml) was added and the resulting mixture stirred for 1 h and then filtered. The organic phase was separated and the aqueous phase extracted with CH_2Cl_2 (2 x 20 ml). The combined organic phases were washed with brine and dried over $MgSO_4$. After evaporation of all volatiles, the residue was purified by flash column chromatography (SiO_2, *n*-hexane/CH_2Cl_2 100 % / 0 % → 0 % / 100 %) to obtain 125 mg (49 % over four steps starting from **31**) of a white, microcrystalline solid. Crystals suitable for X-ray diffraction analysis were obtained by vapor diffusion of *n*-pentane into a concentrated solution in toluene.

$\mathbf{R_f}$ = 0.42 (SiO_2. *n*-hexane/CH_2Cl_2 = 2/1). **M.p.** = 288 °C (Z). **^{1}H-NMR** (300 MHz, CD_2Cl_2): δ = 7.48 (d, *J* = 2.0 Hz, 1 H), 7.46 (ddd, *J* = 7.6, 1.4, 0.5 Hz, 1 H), 7.32 (dd, *J* = 7.7, 1.3 Hz, 1 H), 7.27 (t, *J* = 7.6 Hz, 1 H), 7.17 (ddd, *J* = 7.6, 7.0, 1.8 Hz, 1 H), 7.08 – 7.04 (m, 2 H), 7.07 – 6.98 (m, 1 H), 6.97 (td, *J* = 7.2, 1.4 Hz, 1 H), 3.56 (s, 3 H, C*H*$_3$). **^{13}C-NMR** (101 MHz, CD_2Cl_2): δ = 181.2 (C_q, $C_{(Carben)}$), 157.1 (2 C_q), 155.2 (C_q), 154.6 (C_q), 143.5 (C_q), 136.9 (CH), 128.9 (CH), 128.5 (CH), 127.7 (CH), 123.0 (CH, $CH_{(NHC)}$), 122.6 (CH, $CH_{(NHC)}$), 119.7 (CH), 117.5 (CH), 110.6 (CH), 38.5 (CH_3).[5] **^{19}F-NMR** (282 MHz, CD_2Cl_2): δ = −118.28 – −118.56 (m, 2 F), −160.33 (t, *J* = 19.5 Hz, 1 F), −162.18 – −162.85 (m. 2 F). **IR (ATR):** $\tilde{\nu}$/cm^{-1} = 3172 (vw), 3143 (vw), 3042 (vw), 2959 (vw), 2924 (vw), 2852 (vw), 2190 (vw), 2154 (vw), 2027 (vw), 1970 (vw), 1738 (vw), 1631 (vw), 1601 (vw), 1567 (vw), 1501 (s), 1452 (vs), 1435 (s), 1354 (w), 1307 (vw), 1289 (vw), 1258 (w), 1240 (w), 1177 (vw), 1161 (vw), 1112 (vw), 1057 (m), 1047 (s), 1022 (w), 950 (vs), 887 (vw), 872 (vw), 832 (vw), 784 (m), 756 (vs), 734 (s), 686 (vw), 673 (vw), 658 (vw), 632 (vw), 619 (vw), 595 (vw), 562 (vw), 524 (vw), 496 (vw), 478 (vw), 456 (vw), 446 (vw), 428 (vw), 397 (w). **UV/Vis** (CH_2Cl_2): λ_{max}/nm (ε/[dm^{3}mol^{-1}cm^{-1}]) = 302 (5800), 314 (5400), 336 (600). **Luminescence** (CH_2Cl_2): λ_{ex} = 314 nm, λ_{em} = 470 nm. **MS (APCI)**, m/z (%): 596.2 (100 %) $[M]^+$, 430.5 (38 %) $[M-C_6F_5+H]^+$. **Elemental analysis** calculated (%) for $C_{22}H_{12}N_2AuF_5$: C 44.31, H 2.03, N 4.70, found: C 44.33, H 2.15, N 4.30.

2-(3-Bromo-2-chlorophenyl)pyridine (s2)

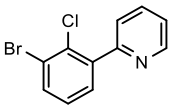

GCA, GWB. A Schlenk tube was charged with a magnetic stirring bar, 1,3-dibromo-2-chlorobenzene (1622 mg, 6.00 mmol, 1.50 eq.), LiCl (678 mg, 16.00 mmol, 4.00 eq.) and $Pd(PPh_3)_4$ (92 mg, 0.08 mmol, 0.02 eq.). Toluene (20 ml) and 2-(tributylstannyl)pyridine (1473 mg, 4.00 mmol, 1.29 ml, 1.00 eq.) were added. The tube was screw-sealed, and the light-yellow mixture heated to 115 °C under continuous stirring in an oil-bath. The reaction progress was monitored via TLC. After 15 h, all 2-(tributylstannyl)pyridine was consumed. After cooling the mixture to room temperature, 20 ml of a 7 M aqueous solution of KF were added and stirring continued for 30 min. The greyish suspension was filtered over a plug of Celite®, and the plug extracted with CH_2Cl_2 (3 x 20 ml). The combined organic phases were washed with brine and dried over $MgSO_4$. After evaporating all volatiles, the crude yellow oil was purified by column chromatography (SiO_2, cyclohexane/EtOAc/TEA = 100/10/1) to give 956 mg (90 %) of a colourless solid.

$\mathbf{R_f}$ = 0.21 (SiO_2, cyclohexane/EtOAc/TEA = 100/10/1). **M.p.** = 79 °C. **^{1}H-NMR** (300 MHz, CD_2Cl_2): δ = 8.71 (ddd, *J* = 4.8, 1.8, 1.0 Hz, 1 H), 7.81 (td, *J* = 7.7, 1.8 Hz, 1 H), 7.73 (dd, *J* = 8.0, 1.6 Hz, 1 H), 7.60 (dt, *J* = 7.9, 1.1 Hz, 1 H), 7.51 (dd, *J* = 7.7, 1.6 Hz, 1 H), 7.34 (ddd, *J* = 7.9, 4.9, 1.2 Hz, 1 H), 7.28 (t, *J* = 7.8 Hz, 1 H). **^{13}C-NMR** (75 MHz, CD_2Cl_2): δ = 157.5 (C_q), 150.1 (CH), 142.3 (C_q), 136.5 (CH), 134.2 (CH), 131.0 (CH), 128.3

[4] Amount of substance and equivalents are given assuming the weighed-in mass corresponds to a pure sample; however, the real content of **39** inside the crude mixture could not be detected.

[5] The resonances of the carbon atoms of the C_6F_5-group could not be detected, probably because of weak signal intensities due to coupling with ^{19}F; please compare the spectrum of $[(C^C^N)AuC_6F_5]$ (**35**).

(CH), 125.2 (CH), 124.3 (C_q), 123.3 (CH), 78.1 (C_q). **IR (ATR):** $\tilde{\nu}$/cm^{-1} = 3046 (vw), 2154 (vw), 2125 (vw), 2029 (vw), 1977 (vw), 1590 (vw), 1567 (vw), 1551 (vw), 1473 (vw), 1449 (vw), 1431 (w), 1401 (w), 1300 (vw), 1288 (vw), 1189 (vw), 1148 (vw), 1118 (vw), 1046 (vw), 1029 (vw), 992 (vw), 963 (vw), 892 (vw), 802 (vw), 789 (w), 767 (vs), 747 (w), 726 (vw), 711 (w), 654 (w), 620 (vw), 570 (vw), 549 (vw), 502 (vw), 474 (vw), 460 (vw), 433 (vw), 422 (vw), 413 (vw), 402 (w). **MS (EI, 70 eV)**, m/z (%): 268.9 (58 %) $[M]^+$, 232.0 (100 %) $[M–Cl]^+$, 153.0 (59 %) $[M–Cl–Br]^+$. **Elemental analysis** calculated (%) for $C_{11}H_7BrClN$: C 49.20, H 2.63, N 5.22, found: C 48.92, H 2.62, N 5.14.

2-(2,2'-Dichloro-[1,1'-biphenyl]-3-yl)pyridine (s3)

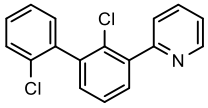

GCA, GWB. A Schlenk tube was charged with a magnetic stirring bar, 2-(3-brom-2-chlorophenyl)pyridine (**s2**) (537 mg, 2.00 mmol, 1.00 eq.), 2-chlorophenylboronic acid (469 mg, 3.00 mmol, 1.50 eq.), K_3PO_4 (849 mg, 4.00 mmol, 2.00 eq.) and XPhos Pd G3[2] (51 mg, 0.06 mmol, 0.03 eq.). THF (8 ml) and deoxygenated water (8 ml) were added. The tube was screw-sealed, and the yellow mixture heated to 70 °C under continuous stirring in an oil-bath. After 18 h the mixture was cooled to room temperature and diluted with water (40 ml) and Et_2O (40 ml). The aqueous phase was extracted with Et_2O (3 x 30 ml) and the combined organic phases washed with brine and dried over $MgSO_4$. After removal of all volatiles in vacuo the residue was purified by column chromatography (SiO_2, cyclohexane/EtOAc = 10/1, then 5/1) yielding a colourless oil (552 mg, 92 %), which solidifies after a couple of weeks.

$\mathbf{R_f}$ = 0.43 (SiO_2. cyclohexane/EtOAc = 5/1). **M.p.** = 35 °C. **^{1}H-NMR** (300 MHz, CD_2Cl_2): δ = 8.73 (ddd, *J* = 4.9, 1.8, 1.0 Hz, 1 H), 7.81 (ddd, *J* = 7.9, 7.5, 1.8 Hz, 1 H), 7.68 (dt, *J* = 7.9, 1.1 Hz, 1 H), 7.62 (dd, *J* = 7.6, 1.8 Hz, 1 H), 7.58 – 7.46 (m, 1 H), 7.47 (t, *J* = 7.6 Hz, 1 H), 7.44 – 7.28 (m, 5 H). **^{13}C-NMR** (75 MHz, CD_2Cl_2): δ = 157.17 (C_q), 149.45 (CH), 140.18 (C_q), 139.32 (C_q), 138.72 (C_q), 135.75 (CH), 133.40 (C_q), 131.35 (C_q), 131.24 (CH), 131.14 (CH), 131.01 (CH), 129.32 (2 CH), 126.67 (CH), 126.49 (CH), 124.89 (CH), 122.43 (CH). **IR (ATR):** $\tilde{\nu}$/cm^{-1} = 3056 (vw), 1586 (w), 1565 (w), 1474 (w), 1452 (w), 1432 (m), 1400 (m), 1314 (vw), 1287 (vw), 1253 (vw), 1161 (vw), 1115 (vw), 1093 (vw), 1069 (w), 1043 (w), 1029 (w), 1016 (w), 992 (w), 974 (vw), 948 (vw), 895 (vw), 808 (w), 775 (s), 759 (vs), 747 (s), 733 (s), 695 (s), 663 (w), 634 (vw), 622 (w), 610 (m), 572 (vw), 540 (w), 513 (vw), 468 (m), 441 (w), 403 (w). **MS (EI, 70 eV)**, m/z (%): 299.0 (54 %) $[M]^+$, 264.1 (93 %) $[M–Cl]^+$. **Elemental analysis** calculated (%) for $C_{17}H_{11}Cl_2N$: C 68.02, H 3.69, N 4.67, found: C 68.08, H 3.28, N 4.77.

2-Iodo-6-(pyridin-2-yl)aniline (s6)

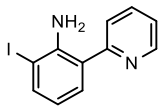

GCA, GWB. **19** (2.51 g, 7.70 mmol, 1.00 eq.) and $SnCl_2{\cdot}2H_2O$ (8.69 g, 38.50 mmol, 5.00 eq.) were dissolved in dry and deoxygenated EtOH (40 ml). The resulting mixture was heated to 70 °C under stirring for 30 min upon which a grey slurry formed. After cooling to room temperature, the mixture was neutralized with conc. aqueous $NaHCO_3$ (pH ~ 8). The slurry was extracted with EtOAc (3 x 50 ml) and the combined organic phases washed with brine and dried over $MgSO_4$. After evaporating all volatiles, the crude was purified by column chromatography (SiO_2, *n*-heptane/EtOAc = 4/1) to obtain a yellowish oil (1.65 g, 72 %).

$\mathbf{R_f}$ = 0.29 (SiO_2. *n*-heptane/EtOAc = 4/1). **^{1}H-NMR** (300 MHz, $CDCl_3$): δ = 8.61 (ddd, *J* = 4.9, 1.9, 1.0 Hz, 1 H), 7.77 (ddd, *J* = 8.2, 7.5, 1.9 Hz, 1 H), 7.70 (dd, *J* = 7.8, 1.5 Hz, 1 H), 7.63 (dt, *J* = 8.1, 1.1 Hz, 1 H), 7.47 (dd, *J* = 7.8, 1.4 Hz, 1 H), 7.22 (ddd, *J* = 7.5, 4.9, 1.2 Hz, 1 H), 6.52 (t, *J* = 7.8 Hz, 1 H), 6.08 (br, 2 H, N*H*$_2$). **^{13}C-NMR** (75 MHz, $CDCl_3$): δ = 158.8 (C_q), 147.8 (CH), 146.3 (C_q), 140.1 (CH), 137.3 (CH), 129.9 (CH), 122.7 (CH), 122.6 (C_q), 121.7 (CH), 118.8 (CH), 87.5 (C_q). **IR (ATR):** $\tilde{\nu}$/cm^{-1} = 3434 (w), 3286 (vw), 3053 (vw), 3007 (vw), 2923 (vw), 2852 (vw), 1852 (vw), 1678 (vw), 1586 (vs), 1569 (vs), 1539 (m), 1474 (s), 1454 (m), 1443 (s), 1417 (vs), 1316 (vw), 1286 (w), 1263 (w), 1234 (m), 1152 (w), 1095 (w), 1066 (w), 1053 (s), 1026 (w), 991 (w), 951 (vw), 907 (vw), 885 (vw), 835 (vw), 796 (m), 752 (vs), 727 (s), 648 (s), 630 (m), 559 (m), 523 (w), 451 (vw), 404 (w). **HR-MS (FAB)**, m/z, calculated for $C_{11}H_9N_2I$: 295.9811 $[M]^+$, found: 295.9810. **Elemental analysis** could not be done for oils.

2-(3-Bromo-2-nitrophenyl)pyridine (s8)

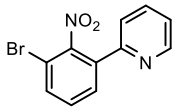

GCB, GWB. **18** (2.36 g, 10.94 mmol, 1.00 eq.) was dissolved in MeCN (20 ml) and conc. HBr_{aq} (4.4 ml) and cooled to –20 °C. $NaNO_2$ (906 mg, 13.13 mmol, 1.20 eq.) in water (6 ml) was added dropwise into the vigorously stirred solution. The mixture was stirred for 30 min at –20 °C and was then added dropwise to a solution of CuBr (2.37 g, 16.52 mmol, 1.50 eq.) in MeCN (20 ml) at –20 °C. The resulting mixture was warmed to room temperature and stirred overnight. The reaction was neutralized with 1 M $NaOH_{(aq)}$ The aqueous layer was extracted with EtOAc (3 x 50 ml) and the combined organic layers washed with aqueous NH_3, water and brine. After drying over $MgSO_4$ all volatiles were removed. The resulting crude solid was directly used in the next step.

^{1}H-NMR (300 MHz, $CDCl_3$): δ = 8.63 (d, *J* = 4.7 Hz, 1 H), 7.77 (td, *J* = 7.7, 1.5 Hz, 1 H), 7.70 (dd, *J* = 8.0, 1.0 Hz, 1 H), 7.63 (dd, *J* = 7.8, 1.2 Hz, 1 H), 7.51 (d, *J* = 7.8 Hz, 1 H), 7.43 (t, *J* = 7.9 Hz, 1 H), 7.30 (ddd, *J* = 7.7, 4.7, 0.9 Hz, 1 H).

2-Bromo-6-(pyridin-2-yl)aniline (s9)

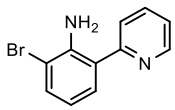

GCA, GWB. Crude **s8** (3.05 g, 10.94 mmol, 1.00 eq.) and $SnCl_2{\cdot}2H_2O$ (12.34 g, 54.70 mmol, 5.00 eq.) were dissolved in dry EtOH and stirred at 70 °C for 60 min. After cooling to room temperature, the mixture was neutralized with conc. aqueous $NaHCO_3$ (pH ~ 8) and diluted with EtOAc. The mixture was filtered through a plug of Celite® and the residue extracted with EtOAc (3 x 50 ml). The aqueous layer was separated, and the combined organic layers washed with brine and dried over $MgSO_4$. After evaporating all volatiles, the residue was purified by column chromatography (SiO_2, *n*-heptane/EtOAc = 10/1) to obtain 1.36 g (50 % over two steps starting from **s11**) of a yellowish oil.

$\mathbf{R_f}$ = 0.3 (SiO_2. *n*-heptane/EtOAc = 10/1). **^{1}H-NMR** (300 MHz, $CDCl_3$): δ = 8.59 (ddd, *J* = 4.9, 1.9, 1.0 Hz, 1 H), 7.68 (ddd, *J* = 8.1, 7.4, 1.9 Hz, 1 H), 7.58 (dt, *J* = 8.1, 1.1 Hz, 1 H), 7.47 (ddd, *J* = 11.3, 7.9, 1.5 Hz, 2 H), 7.14 (ddd, *J* = 7.4, 4.9, 1.2 Hz, 1 H), 6.63 (t, *J* = 7.8 Hz, 1 H), 6.43 (br, 2 H, N*H*$_2$). **^{13}C-NMR** (75 MHz, $CDCl_3$): δ = 158.4 (C_q), 147.5 (CH), 144.0 (C_q), 136.9 (CH), 133.0 (CH), 128.5 (CH), 122.9 (C_q), 122.2 (CH), 121.3 (CH), 117.4 (CH), 111.3 (C_q). **IR (**ATR): $\tilde{\nu}$/cm^{-1} = 3451 (w), 3295 (vw), 3051 (vw), 3008 (vw), 1586 (s), 1572 (s), 1543 (m), 1477 (s), 1460 (m), 1446 (s), 1419 (vs), 1320 (vw), 1289 (w), 1265 (w), 1235 (m), 1198 (vw), 1152 (w), 1096 (w), 1058 (s), 1032 (w), 991 (w), 952 (vw), 905 (vw), 885 (vw), 835 (vw), 798 (w), 753 (vs), 726 (s), 655 (s), 630 (m), 575 (vw), 560 (m), 527 (w), 453 (vw), 403 (w), 380 (vw). **HR-MS (FAB)**, m/z, calculated for $C_{11}H_9N_2{}^{79}Br1$: 247.9949 $[M]^+$, found: 247.9948. **Elemental analysis** could not be done for oils.

3'-(Pyridin-2-yl)-2'-(pyrrolidin-1-yldiazenyl)-[1,1'-biphenyl]-2-amine (s15)

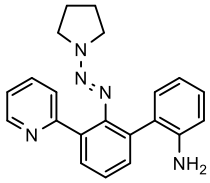

GCA, GWB. A Schlenk-tube was charged with **8** (1324 mg, 4.00 mmol, 1.00 eq.), 2-aminophenylboronic acid pinacol ester (1314 mg, 6.00 mmol, 1.50 eq.), K_3PO_4 (849 mg, 8.00 mmol, 2.00 eq.) and XPhos Pd G3[2] (102 mg, 0.12 mmol, 0.03 eq.). 16 ml 1,4-dioxane and 4 ml H_2O were added, the tube screw-sealed and the resulting mixture heated to 80 °C for 24 h. After cooling to room temperature, the mixture was diluted with CH_2Cl_2 (10 ml) and filtered over a plug of Celite. The plug was extracted with CH_2Cl_2 (3 x 20 ml) and the combined organic phases washed with aqueous 1 M NaOH, H_2O and brine. After drying over $MgSO_4$ all volatiles were removed. The crude was purified by column chromatography using neutral alumina as stationary phase (cyclohexane/EtOAc = 2/1). 3.63 g (91 %) of a light yellow microcrystalline solid were obtained, which is sensitive against acid and should be stored under a dry atmosphere. Single crystals suitable for X-Ray diffraction were obtained by layering a concentrated solution in toluene with *n*-pentane.

R_f = 0.17 (Al_2O_3. cyclohexane/EtOAc = 2/1). **M.p.** = 132 °C. **^{1}H-NMR** (300 MHz, CD_2Cl_2): δ = 8.63 (ddd, *J* = 4.9, 1.9, 1.0 Hz, 1 H), 7.67 (dd, *J* = 6.1, 3.1 Hz, 1 H), 7.60 (ddd, *J* = 8.0, 7.5, 1.9 Hz, 1 H), 7.39 (dt, *J* = 8.0, 1.1 Hz, 1 H), 7.32 (d, *J* = 3.1 Hz, 1 H), 7.31 (s, 1 H), 7.15 (ddd, *J* = 7.5, 4.9, 1.2 Hz, 1 H), 7.12 – 7.05 (m, 2 H), 6.74 (ddd, *J* = 7.7, 7.2, 1.2 Hz, 1 H), 6.69 – 6.63 (m, 1 H), 3.79 (br, 2 H, N*H*$_2$), 3.28 (td, *J* = 6.8, 3.7 Hz, 4 H), 1.77 (s, 4 H). **^{13}C-NMR** (75 MHz, CD_2Cl_2): δ = 159.2 (C_q), 149.7 (CH), 148.5 (C_q), 144.6 (C_q), 135.3 (CH), 134.8 (C_q), 133.8 (C_q), 132.2 (CH), 131.9 (CH), 130.7 (CH), 128.2 (CH), 127.8 (C_q), 126.4 (CH), 125.7 (CH), 121.5 (CH), 118.3 (CH), 115.7 (CH), 50.7 (CH_2)[1], 46.9 (CH_2), 24.2 (2 CH_2). **^{15}N-NMR** (30 MHz, ^{1}H/^{15}N HMBC, CD_2Cl_2): δ = -65.46, -324.76, -198.86. **IR (ATR):** $\tilde{\nu}$/cm^{-1} = 3437 (vw), 3354 (vw), 3053 (vw), 2964 (vw), 2883 (vw), 1992 (vw), 1611 (w), 1581 (w), 1561 (vw), 1496 (vw), 1472 (w), 1461 (vw), 1450 (vw), 1429 (w), 1399 (s), 1329 (m), 1318 (m), 1297 (w), 1259 (vw), 1207 (w), 1150 (w), 1098 (vw), 1074 (w), 1054 (vw), 1031 (vw), 1017 (vw), 988 (vw), 969 (vw), 942 (vw), 906 (vw), 865 (vw), 842 (vw), 810 (vw), 777 (s), 749 (vs), 715 (w), 673 (vw), 631 (vw), 623 (w), 612 (w), 603 (w), 585 (w), 572 (w), 539 (w), 517 (w), 484 (s), 434 (vw), 407 (w). **MS (ESI)**, m/z (%): 344.2 (93 %) $[M+H]^+$, 245.1 (100 %) $[M–Pyrrolidin–N_2]^+$. **Elemental analysis** calculated (%) for $C_{21}H_{21}N_5$: C 73.44, H 6.16, N 20.39, found: C 73.29, H 6.16, N 19.53. We repeated elemental analysis several times with recrystallized samples, however, percentage of N was always too low, maybe due to the facile loss of nitrogen.

4-(Pyridin-2-yl)benzo[c]cinnoline (s16)

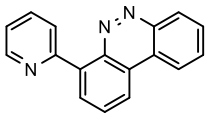

GCB, GWB. The synthesis of **s16** was not intended. It forms upon treatment of **s15** with acid (Brønsted or Lewis acid). Originally, we wanted to substitute the triazene group of **S15** by iodide.

S15 (343 mg, 1.00 mmol, 1.00 eq.) was dissolved in MeCN (4 ml) and treated with acid (~ 10 eq. aqueous HI). After stirring for 30 min, the reaction was neutralized with concentrated K_2CO_3. The mixture was extracted with CH_2Cl_2 (3 x 10 ml) and the combined extracts were washed with brine and dried over $MgSO_4$. After evaporating all volatiles in vacuo, the residue was purified by column chromatography (SiO_2, cyclohexane/EtOAc = 1/1). Analytically pure samples were not obtained, neither was the yield determined.

R_f = 0.29 (SiO_2. cyclohexane/EtOAc = 1/1). **^{1}H-NMR** (300 MHz, CD_2Cl_2): δ = 8.84 (ddd, *J* = 4.9, 1.9, 1.0 Hz, 1 H), 8.79 – 8.68 (m, 3 H), 8.32 (dd, *J* = 7.4, 1.3 Hz, 1 H), 8.18 (dt, *J* = 7.9, 1.1 Hz, 1 H), 8.09 (dd, *J* = 8.2, 7.4 Hz, 1 H), 8.07 – 7.92 (m, 2 H), 7.91 (ddd, *J* = 7.5, 1.8 Hz, 1 H), 7.43 (ddd, *J* = 7.5, 4.9, 1.2 Hz, 1 H). **^{13}C-NMR** (75 MHz, CD_2Cl_2): δ = 156.7 (C_q), 150.1 (CH), 145.7 (C_q), 143.0 (C_q), 141.5 (C_q), 135.8 (CH), 132.2 (CH), 132.0 (CH), 131.6 (2 x CH), 130.0 (CH), 128.6 (CH), 123.1 (CH), 122.7 (CH), 122.3 (CH), 121.4 (C_q), 121.3 (C_q). **MS (ESI)**, m/z (%): 258.1 (100 %) $[M+H]^+$.

(*9H*-Fluoren-9-yl)methyl-(3'-(pyridin-2-yl)-2'-(pyrrolidin-1-yldiazenyl)-[1,1'-biphenyl]-2-yl)carbamate (s17)

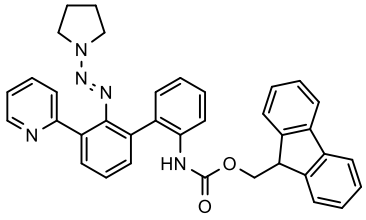

GCB, GWB. A mixture of **s15** (343 mg, 1.00 mmol, 1.00 eq.), Na_2CO_3 (250 mg, 2.36 mmol, 2.36 eq.), water (2.5 ml) and 1,4-dioxane (2.5 ml) was cooled to 0 °C under stirring. Then, Fmoc-Cl (259 mg, 1.00 mmol, 1.00 eq.) in a mixture of water (2.5 ml) and 1,4-dioxane (2.5 ml) was added dropwise. The resulting mixture was stirred for 1 h at 0 °C and then at room temperature for additional 3 h. The mixture was extracted with EtOAc (3 x 20 ml) and the combined organic phases washed with brine and dried over $MgSO_4$. After removing all volatiles in vacuo, the residue was filtered through a short column with silica (cyclohexane/EtOAc = 2/1) to obtain 540 mg (95 %) of a yellowish solid, which was used without further purification.

R_f = 0.36 (SiO_2. cyclohexane/EtOAc = 2/1). **^{1}H-NMR** (300 MHz, CD_2Cl_2): δ = 8.64 (ddd, *J* = 4.9, 1.9, 1.0 Hz, 1 H), 8.06 (s, 1 H, N*H*), 7.80 – 7.74 (m, 3 H), 7.71 (dd, *J* = 6.9, 2.3 Hz, 1 H), 7.62 (ddd, *J* = 8.0, 7.5, 1.8 Hz, 1 H), 7.56 (ddd, *J* = 7.4, 5.2, 1.0 Hz, 2 H), 7.42 – 7.11 (m, 11 H), 4.50 – 4.32 (m, 2 H), 3.25 (m, 4 H), 1.79 (br, 4 H).

(*9H*-Fluoren-9-yl)methyl 1-(pyridin-2-yl)-9*H*-carbazole-9-carboxylate

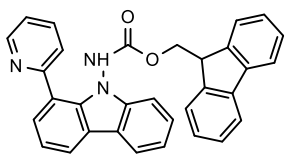

GCA, GWB. The synthesis of the protected carbazole was not intended. It forms upon treatment of **s17** with Lewis acid. Originally, we wanted to substitute the triazene group of **S17** by iodide.

s17 (566 mg, 1.00 mmol, 1.00 eq.) and NaI (150 mg, 1.00 mmol, 1.00 eq.) were dissolved in MeCN (10 ml) and treated with TMS-I (300 mg, 213 µl, 1.50 mmol, 1.50 eq.). The brown mixture was heated to 60 °C under stirring upon which the evolution of gas bubbles was observable. After 1 h the mixture was cooled to room temperature and basifisized with 5 % $NaHCO_3$ (pH = 8 ~ 9). The mixture was extracted with Et_2O (3 x 20 ml) and the combined organic phases were washed with brine and drive over $MgSO_4$. After evaporating all volatiles in vacuo, the remaining foam (~ 600 mg) was directly used in the next step.

1-(Pyridin-2-yl)-9*H*-carbazole (s18)

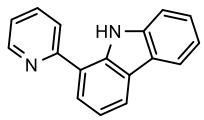

GCB, GWB. The crude protected carbazole **s17** (~ 600 mg) was dissolved in DMF (8 ml). Under stirring 2 ml Piperidine were added dropwise. The resulting mixture was stirred for 30 min and then diluted with EtOAc (20 ml). The organic phase was washed several times with water and then brine. After drying over $MgSO_4$ all volatiles were removed and the brown residue purified by column chromatography (SiO_2, cyclohexane/EtOAc = 10 / 1) to obtain 120 mg (32 % over three steps starting from **s15**) of a pale yellow solid.

$\mathbf{R_f}$ = 0.37 (SiO_2, cyclohexane/EtOAc = 10/1). The analytical data were in accordance with the ones reported in the literature.[36]

6-(2-Bromophenyl)benzo[e]imidazo[5,1-c][1,2,4]triazine (s19)

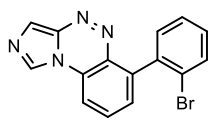

GCB, GWB. In a round bottom flask, thoroughly powdered **30** (1104 mg, 3.51 mmol, 1.00 eq.) was treated with MeCN (10 ml) and conc. $HCl_{(aq)}$ (1.5 ml). The resulting red mixture was cooled to –15 °C. Under stirring, a solution of $NaNO_2$ in water (5 ml) was added dropwise. The resulting yellow mixture was warmed to 0 °C and stirred for 30 min. The mixture was recooled to –15 °C and a solution of KI (875 mg, 5.27 mmol, 1.50 eq.) in water/MeCN (5 ml / 5 ml) was added dropwise (addition of KI at this stage was not necessary anymore, since the cyclized triazine has already formed at this stage; however, when performing the reaction this was not yet clear). The resulting mixture was stirred at room temperature overnight. The reaction was neutralized using conc. $K_2CO_{3(aq)}$ (pH ~ 8) and extracted with CH_2Cl_2 (2 x 30 ml). The combined extracts were washed with conc. $NaS_2O_{3(aq)}$, brine and dried over $MgSO_4$. After evaporation of all volatiles, the crude was purified by column chromatography (SiO_2, cyclohexane/EtOAc = 1/3) to obtain a brownish solid. Recrystallization from CH_2Cl_2 gave 260 mg (23 %) lemon-colored crystals.$\mathbf{R_f}$ = 0.25 (SiO_2. cyclohexane/EtOAc = 1/3). **M.p.** = 226 °C (Z). **^{1}H-NMR** (300 MHz, $CDCl_3$): δ = 8.65 (d, *J* = 0.6 Hz, 1 H), 8.38 (d, *J* = 0.6 Hz, 1 H), 8.00 (dd, *J* = 8.2, 1.3 Hz, 1 H), 7.88 (dd, *J* = 8.3, 7.5 Hz, 1 H), 7.73 (dt, *J* = 8.0, 0.9 Hz, 1 H), 7.61 (dd, *J* = 7.5, 1.3 Hz, 1 H), 7.48 – 7.39 (m, 2 H), 7.40 – 7.25 (m, 1 H). **^{13}C-NMR** (75 MHz, $CDCl_3$): δ = 143.0 (C_q), 139.3 (C_q), 138.7 (C_q), 134.0 (C_q), 133.0 (CH), 132.9 (CH), 132.0 (CH), 129.9 (CH), 129.5 (CH), 128.9 (CH), 127.2 (CH), 125.9 (CH), 124.1 (CH), 122.2 (C_q), 114.0 (C_q). **IR (ATR):** $\tilde{\nu}$/cm^{-1} = 3105 (vw), 2007 (vw), 1969 (vw), 1935 (vw), 1822 (vw), 1732 (vw), 1700 (vw), 1629 (vw), 1596 (w), 1527 (vw), 1501 (w), 1474 (vw), 1458 (vw), 1430 (w), 1418 (w), 1396 (vw), 1355 (w), 1310 (w), 1288 (w), 1245 (vw), 1215 (vw), 1166 (w), 1135 (w), 1118 (m), 1060 (w), 1025 (vw), 1010 (w), 957 (vw), 925 (w), 908 (vw), 898 (m), 851 (m), 821 (vw), 809 (m), 796 (vs), 766 (s), 748 (vs), 726 (m), 696 (w), 678 (w), 659 (w), 646 (s), 625 (w), 609 (vw), 568 (vw), 536 (vw), 521 (vw), 489 (w), 468 (vw), 442 (w), 404 (vw), 384 (vw). **MS (APCI)**, m/z (%): 325.1 (100 %) $[M+H]^+$. **Elemental analysis** calculated (%) for $C_{15}H_9N_4Br$: C 55.41, H 2.79, N 17.23, found: C 54.31, H 2.75, N 16.99.

1-(2'-Bromo-2-iodo-[1,1'-biphenyl]-3-yl)-3-methyl-1H-imidazol-3-ium iodide (s20)

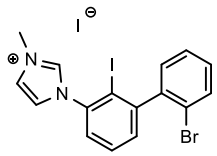

GCA, GWB. In a round bottom flask, **31** (2.48 g, 5.83 mmol, 1.00 eq.) was dissolved in THF (30 ml). MeI (2.48 g, 17.50 mmol, 1.09 ml, 3.00 eq.) was added and the resulting mixture stirred for 3 days during which a voluminous colorless precipitate formed. The mixture was filtered and the residue washed with Et_2O (3 x 20 ml) and dried in vacuo to obtain 3.31 g (quant.) of a colorless solid.**M.p.** = 298 °C (Z). **^{1}H-NMR** (300 MHz, Methanol-*d4*): δ = 9.45 (d, *J* = 2.1 Hz, 1 H), 9.41 (d, *J* = 2.0 Hz, 1 H), 9.32 – 9.21 (m, 3 H), 9.07 (dd, *J* = 7.0, 2.2 Hz, 1 H), 9.05 (td, *J* = 7.5, 1.3 Hz, 1 H), 8.93 (ddd, *J* = 8.0, 7.5, 1.8 Hz, 1 H), 8.83 (ddd, *J* = 7.6, 1.8, 0.4 Hz, 1 H), 5.65 (s, 3 H, C*H*$_3$).[6] **^{1}H-NMR** (300 MHz, MeCN-*d3*): δ = 8.82 (td, *J* = 1.7, 0.8 Hz, 1 H, (H$_3$C)NC*H*N), 7.76 (ddd, *J* = 7.9, 1.1, 0.4 Hz, 1 H), 7.68 (t, *J* = 7.7 Hz, 1 H), 7.61 – 7.53 (m, 3 H), 7.51 (t, *J* = 1.4 Hz, 1 H), 7.49 (t, *J* = 1.5 Hz, 1 H), 7.40 (ddd, *J* = 8.0, 7.5, 1.8 Hz, 1 H), 7.28 (ddd, *J* = 7.6, 1.9, 0.3 Hz, 1 H), 3.98 (d, *J* = 0.7 Hz, 3 H, C*H*$_3$). **^{1}H-NMR** (300 MHz, DMSO-*d6*): δ = 9.54 (s, 1 H, (H$_3$C)NC*H*N), 8.01 (t, J = 1.8 Hz, 1 H), 7.92 (t, J = 1.8 Hz, 1 H), 7.77 (d, J = 8.1 Hz, 1 H), 7.73 – 7.65 (m, 2 H), 7.58 – 7.46 (m, 2 H), 7.40 (td, J = 7.7, 1.8 Hz, 1 H), 7.26 (dd, J = 7.5, 1.8 Hz, 1 H), 3.97 (s, 3 H, NC*H*$_3$). **^{13}C-NMR** (75 MHz, DMSO-*d6*): δ = 148.2 (C_q), 143.9 (C_q), 138.2 (C_q), 137.9 (CH), 132.6 (CH), 131.9 (CH), 130.9 (CH), 130.4 (CH), 129.5 (CH), 128.0 (CH), 127.4 (CH), 124.3 (CH), 123.8 (CH), 122.4 (C_q), 102.7 (C_q), 36.2 (CH_3). **IR (ATR):** $\tilde{\nu}$/cm^{-1} = 3162 (vw), 3125 (vw), 3070 (vw), 3037 (w), 2295 (vw), 2169 (vw), 2150 (vw), 2041 (vw), 2019 (vw), 1996 (vw), 1941 (vw), 1718 (vw), 1610 (vw), 1576 (vw), 1566 (vw), 1549 (m), 1536 (w), 1481 (vw), 1451 (m), 1426 (w), 1342 (vw), 1296 (vw), 1273 (vw), 1248 (vw), 1223 (m), 1174 (vw), 1113 (w), 1071 (w), 1022 (w), 972 (w), 951 (vw), 919 (vw), 896 (vw), 866 (vw), 842 (w), 799 (vs), 766 (vs), 755 (s), 745 (vs), 720 (vs), 707 (w), 667 (w), 645 (vs), 617 (s), 560 (w), 548 (vw), 506 (vw), 464 (w), 443 (w), 409 (w), 391 (vw), 382 (vw). **MS (ESI)**, m/z (%): 438.9 (100 %) $[M]^+$. **Elemental analysis** calculated (%) for $C_{16}H_{13}N_2BrI_2$: C 33.89, H 2.31, N 4.94, found: C 34.05, H 1.86, N 5.07.

[(NHC)Au(I)Cl] (s21)

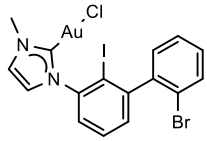

GCA, GWA. In a Schlenk tube **s20** (170 mg, 0.30 mmol, 1.00 eq.), (tht)AuCl (96 mg, 0.30 mmol, 1.00 eq.) and K_2CO_3 (83 mg, 0.60 mmol, 2.00 eq.) were suspended in MeCN (5 ml). The resulting mixture was stirred for 24 h at room temperature. The solvent was removed in vacuo and the yellowish residue washed with Et_2O (10 ml), taken up in CH_2Cl_2 (5 ml), filtered and layered with *n*-hexane. After a couple of days, yellow crystals formed. The supernatant solution was taken off and the crystals dried in vacuo (96 mg, 60 %). Two rotamers with respect to the bromo-phenyl ring form as evidenced from X-ray diffraction analysis and NMR (ratio a:b = 1:0.57).

M.p. = 230 °C (Z).

^{1}H-NMR (300 MHz, $CDCl_3$) **rotamer a**: δ = 7.62 (dd, J = 8.0, 1.2 Hz, 1 H), 7.48 (t, J = 7.7 Hz, 1 H), 7.43 – 7.20 (m, 5 H), 7.18 – 7.03 (m, 2 H), 3.91 (s, 3 H).

^{1}H-NMR (300 MHz, $CDCl_3$) **rotamer b**: δ = 7.63 (dd, J = 7.9, 1.3 Hz, 1 H), 7.49 (t, J = 7.7 Hz, 1 H), 7.43 – 7.20 (m, 5 H), 7.18 – 7.03 (m, 2 H), 3.91 (s, 1 H).

^{13}C-NMR (75 MHz, $CDCl_3$) **rotamer a**: δ = 172.8 (C_q, $C_{(carbene)}$), 148.8 (C_q), 144.6 (C_q), 142.0 (C_q), 132.7 (CH), 131.5 (CH), 131.3 (CH), 130.1 (CH), 129.2 (CH), 128.1 (CH), 127.8 (CH), 123.2 (CH), 122.9 (C_q), 121.8 (CH), 102.5 (C_q), 38.7 (CH_3),

[6] The protic H of the imidazolium group could not be detected in deuterated methanol.

^{13}C-NMR (75 MHz, $CDCl_3$) **rotamer b**: δ = 173.8 (C_q, $C_{(carbene)}$), 149.2 (C_q), 144.7 (C_q), 142.0 (C_q), 133.0 (CH), 131.5 (CH), 131.1 (CH), 129.9 (CH), 129.4 (CH), 127.7 (CH), 127.3 (CH), 124.2 (C_q), 122.5 (CH), 121.8 (CH), 103.8 (C_q), 38.7 (CH_3).

IR (ATR): $\tilde{\nu}$/cm^{-1} = 3166 (vw), 3128 (vw), 3099 (vw), 2256 (vw), 2189 (vw), 2174 (vw), 2122 (vw), 2023 (vw), 1997 (vw), 1956 (vw), 1942 (vw), 1926 (vw), 1885 (vw), 1567 (vw), 1466 (w), 1435 (vw), 1418 (w), 1396 (vw), 1356 (vw), 1312 (vw), 1241 (w), 1181 (vw), 1159 (vw), 1132 (vw), 1104 (vw), 1078 (vw), 1021 (w), 974 (vw), 946 (vw), 919 (vw), 864 (vw), 844 (vw), 800 (s), 754 (vs), 724 (vs), 677 (m), 665 (m), 620 (vw), 562 (w), 530 (vw), 513 (vw), 486 (vw), 472 (vw), 444 (m), 418 (vw), 405 (vw), 398 (vw), 388 (vw). **MS (APCI)**, m/z (%): 634.6 (100 %) $[M–Cl]^+$. **Elemental analysis** calculated (%) for $C_{16}H_{12}N_2ClBrIAu$: C 28.62, H 1.80, N 4.17, found: C 28.62, H 1.97, N 4.52.

S 5 Crystallographic Details and Structures not Reported in the Main Text

In order to avoid degradation, single crystals were mounted in perfluoropolyalkylether-oil on top of the edge of an open Mark tube and then brought into the cold nitrogen stream of a low-temperature device (Oxford Cryosystems Cryostream unit) so that the oil solidified. Diffraction data were measured using a Stoe IPDS II diffractometer (monochromatic Mo K_α (0.71073 Å) radiation), Stoe Stadivari (monochromatic Mo K_α (0.71073 Å) radiation) or Stoe Stadivari (monochromatic Ga K_α (1.34143 Å) radiation). The structures were solved by dual-space direct methods with SHELXT,[37] followed by full-matrix least-squares refinement using SHELXL-2014/7.[38] All non-hydrogen atoms were refined anisotropically, with organic hydrogen atoms placed in calculated positions using a riding model. Absorption corrections were applied for compounds **25**, **29**, **33_1**, **33_2**, **35**, **39**, **40** and **s22** (multi-scan) and compound **s20** (gaussian). Crystallographic data, data collection, and refinement details are summarized in the following tables. Crystallographic data (excluding structure factors) for the structures in this paper have been deposited with the Cambridge Crystallographic Data Centre. Copies of the data can be obtained from https://www.ccdc.cam.ac.uk/structures/.

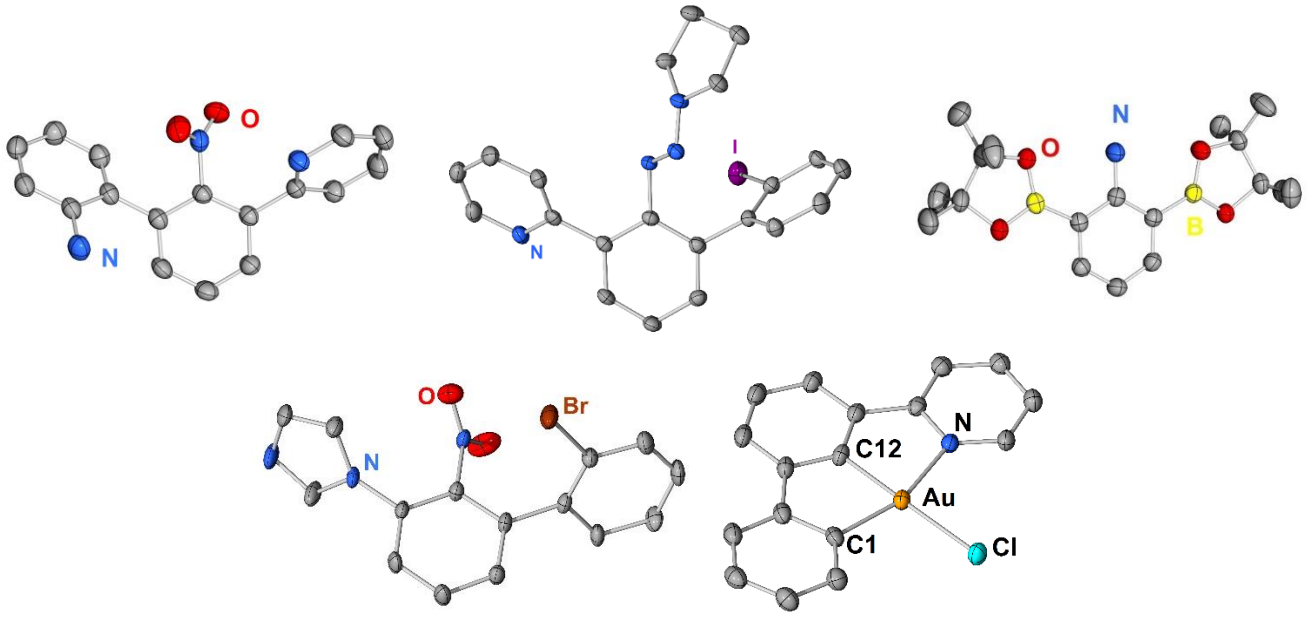

Figure S 9. Solid state molecular structures not reported/ shown in the main text. **20** (top left), **25** (top middle), **s22** (top right),[39] **29** (bottom left); **33** (bottom right). Thermal ellipsoids are set at 30 % probability. Hydrogen atoms are omitted for clarity. Only one molecule of the elementary cell is shown (if applicable). Selected bond lengths (pm) and angles (°) of **33**: Au–Cl 236.88(9), Au–N 213.8(3), Au–C1 203.4(4), Au–C12 197.2(4), C1–Au–C12 80.76(16), N–Au–C12 79.70(14).

The structural parameters of [(C^C^N)Au(III)Cl] (**33**) are comparable to the (C^C^N) complexes reported by Nevado and co-workers.[40] The Au−Cl (236.9 pm) bond is 9 pm longer than the one of the palindromic (C^N^C) congener[41] resembling the strong *trans* influence of the central phenyl donor.

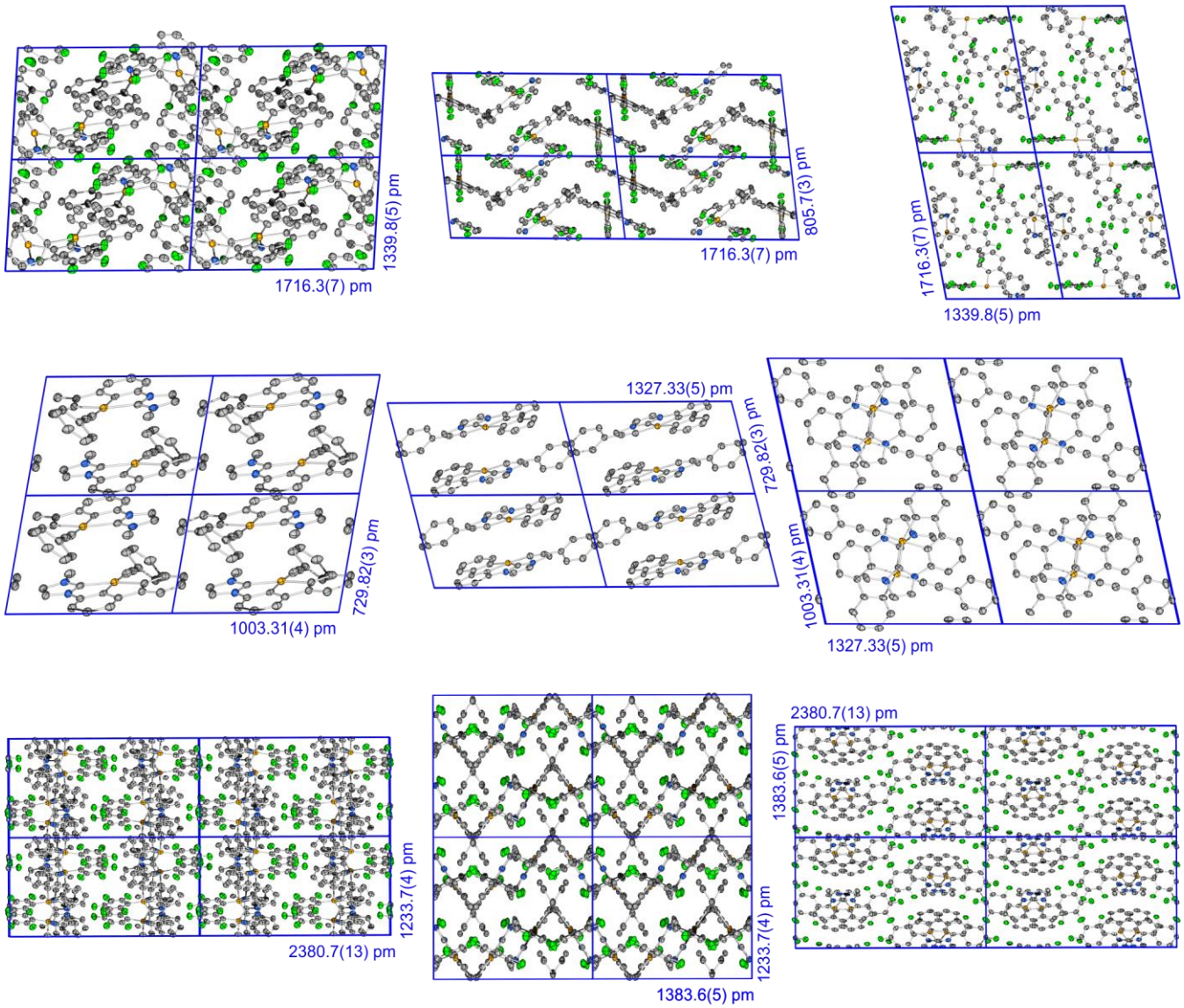

Figure S 10. Molecular packing of [(C^C^N)Au(III)C_6F_5] (**35**), [(C^C^C')Au(III)CCPh] (**39**) and [(C^C^C')Au(III)C_6F_5] (**40**) in the solid state. The distance of one molecule's gold atom to the plane spanned by the pincer of the closest neighbouring molecule is d_{Au-CCN} = 346.12(6) pm for **35**, $d_{Au-CCC'}$ = 345.80(3) pm for **39** and $d_{Au-CCC'}$ = 347.24(5) pm for **40**. We make these rather close distances responsible for the lack of solid state emission due to triplet-triplet annihilation.[42]

Compound	**20**	**25**	**29**
Empirical Formula	$C_{17}H_{13}N_3O_2$	$C_{21}H_{19}N_4I$	$C_{15}H_{10}BrN_3O_2$
M	291.30	454.30	344.17
Temperature / K	200	200	200
Crystal system	monoclinic	monoclinic	triclinic
Space group	*Cc*	$P2_1/c$	$P\bar{1}$
a / Å	14.206(3)	10.356(4)	7.395(5)
b / Å	14.403(3)	14.018(7)	7.780(4)
c / Å	14.332(3)	13.319(5)	12.552(7)
α / °	90	90	102.52(4)
β / °	96.80(3)	96.78(3)	96.50(5)
γ / °	90	90	92.43(5)
V / Å³	2911.8(10)	1920.1(13)	698.7(7)
Z	8	1	2
ρ_{calc} g/cm^3	1.329	1.572	1.636
μ /mm^{-1}	0.090	1.679	2.949
Crystal size / mm^3	0.5 × 0.5 × 0.25	0.3 × 0.3 × 0.1	0.6 × 0.6 × 0.25
Radiation	Mo K_α (λ = 0.71073)	Mo K_α (λ = 0.71073)	Mo K_α (λ = 0.71073)
$2\theta_{min}$ / °	4.042	3.96	3.35
$2\theta_{max}$ / °	51.992	51.996	51.988
Reflections collected	15949	14001	5227
Independent Reflections	5150 (R_{int} = 0.0385)	3774 (R_{int} = 0.0545)	2738 (R_{int} = 0.0853)
Data/restraints/parameters	5150/2/400	3774/0/236	2738/0/190
GooF on F²	1.047	1.063	1.422
*R*1 [$I \geq 2\sigma(I)$]	0.0329	0.0418	0.0869
*wR*2 [$I \geq 2\sigma(I)$]	0.0864	0.1077	0.2485
*R*1 (all data)	0.0337	0.0592	0.0998
*wR*2 (all data)	0.0872	0.1154	0.3041
Largest diff. peak/holes /e · Å³	0.17 / –0.18	0.57 / –0.99	2.27/−2.18
Diffractometer	Stoe IPDS II	Stoe IPDS II	Stoe IPDS II
CCDC number	1986483	1986486	2009470

Compound	**33_1**	**33_2**	**35**
Empirical Formula	$C_{17}H_{11}AuClN$	$C_{20}H_{18}AuClN$	$C_{92}H_{44}Au_4F_{20}N_4$
M	461.68	504.77	2373.18
Temperature / K	180.15	150.15	200
Crystal system	monoclinic	monoclinic	triclinic
Space group	$P2_1/n$	$P\bar{1}$	$P\bar{1}$
a / Å	8.8866(5)	6.9945(4)	8.057(3)
b / Å	16.7066(7)	9.5227(5)	13.398(5)
c / Å	9.0688(4)	12.7862(6)	17.163(7)
α / °	90.00	79.204(4)	100.22(3)
β / °	93.037(4)	78.150(4)	96.17(3)
γ / °	90.00	85.442(4)	92.43(3)
V / Å³	1344.50(11)	818.01(7)	1809.2(12)
Z	4	2	1
ρ_{calc} g/cm^3	2.281	2.049	2.178
μ /mm^{-1}	11.127	12.952	8.191
Crystal size / mm^3	0.25 × 0.18 × 0.15	0.12 × 0.07 × 0.05	0.5 × 0.35 × 0.3
Radiation	Mo K_α (λ = 0.71073)	Ga K_α (λ = 1.34143)	Mo K_α (λ = 0.71073)
$2\theta_{min}$ / °	4.876	6.242	3.094
$2\theta_{max}$ / °	59.995	124.964	51.998
Reflections collected	7983	9051	13920
Independent Reflections	3864 (R_{int} = 0.0435)	3782 (R_{int} = 0.0189)	7095 (R_{int} = 0.0727)
Data/restraints/parameters	3864/0/181	3782/0/209	7095/0/542
GooF on F²	1.057	1.134	1.012
*R*1 [$I \geq 2\sigma(I)$]	0.0422	0.0228	0.0781
*wR*2 [$I \geq 2\sigma(I)$]	0.1188	0.0594	0.1947
*R*1 (all data)	0.0471	0.0244	0.0856
*wR*2 (all data)	0.1251	0.0630	0.2033
Largest diff. peak/holes /e · Å³	2.12/−2.29	0.76/−089	4.55/−3.96
Diffractometer	Stoe Stadivari	Stoe Stadivari	Stoe IPDS II
CCDC number	2009476	2009473	2009475

Compound	**39**	**40**	**s15**[7]
Empirical Formula	$C_{24}H_{17}N_2Au$	$AuC_{22}F_5N_2$	$C_{21}H_{21}N_5$
M	530.36	584.21	343.43
Temperature / K	150(2)	200	200
Crystal system	triclinic	orthorhombic	triclinic
Space group	$P\bar{1}$	*Pbca*	$P\bar{1}$
a / Å	7.2982(3)	12.337(4)	7.8037(11)
b / Å	10.0331(4)	13.836(5)	11.0082(15)
c / Å	13.2733(5)	23.807(13)	11.5587(13)
α / °	100.268(3)	90.00	65.128(9)
β / °	102.299(3)	90.00	77.063(10)
γ / °	97.580(3)	90.00	85.788(11)
V / Å³	919.70(6)	4063.8(31)	877.75(20)
Z	2	8	2
ρ_{calc} g/cm³	1.915	1.910	1.299
μ /mm^{-1}	10.705	7.294	0.080
Crystal size / mm³	0.080 × 0.010 × 0.010	0.2 × 0.2 × 0.15	0.4 × 0.25 × 0.25
Radiation	Ga K_α (λ = 1.34143)	Mo K_α (λ = 0.71073)	Mo K_α (λ = 0.71073)
$2\theta_{min}$ / °	6.068	4.742	3.976
$2\theta_{max}$ / °	124.976	51.998	58.388
Reflections collected	11082	11160	4472
Independent Reflections	4369 (R_{int} = 0.0426)	3986 (R_{int} = 0.0728)	3491 (R_{int} = 0.0238)
Data/restraints/parameters	4369/0/245	3986/0/272	3491/0/237
GooF on F²	1.118	1.045	1.170
*R*1 [$I \geq 2\sigma(I)$]	0.0439	0.0855	0.0550
*wR*2 [$I \geq 2\sigma(I)$]	0.1183	0.2370	0.1383
*R*1 (all data)	0.0540	0.1000	0.0814
*wR*2 (all data)	0.1266	0.2620	0.1994
Largest diff. peak/holes /e · Å³	1.68/−1.89	3.30/−5.89	0.27 / −0.28
Diffractometer	Stoe Stadivari	Stoe IPDS II	Stoe IPDS II
CCDC number	2009471	2009477	1986481

[7] The crystal slipped during measurement, hence, a part of the data set had to be discarded (completeness 73 %).

Compound	**s19**	**s21**	**s22**
Empirical Formula	$C_{15}H_9BrN_4$	$C_{16}H_{12}AuBrClIN_2$	$C_{18}H_{29}B_2NO_4$
M	325.17	671.50	345.04
Temperature / K	200	200	200
Crystal system	orthorhombic	monoclinic	monoclinic
Space group	*Pbca*	$P2_1/n$	$P2_1/c$
a / Å	7.449(2)	11.261(7)	13.097(3)
b / Å	8.508(2)	8.865(3)	12.656(3)
c / Å	40.758(15)	18.859(12)	12.574(3)
α / °	90.00	90.00	90
β / °	90.00	101.47(5)	106.97(3)
γ / °	90.00	90.00	90
V / Å³	2583.0(13)	1845.0(17)	1993.4(7)
Z	8	4	4
ρ_{calc} g/cm³	1.672	2.417	1.150
μ /mm^{-1}	3.177	11.954	0.078
Crystal size / mm³	0.4 × 0.4 × 0.2	0.65 × 0.25 × 0.1	0.3 × 0.3 × 0.01
Radiation	Mo K_α (λ = 0.71073)	Mo K_α (λ = 0.71073)	Mo K_α (λ = 0.71073)
$2\theta_{min}$ / °	3.998	3.904	3.252
$2\theta_{max}$ / °	51.992	51.992	53.99
Reflections collected	11749	6762	21152
Independent Reflections	2513 (R_{int} = 0.0574)	3612 (R_{int} = 0.1045)	4349 (R_{int} = 0.0586)
Data/restraints/parameters	2513/0/182	3612/210/241	4349/0/236
GooF on F²	1.090	1.048	1.040
*R*1 [$I \geq 2\sigma(I)$]	0.0582	0.0887	0.0570
*wR*2 [$I \geq 2\sigma(I)$]	0.1622	0.2365	0.1443
*R*1 (all data)	0.0660	0.1038	0.0958
*wR*2 (all data)	0.1720	0.2563	0.1804
Largest diff. peak/holes /e · Å³	1.36/−0.74	4.71/−2.28	0.39 / −0.44
Diffractometer	Stoe IPDS II	Stoe IPDS II	Stoe IPDS II
CCDC number	2009474	2009472	1991871

S 6 NMR and mass spectra

In order of appearance in the text and the SI.

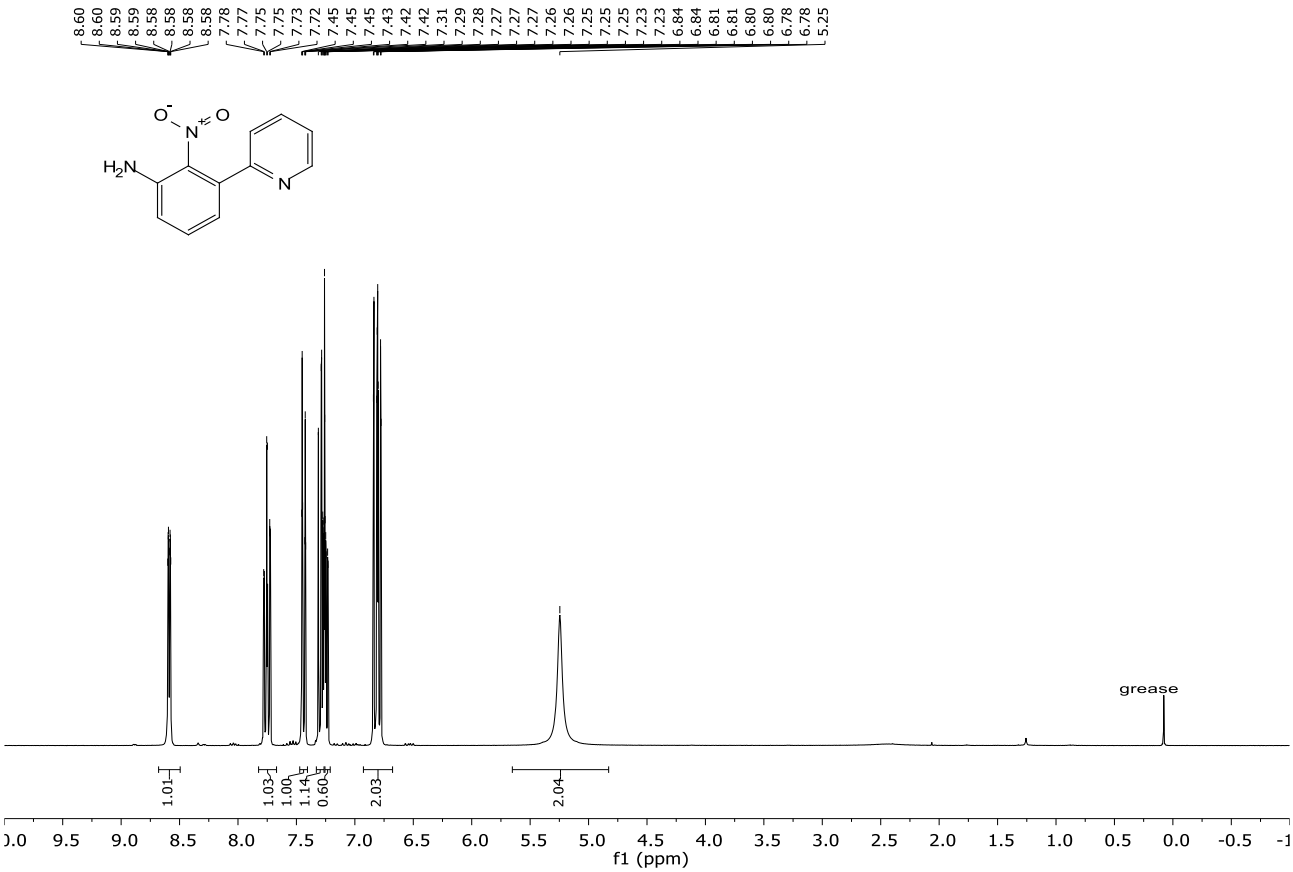

Figure S 11. ^{1}H NMR spectrum (300 MHz, $CDCl_3$) of **18**.

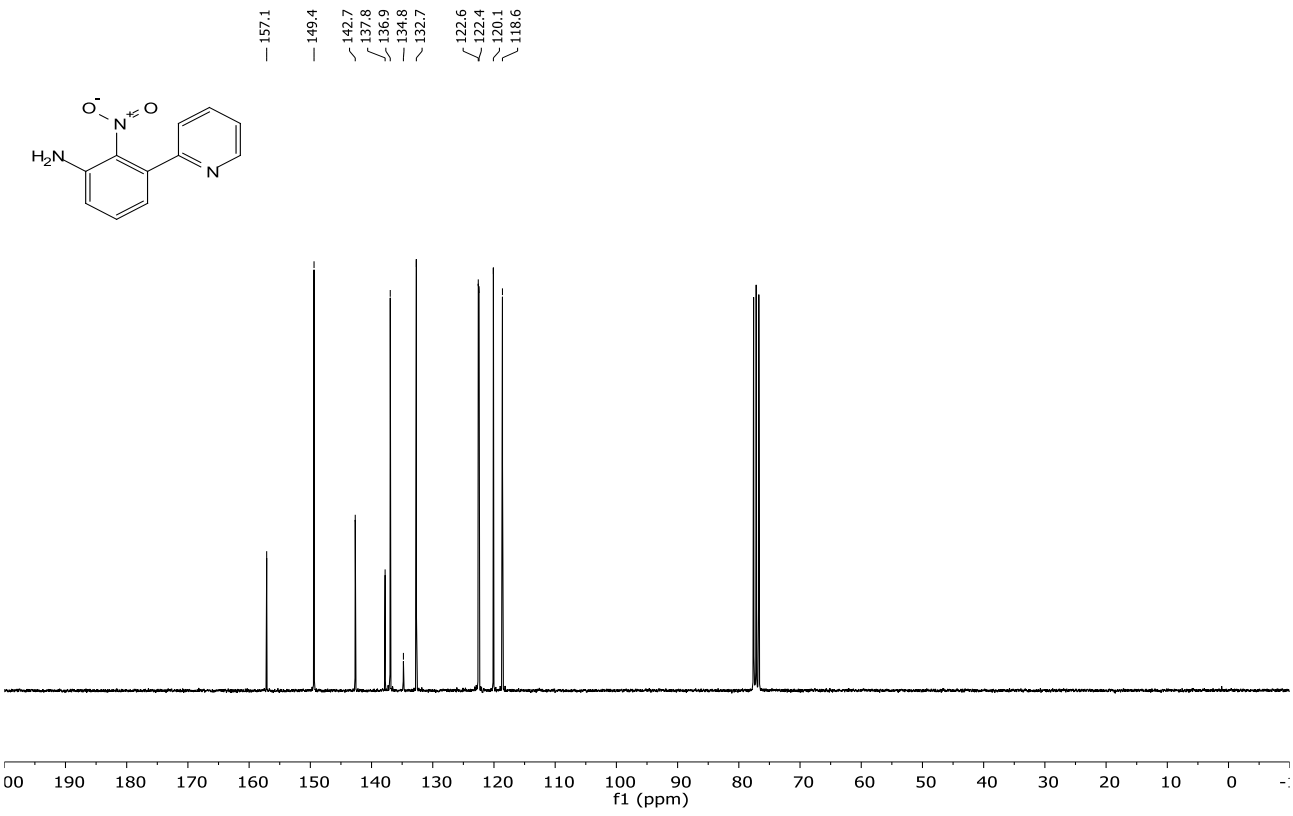

Figure S 12: ^{13}C NMR spectrum (75 MHz, $CDCl_3$) of **18**.

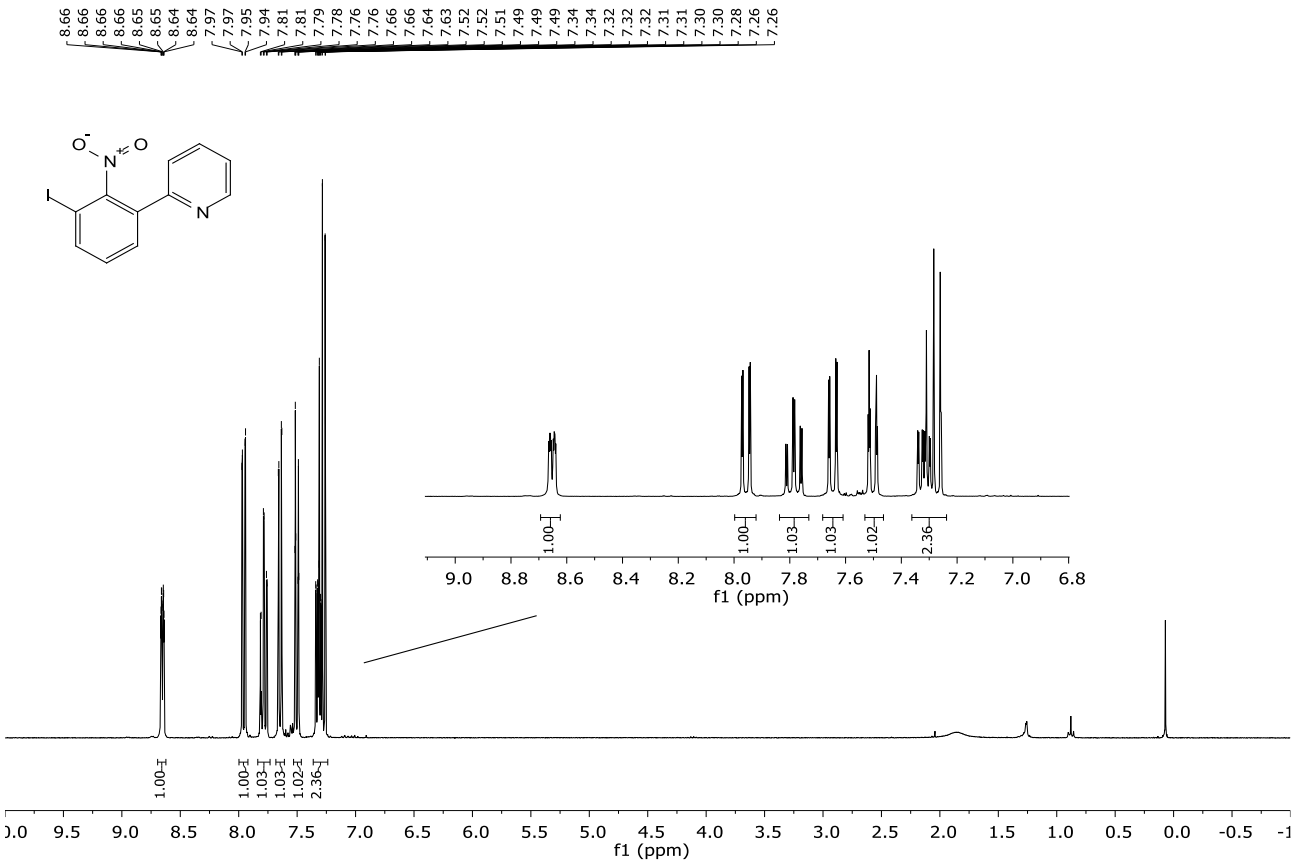

Figure S 13. ^{1}H NMR spectrum (300 MHz, $CDCl_3$) of **19**.

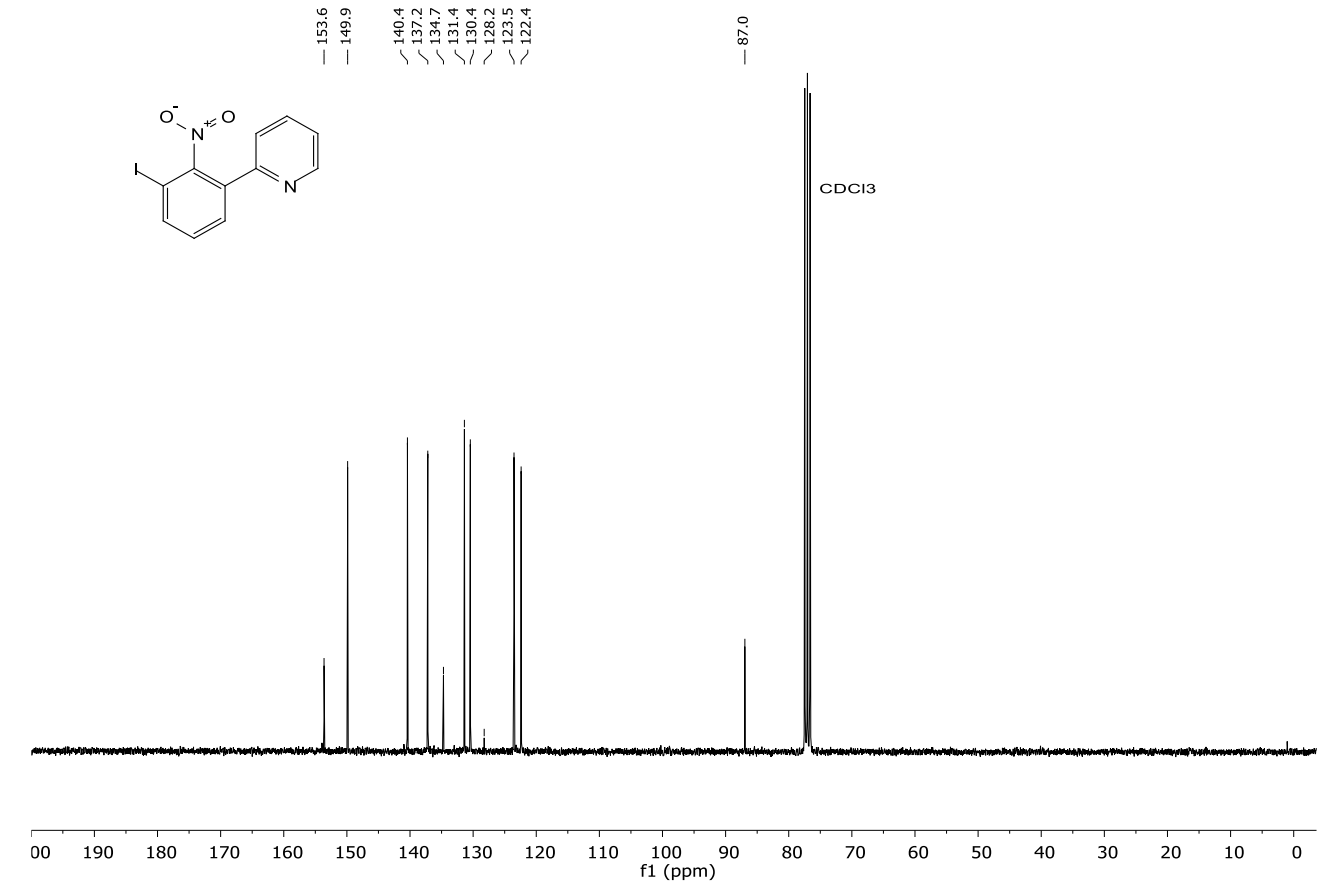

Figure S 14. ^{13}C NMR spectrum (75 MHz, $CDCl_3$) of **19**.

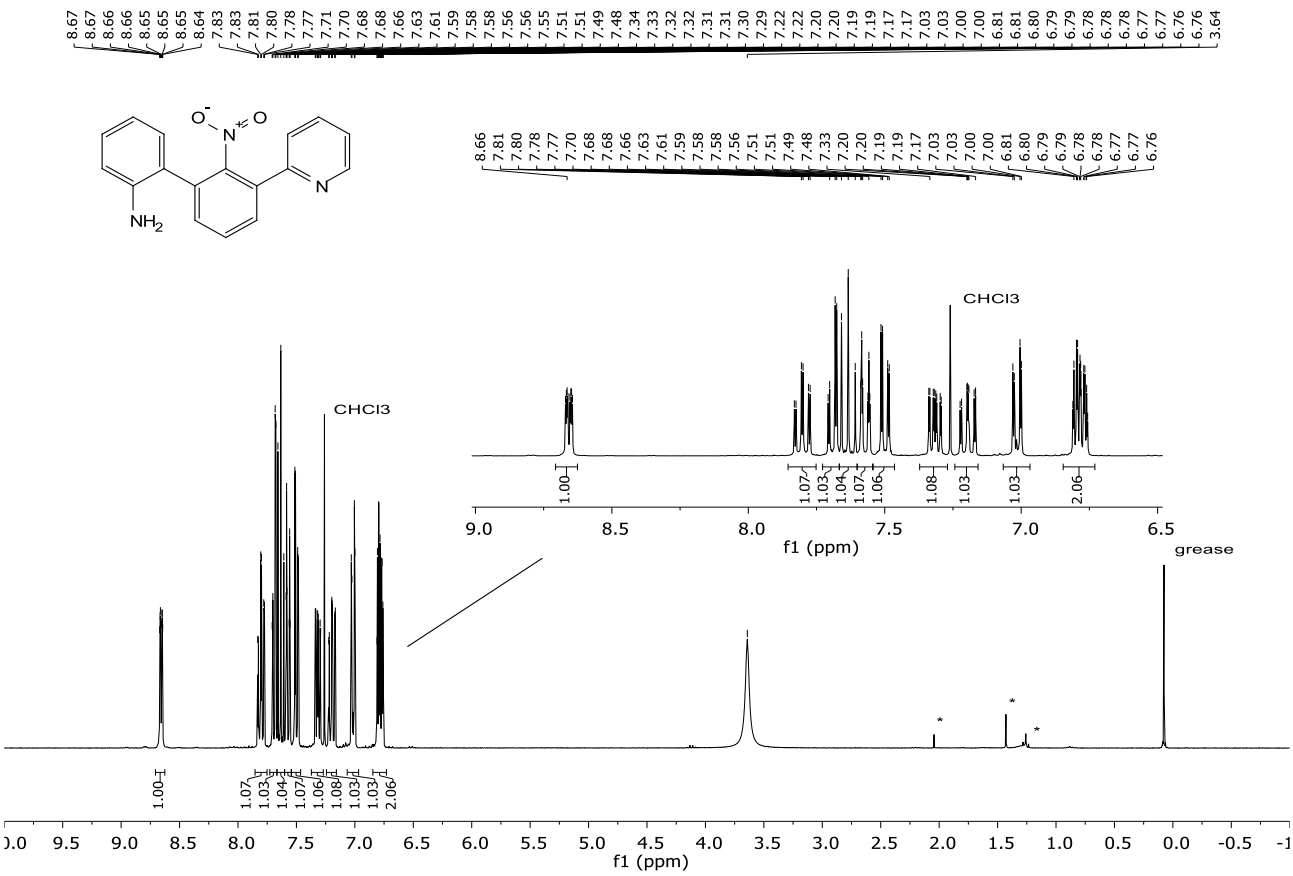

Figure S 15. ^{1}H NMR spectrum (300 MHz, $CDCl_3$) of **20**. Impurities are marked with an asterisk.

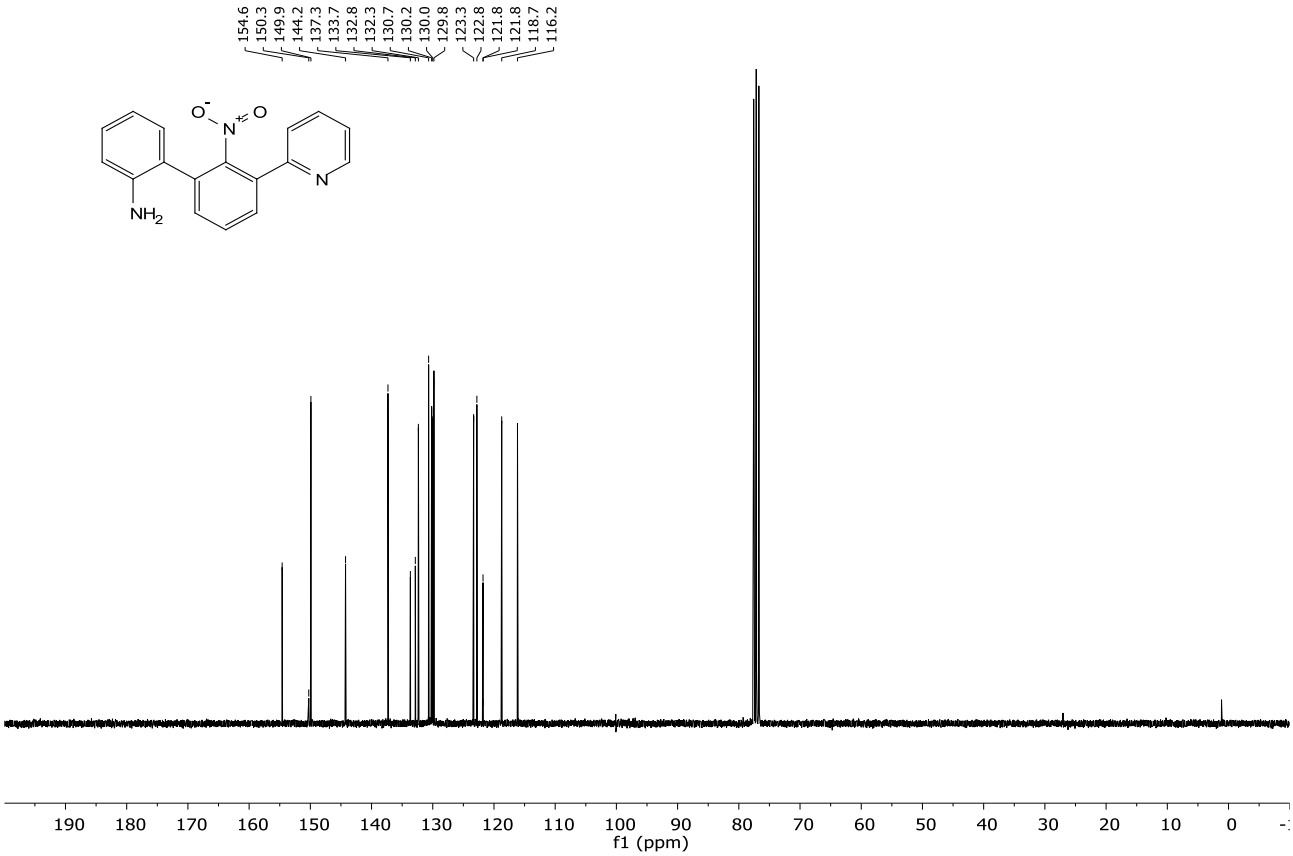

Figure S 16. ^{13}C NMR spectrum (75 MHz, $CDCl_3$) of **20**.

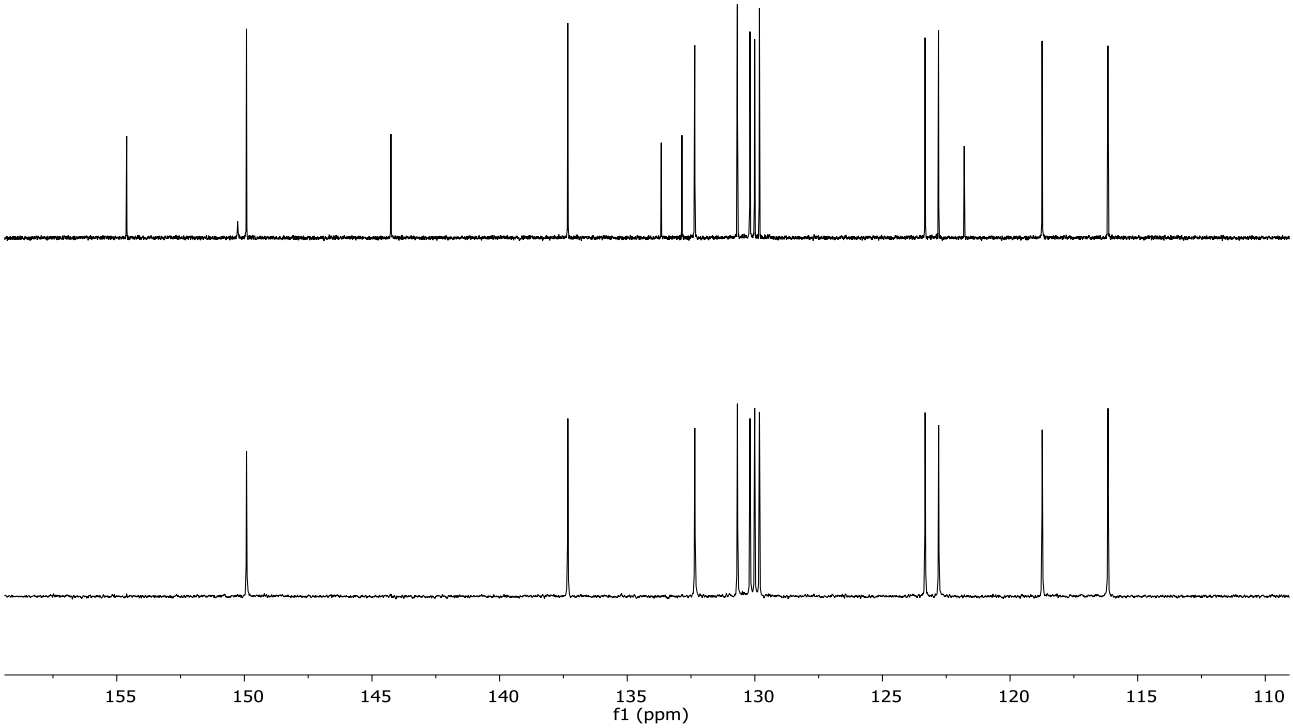

Figure S 17. ^{13}C (top) and dept135 (bottom) **20** in $CDCl_3$.

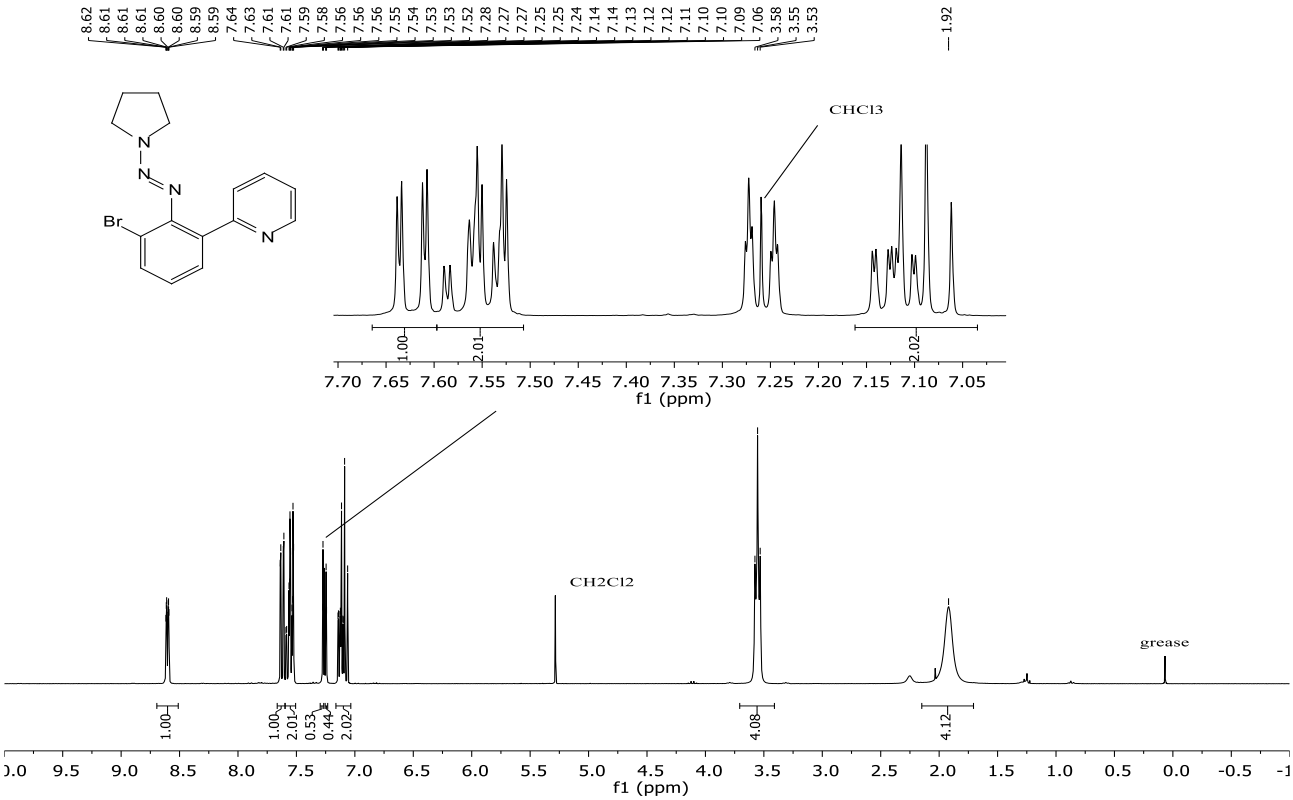

Figure S 18. ^{1}H NMR spectrum (300 MHz, $CDCl_3$) of **24**.

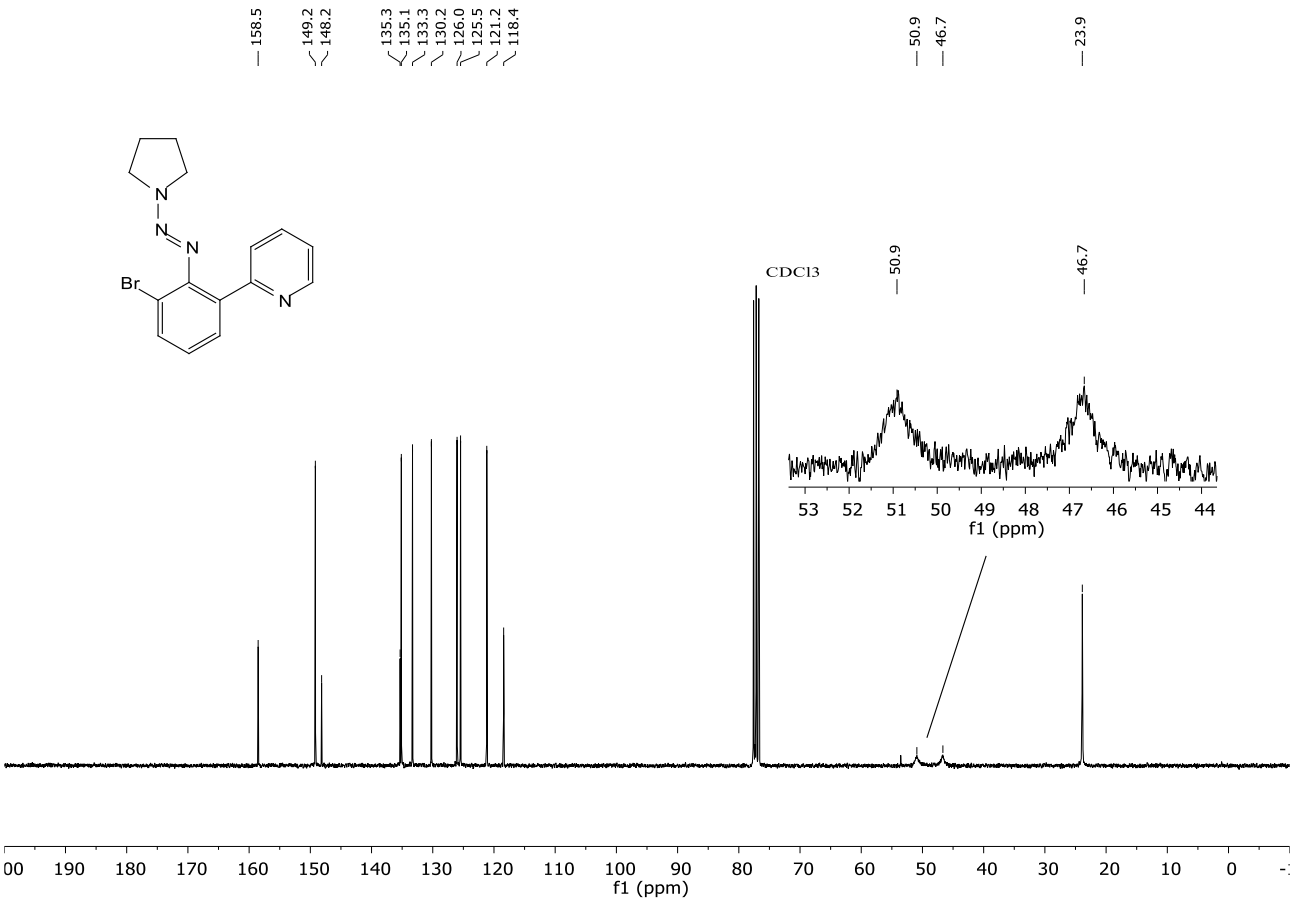

Figure S 19. ^{13}C NMR spectrum (75 MHz, $CDCl_3$) of **24**. The inset shows the two signals of the *NN*-(CH_2) atoms of the pyrrolidine moiety which show different chemical shifts probably due to a hindered rotation around the *N-N*-axis and/or the ability of fast *E/Z*-isomerization of the N-N-double bond. Please refer to the HMQC-spectrum Figure S 20 as well.

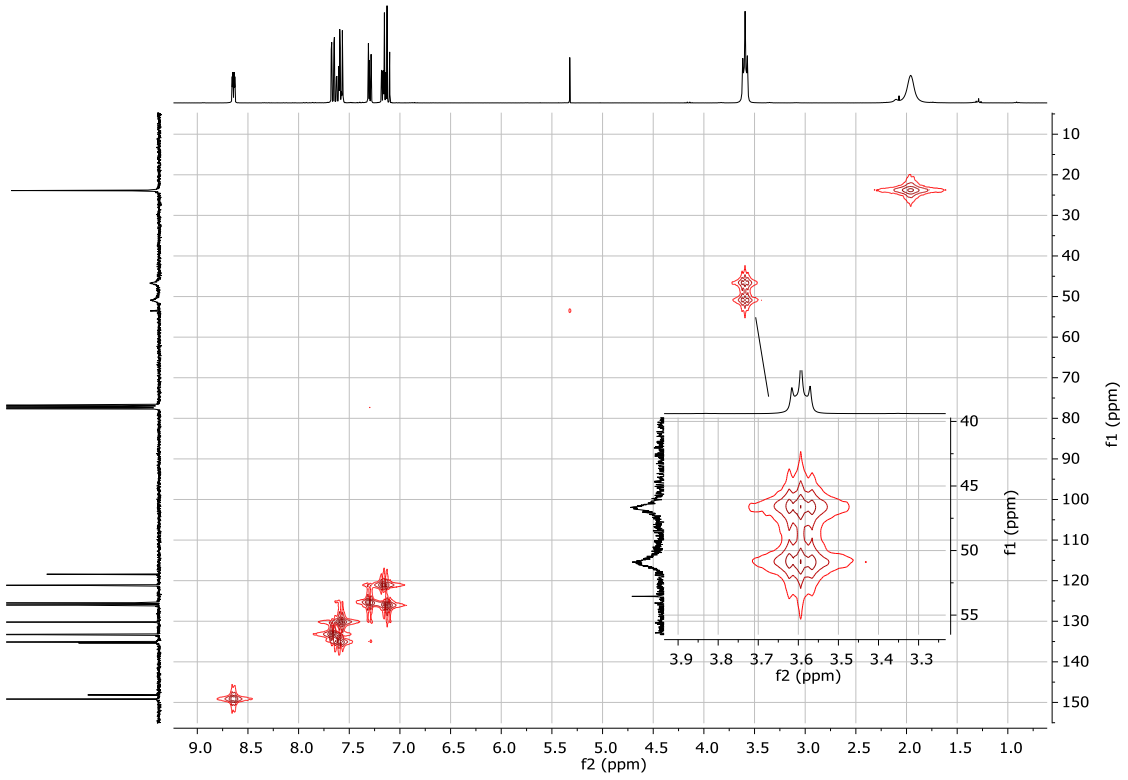

Figure S 20. ^{1}H/^{13}C HMQC of **24** in $CDCl_3$. The inset shows the signals due to the NN-(CH_2) carbon atoms of the pyrrolidine moiety.

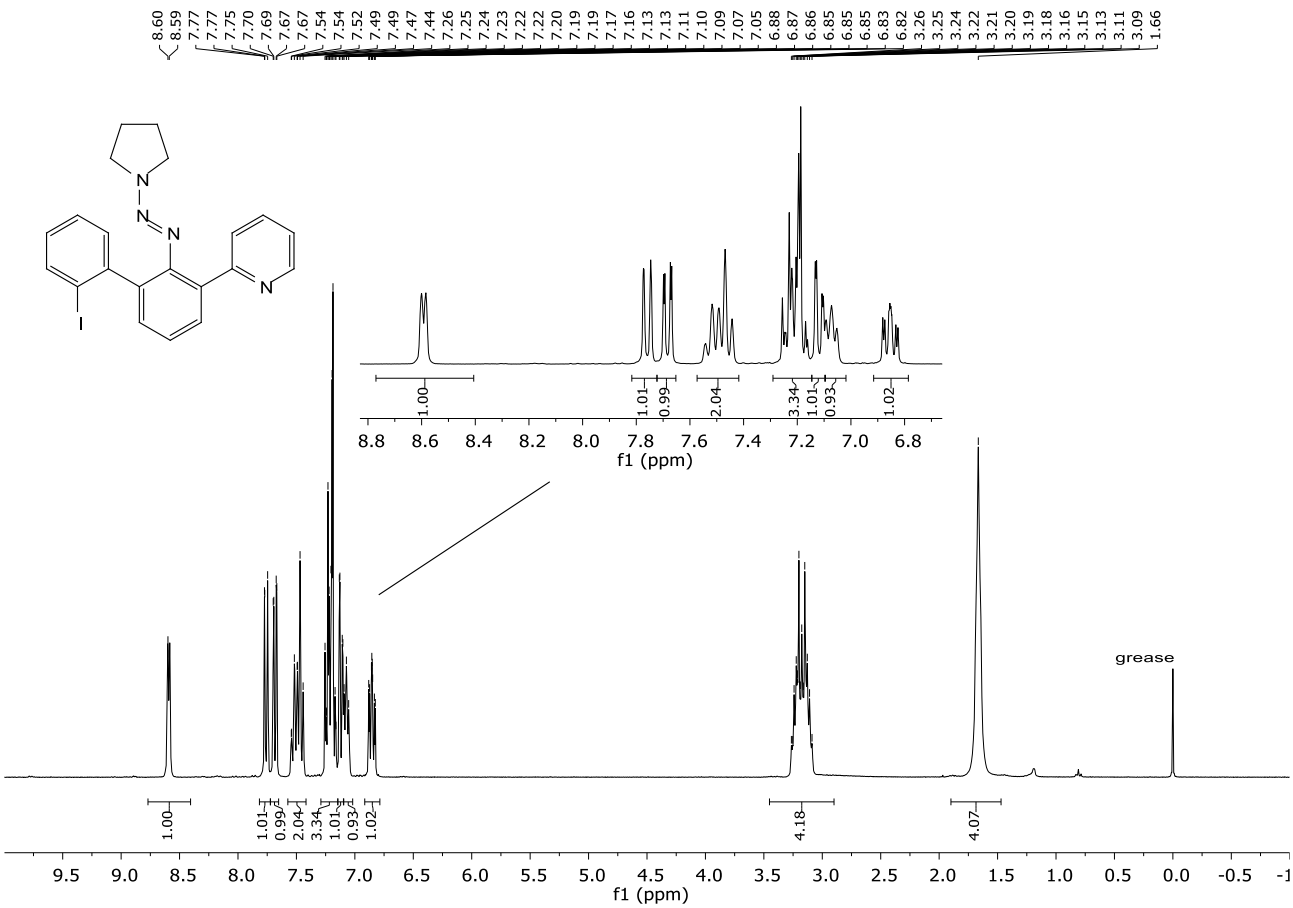

Figure S 21. ^{1}H NMR spectrum (300 MHz, $CDCl_3$) of **25**. One integral in the aromatic region (3.34) contains the proton signal of $CHCl_3$.

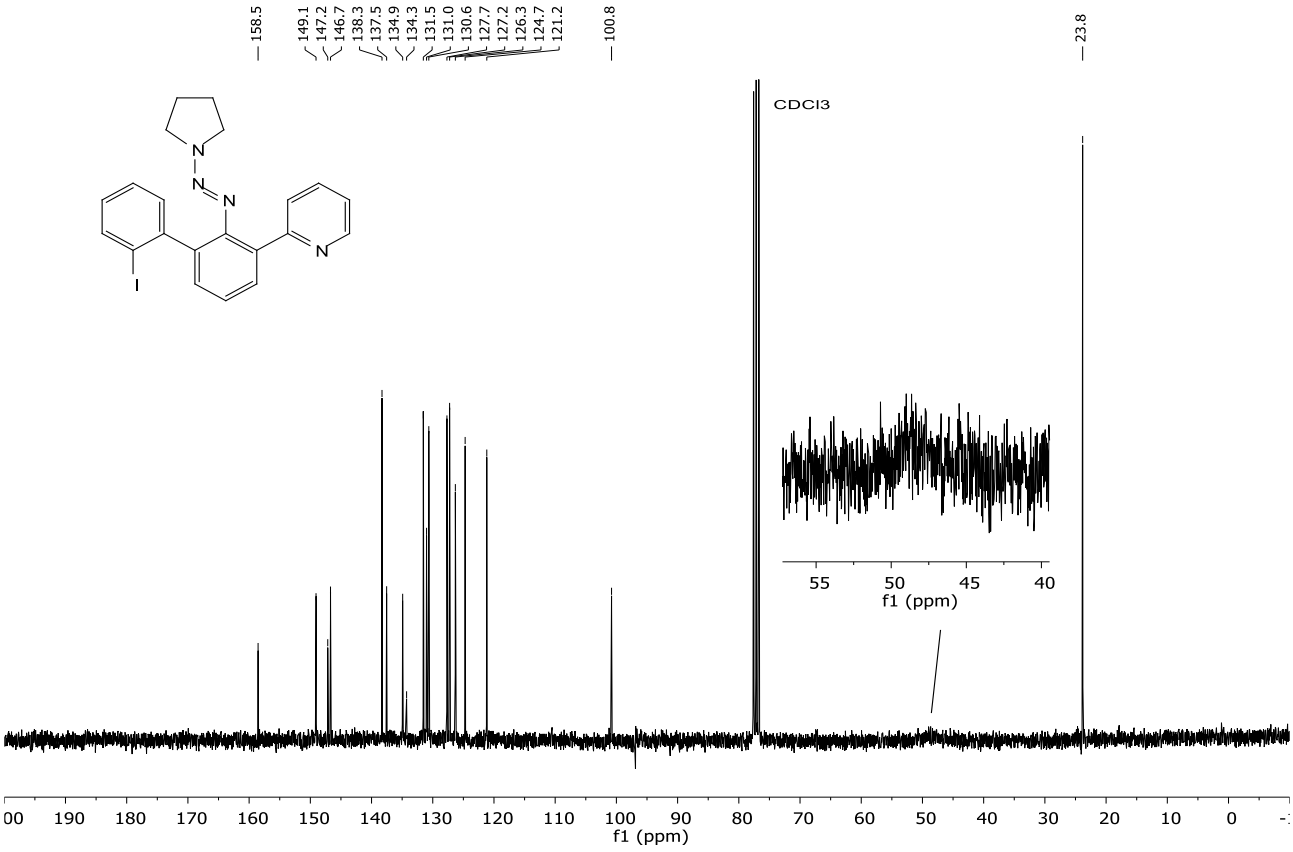

Figure S 22. ^{13}C NMR spectrum (75 MHz, $CDCl_3$) of **25**. Signals of the NN-(CH_2) atoms of the pyrrolidine moiety are significantly broadened probably due to hindered rotation around the *N-N*-axis and/or the ability of fast *E/Z*-isomerization of the N-N-double bond.

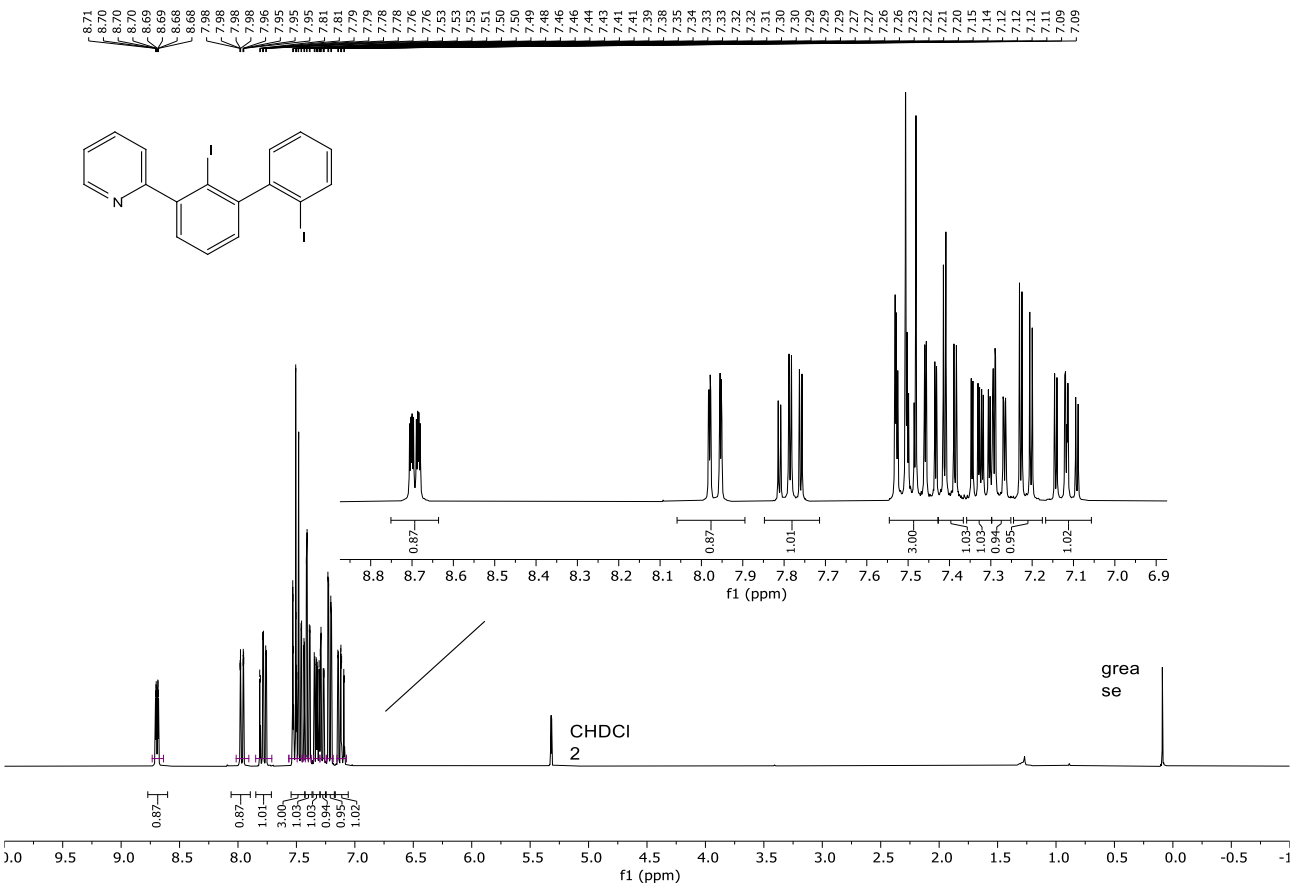

Figure S 23. ^{1}H NMR spectrum (300 MHz, CD_2Cl_2) of **26**.

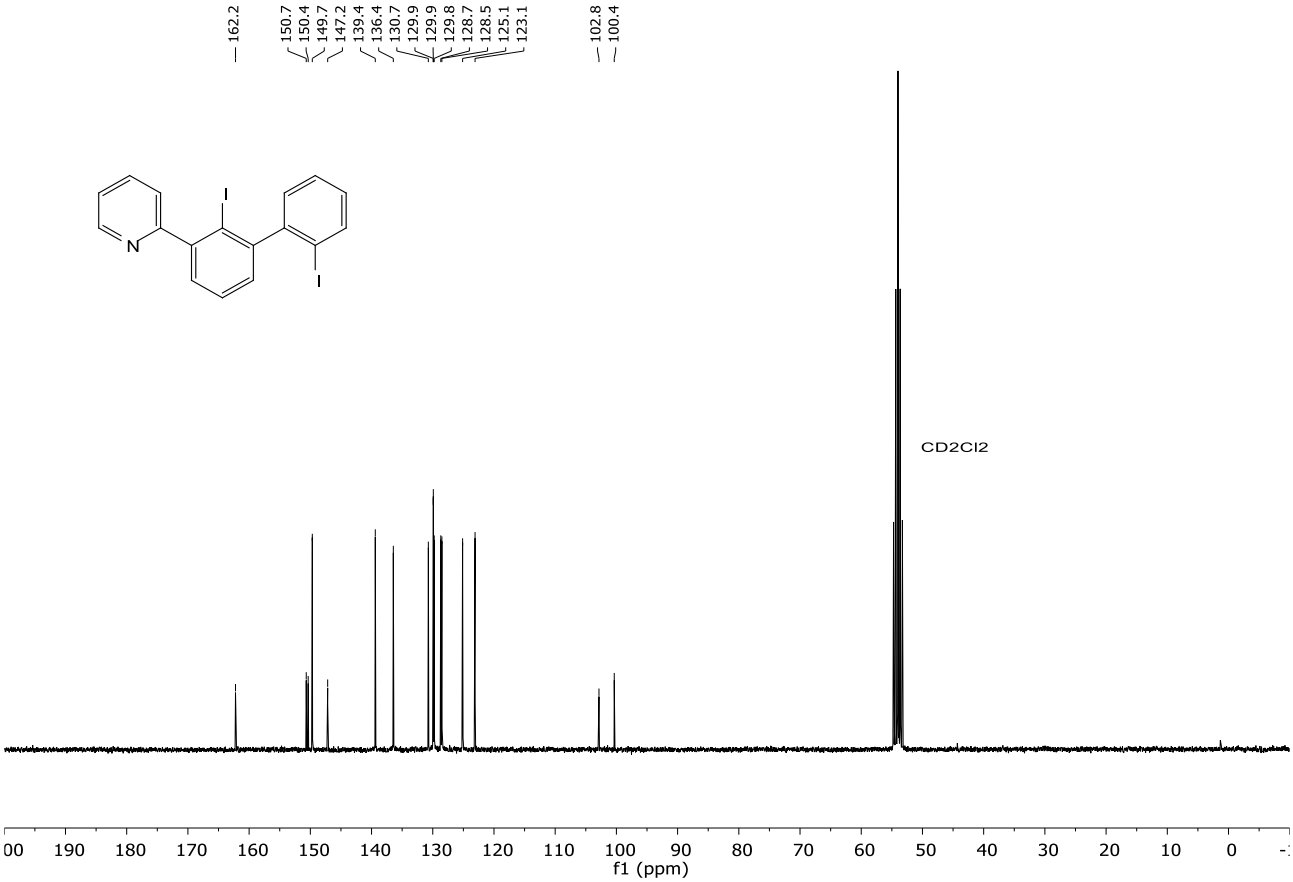

Figure S 24. ^{13}C NMR spectrum (75 MHz, CD_2Cl_2) of **26**.

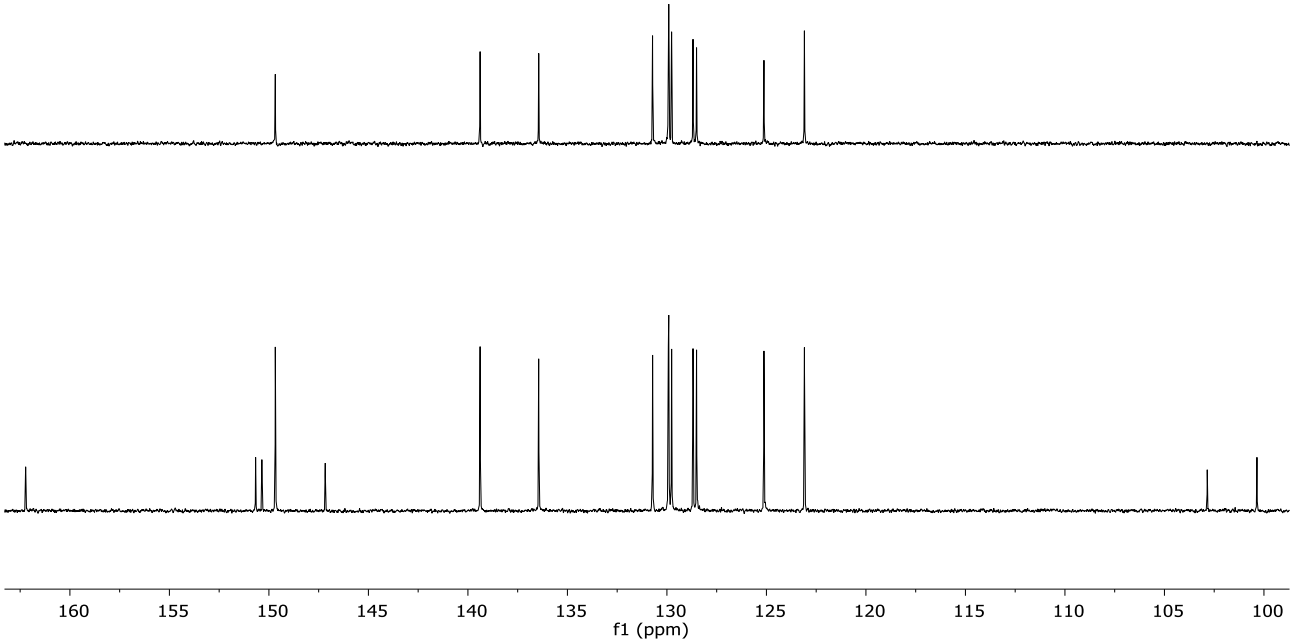

Figure S 25. Dept135 (top) and ^{13}C (bottom) spectra of **26**.

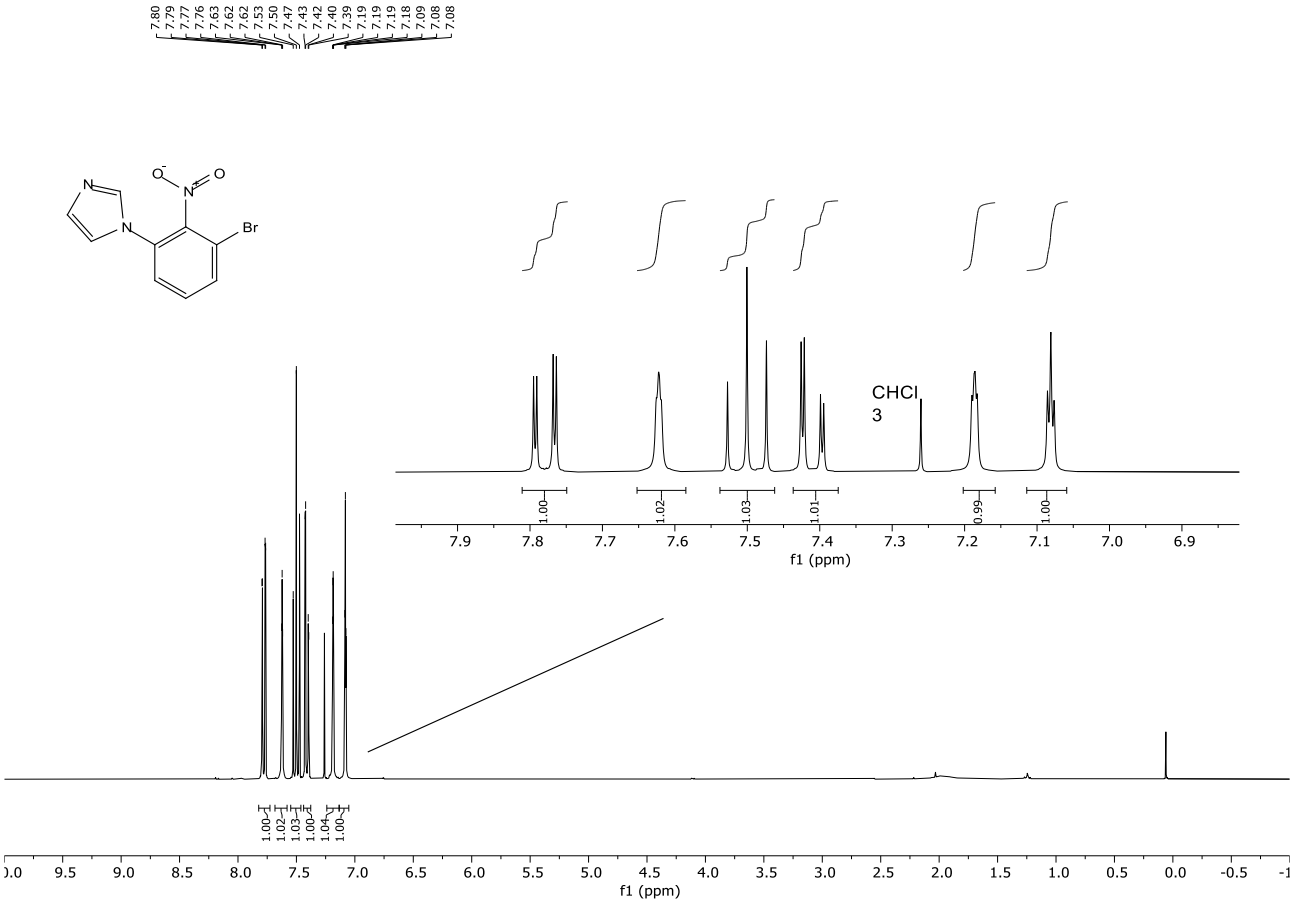

Figure S 26. ^{1}H NMR (300 MHz, CDCl3) of **28**.

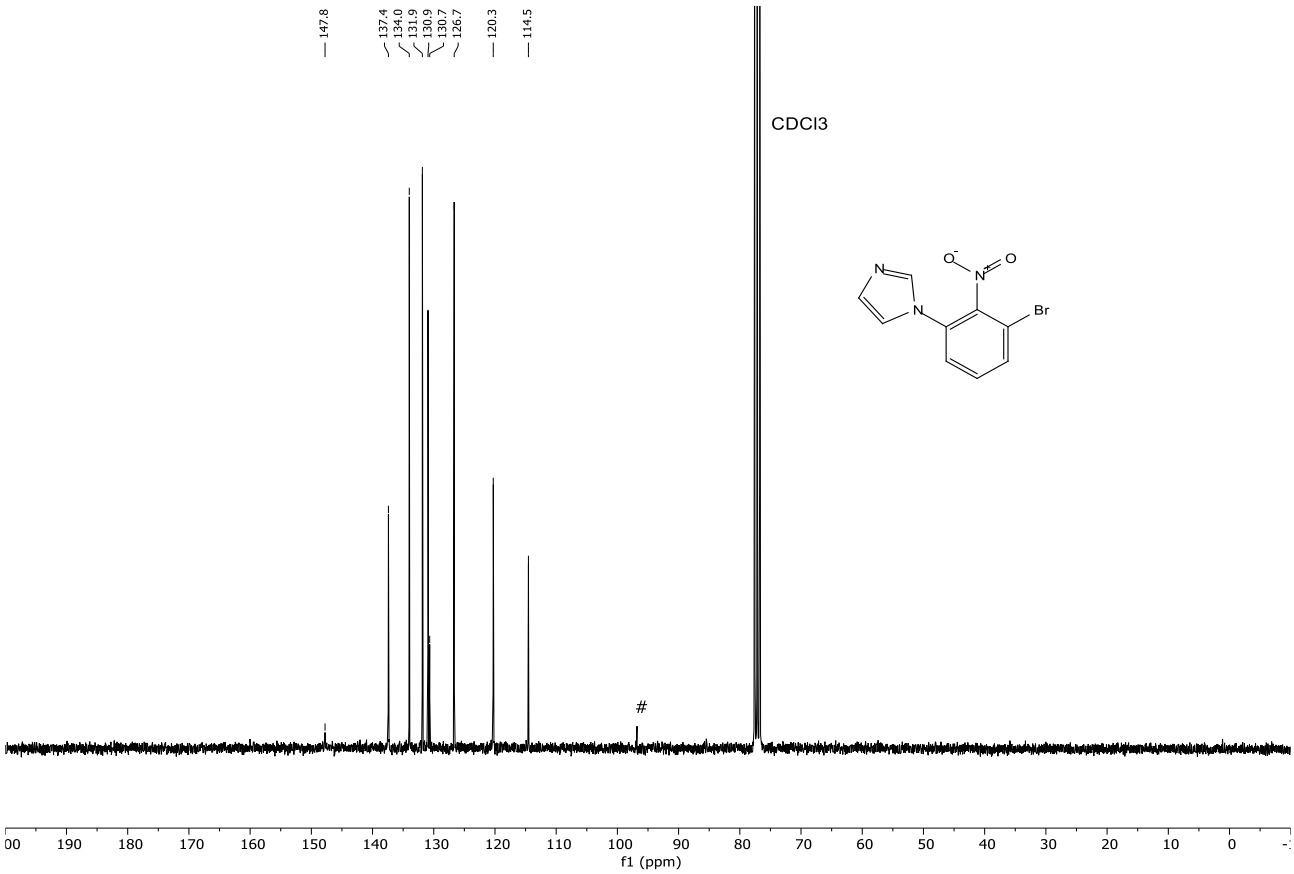

Figure S 27. ^{13}C NMR (75 MHz, $CDCl_3$) of **28**. The signal marked with # is due to an artefact of the spectrometer.

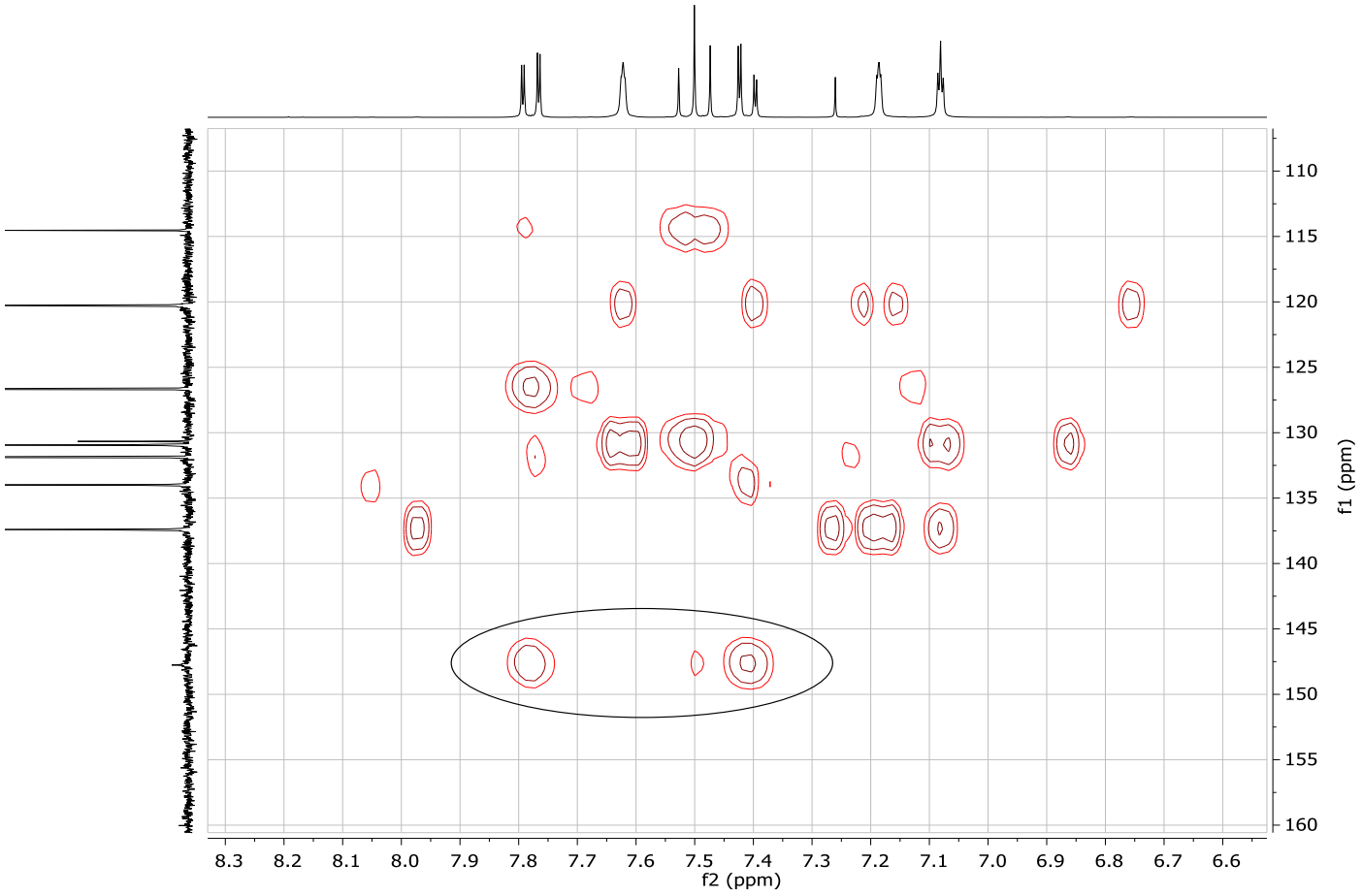

Figure S 28: ^{1}H/^{13}C HMBC spectrum of **28** in $CDCl_3$. The marked signals belong to the quaternary carbon bound to the nitro group which is of very poor intensity in ^{13}C NMR.

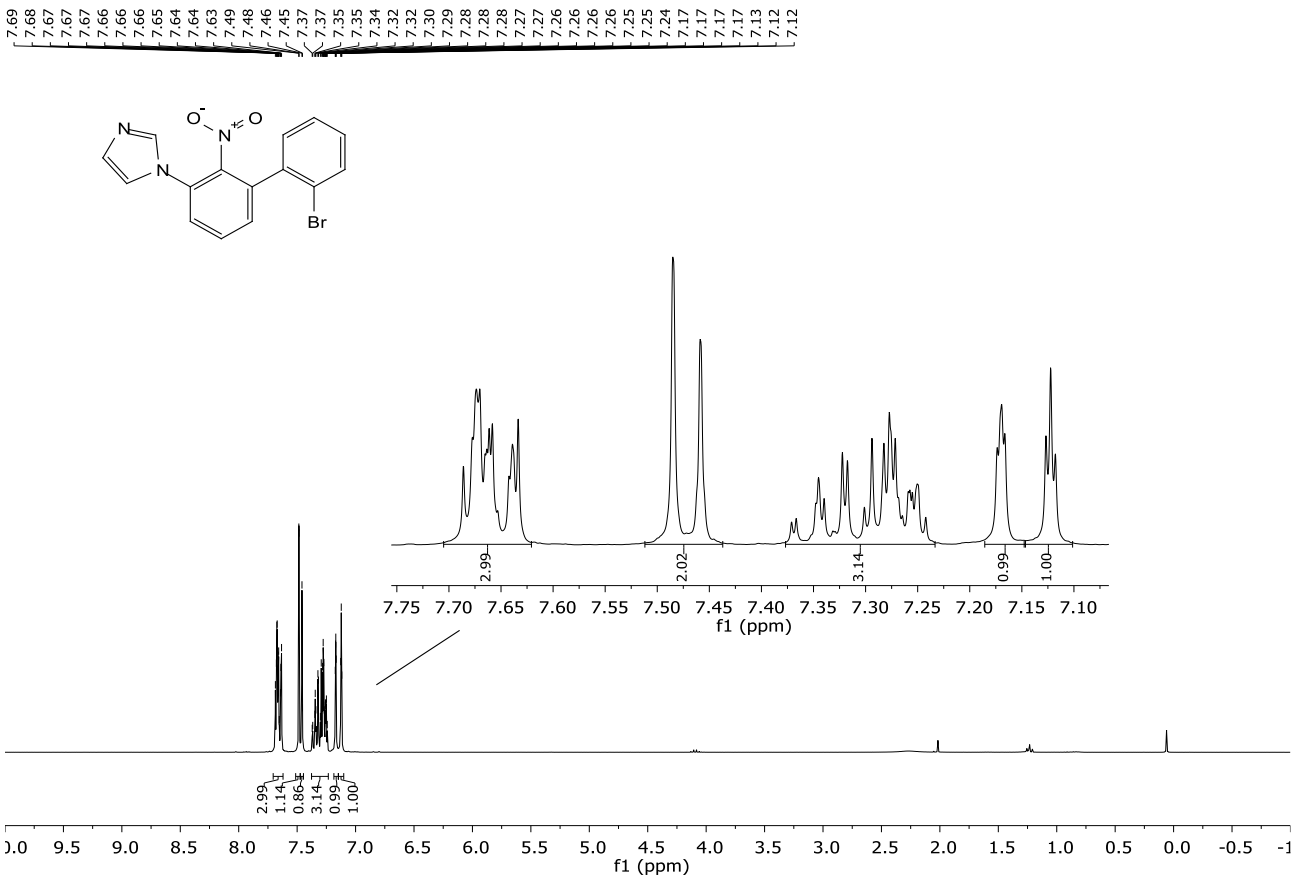

Figure S 29. ^{1}H NMR (300 MHz, $CDCl_3$) of **29**.

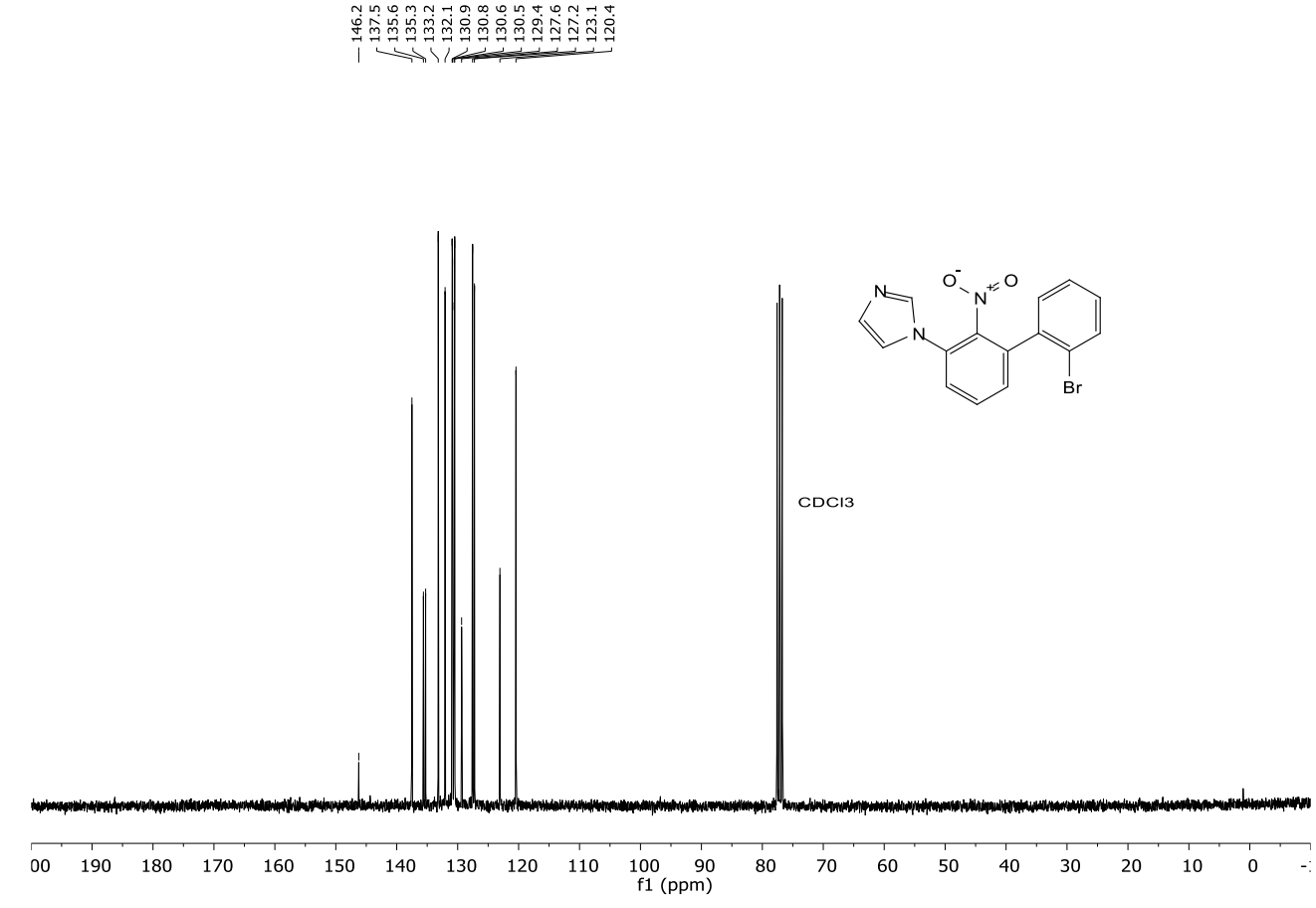

Figure S 30. ^{13}C NMR (75 MHz, $CDCl_3$) of **29**.

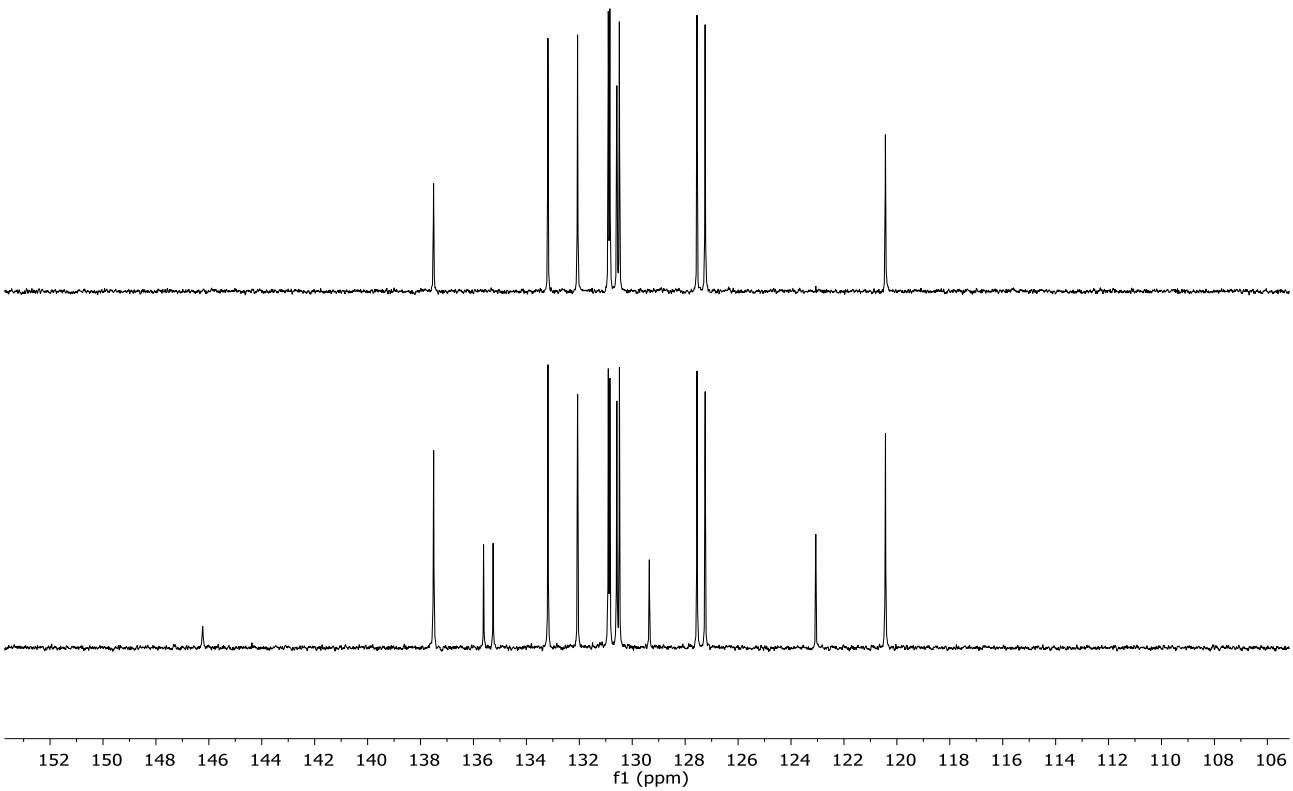

Figure S 31. Dept90 (top) and ^{13}C NMR (bottom) of **29** in $CDCl_3$.

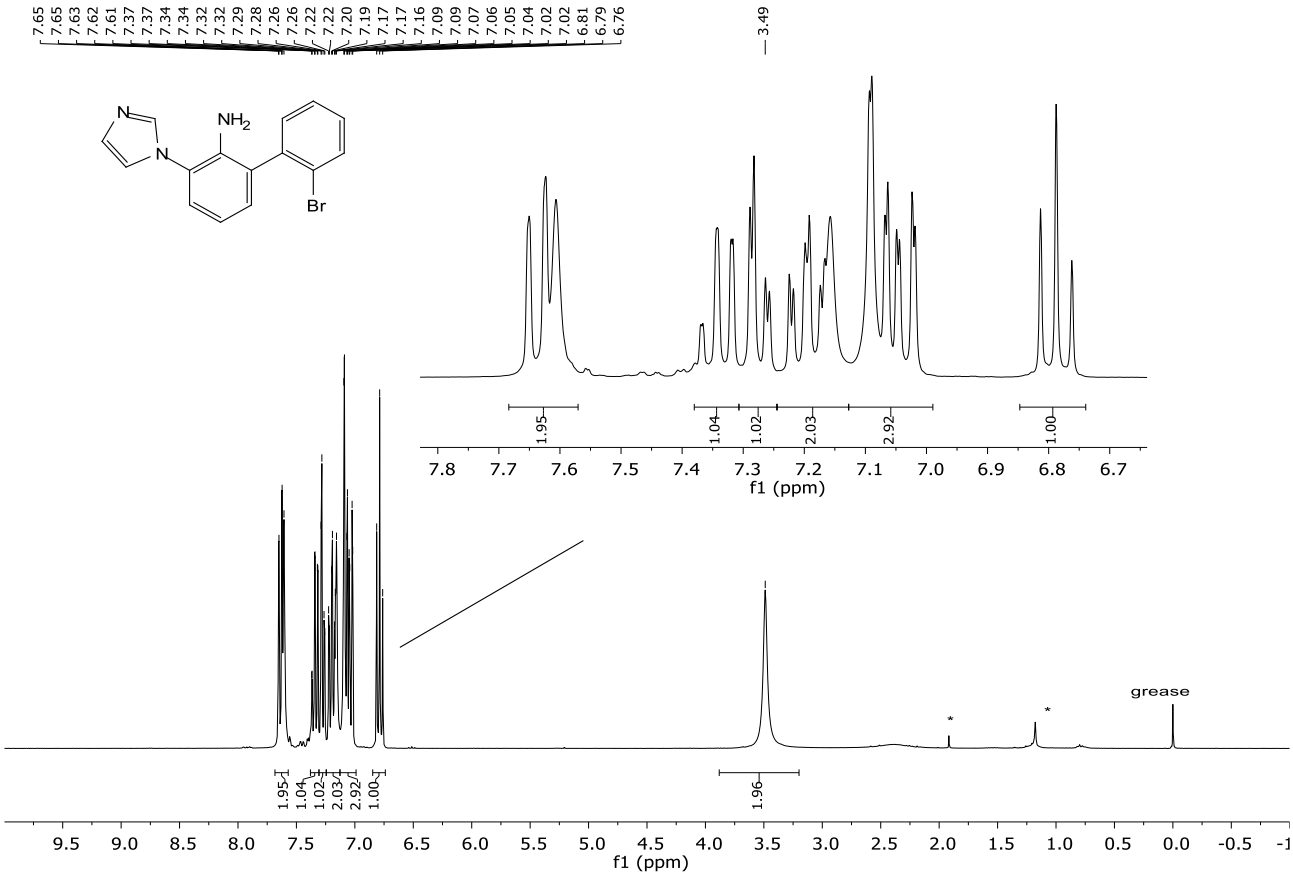

Figure S 32. ^{1}H NMR (300 MHz, $CDCl_3$) of **30**. Impurities are marked with an asterisk.

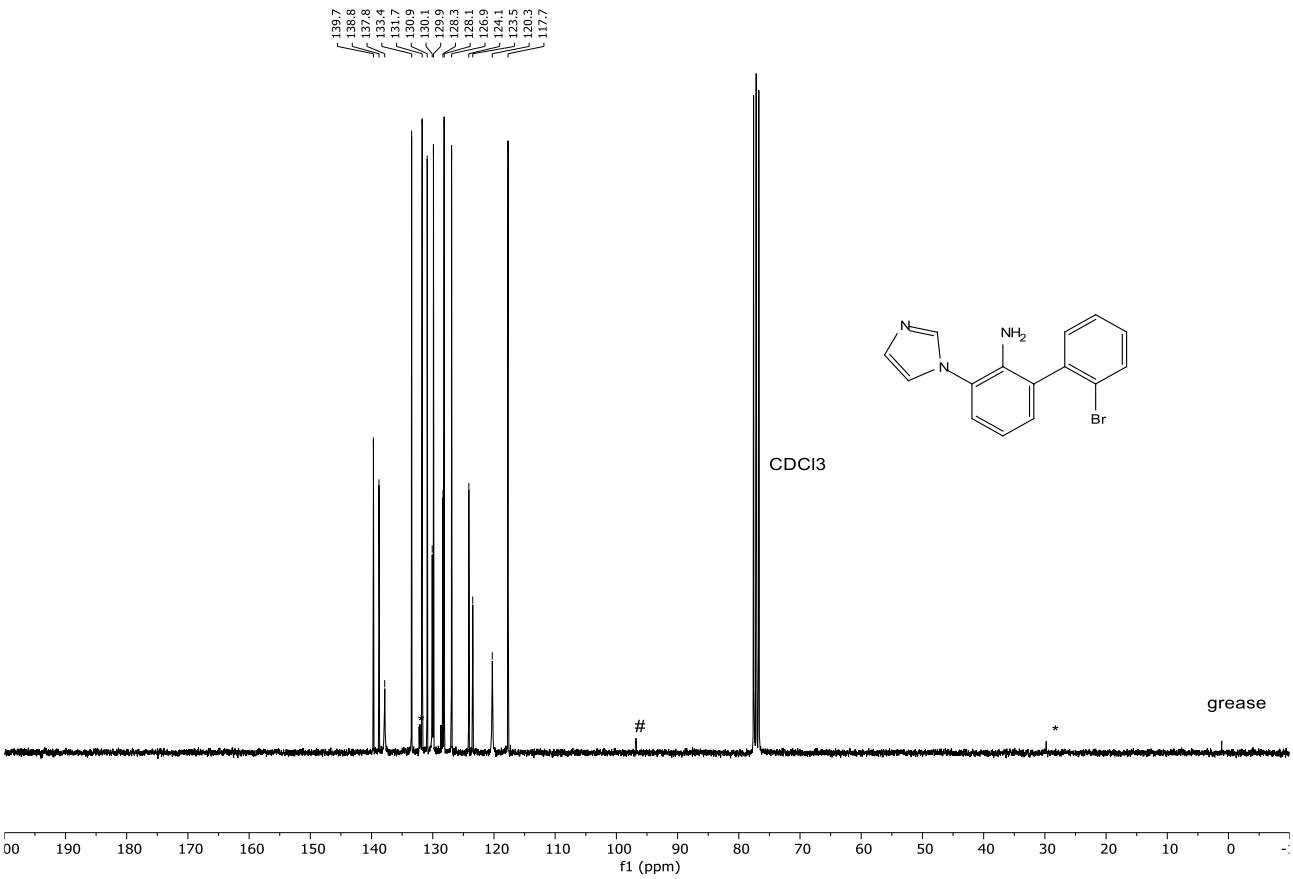

Figure S 33. 13C NMR (75 MHz, $CDCl_3$) of **30**. Impurities are marked with an asterisk. The signal marked with a # is due to an artefact of the spectrometer.

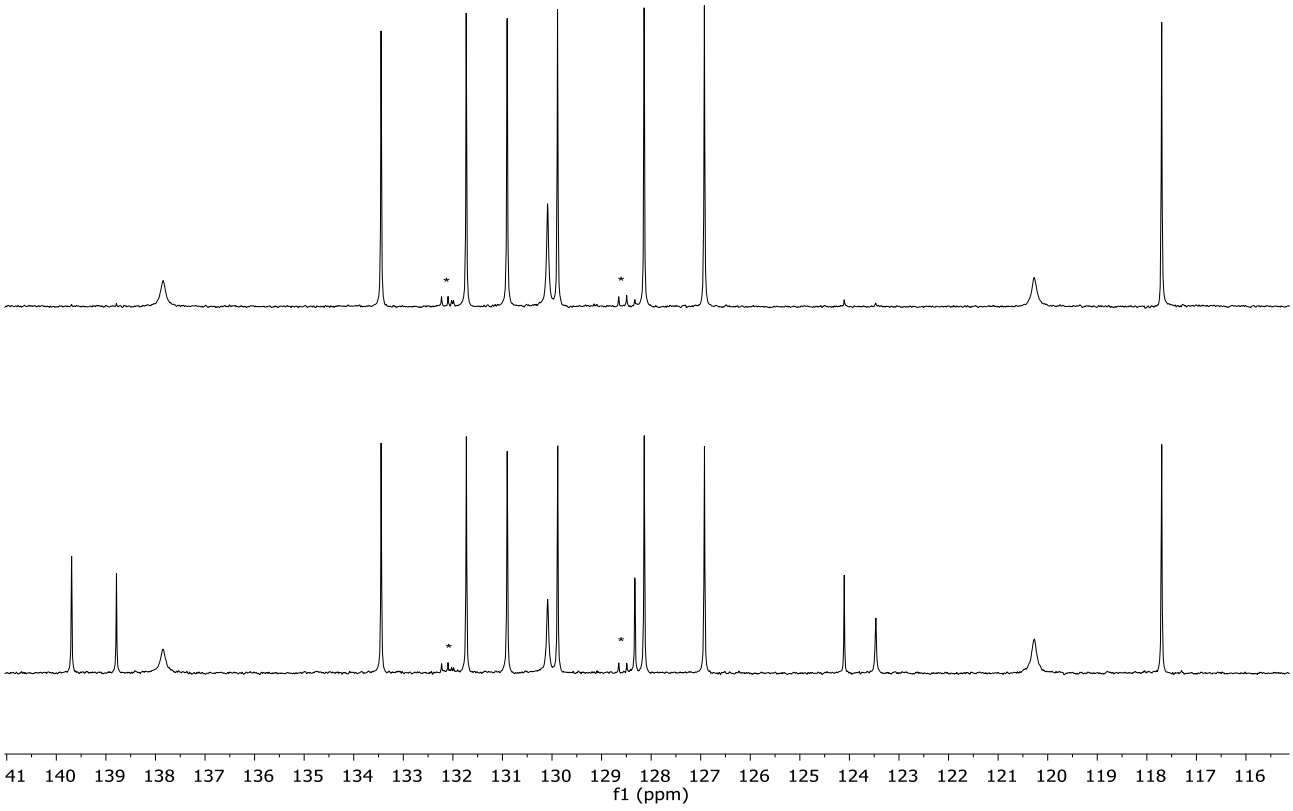

Figure S 34. Dept90 (top) and ^{13}C NMR (bottom) of **30** in $CDCl_3$. Impurities are marked with an asterisk.

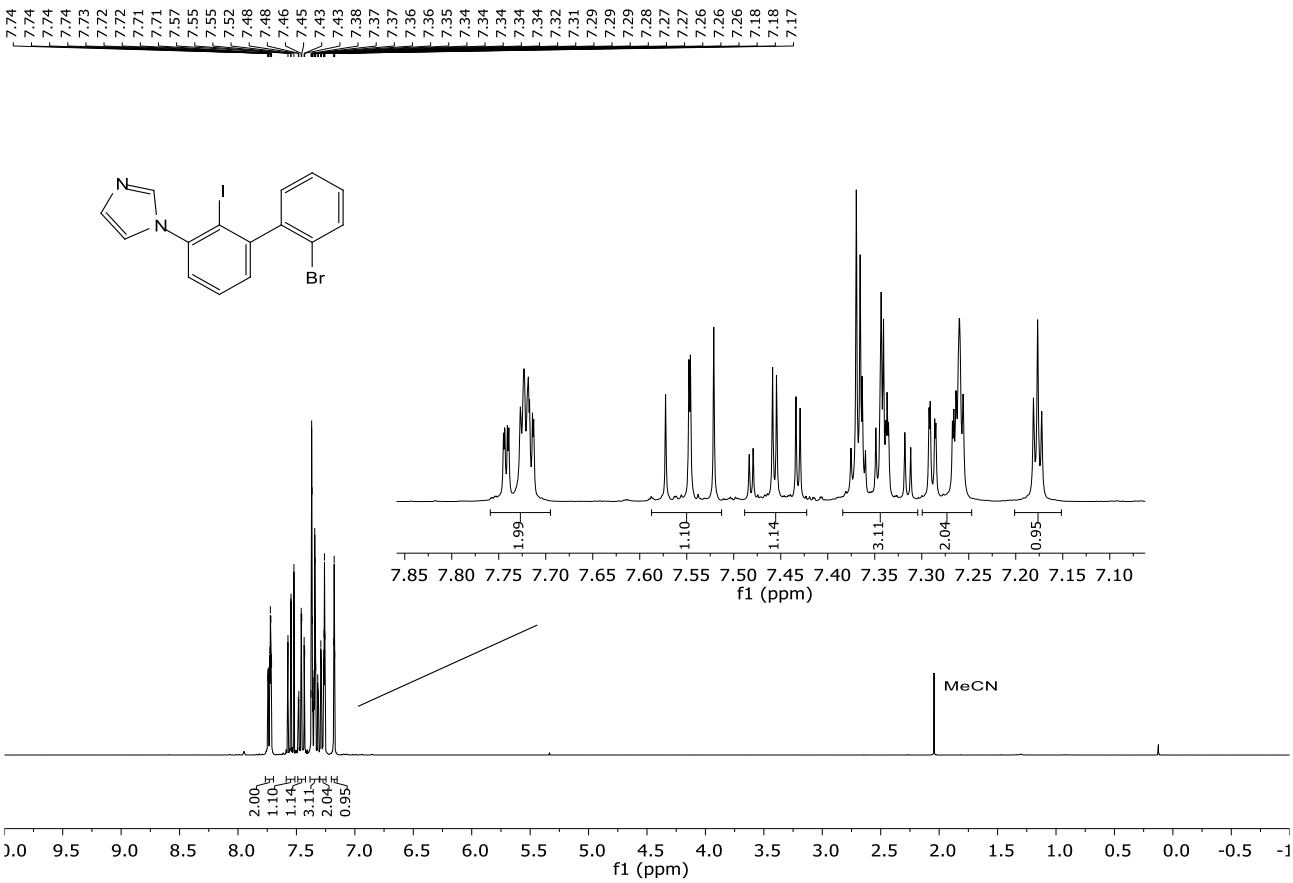

Figure S 35. ^{1}H NMR (300 MHz, $CDCl_3$) of **31**.

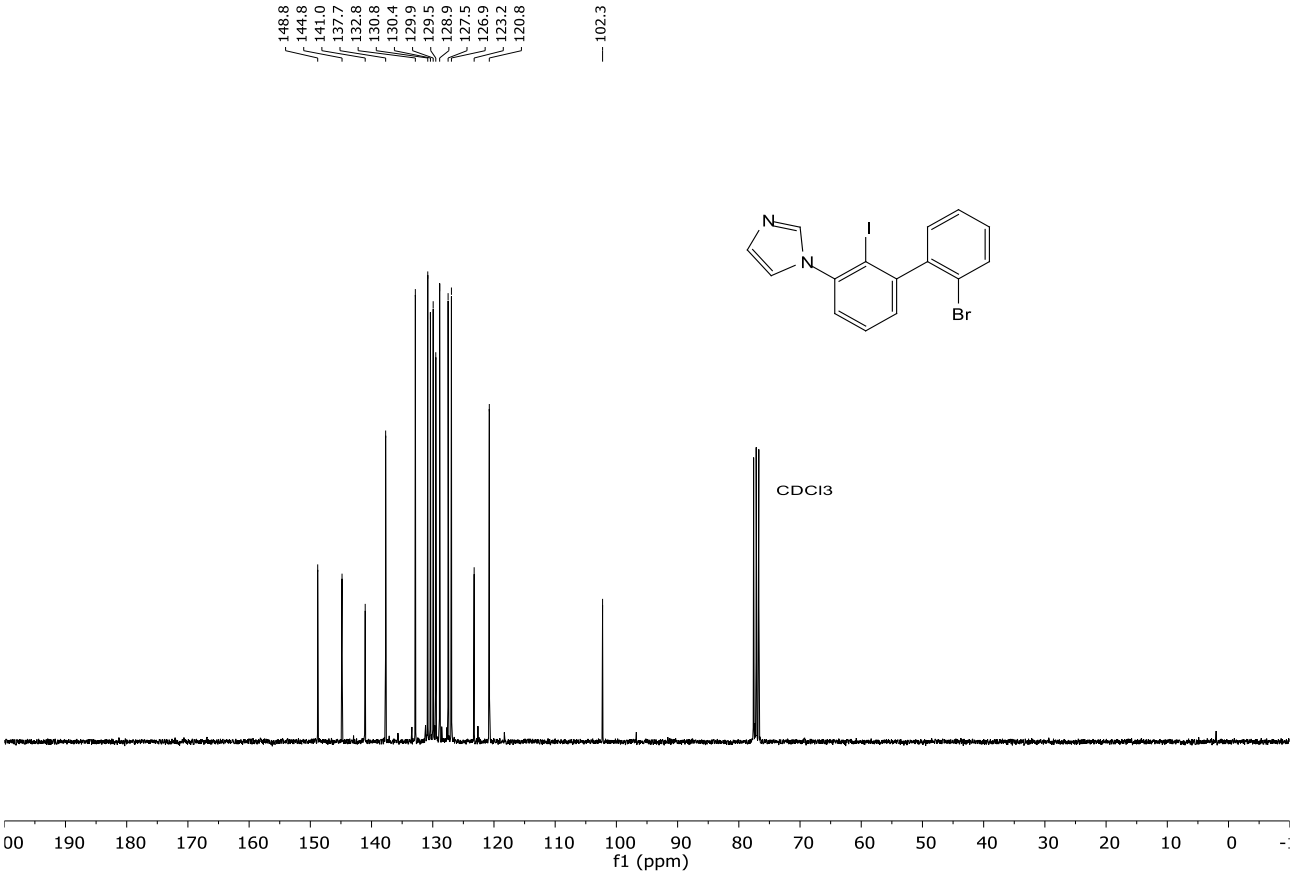

Figure S 36. ^{13}C NMR (75 MHz, $CDCl_3$) of **31**.

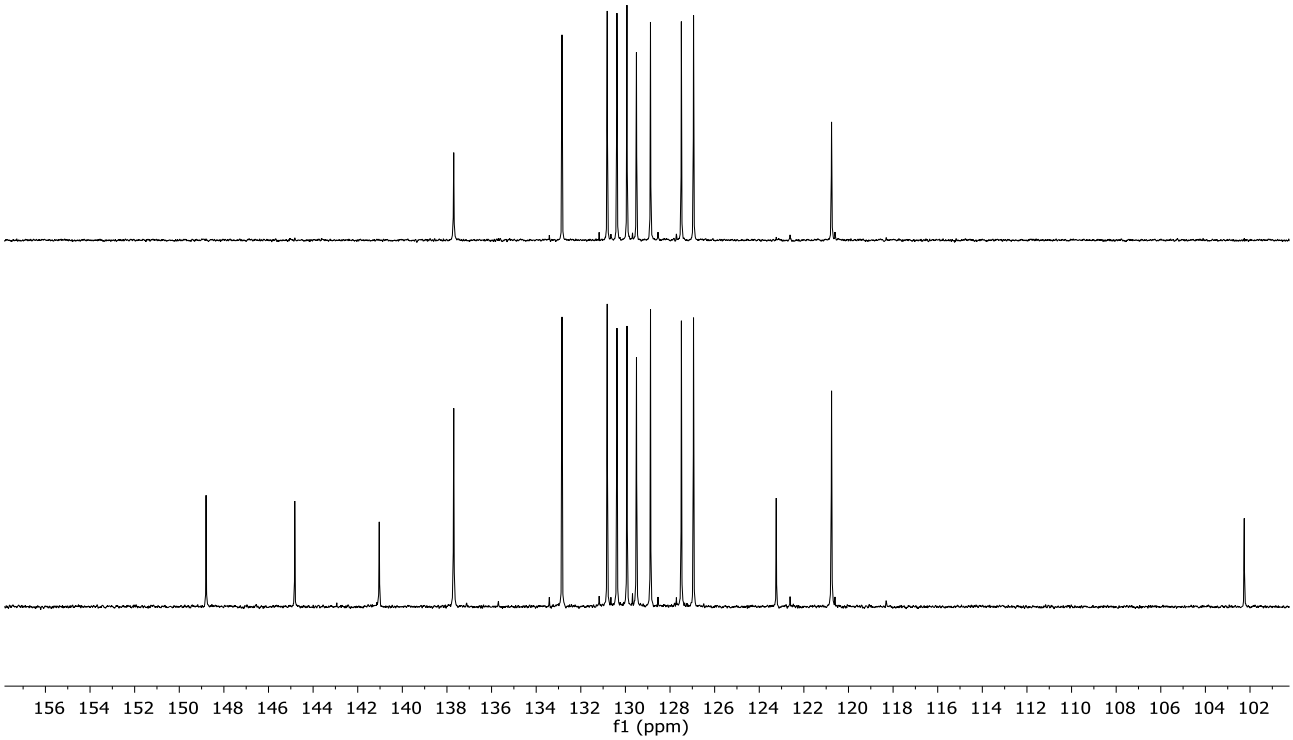

Figure S 37. Dept135 (top) and ^{13}C NMR (bottom) of **31** in $CDCl_3$.

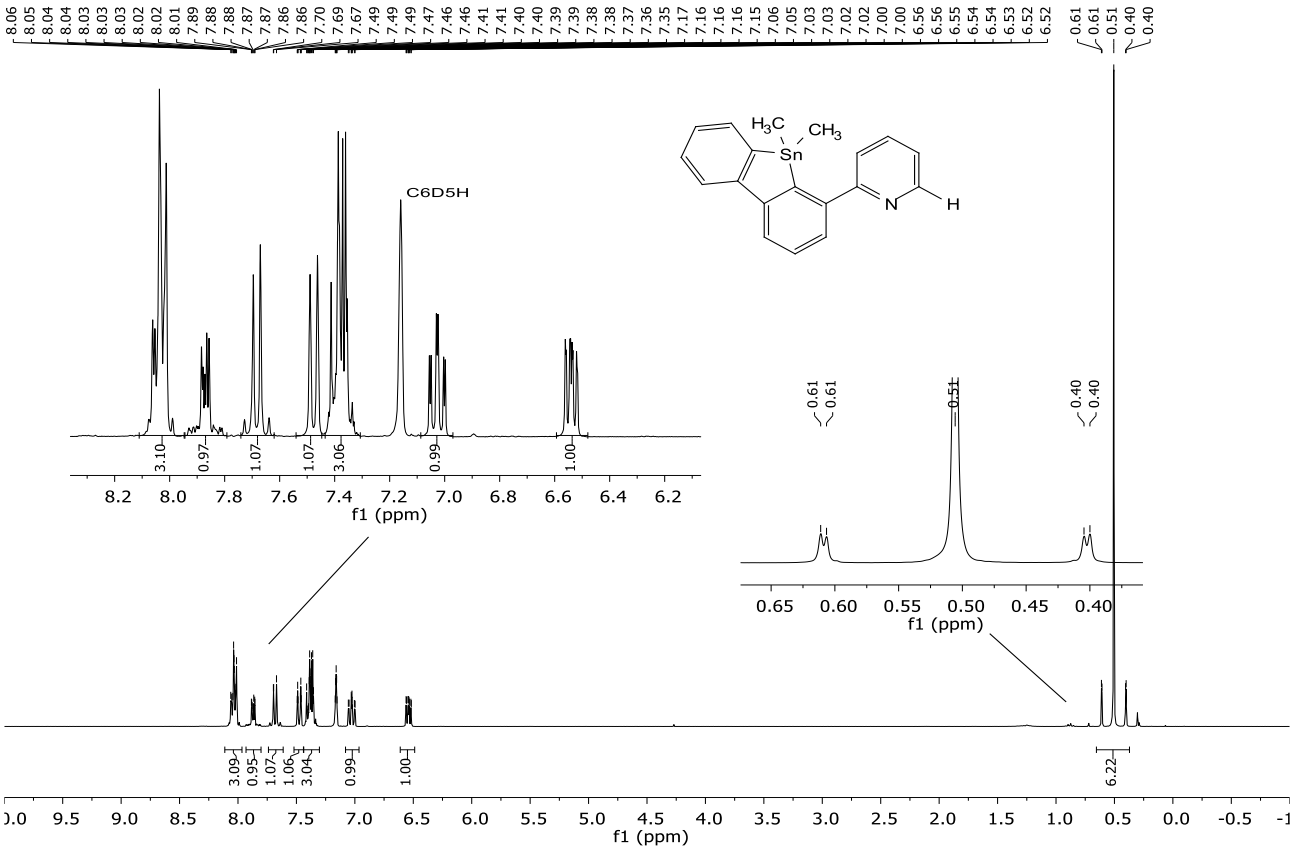

Figure S 38. ^{1}H NMR spectrum (300 MHz, C_6D_6) of **32**. Signals at δ = 0.51 ppm, δ = 7.69 ppm and δ = 7.87 ppm show characteristic $^{117}Sn/^{119}Sn$ couplings. The signal of the proton in α-position to pyridine-N appears at δ = 6.54 ppm.

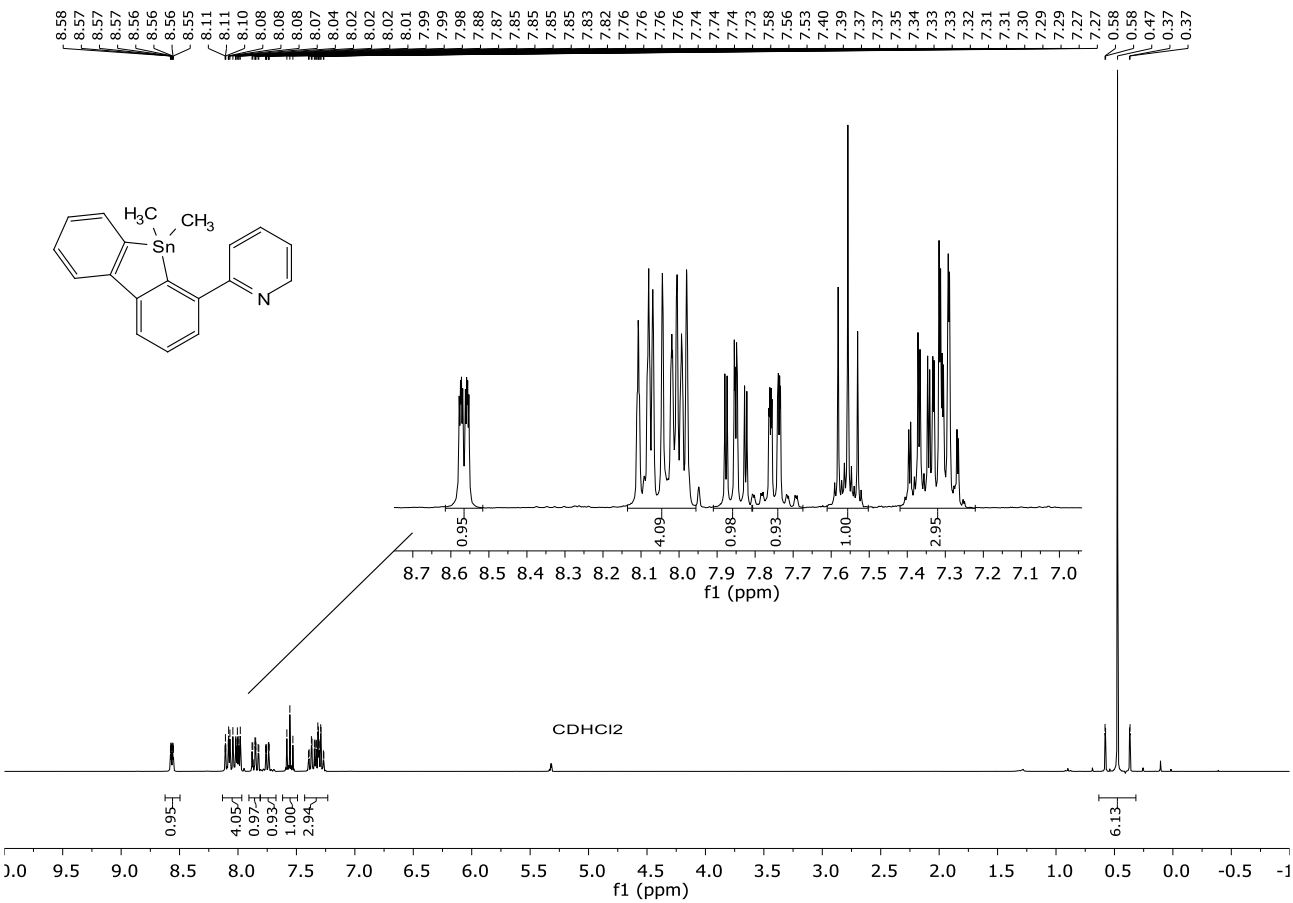

Figure S 39. ^{1}H NMR spectrum (300 MHz, CD_2Cl_2) of **32**. In CD_2Cl_2, the signal of the proton in α-position to pyridine-N is significantly shifted to lower fields (δ = 8.57 ppm) compared to C_6D_6 (cf. Figure S 38). This may be due to coordination of the pyridine ring to the central Sn atom in the less polar solvent benzene generating a pentacoordinated tin centre.

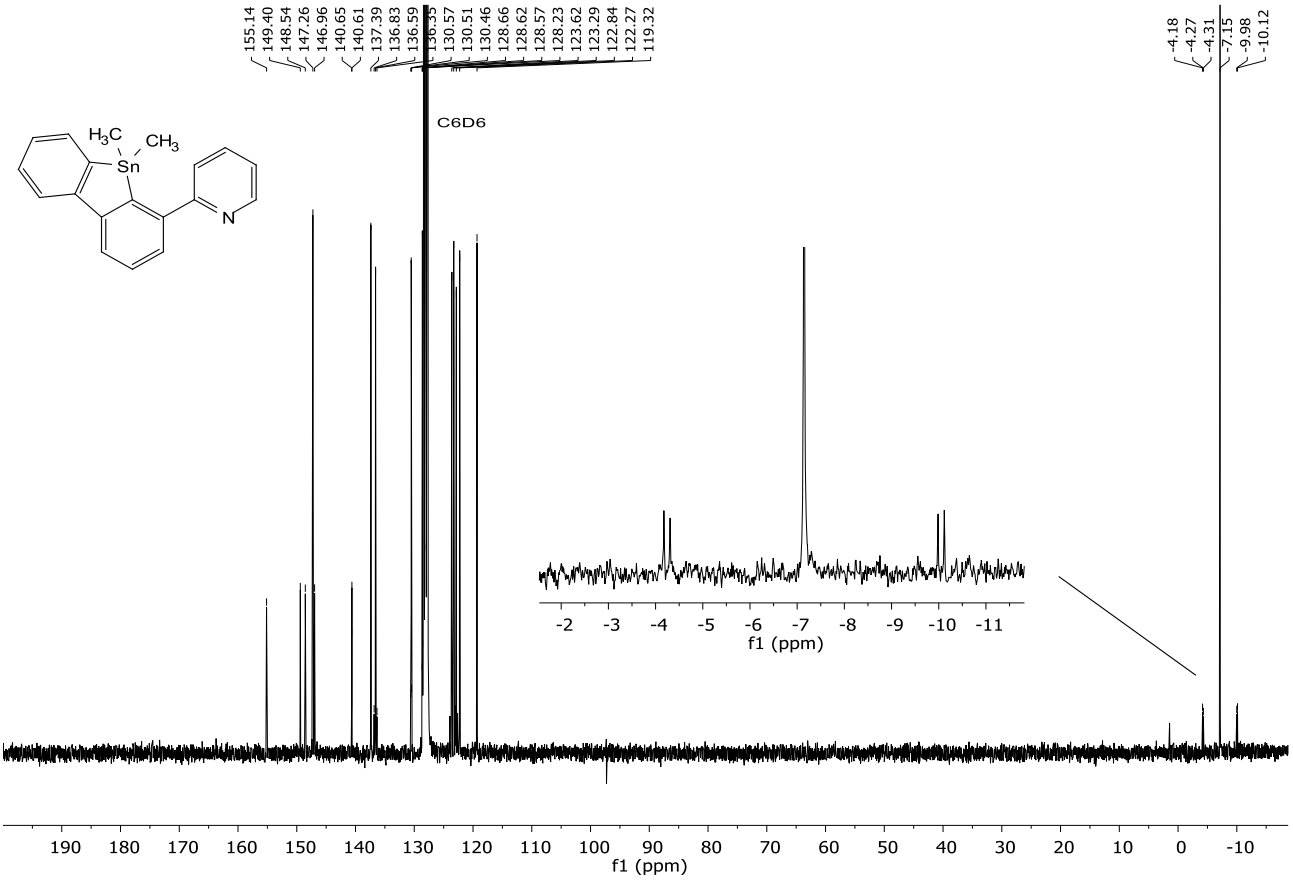

Figure S 40. ^{13}C NMR spectrum (75 MHz, C_6D_6) of **32**. The inset shows the ^{117}Sn/^{119}Sn satellites of the methyl group's ^{13}C signal.

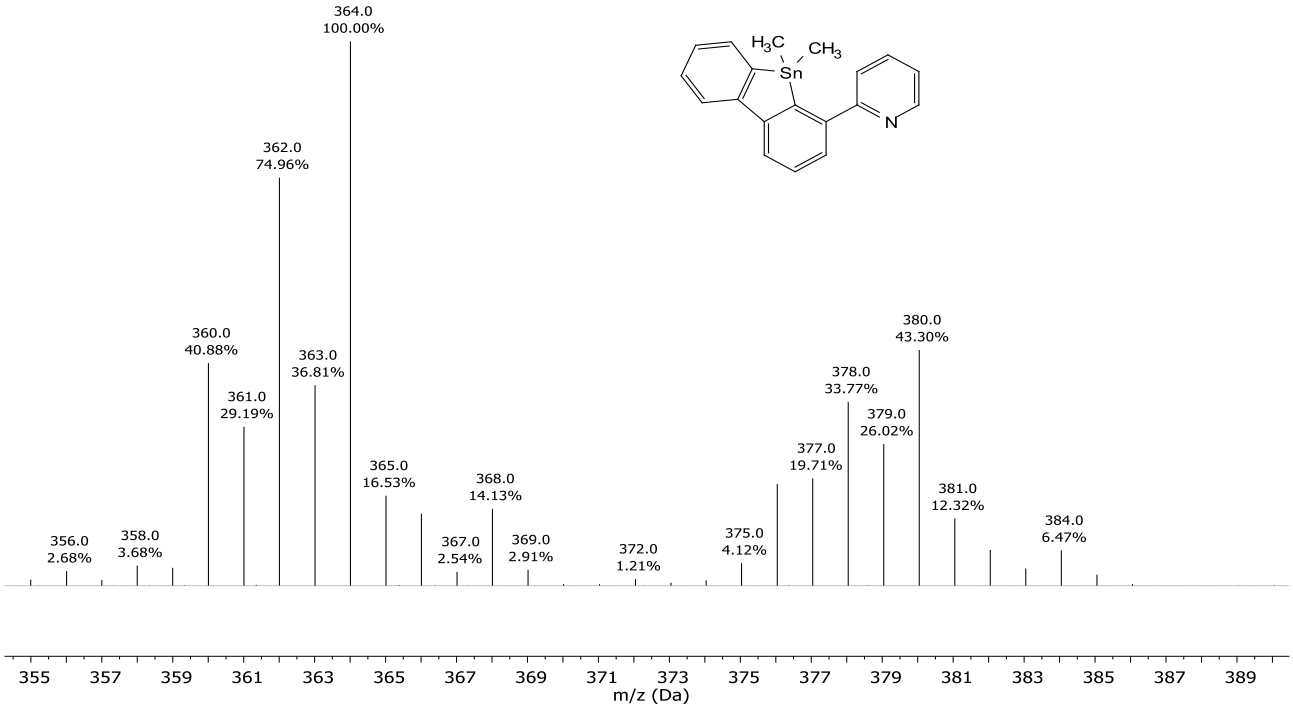

Figure S 41. EI-MS (70 eV) mass spectrum of **32** showing the $[M+H]^+$ and $[M-CH_3]^+$ peaks and typical Sn isotopic patterns (intensity in arbitrary units).

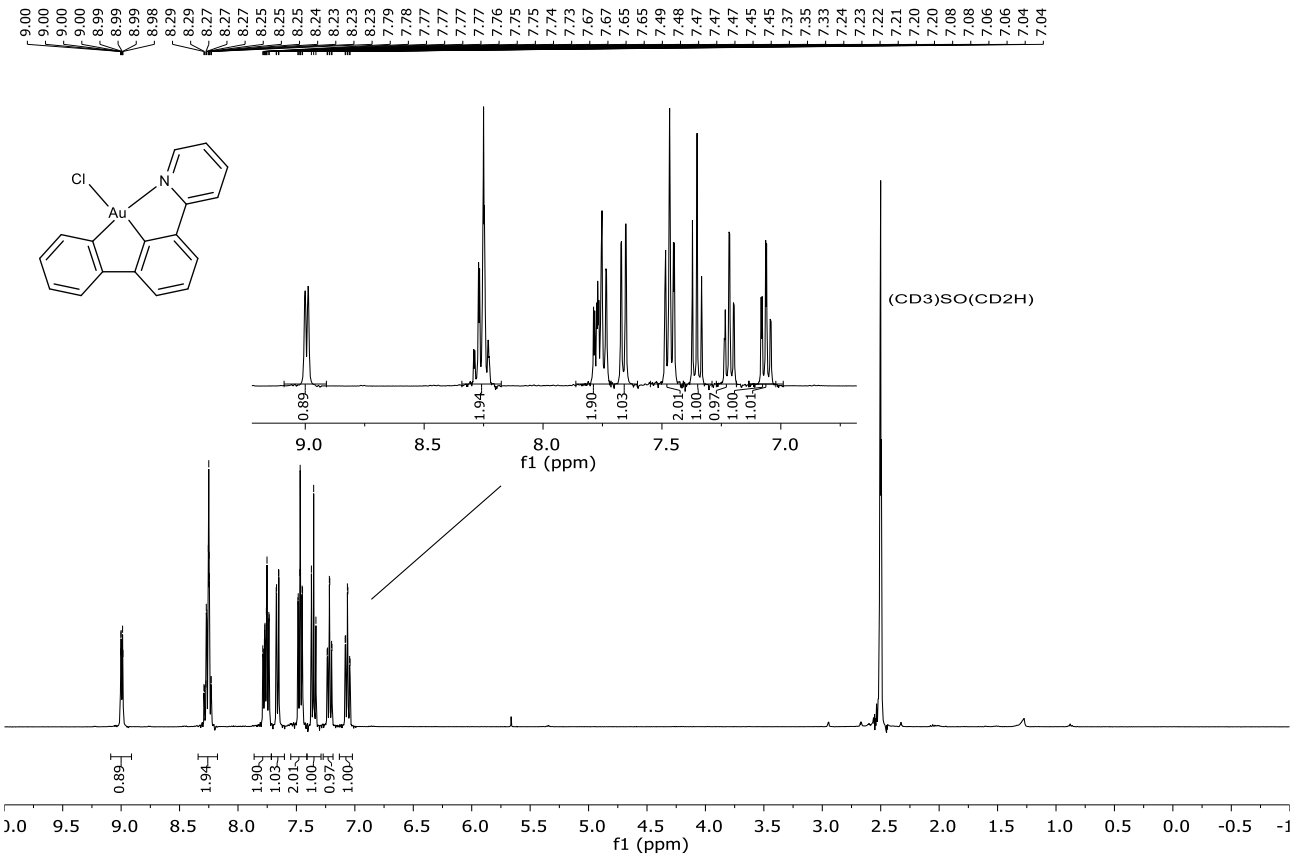

Figure S 42. ^{1}H NMR spectrum (400 MHz, DMSO-*d6*) of **33** recorded at 373 K.

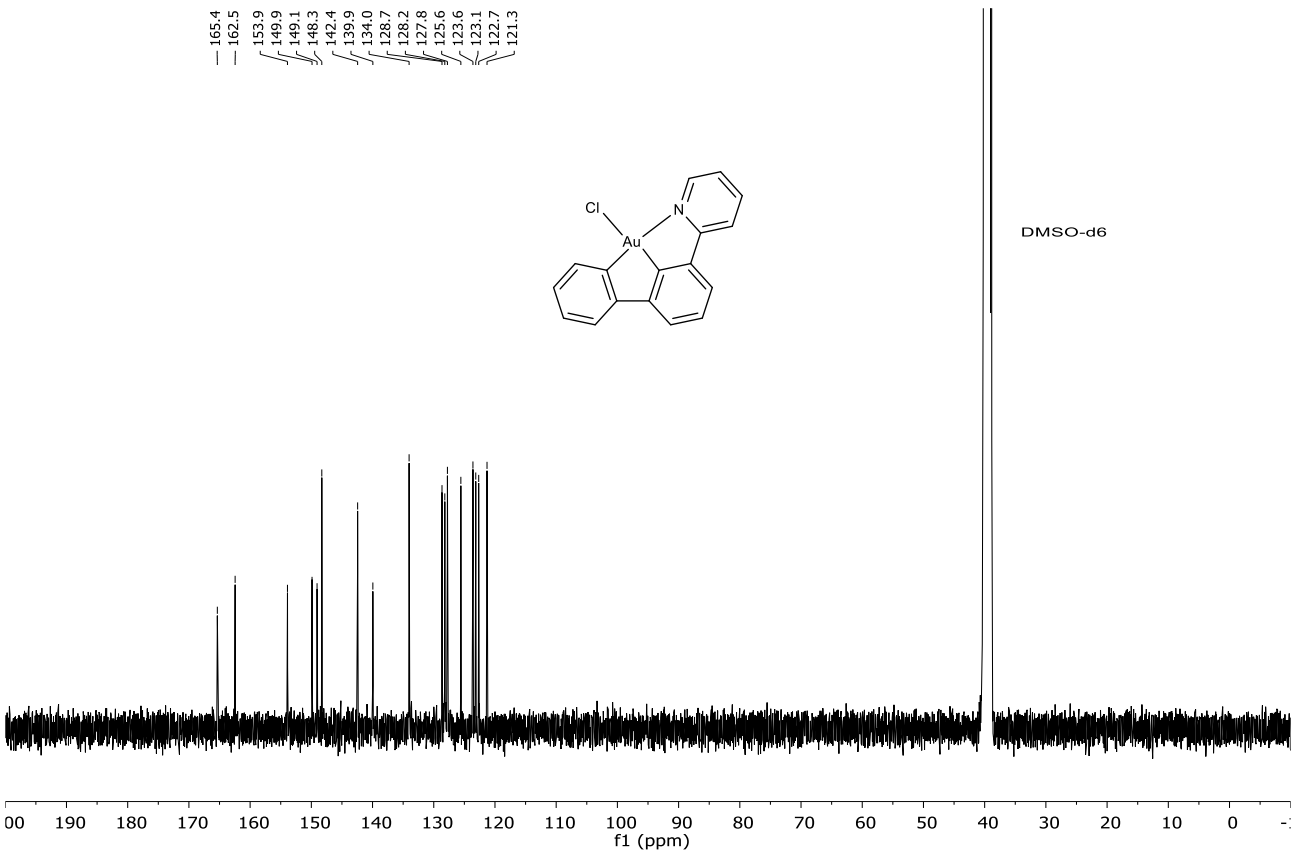

Figure S 43. ^{13}C NMR spectrum (101 MHz, DMSO-*d6*) of **33** recorded at 373 K.

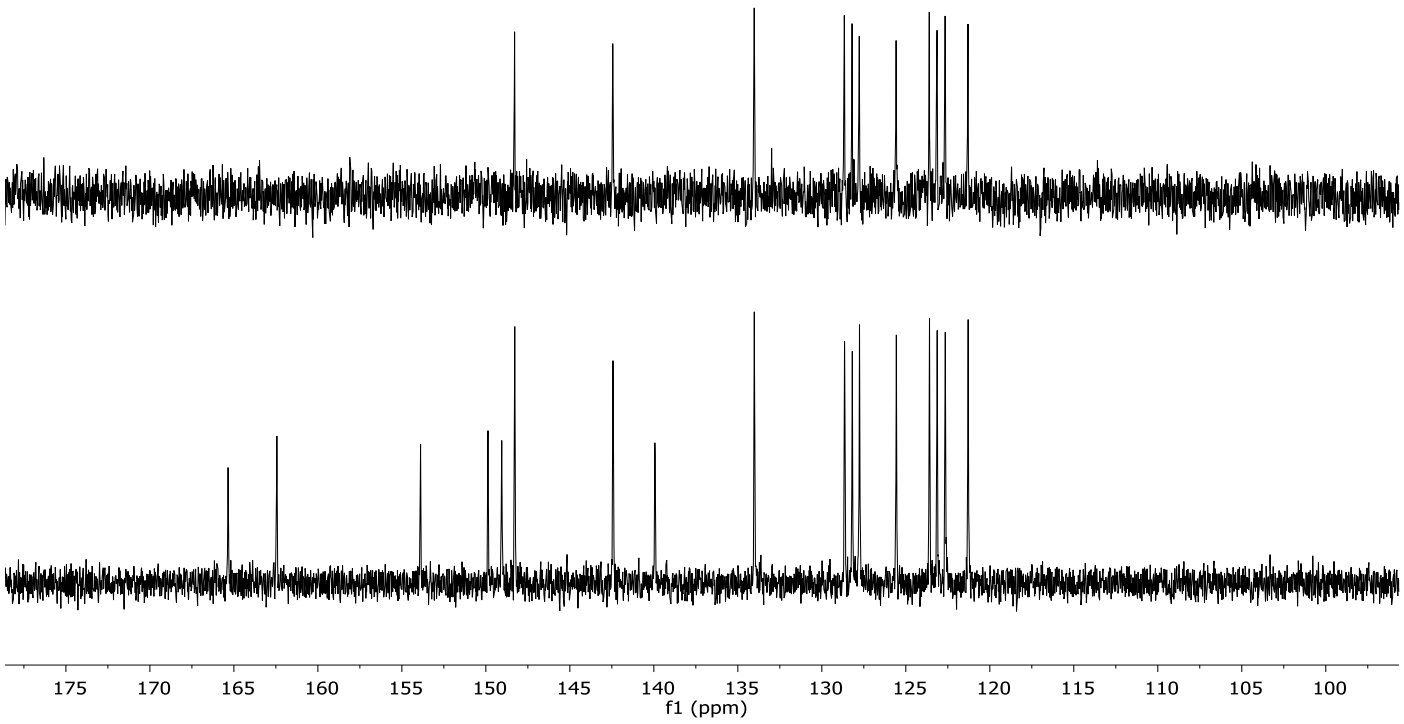

Figure S 44. ^{13}C NMR (bottom) and dept135 (top) spectrum of **33** recorded at 373 K.

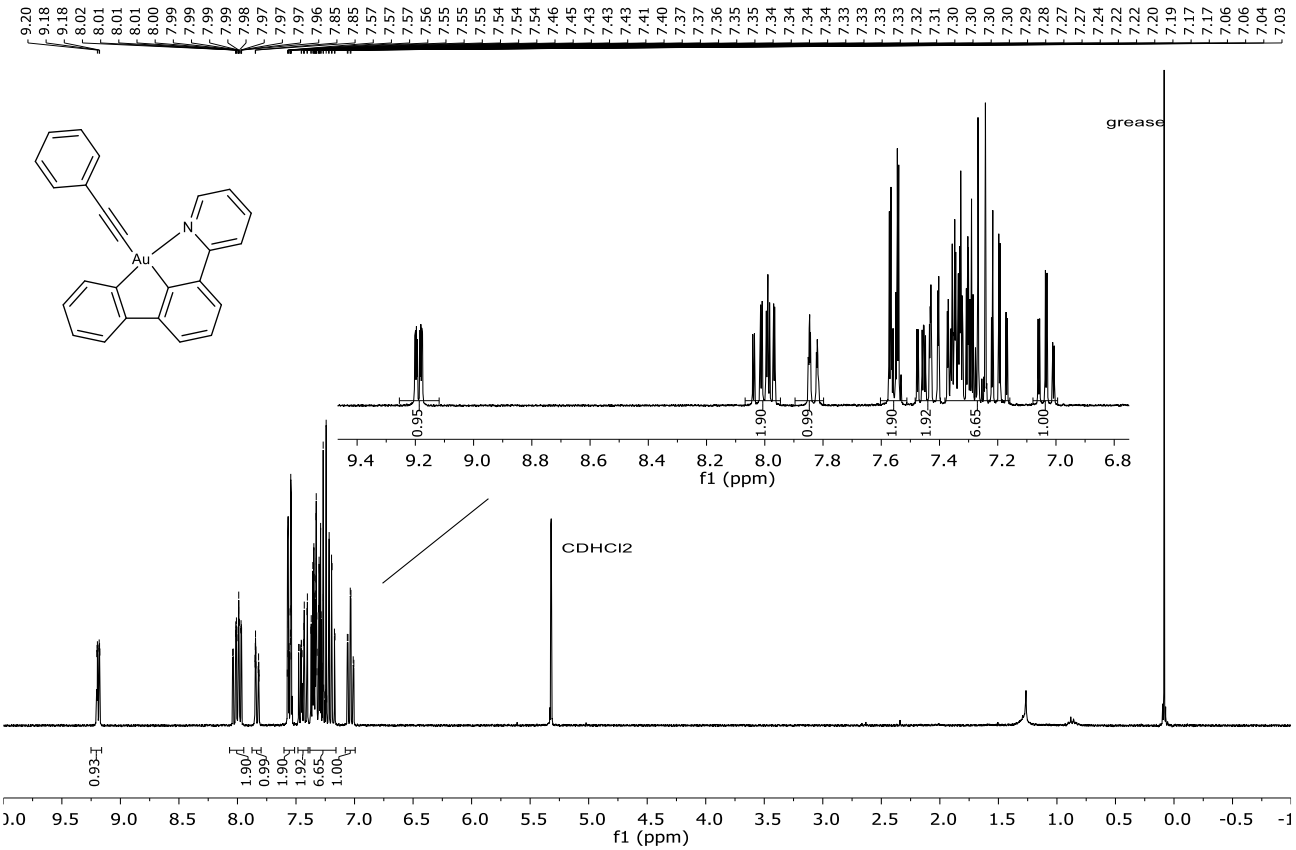

Figure S 45. ^{1}H NMR spectrum (300 MHz, CD_2Cl_2) of **34**.

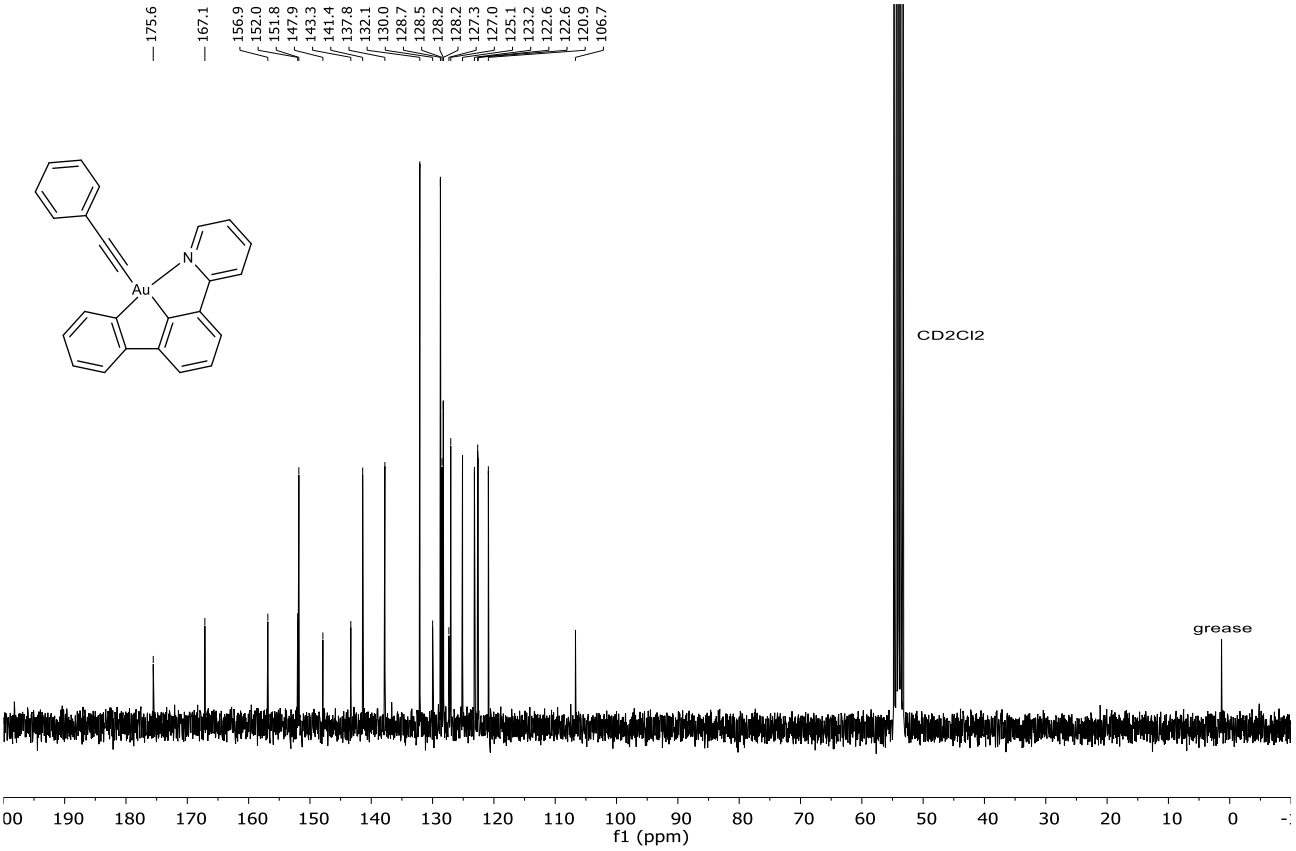

Figure S 46. ^{13}C NMR spectrum (75 MHz, CD_2Cl_2) of **34**.

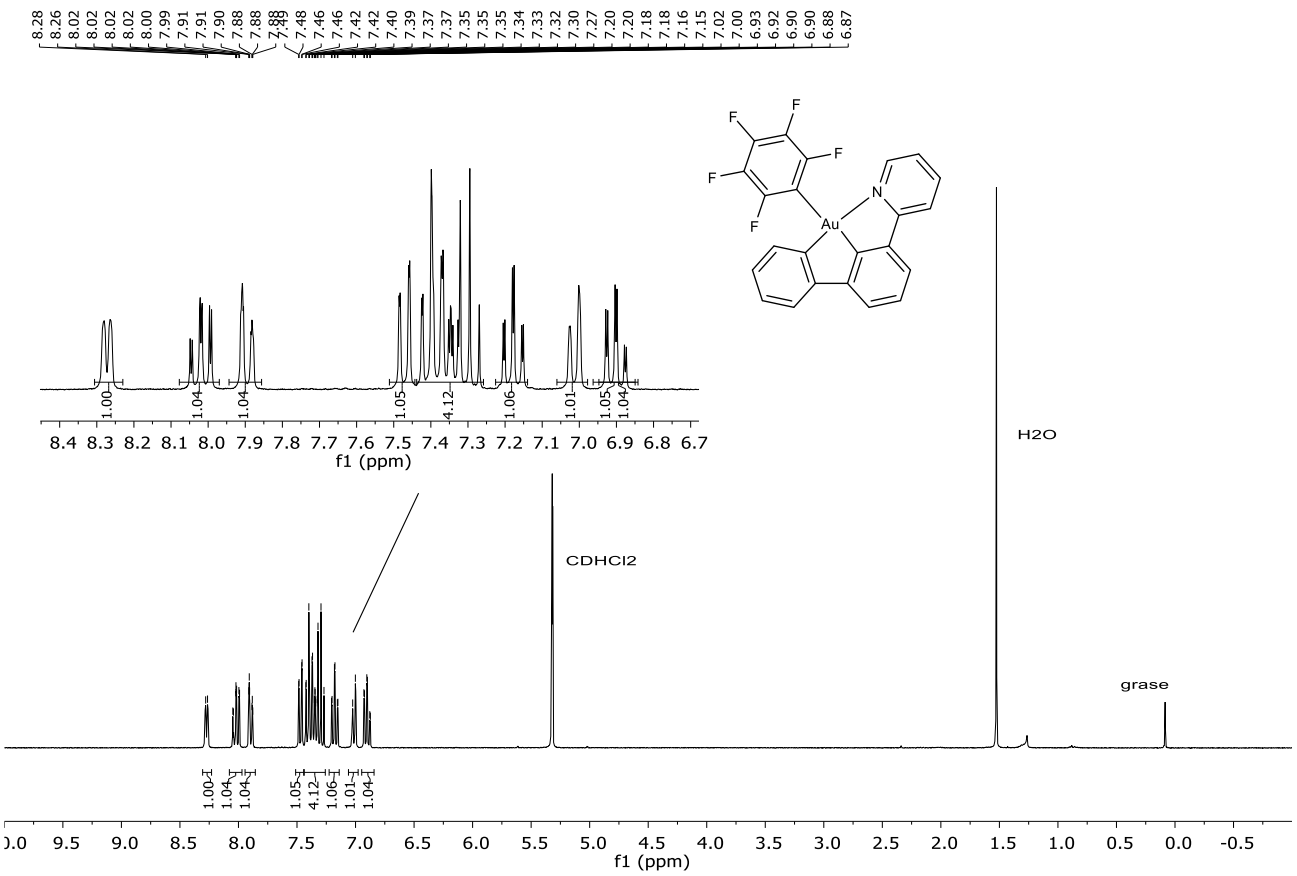

Figure S 47. ^{1}H NMR spectrum (300 MHz, CD_2Cl_2) of **35**.

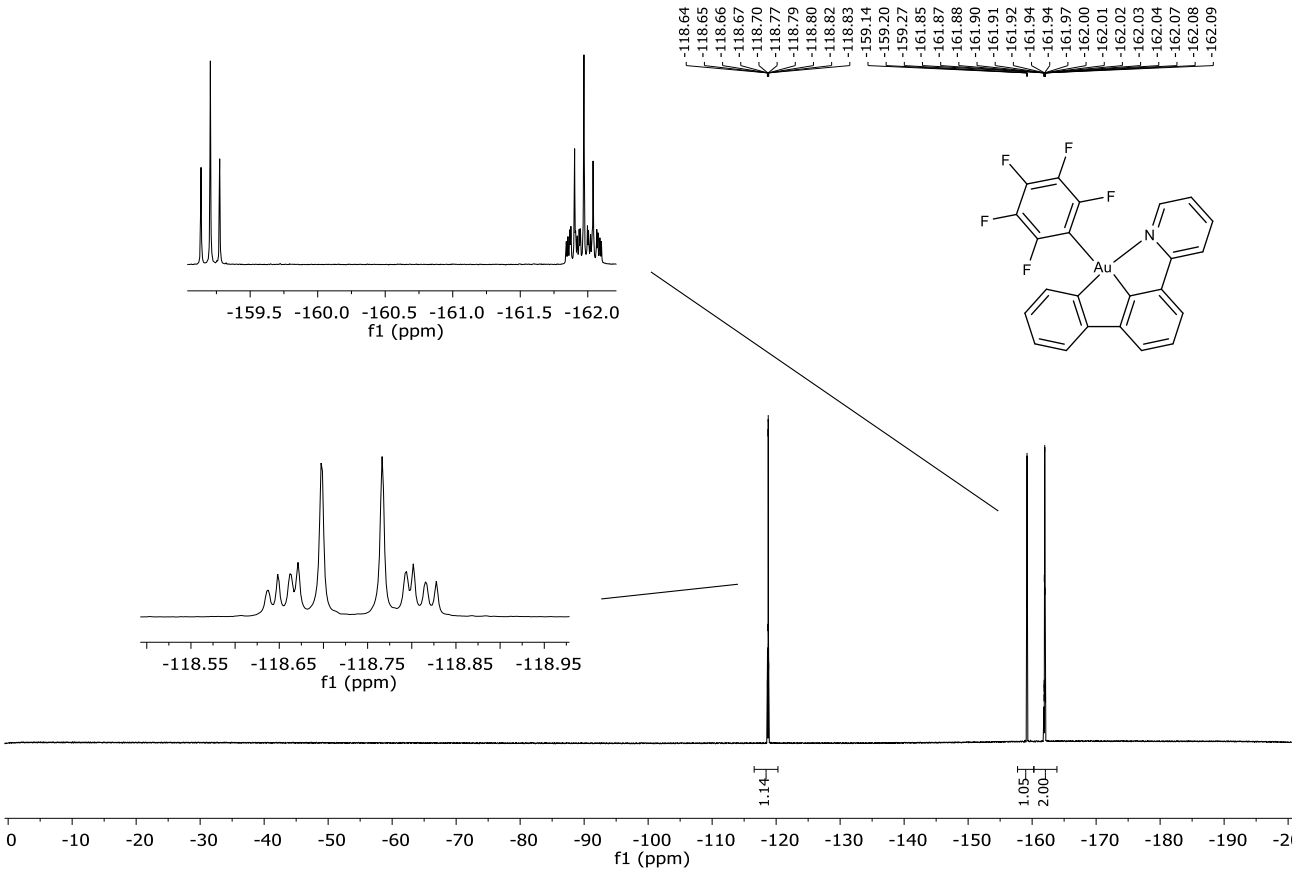

Figure S 48. ^{19}F NMR (282 MHz, CD_2Cl_2) of **35**.

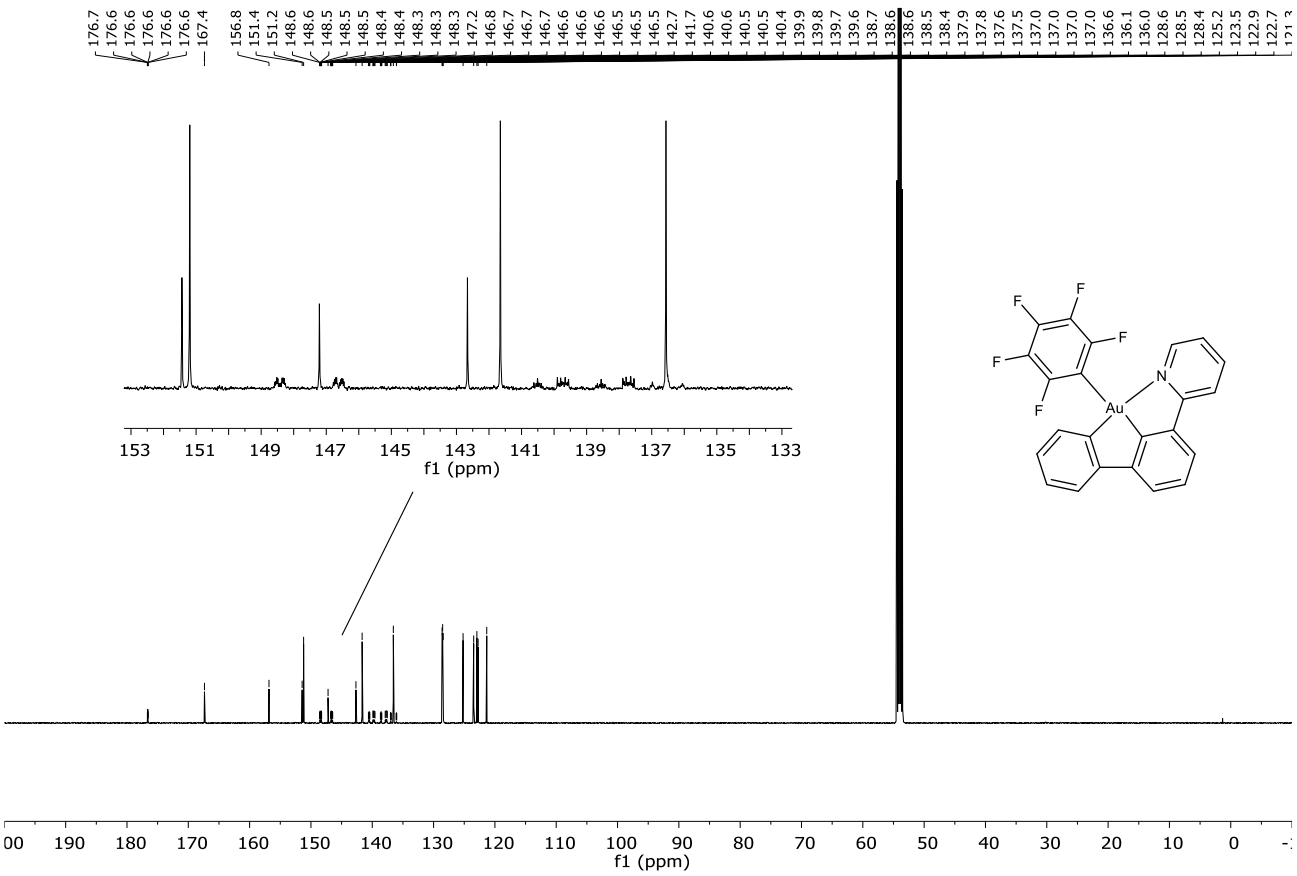

Figure S 49. ^{13}C NMR (126 MHz, CD_2Cl_2) of **35**.

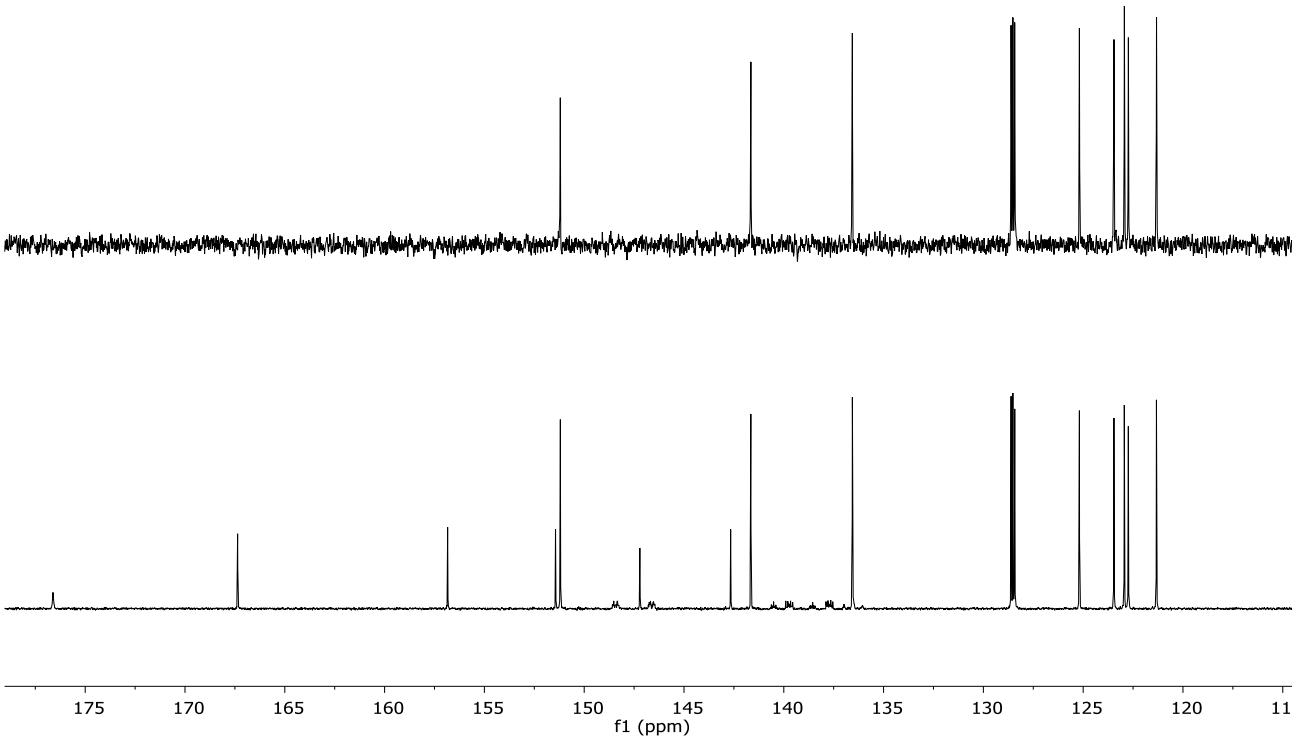

Figure S 50. Dept90 (top) and ^{13}C NMR (bottom) spectra of **35**.

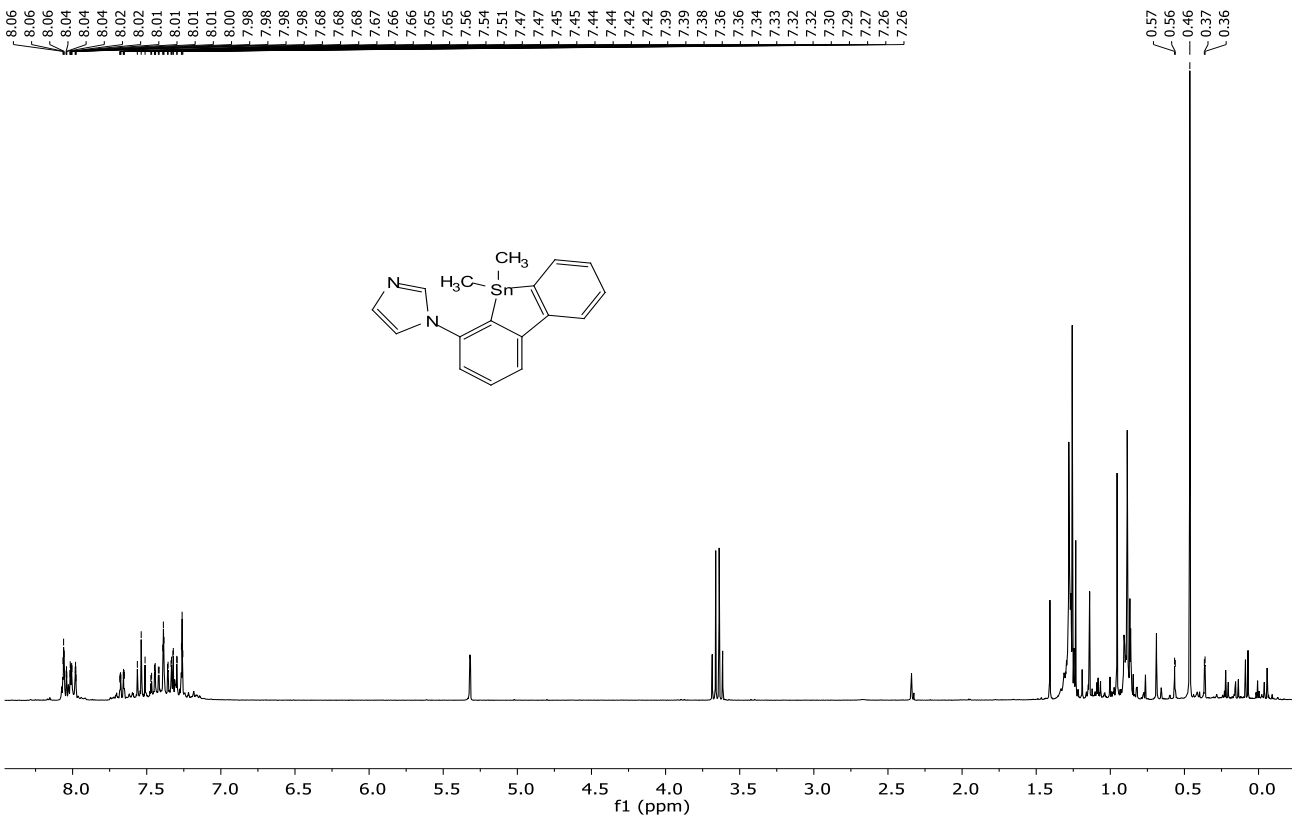

Figure S 51. ^{1}H NMR (300 MHz, CD_2Cl_2) of crude **36**.

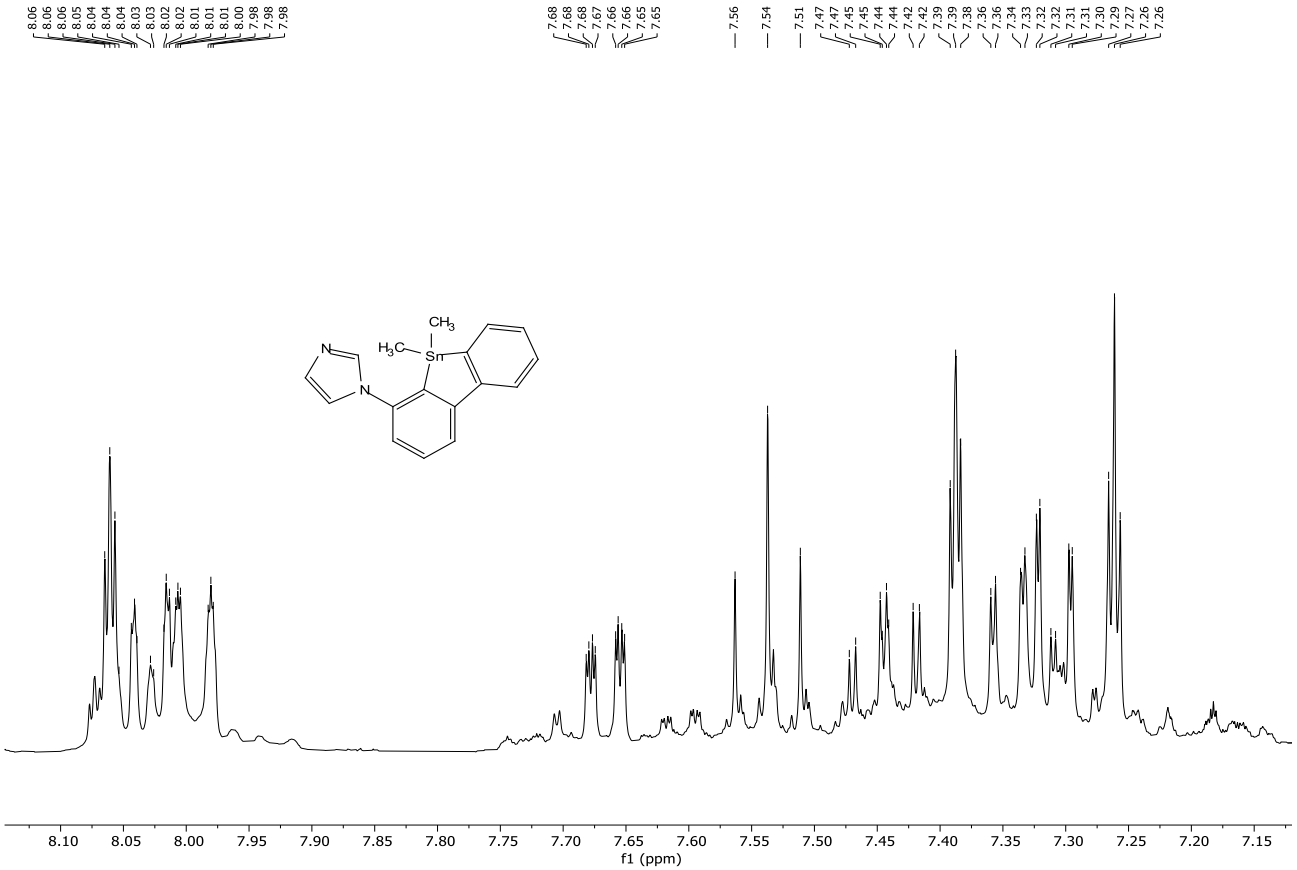

Figure S 52. ^{1}H NMR (300 MHz, CD_2Cl_2) of crude **36** (aromatic region).

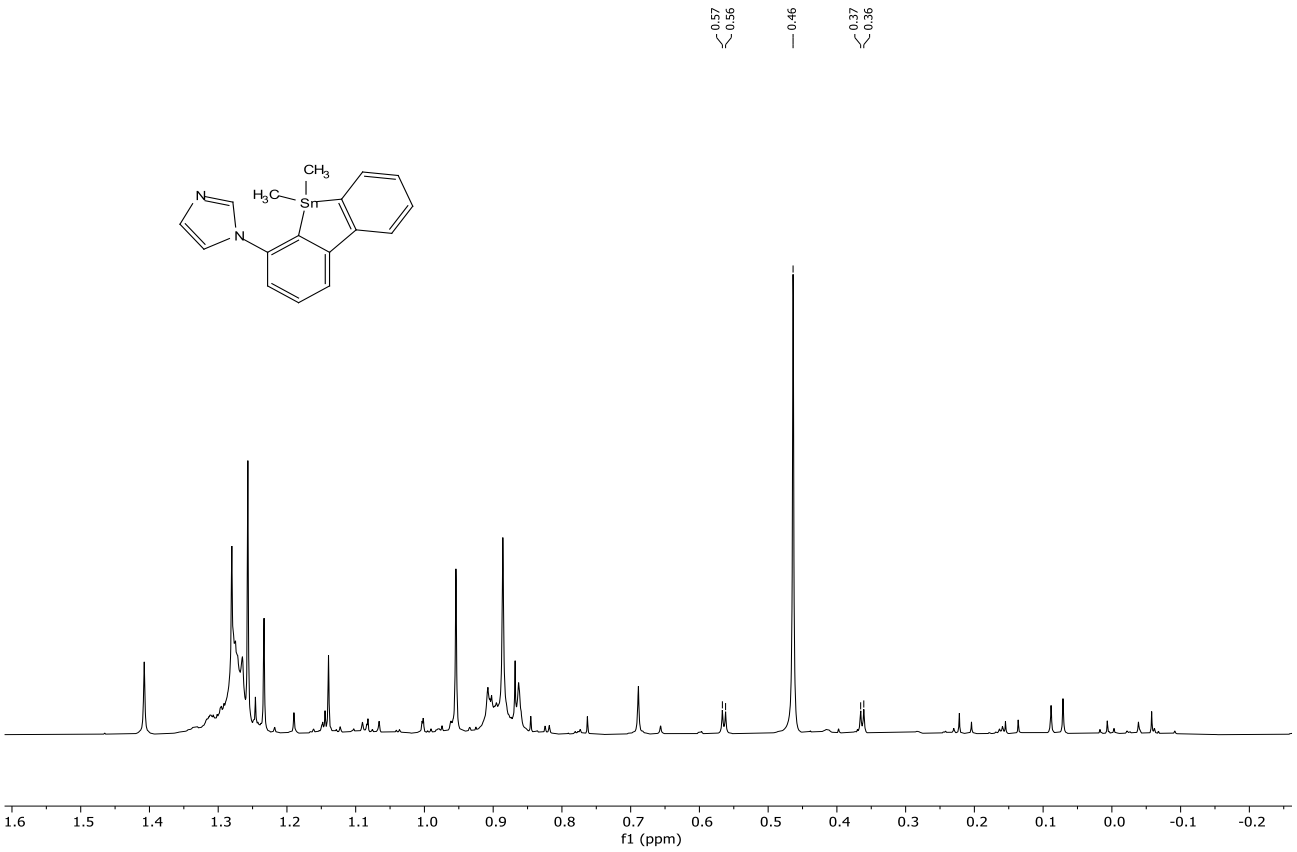

Figure S 53. ^{1}H NMR (300 MHz, CD_2Cl_2) of crude **36** (high-field region). The signal of the *Sn*(CH_3)$_2$ protons at δ = 0.46 clearly shows ^{117}Sn and ^{119}Sn couplings.

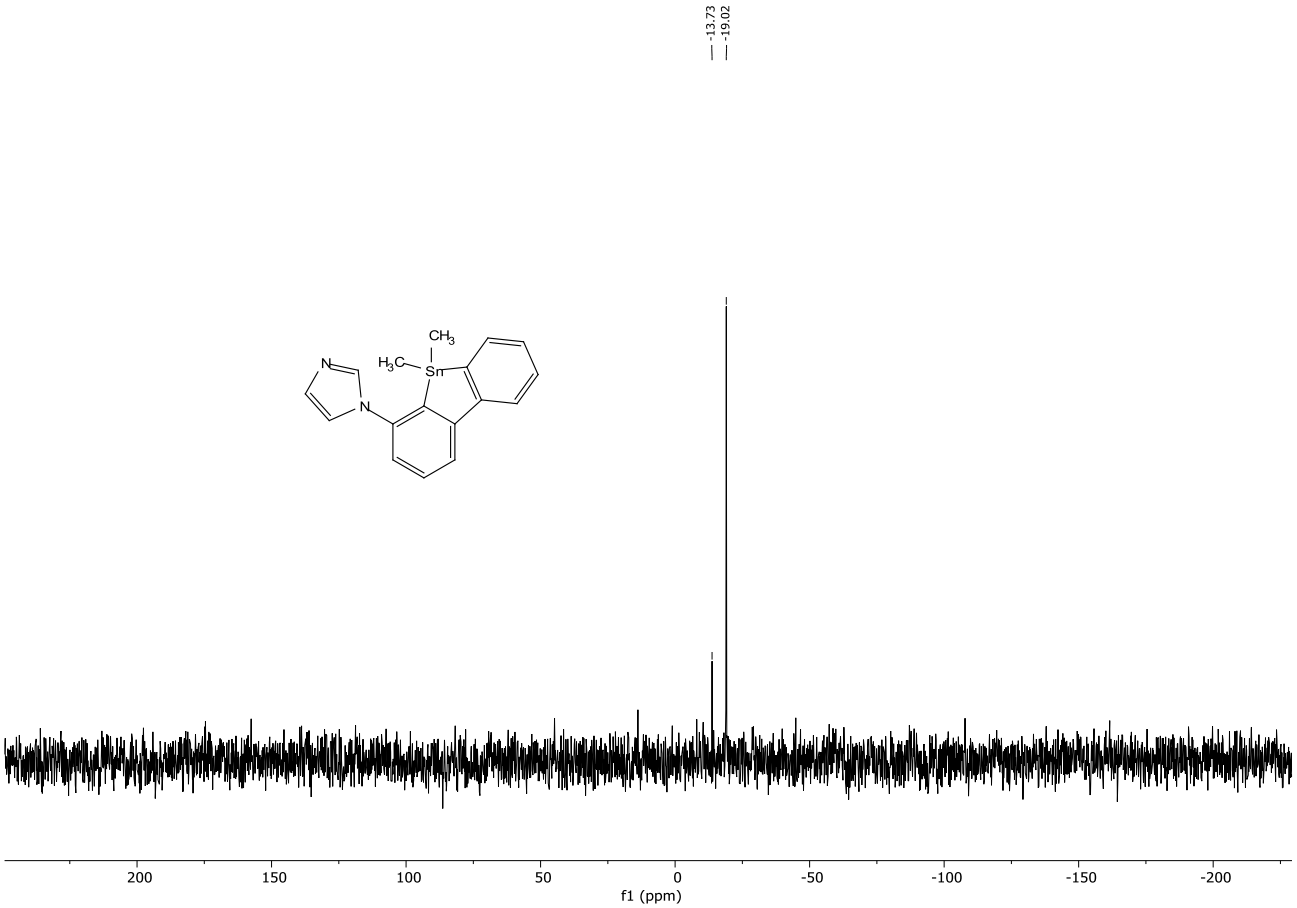

Figure S 54. ^{119}Sn NMR (112 MHz, CD_2Cl_2) of crude **36**. The weaker signal at 13.7 ppm is due to the side product with one *t-b*utyl (instead of one methyl) group.

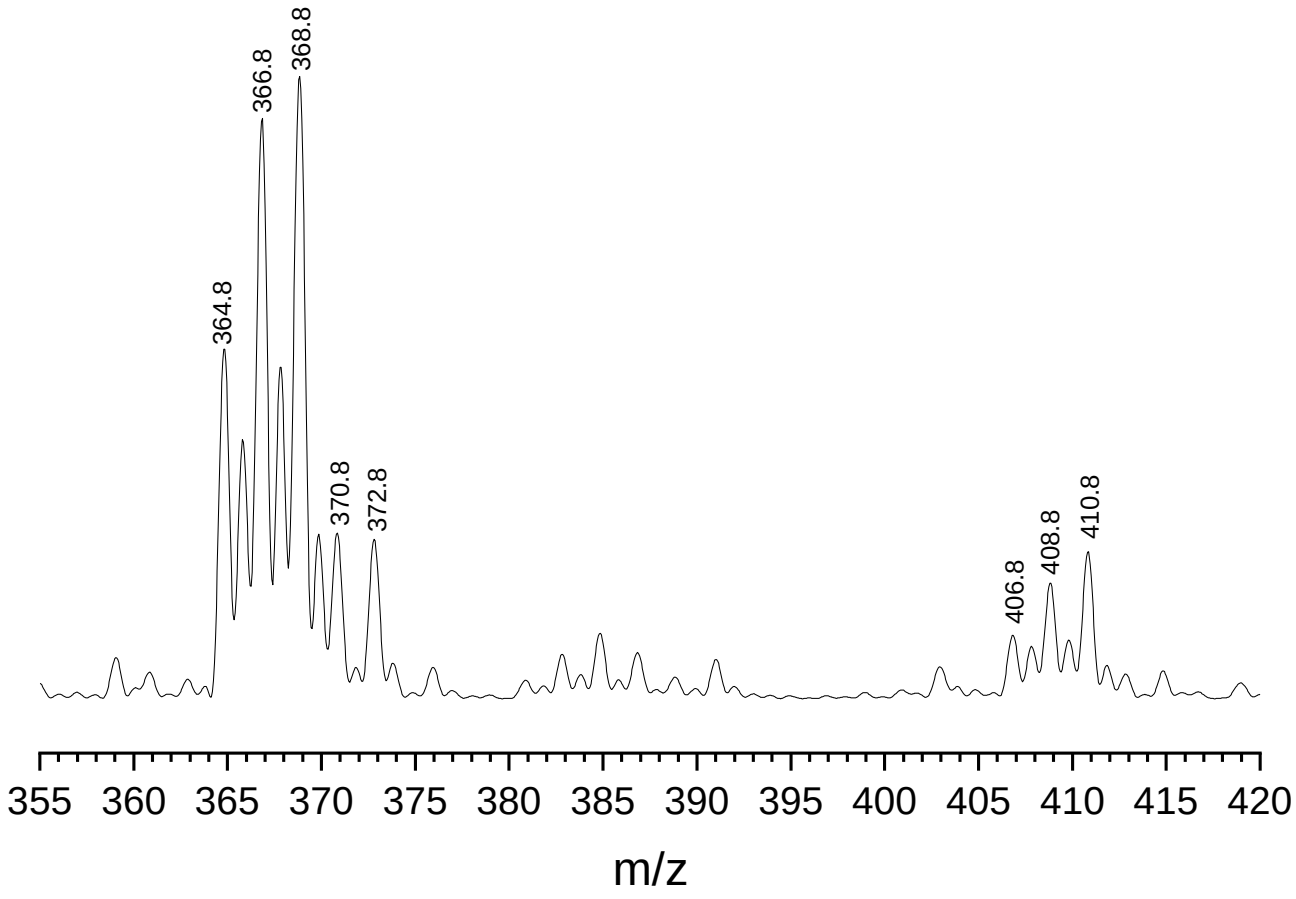

Figure S 55. APCI-MS spectrum of crude **36** showing the $[M+H]^+$ and $[M-CH_3+t\text{-}Bu+H]^+$ peaks and typical Sn isotopic patterns (intensity in arbitrary units).

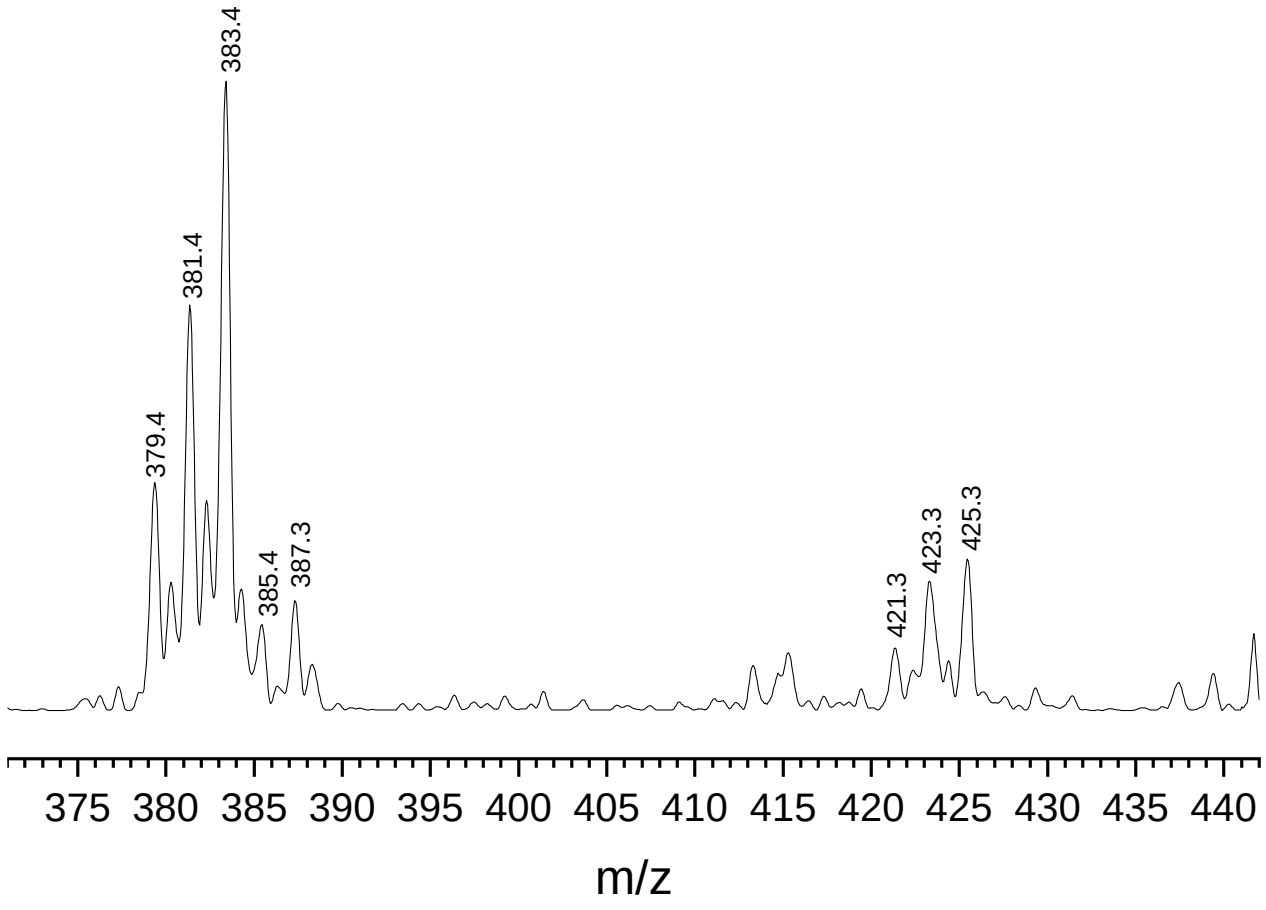

Figure S 56. ESI-MS (positive mode) spectrum of crude **37** showing the $[M]^+$ and $[M-CH_3+t\text{-}Bu]^+$ peaks and typical Sn isotopic patterns (intensity in arbitrary units).

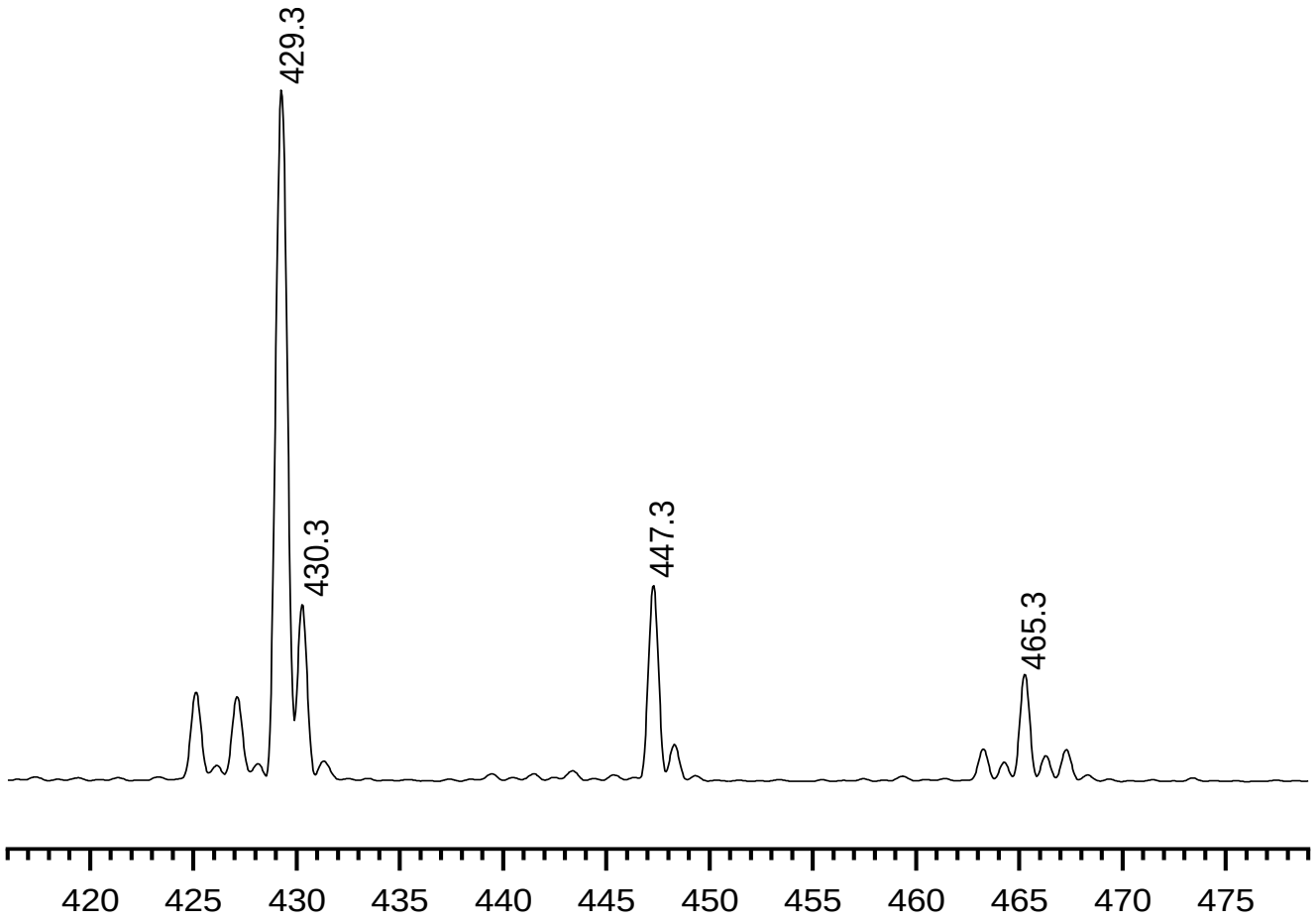

Figure S 57. APCI-MS spectrum of crude **38** showing the $[M]^+$, the $[M-Cl+OH_2]^+$ and $[M-Cl]^+$ peaks.

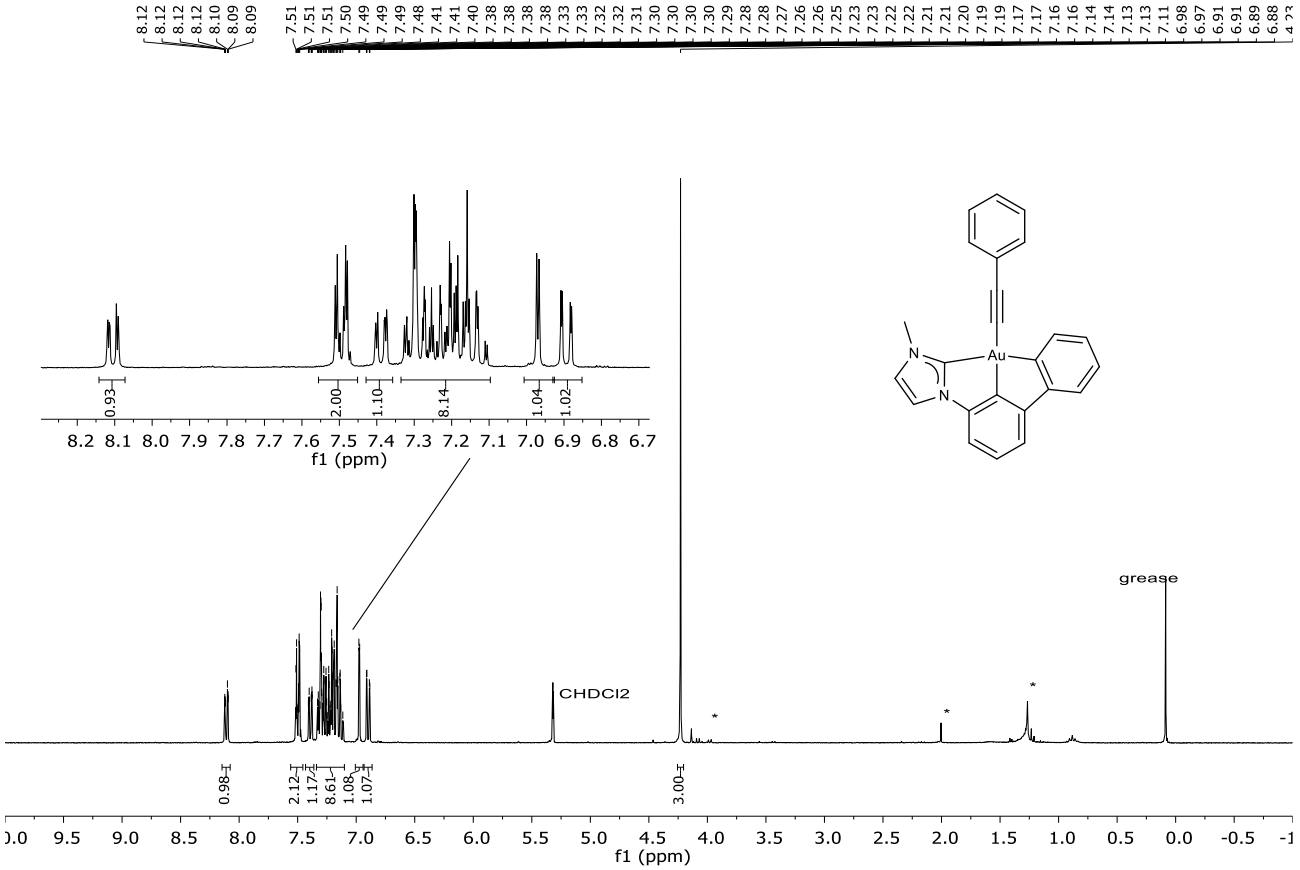

Figure S 58. 1H NMR (300 MHz, CD_2Cl_2) of **39**. Impurities are marked with an asterisk.

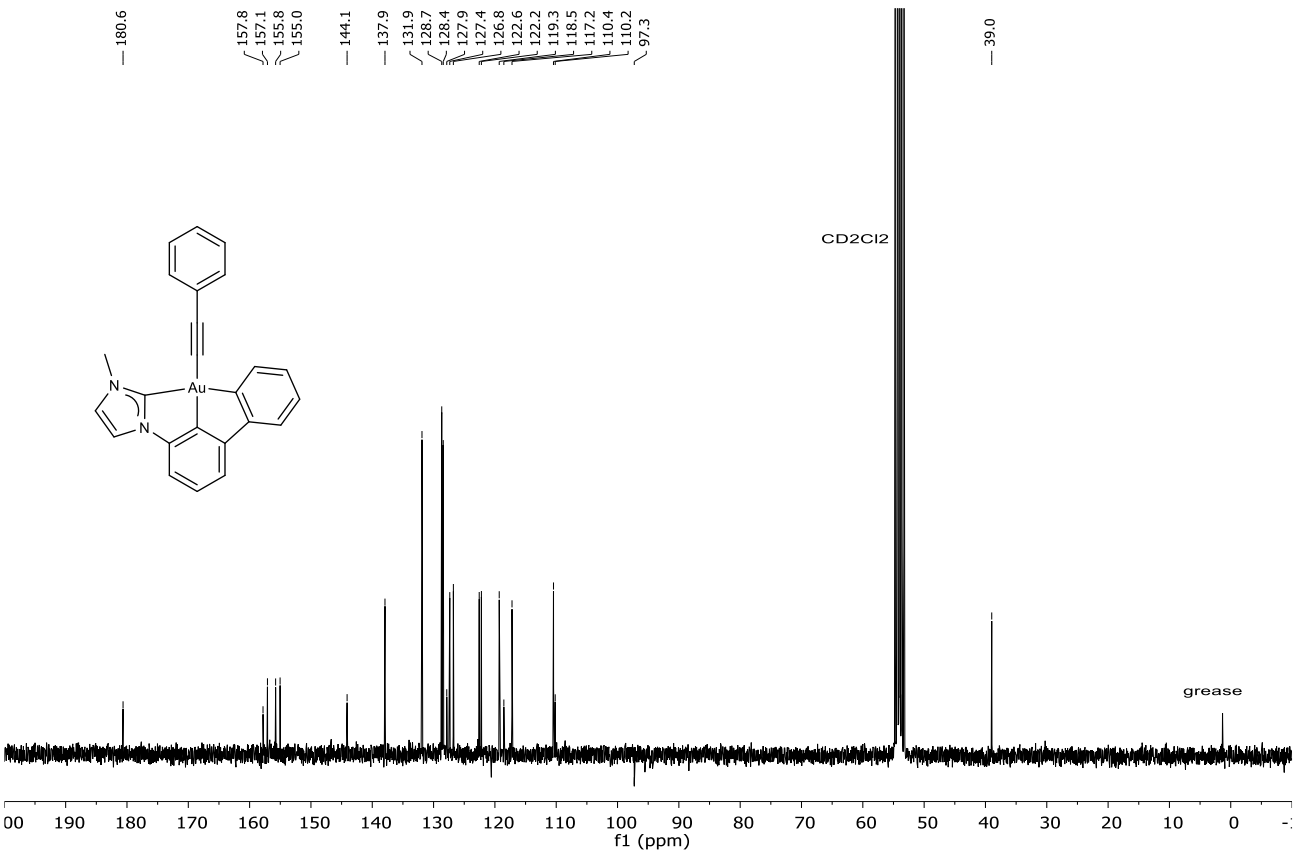

Figure S 59. ^{13}C NMR (75 MHz, CD_2Cl_2) of **39**.

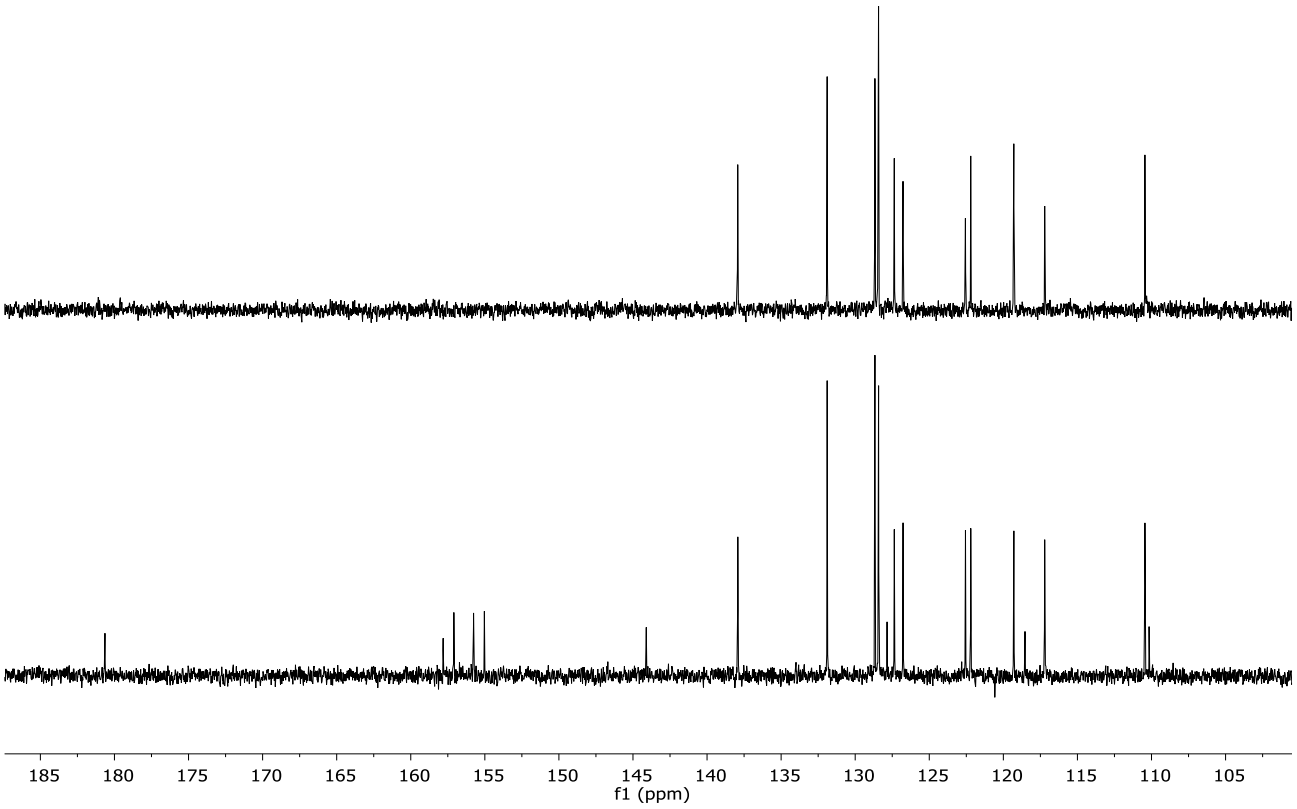

Figure S 60. Dept90 (top) and ^{13}C NMR spectrum (bottom) of **39**.

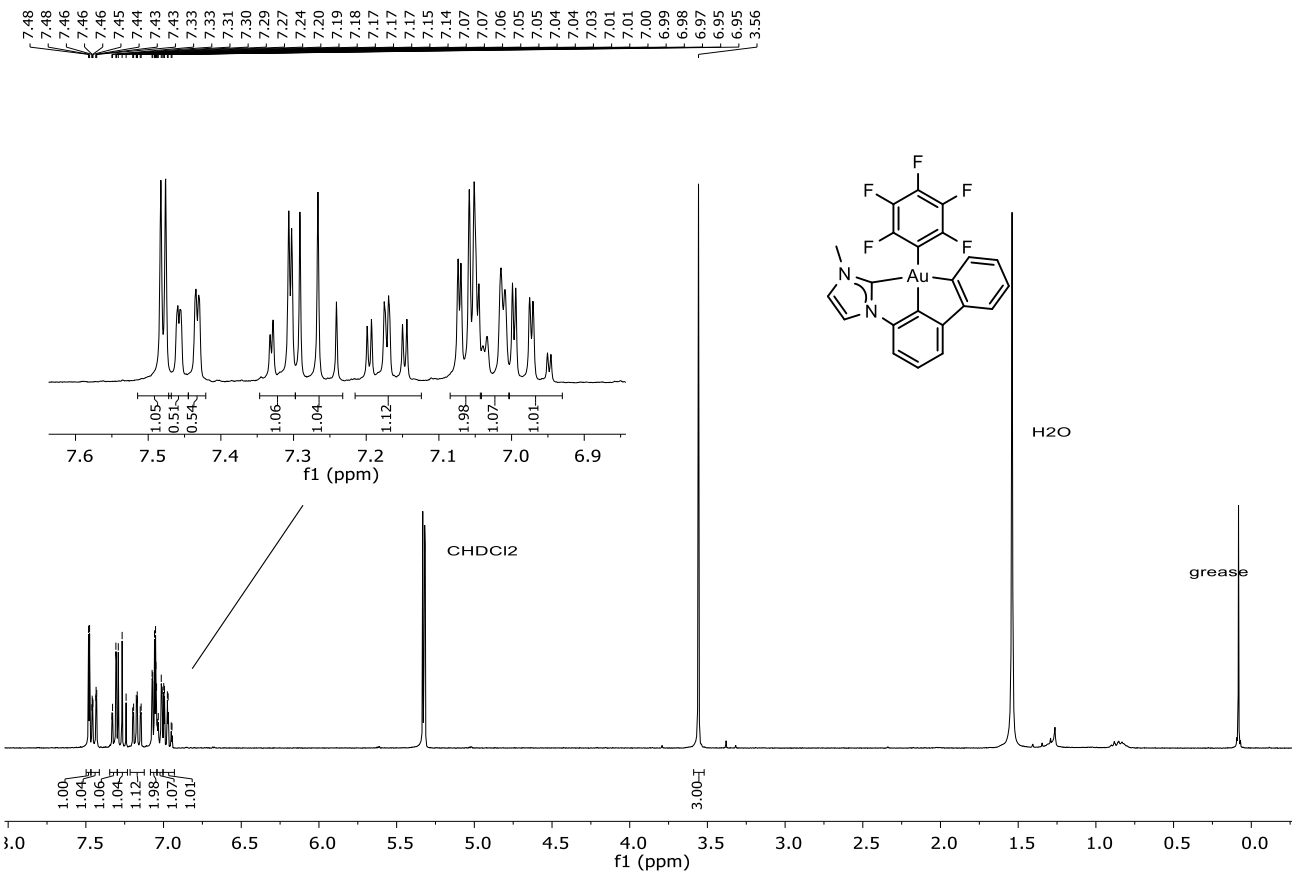

Figure S 61. ^{1}H NMR (300 MHz, CD_2Cl_2) of **40**.

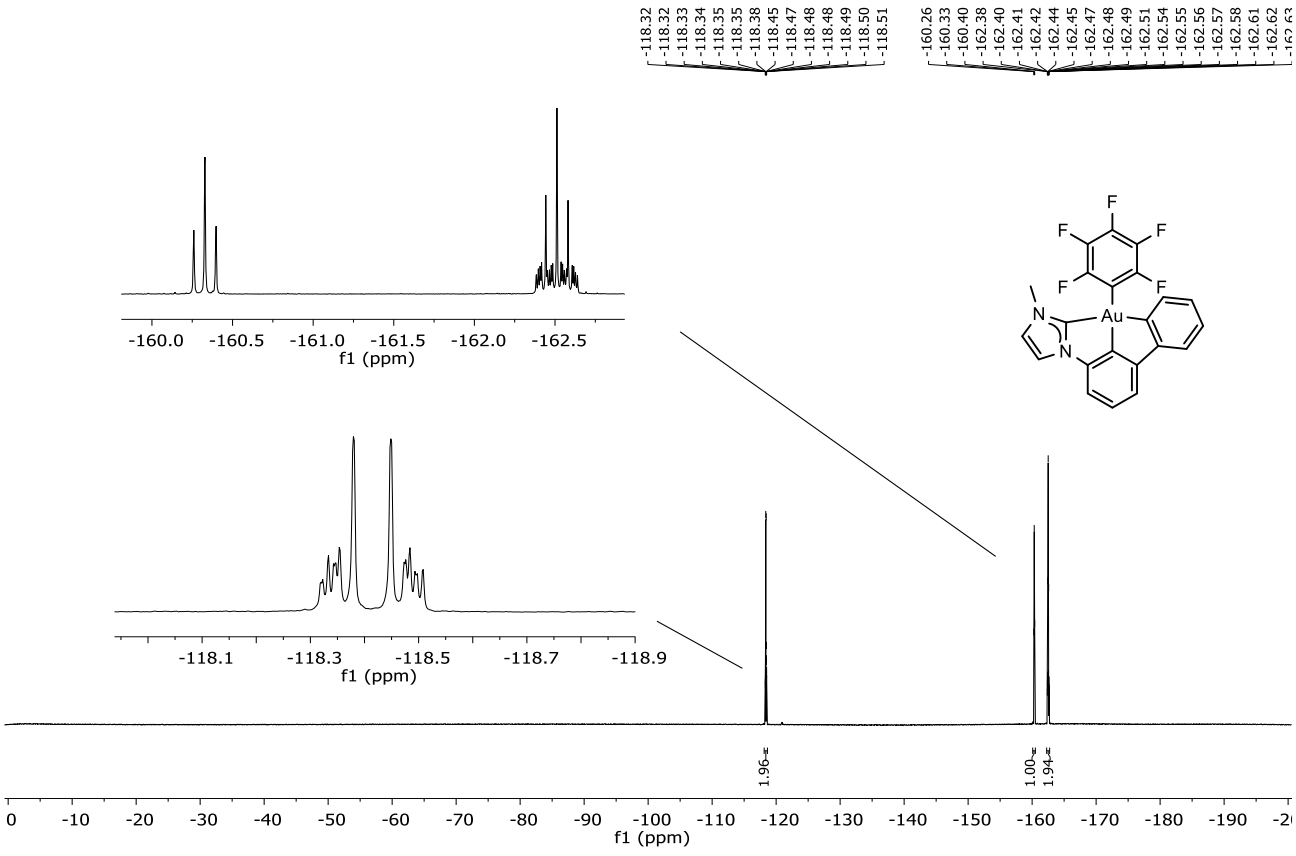

Figure S 62. ^{19}F NMR (282 MHz, CD_2Cl_2) of **40**.

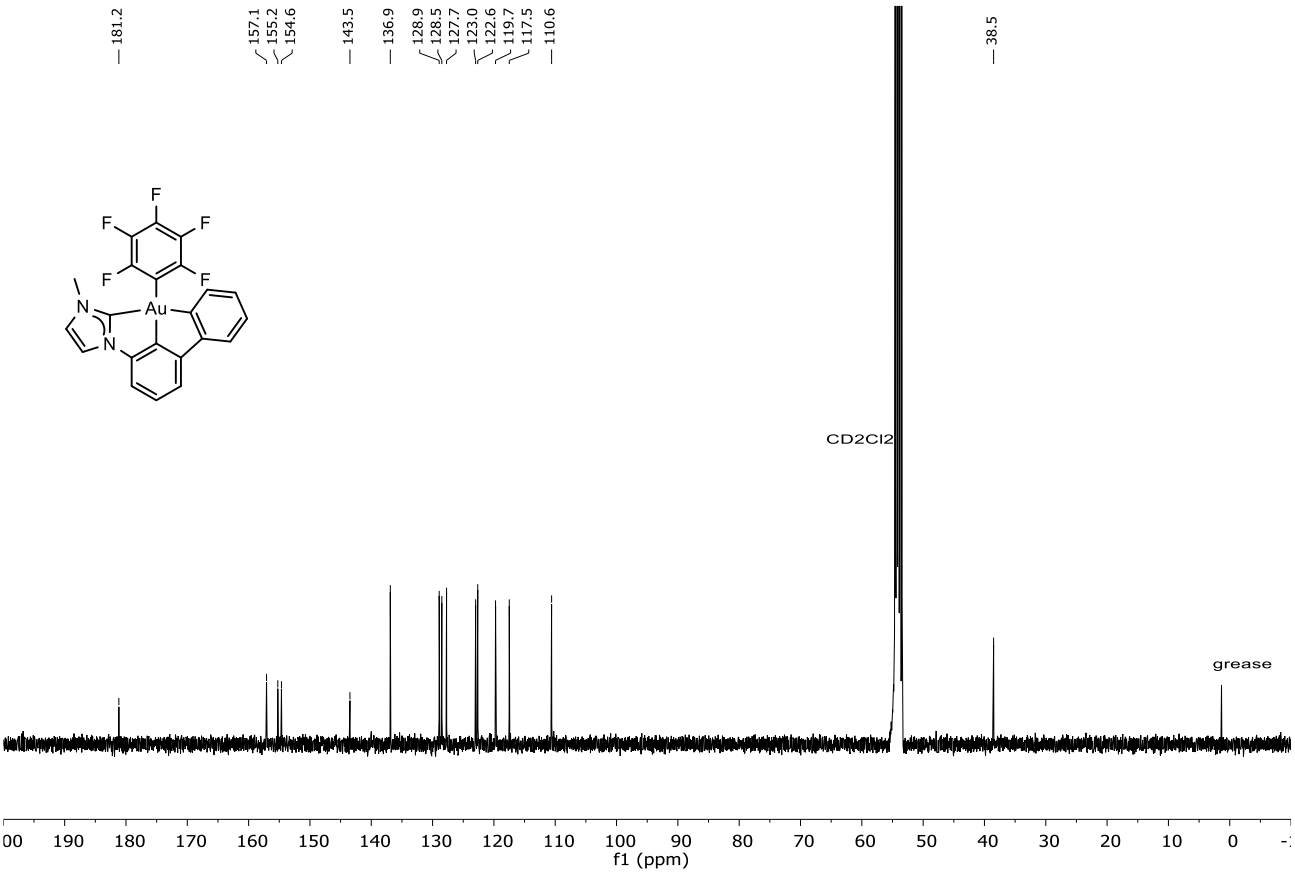

Figure S 63. ^{13}C NMR (75 MHz, CD_2Cl_2) of **40**.

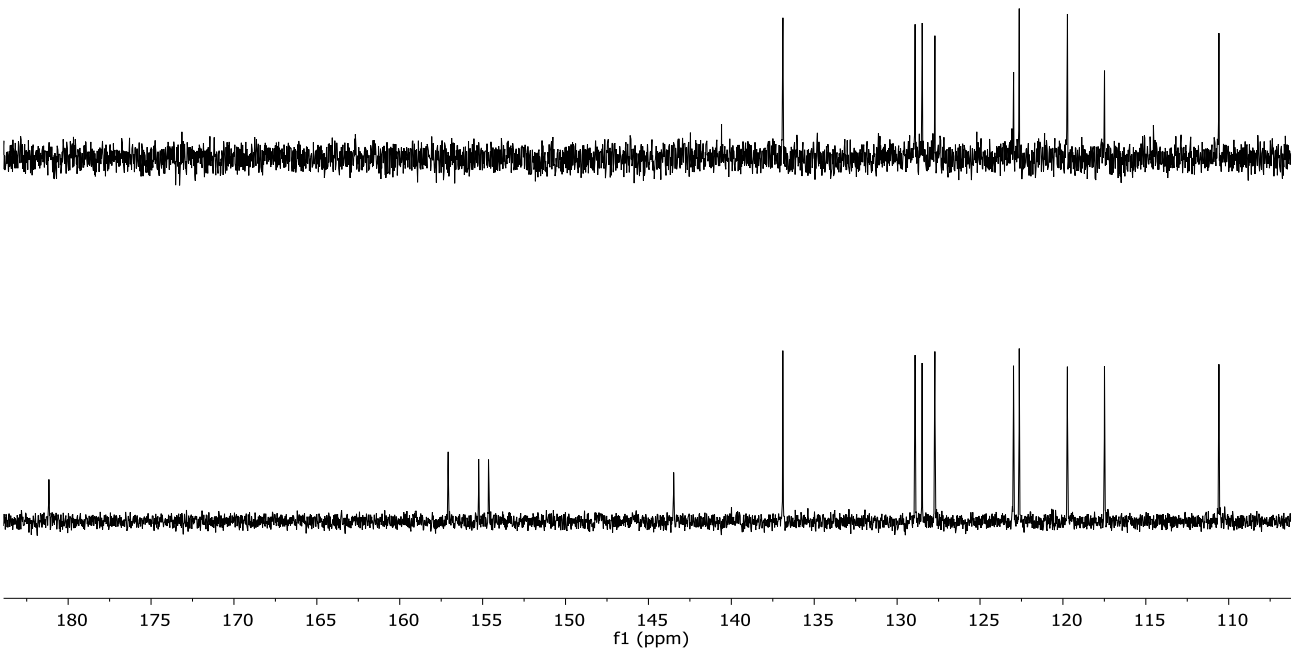

Figure S 64. Dept90 (top) and ^{13}C NMR spectrum (bottom) of **40**.

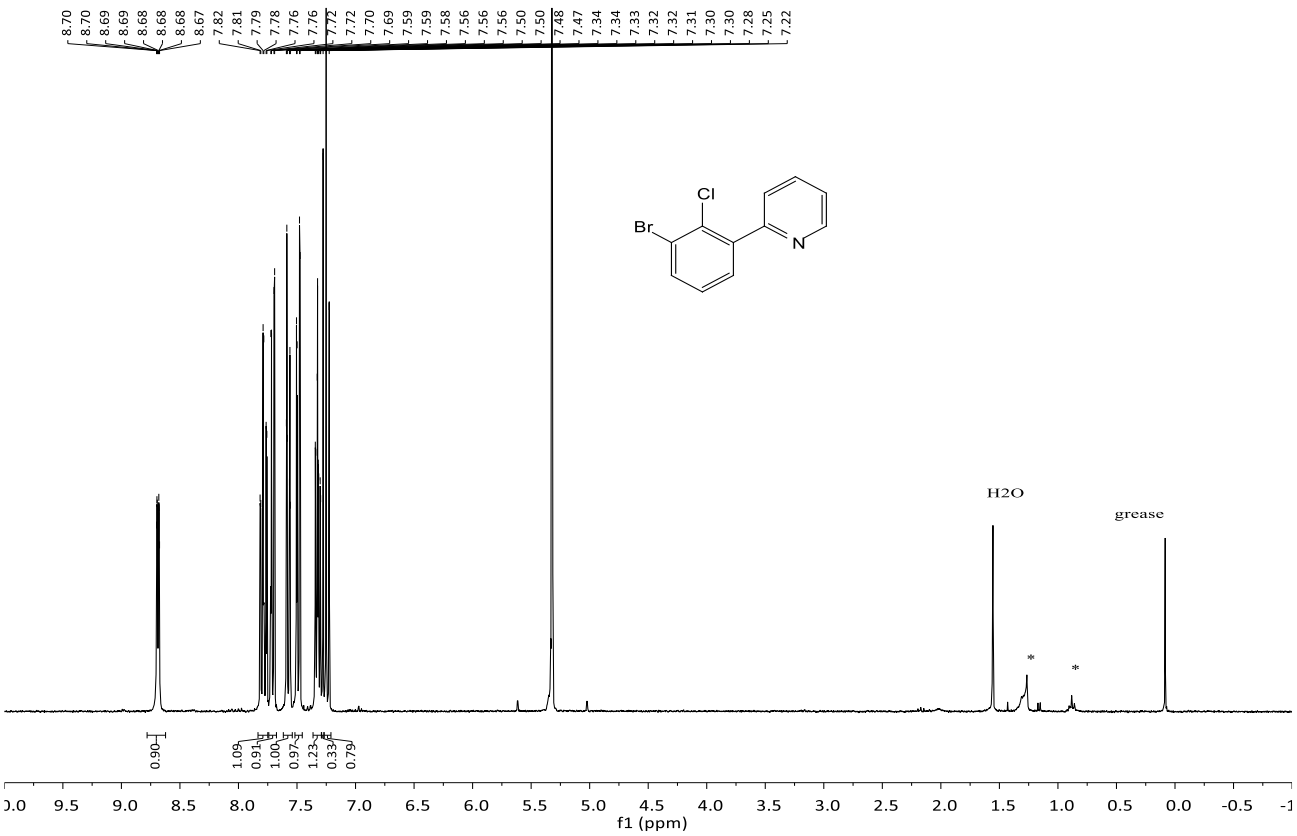

Figure S 65. ^{1}H NMR spectrum (300 MHz, CD_2Cl_2) of **s2**. Impurities are marked with an asterisk.

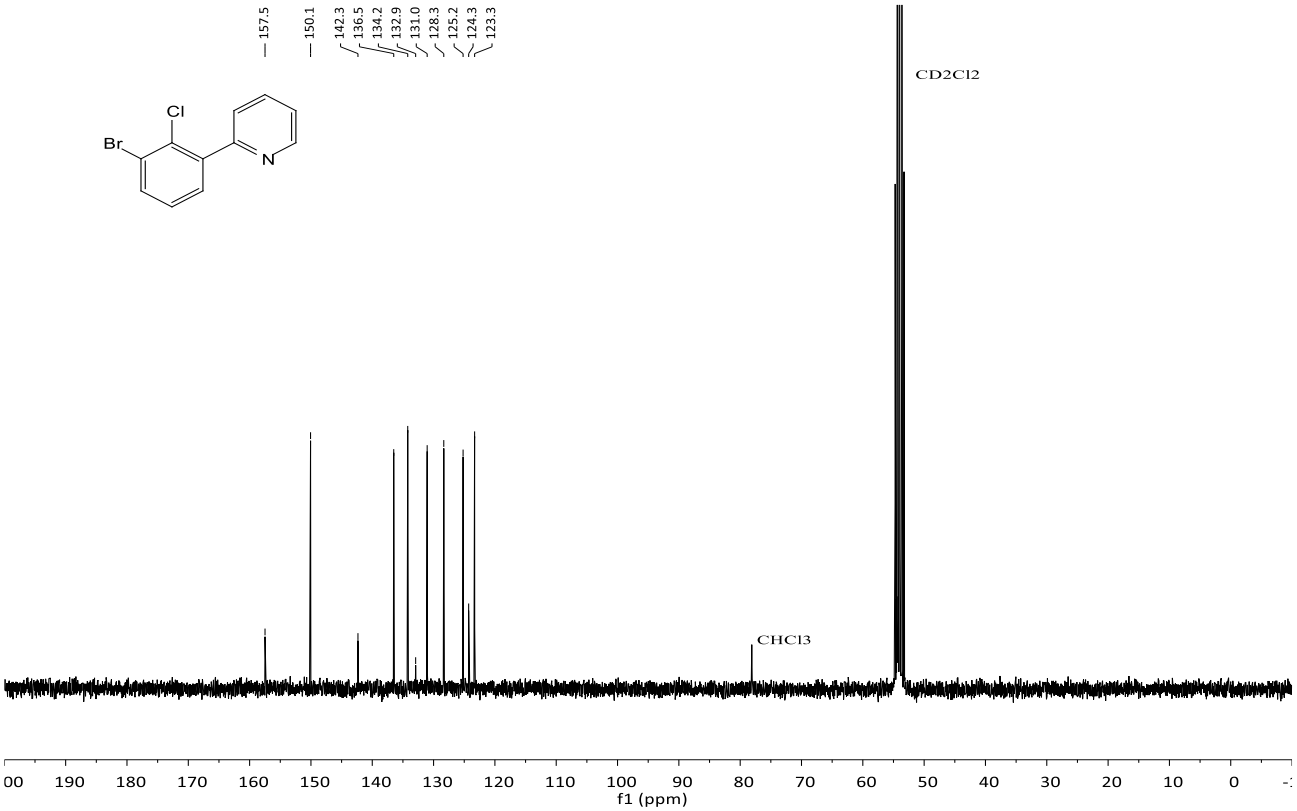

Figure S 66. ^{13}C NMR spectrum (75 MHz, CD_2Cl_2) of **s2**.

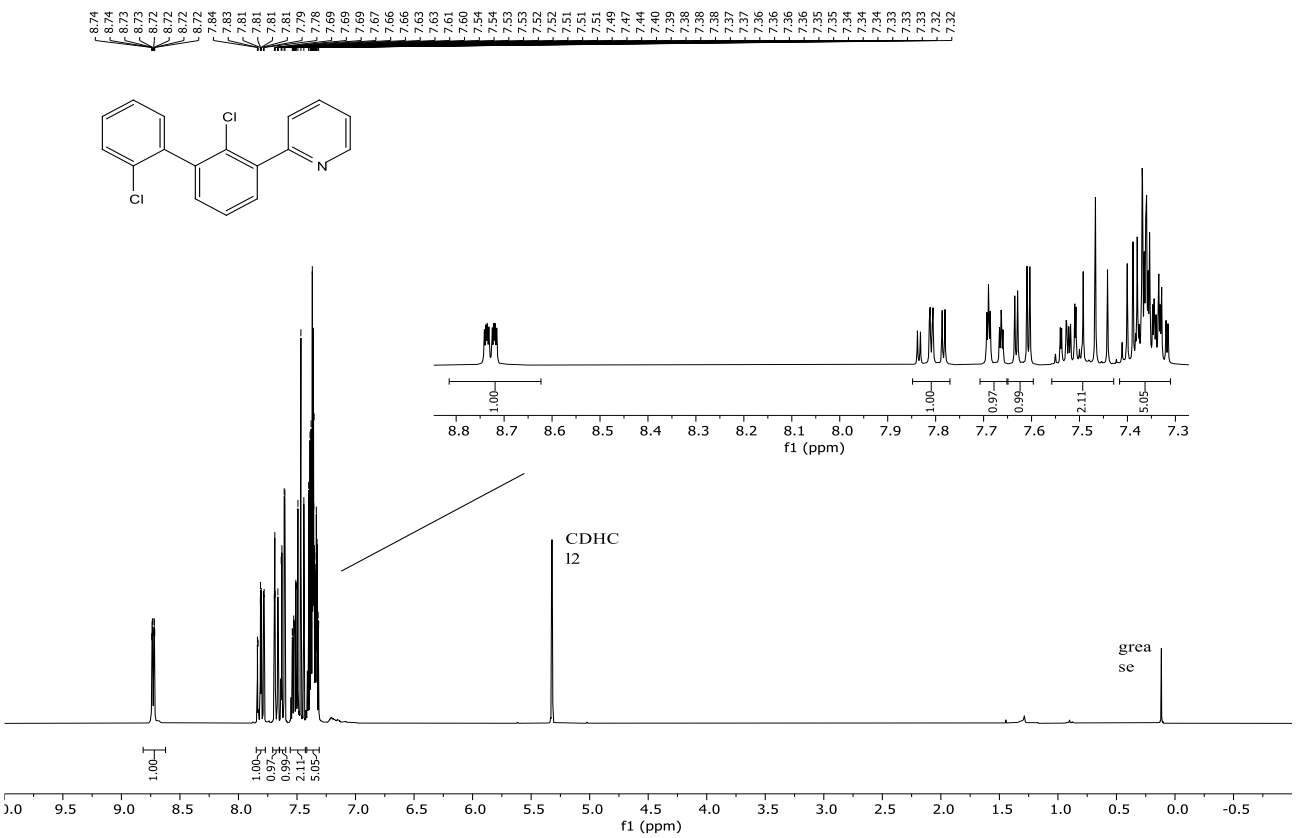

Figure S 67. ^{1}H NMR spectrum (300 MHz, CD_2Cl_2) of **s3**.

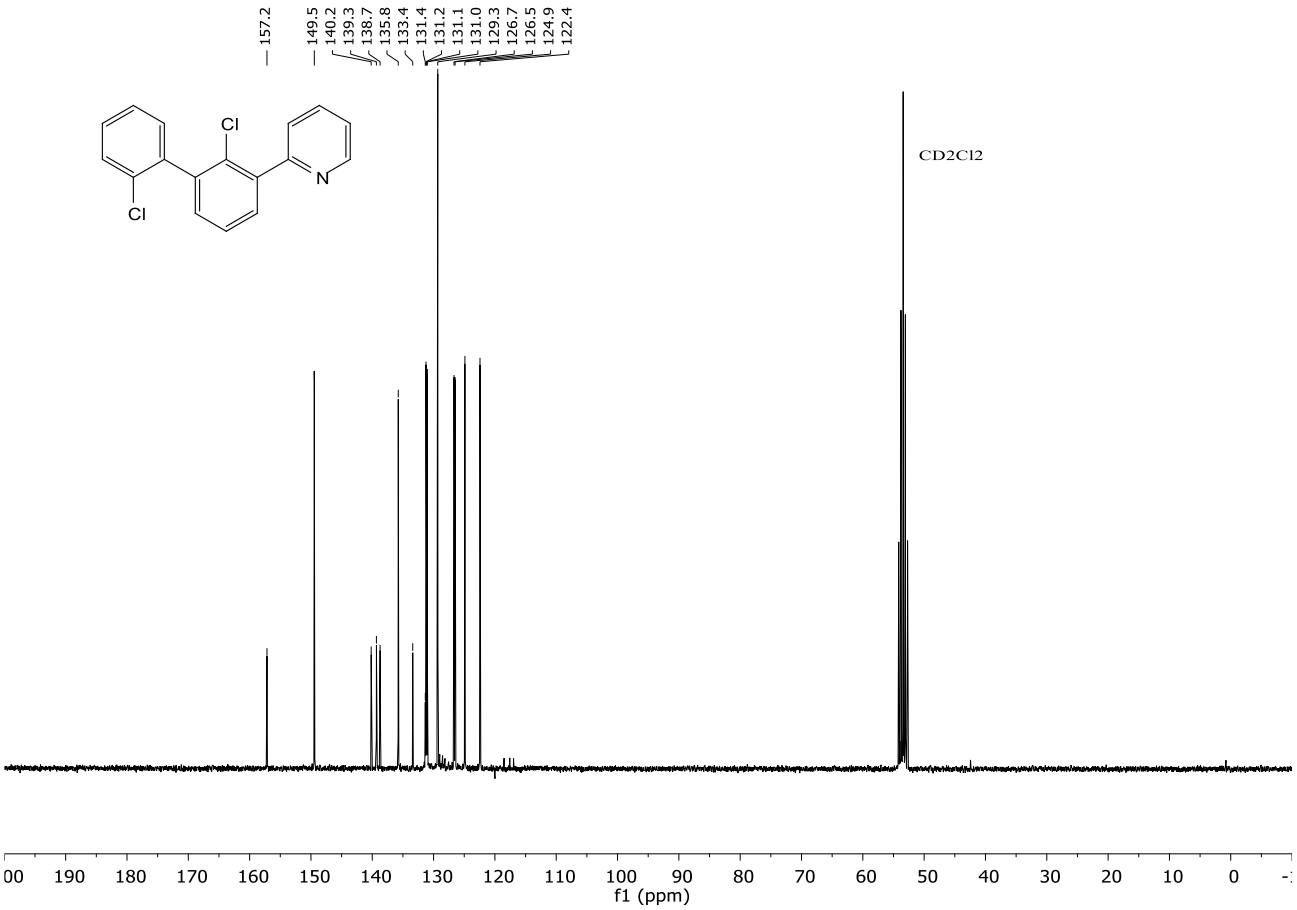

Figure S 68. ^{13}C NMR spectrum (75 MHz, CD_2Cl_2) of **s3**.

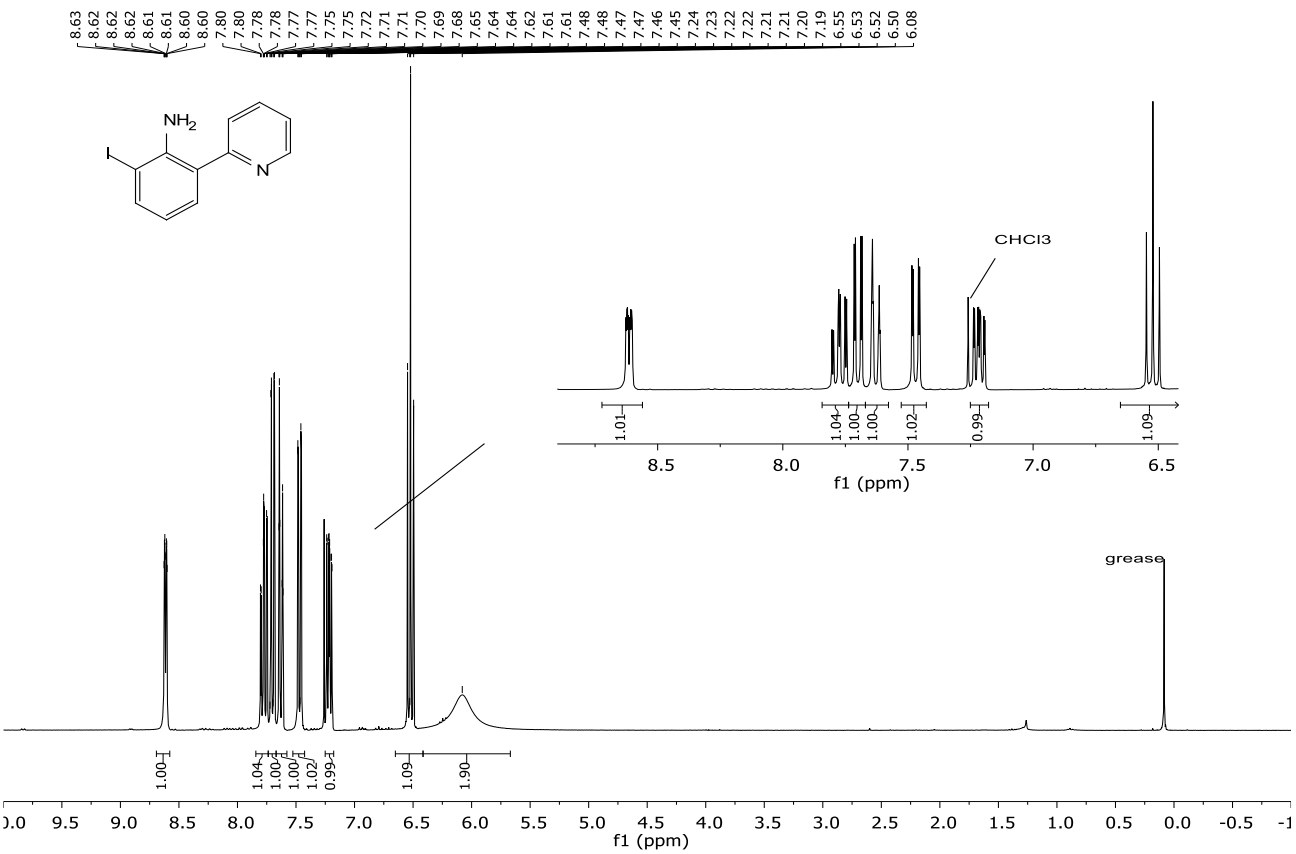

Figure S 69: ^{1}H NMR spectrum (300 MHz, $CDCl_3$) of **s6**.

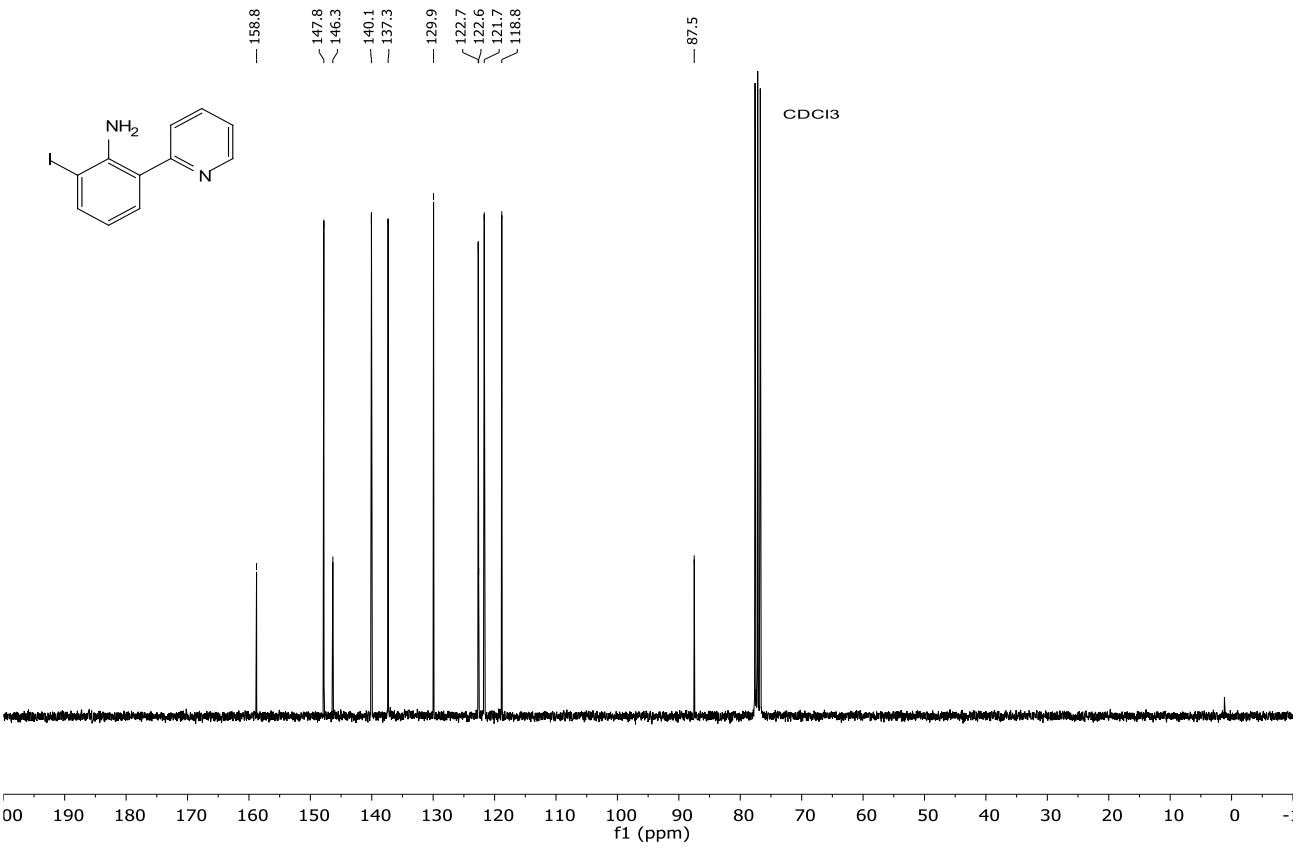

Figure S 70. ^{13}C NMR spectrum (75 MHz, $CDCl_3$) of **s6**.

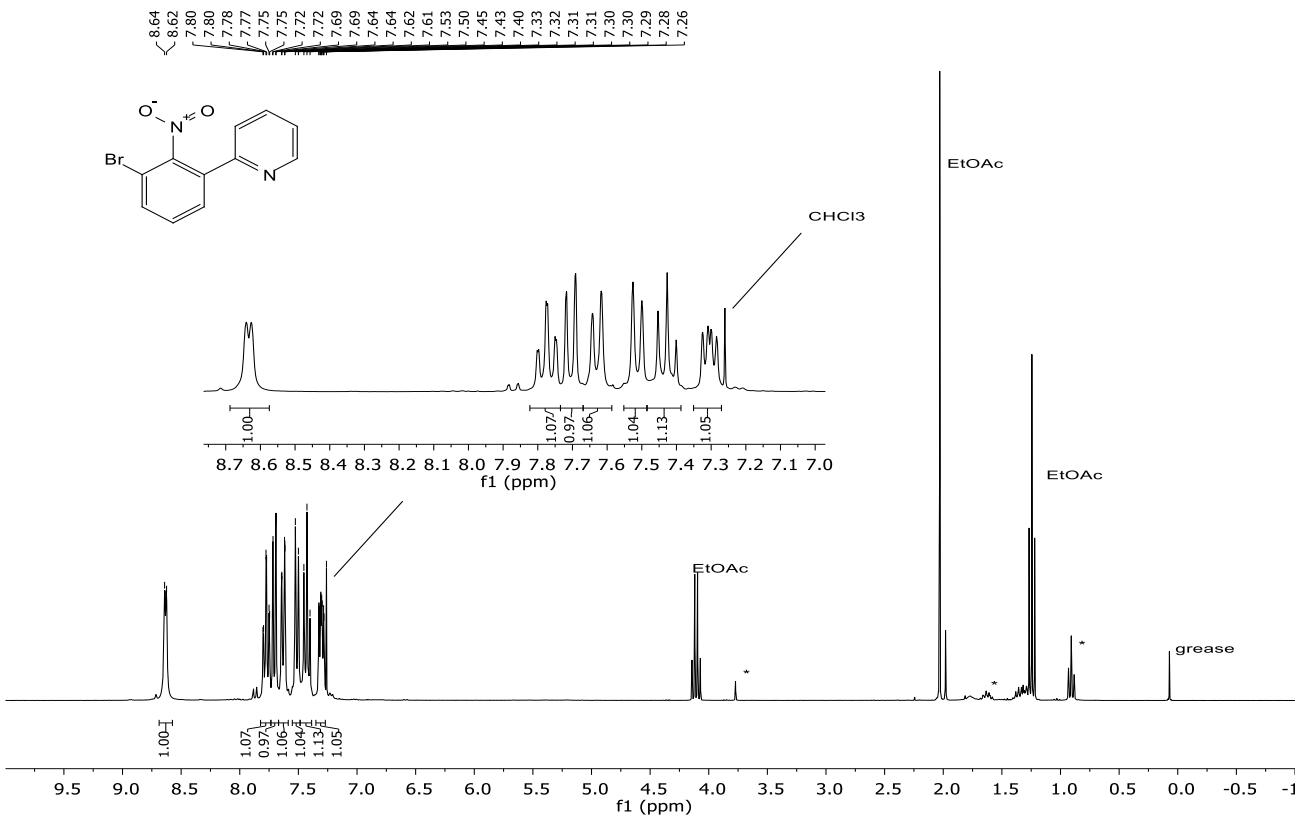

Figure S 71. ^{1}H NMR spectrum (300 MHz, $CDCl_3$) of crude **s8**. Impurities are marked with an asterisk.

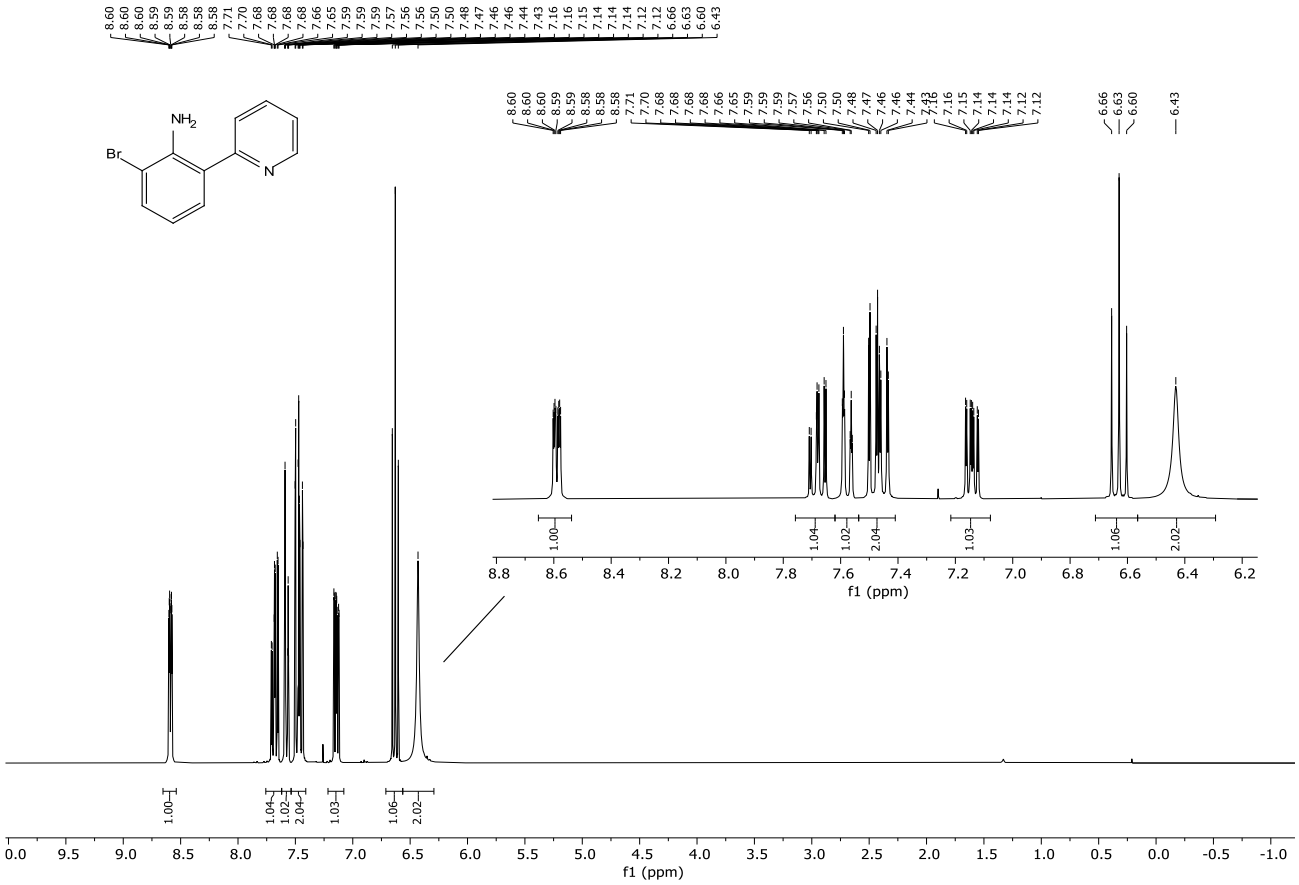

Figure S 72. ^{1}H NMR spectrum (300 MHz, $CDCl_3$) of **s9**.

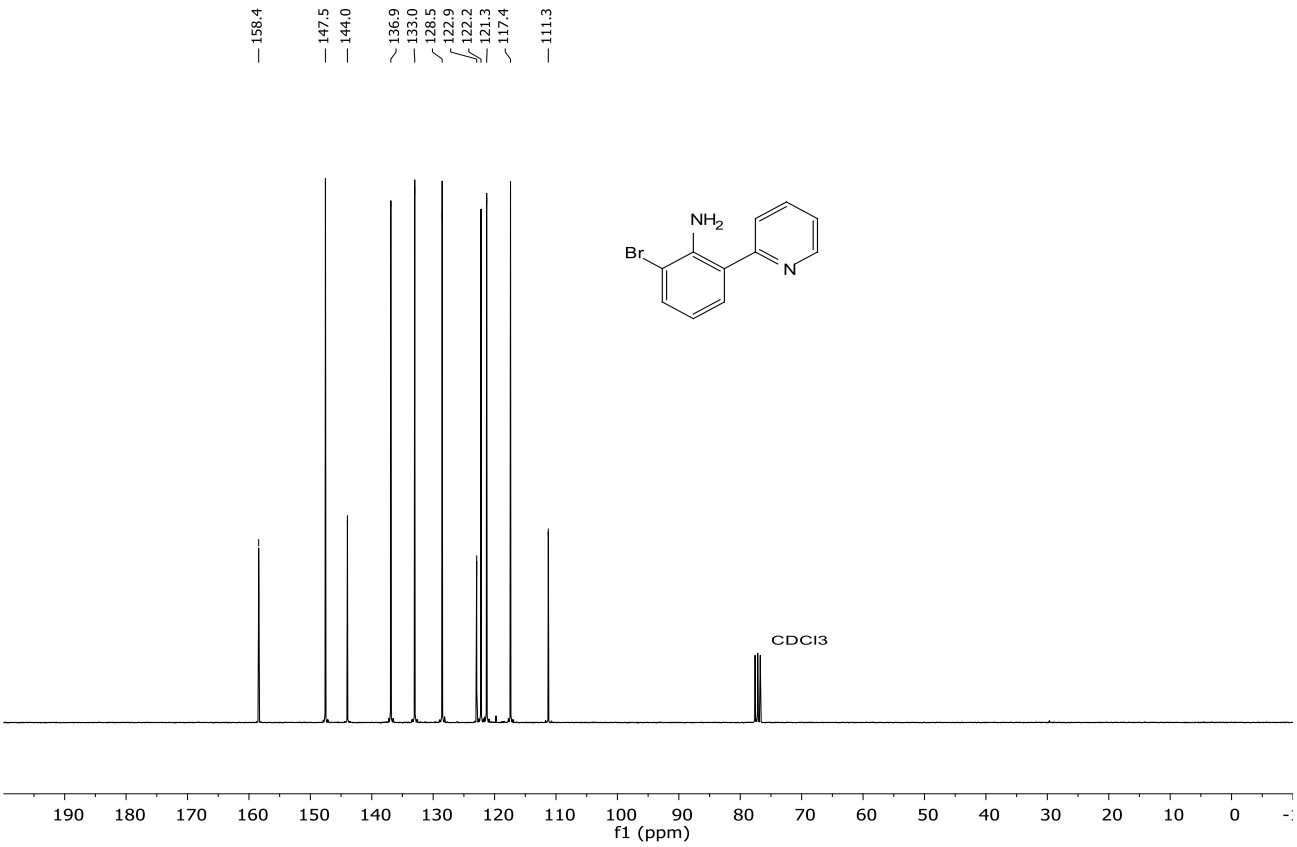

Figure S 73. ^{13}C NMR spectrum (75 MHz, $CDCl_3$) of **s9**.

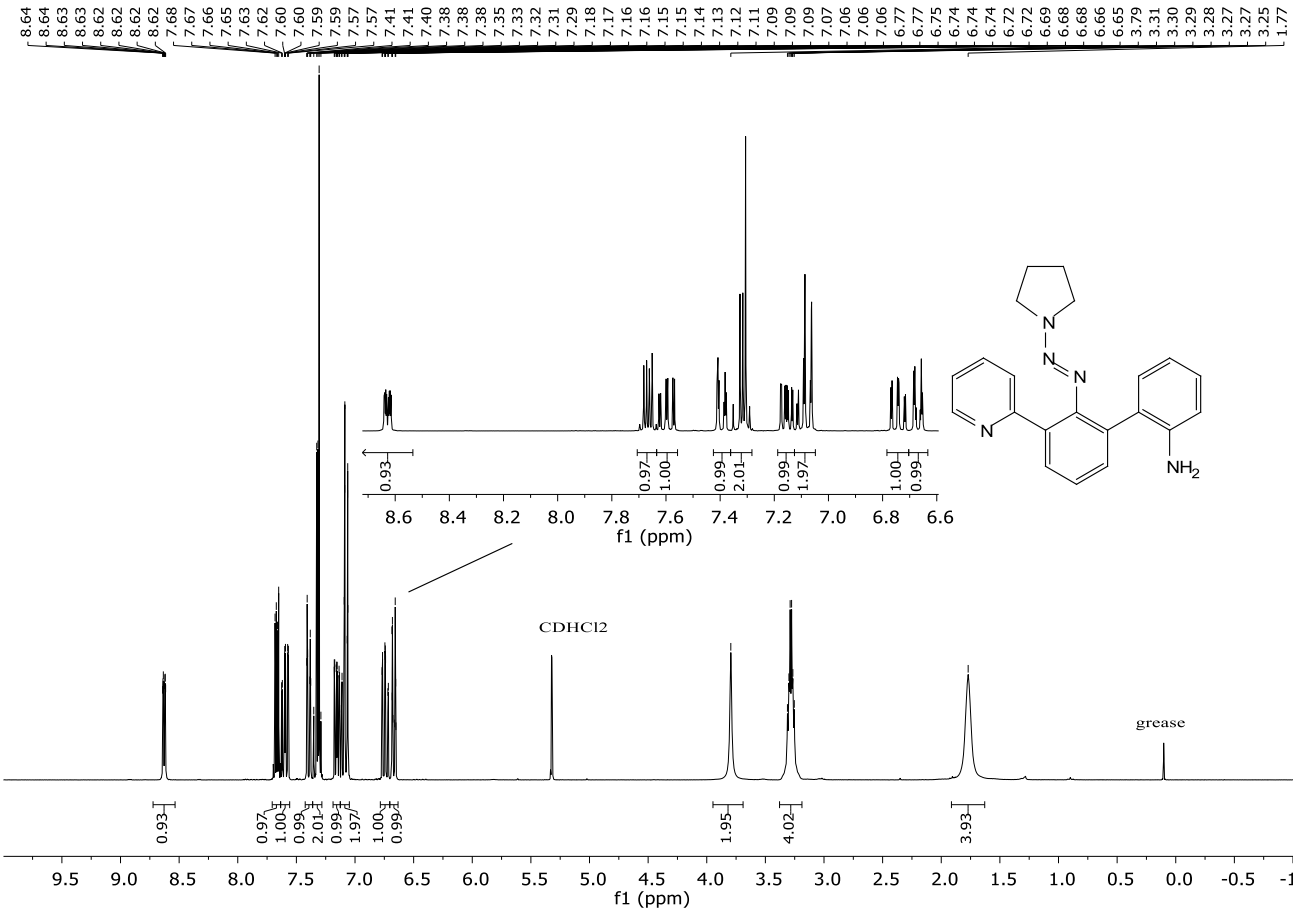

Figure S 74. ^{1}H NMR spectrum (300 MHz, CD_2Cl_2) of **s15**.

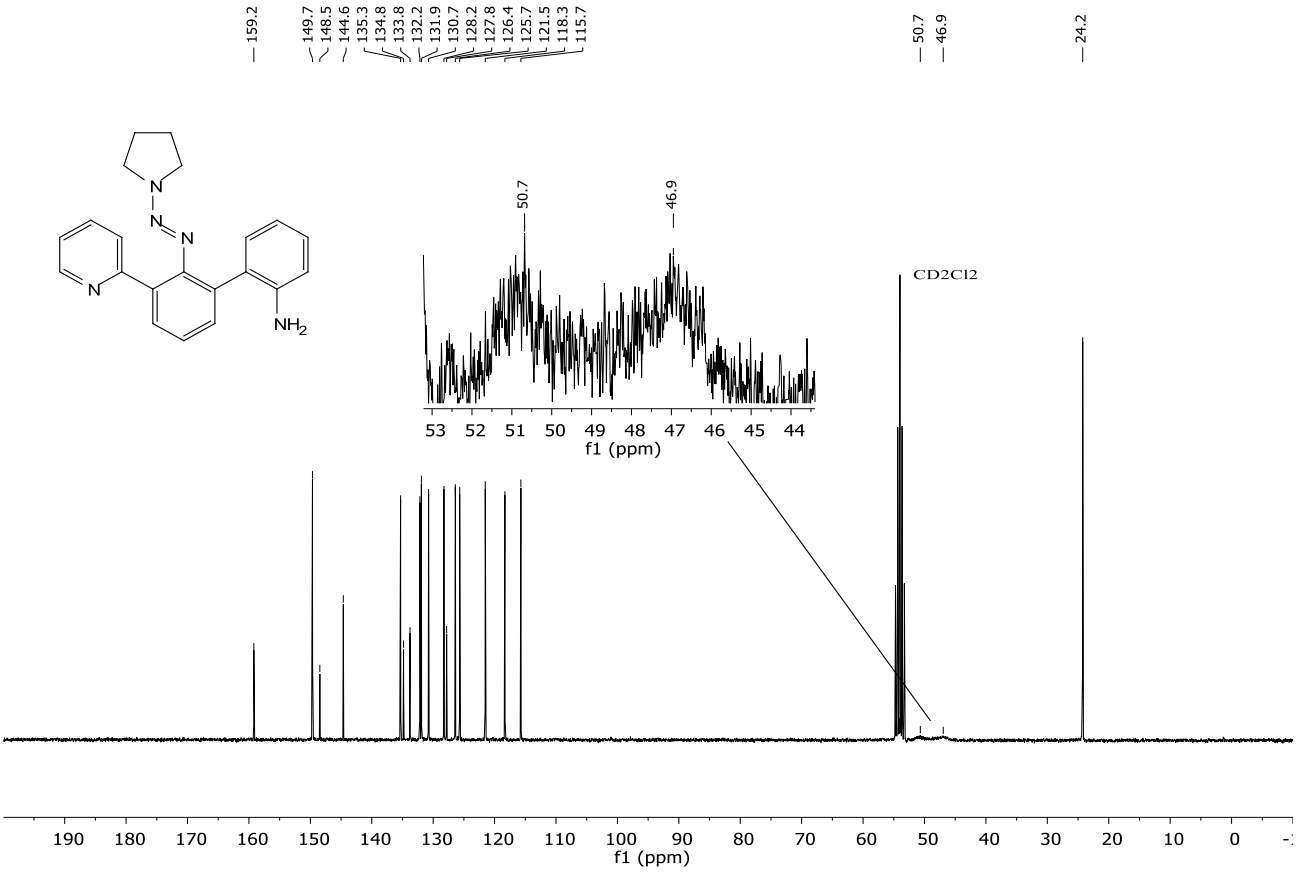

Figure S 75. ^{13}C NMR spectrum (75 MHz, CD_2Cl_2) of **s15**. The inset shows the two signals of the NN-(*CH*$_2$) atoms of the pyrrolidine moiety which show different chemical shifts probably due to a hindered rotation around the *N-N*-axis and/or the ability of fast *E/Z*-isomerization of the N-N-double bond. Please refer to the HSQC-spectrum Figure S 76 as well.

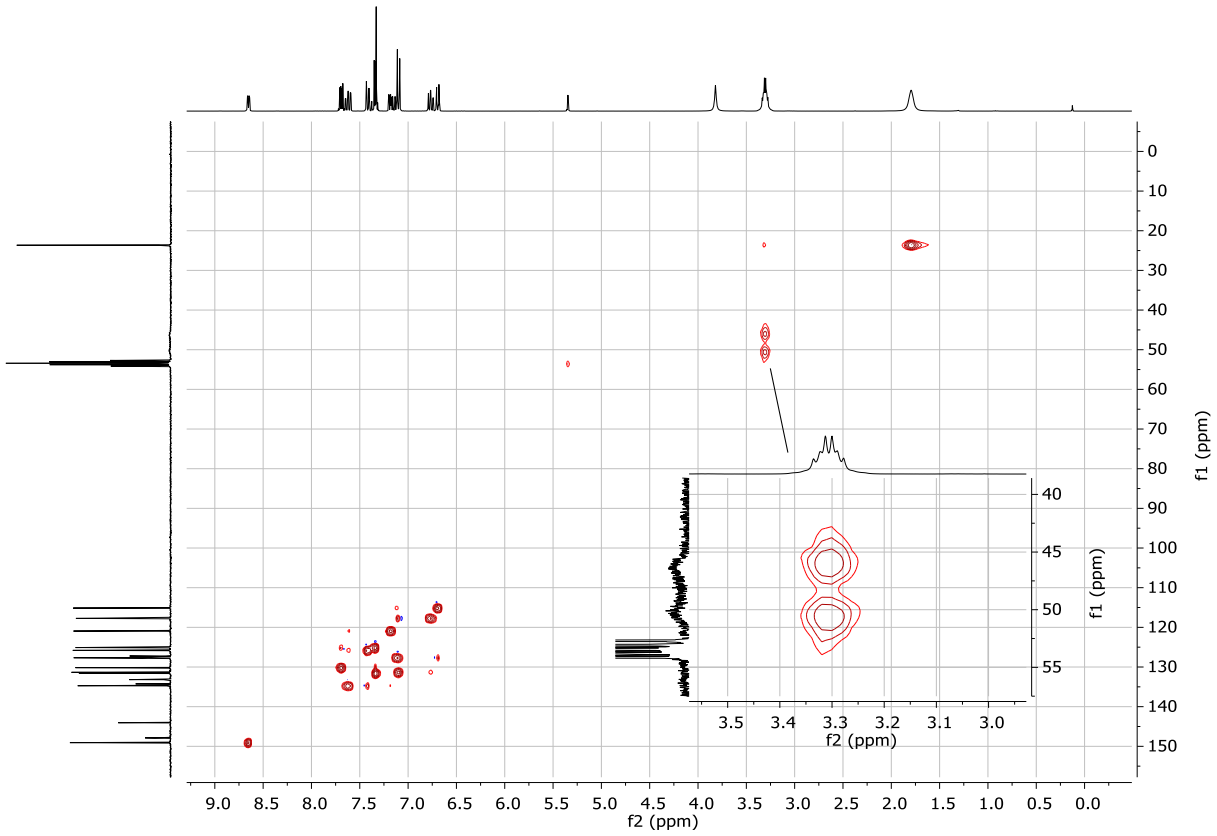

Figure S 76: $^{1}H/^{13}C$ HSQC of **s15** in CD_2Cl_2. The inset shows the signals due to the NN-(*CH*$_2$) carbon atoms of the pyrrolidine moiety.

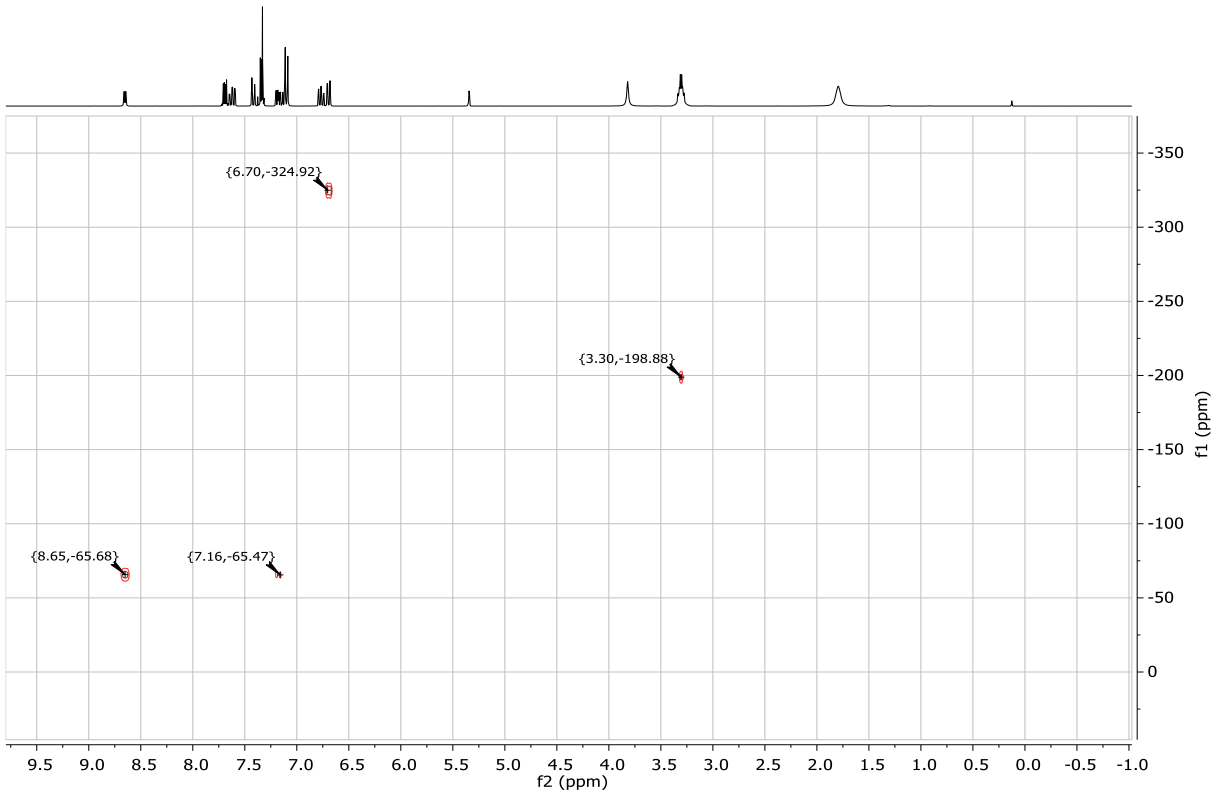

Figure S 77. $^{1}H/^{15}N$ HMBC of **s15** in CD_2Cl_2.

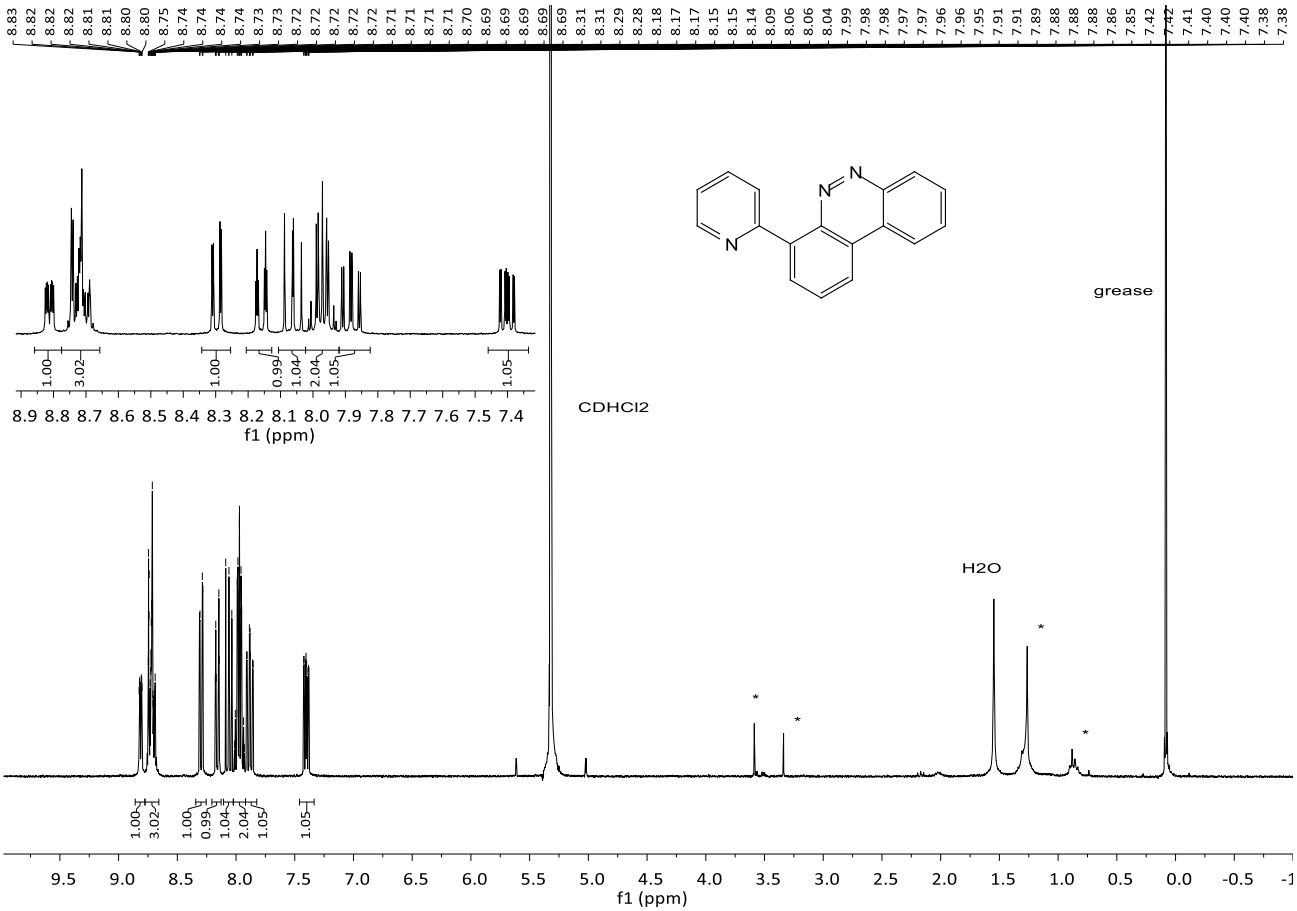

Figure S 78. ^{1}H NMR spectrum (300 MHz, CD_2Cl_2) of **s16**. Impurities are marked with an asterisk.

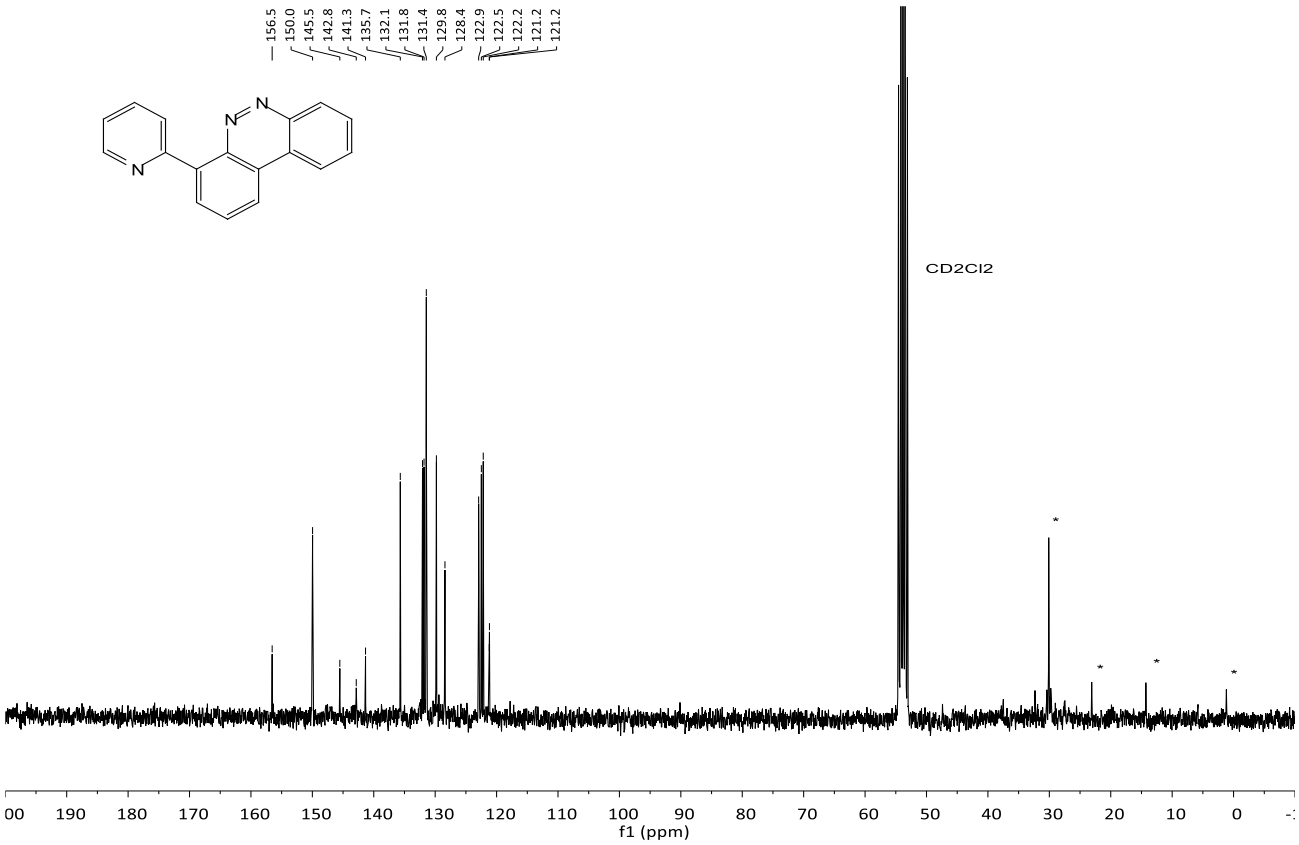

Figure S 79. ^{13}C NMR spectrum (75 MHz, CD_2Cl_2) of **s16**. Impurities are marked with an asterisk.

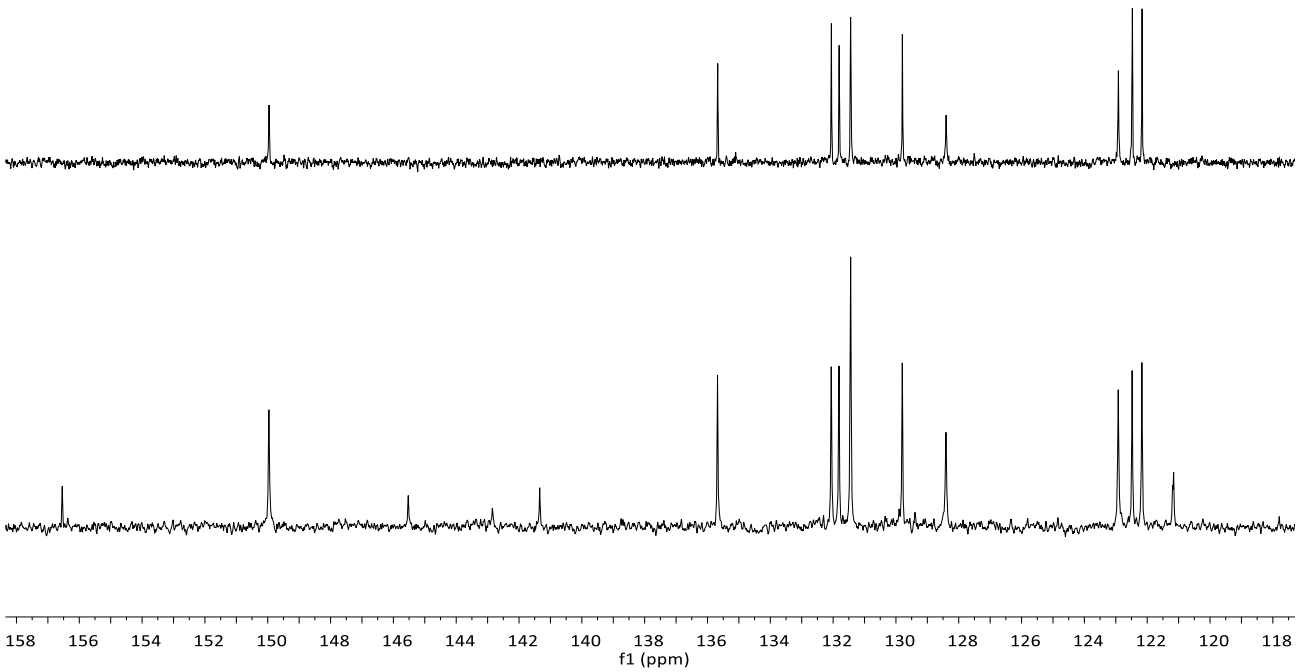

Figure S 80. Dept135 (top) and ^{13}C (bottom) spectra of **s16** in CD_2Cl_2.

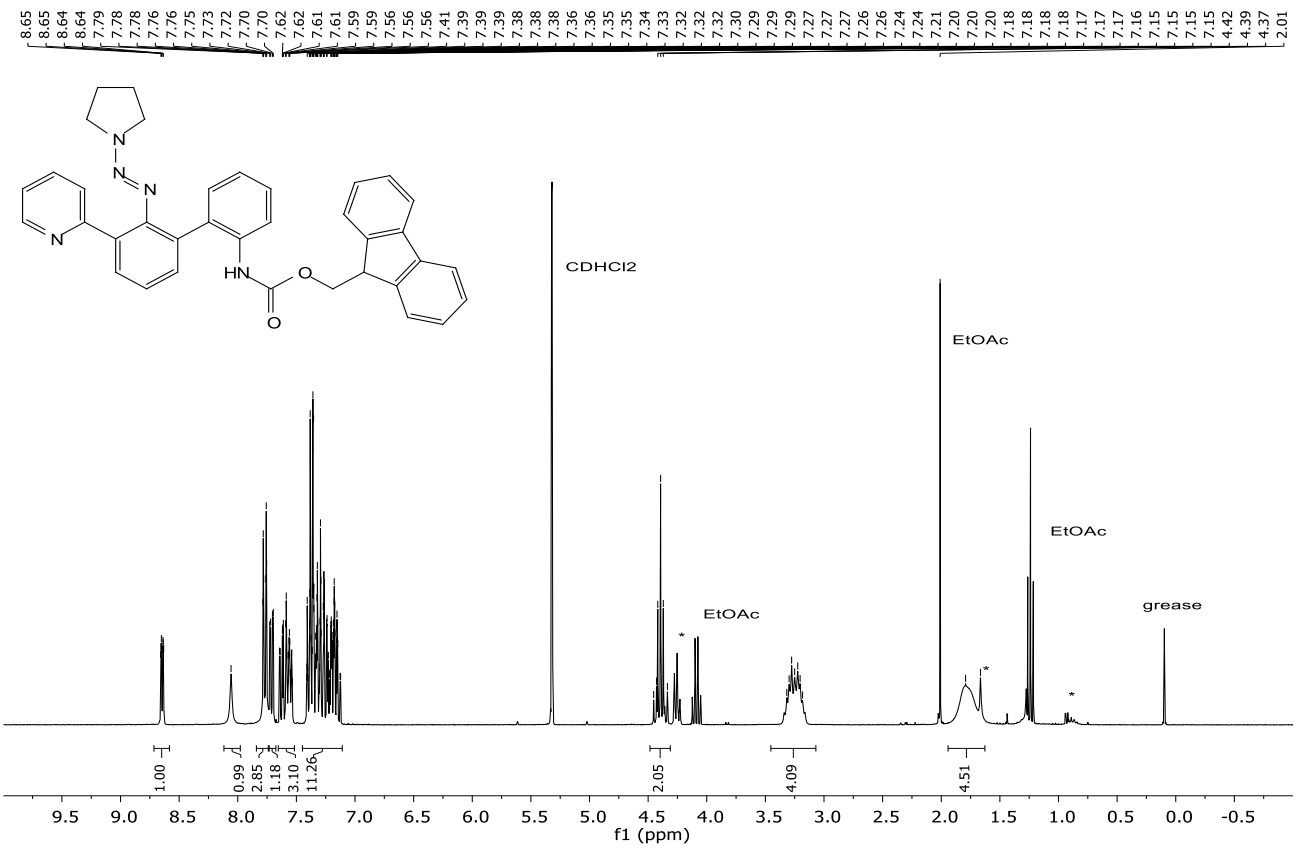

Figure S 81. ^{1}H NMR spectrum (300 MHz, CD_2Cl_2) of crude **s17**. Impurities are marked with an asterisk.

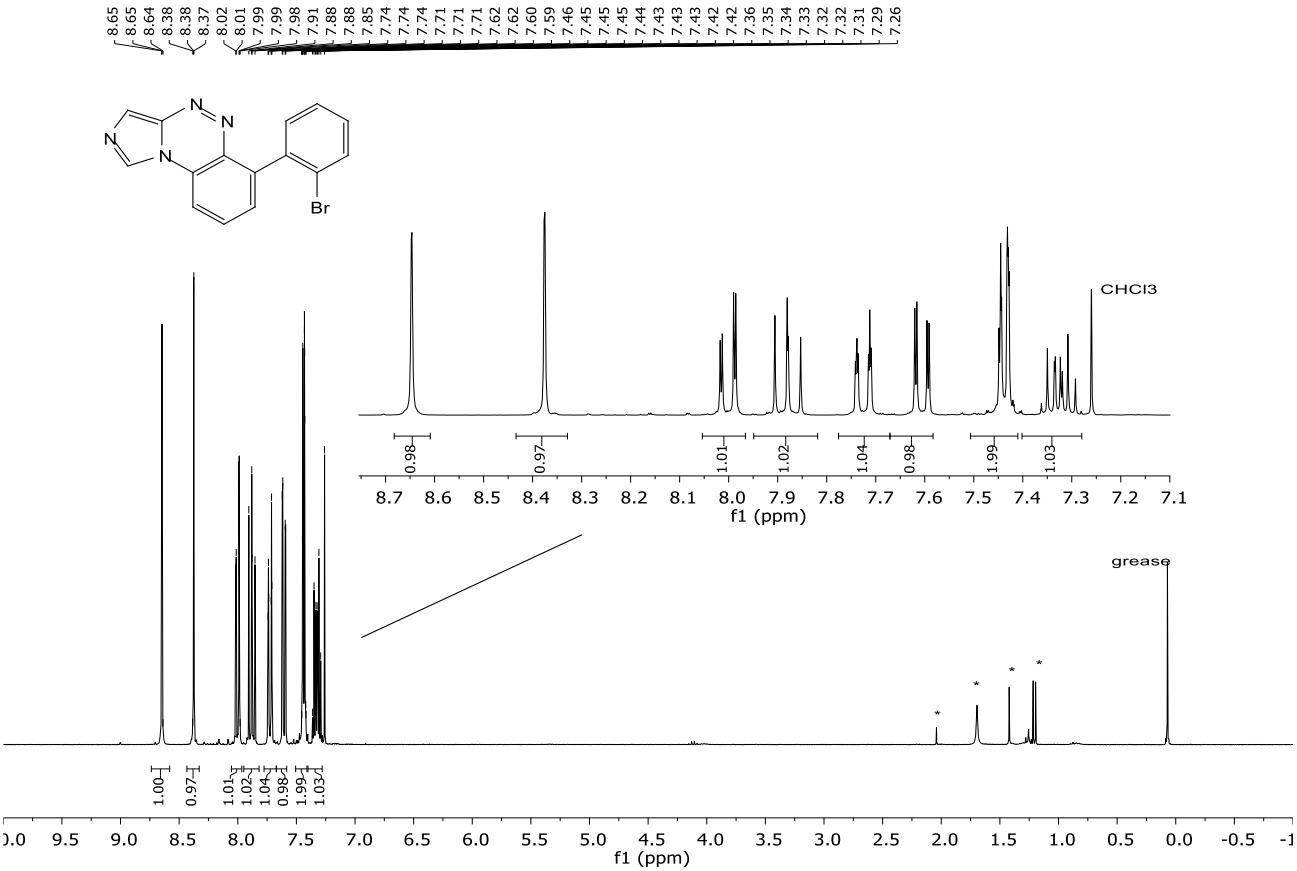

Figure S 82. ^{1}H NMR (300 MHz, $CDCl_3$) of **s19**. Impurities are marked with an asterisk.

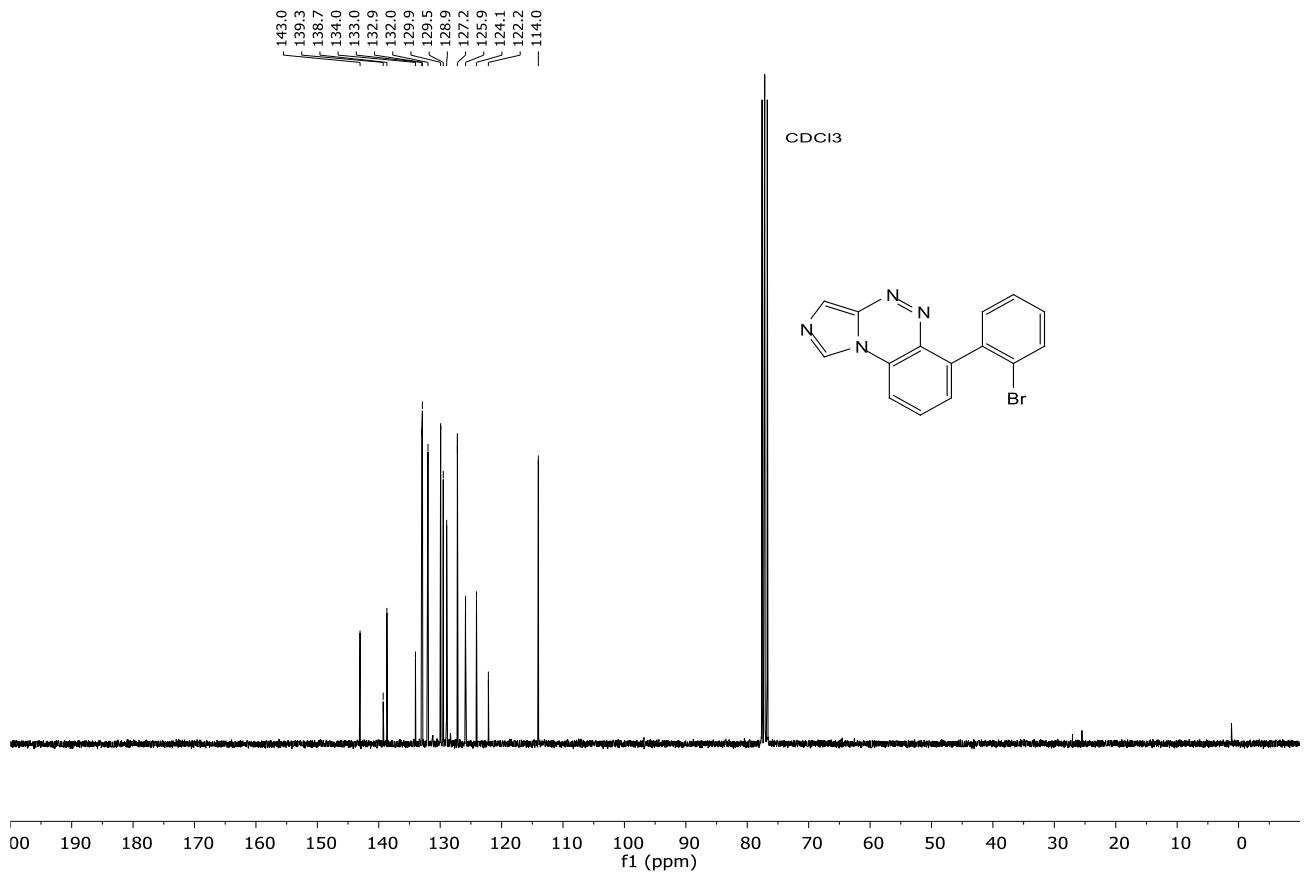

Figure S 83: ^{13}C NMR (75 MHz, $CDCl_3$) of **s19**.

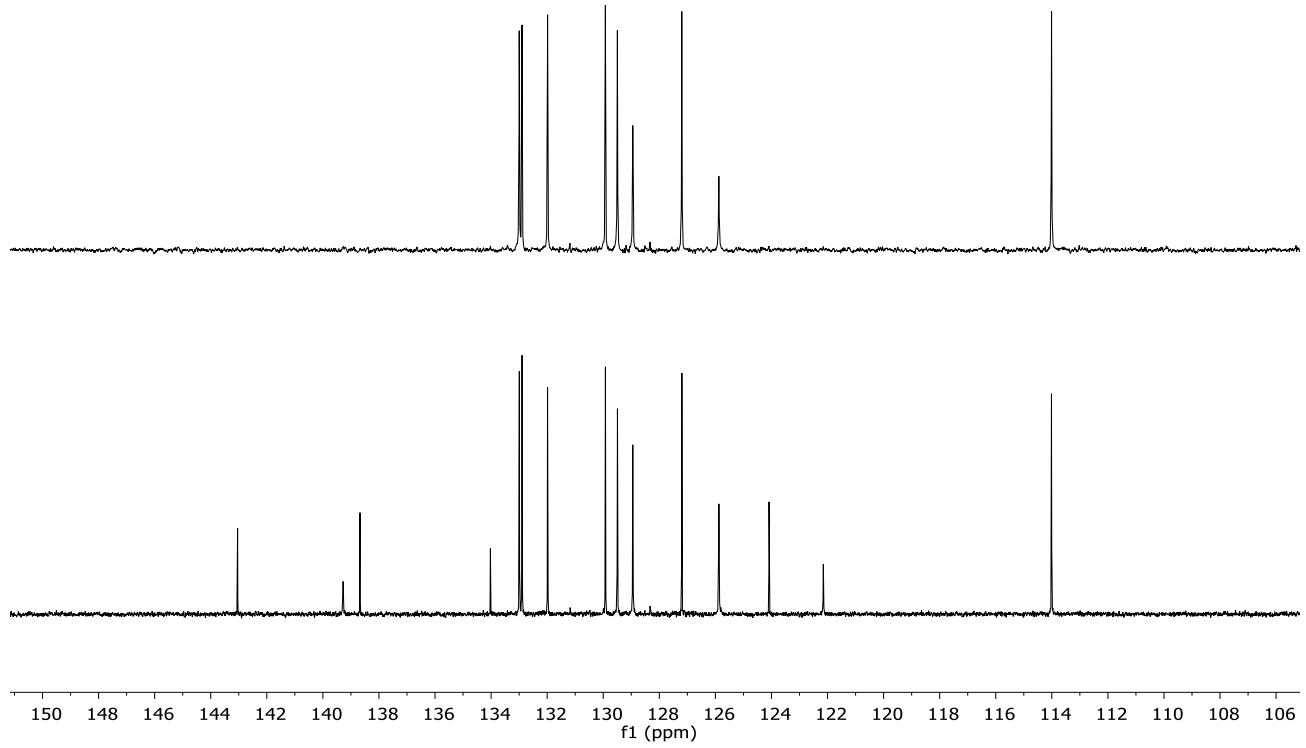

Figure S 84. Dept90 (top) and ^{13}C NMR (bottom) of **s19** in $CDCl_3$.

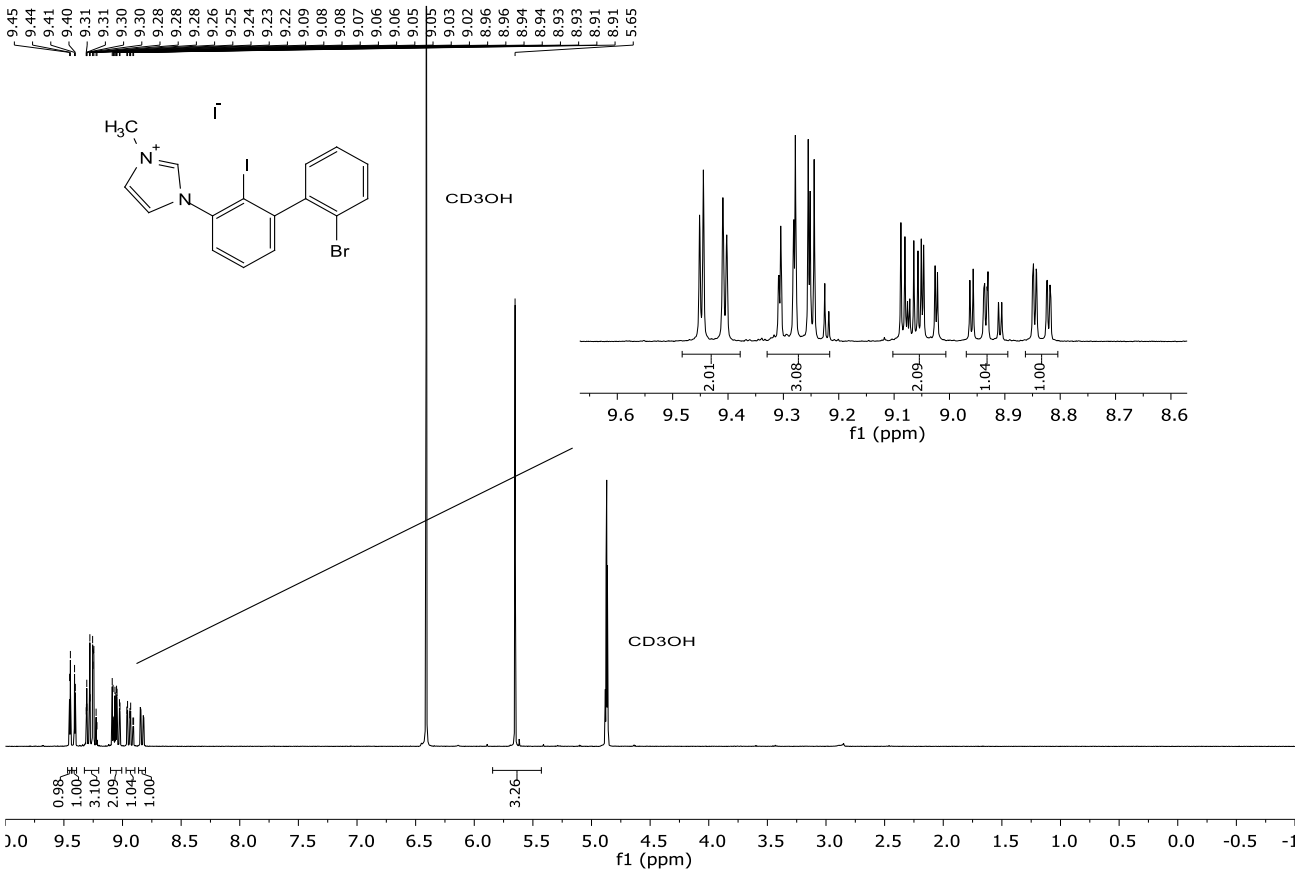

Figure S 85. ^{1}H NMR (300 MHz, MeOH-*d4*) of **s20**.

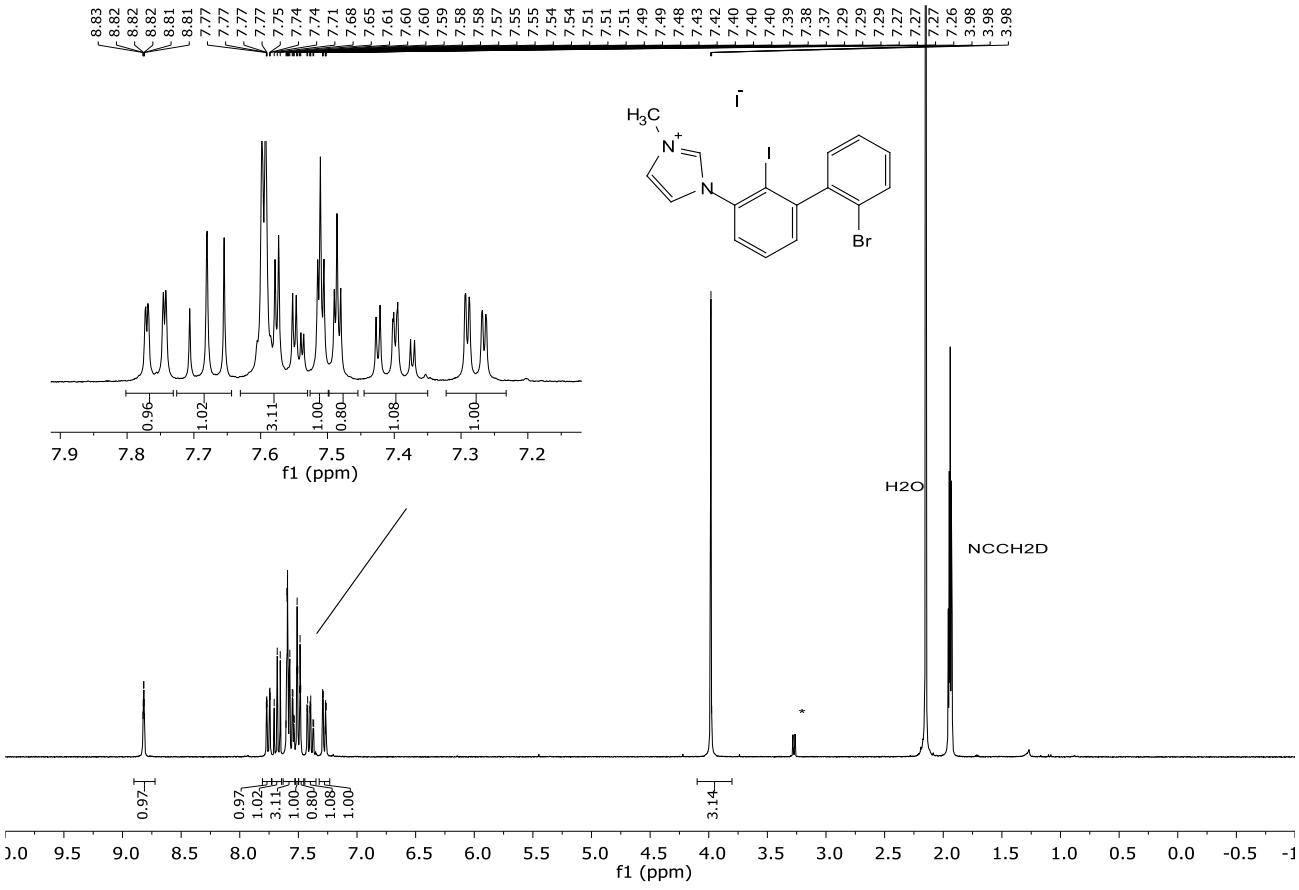

Figure S 86. ^{1}H NMR (300 MHz, MeCN-*d3*) of **s20**. Impurities are marked with an asterisk.

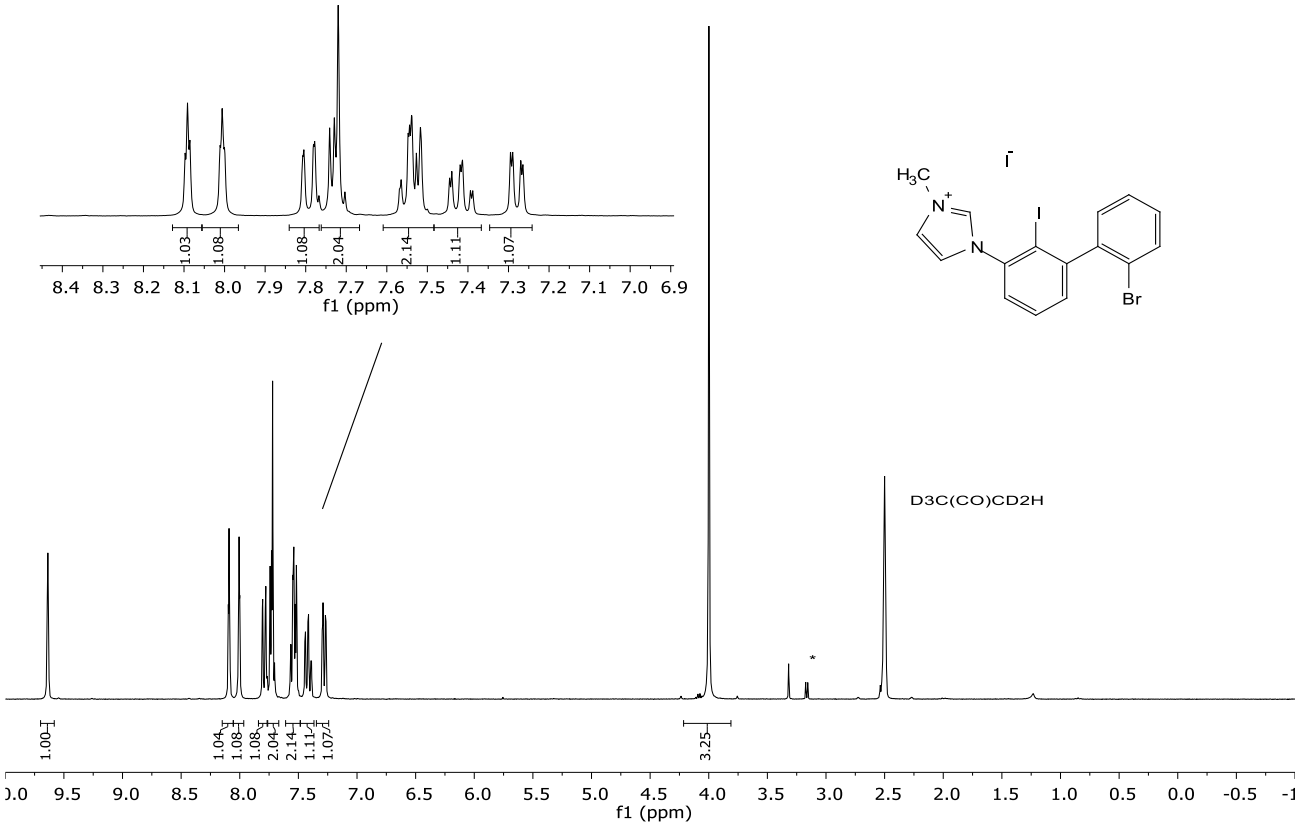

Figure S 87. ^{1}H NMR (300 MHz, DMSO-*d6*) of **s20**. Impurities are marked with an asterisk.

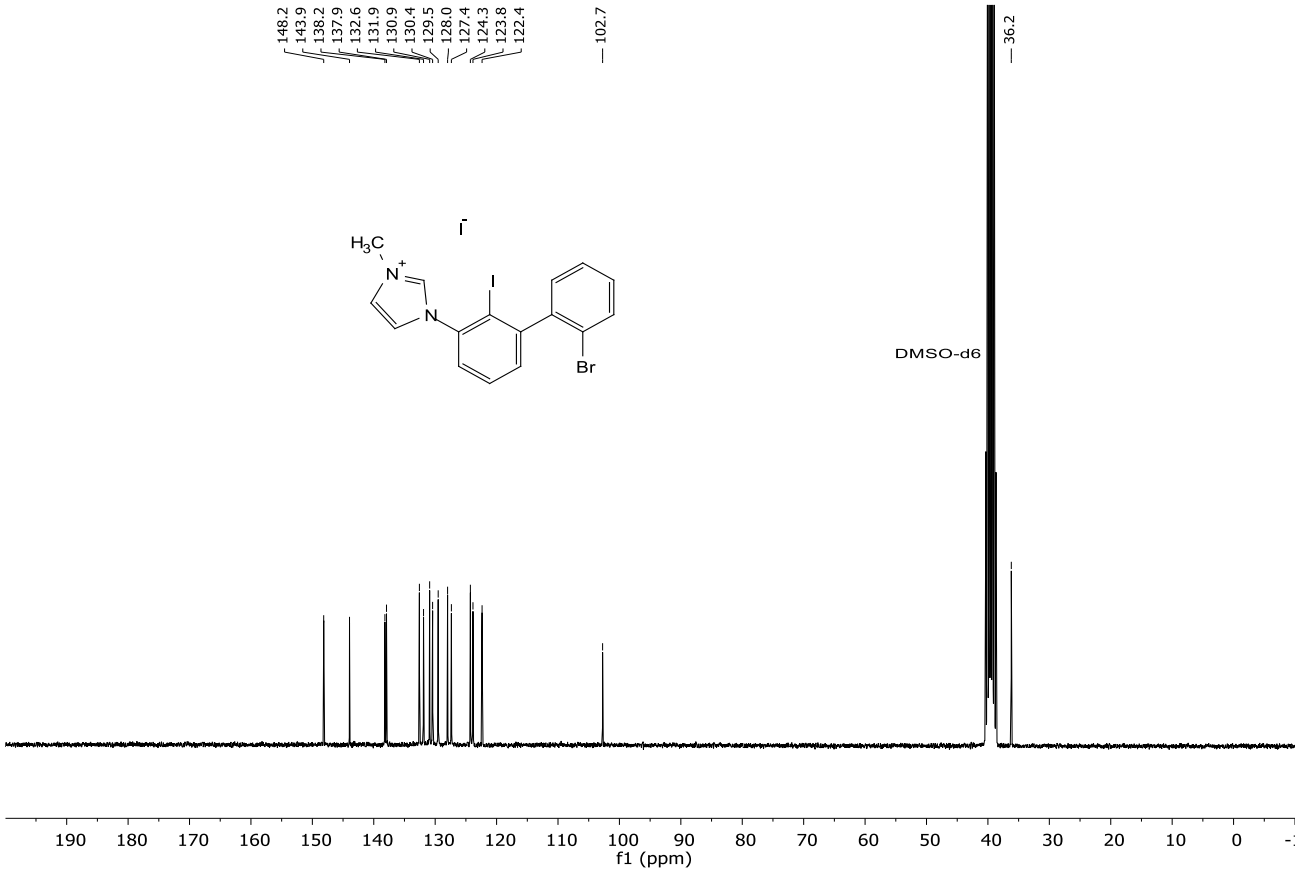

Figure S 88. ^{13}C NMR (75 MHz, DMSO-*d6*) of **s20**.

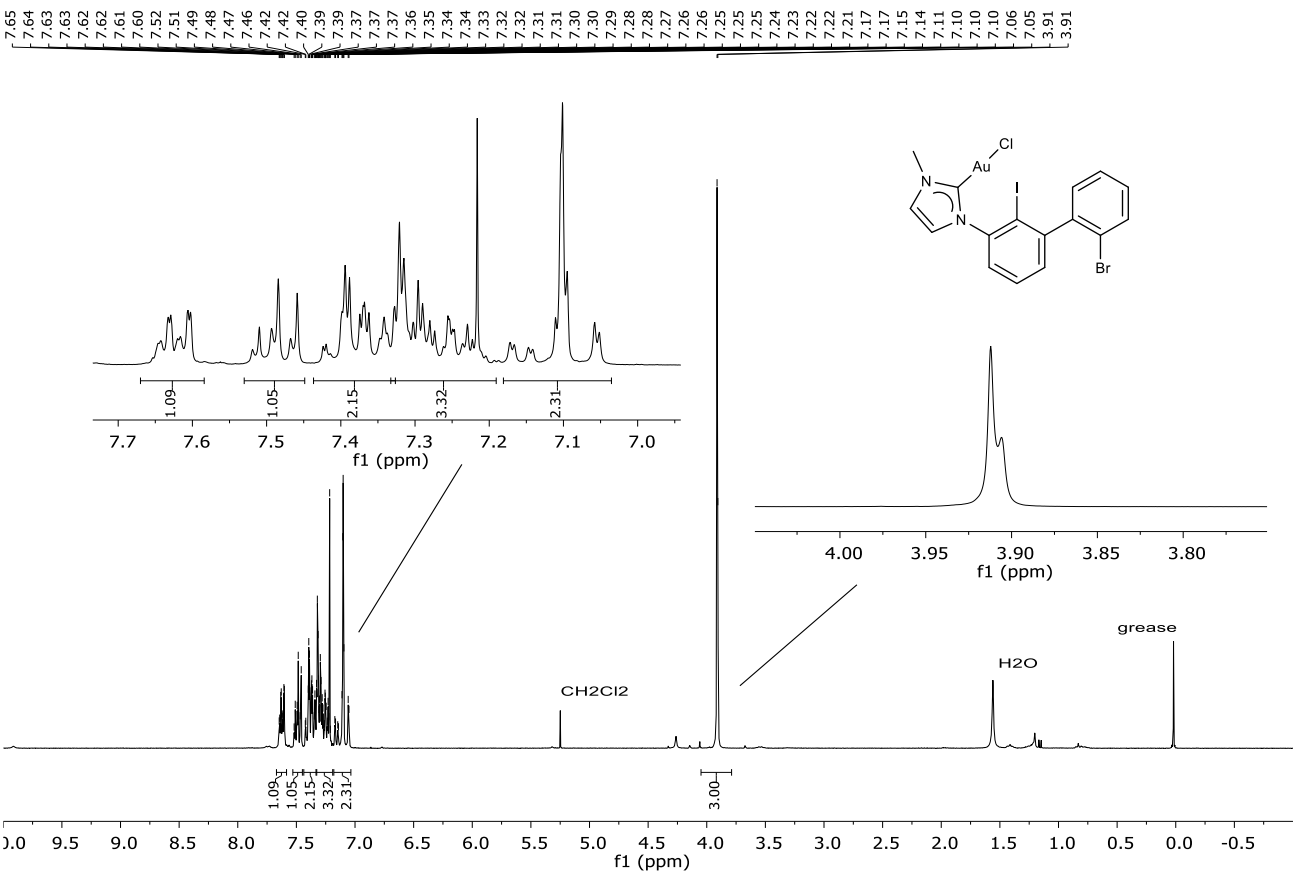

Figure S 89. ^{1}H NMR (300 MHz, $CDCl_3$) of **s21**. The insets show the doubled resonances due to the two rotamers.

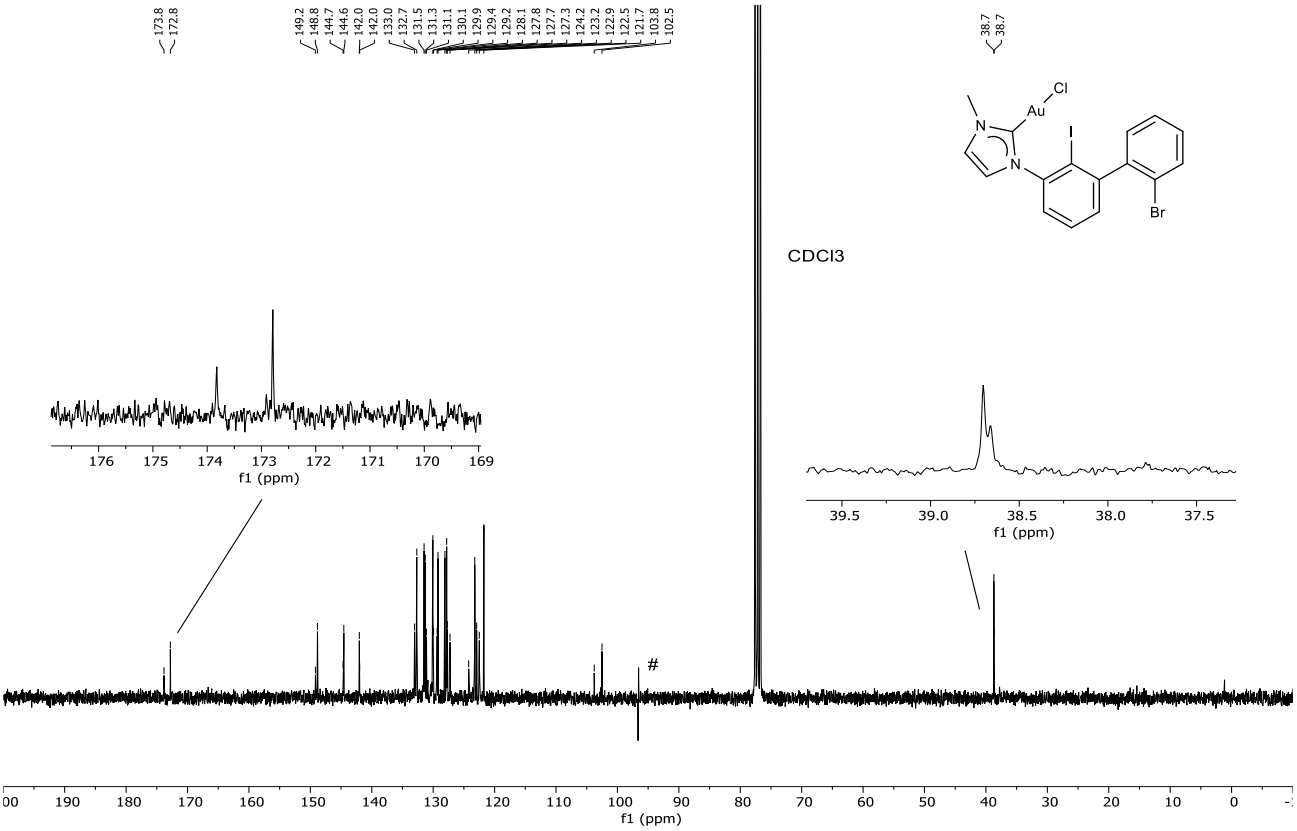

Figure S 90. ^{13}C NMR (75 MHz, $CDCl_3$) of **s21**. Exemplarily, the two insets show doubled resonances due to the two rotamers. The signal marked with # is due to an artefact of the spectrometer.

S 7 Coordinates of Calculated Structures

Attached in this section are the structures of complexes **34**, **35**, **39**, and **40** in the respective S_0 and T_1 geometry. In addition, tor the phenylalkynylide complexes **34** and **35** the planar transition state is listed. All coordinates in TURBOMOLE coord format.

[(C^C^N)Au(III)CCPh] @ S0; TPSSh/def2-TZVP(P)

```
$coord
   -4.44260571829780      3.45772655130228     11.28248830643123  au
   -6.87534754403167      2.22929253861739     14.00806565086017  c
   -2.05284470787977      4.76825060304226      8.69211860850517  c
   -4.28896951096062      0.40022365806585      8.96205410635605  c
   -8.31180894537827      1.59625859574145     15.70301033795938  c
   -1.10475252357055      7.20571132284895      8.98245495704538  c
   -1.41219905206263      3.19039805083448      6.67791236281518  c
   -2.67917548200951      0.72214225754593      6.83530065133900  c
   -5.58396478524990     -1.85047748784977      9.30940213099886  c
   -9.98529903813224      0.84354650212012     17.67448370187307  c
    0.58360775191312      8.12196783767892      7.15158568000869  c
    0.26850634325538      4.12787822706800      4.87153101159605  c
   -2.42618018889441     -1.25604502560603      5.11182787212510  c
   -6.80637504246422     -2.08230515639251     10.93379480010151  h
   -5.30278800727755     -3.80900250442326      7.55847196034451  c
  -12.60687134286508      1.21288641390924     17.45198633548336  c
   -9.05431193247854     -0.28649618626237     19.89153975626394  c
    1.38226841031973     10.00520444256659      7.27991832424176  h
    1.24196079205440      6.57343477304096      5.13082481792408  c
    0.83601560394315      2.99008342723631      3.26305768380084  h
   -1.20474553544306     -1.03837956334420      3.47894350434249  h
   -3.73257853214203     -3.51161676811276      5.47272241366648  c
   -6.31872387834641     -5.56696759210352      7.83686007746256  h
  -13.34401346991525      2.07678308788637     15.74837301088261  h
  -14.22981954575421      0.47909840284045     19.37928550297502  c
  -10.68921550695134     -1.01520619852947     21.81052122897902  c
   -7.03742219267274     -0.58531252569938     20.07851086436902  h
    2.54589039680229      7.28070601478538      3.71808528178116  h
   -3.52215822893509     -5.03709908947895      4.12126239551337  h
  -16.24667744173359      0.77767654911409     19.17126996550033  h
  -13.28273964784960     -0.63647608040240     21.56732893343984  c
   -9.93469717884383     -1.88647236817763     23.50513355950005  h
  -14.55454734983188     -1.20819179318134     23.06802355088552  h
   -2.01277179837528      8.55373608629762     11.22996647062431  c
   -3.65507182856438      7.22996549925665     12.71831599669515  n
   -1.33422096732300     11.00709732910880     11.92079194413178  c
   -4.61279462871992      8.25638161465281     14.81766678434034  c
   -2.32744359438562     12.07427280821040     14.09879098399243  c
   -3.99650855135062     10.68549026904485     15.58172317375089  c
   -5.89754773796438      7.05908119519715     15.87234066951591  h
   -1.80232075267526     13.97962051376417     14.63661002419146  h
   -4.80921357488122     11.45448338652393     17.29308698045390  h
   -0.03309413653461     12.06022043582780     10.74598971836487  h
$end
```

[(C^C^N)Au(III)C_6F_5] @ S0; TPSSh/def2-TZVP(P)

```
$coord
   -0.00801154828288      0.04146639243581     -0.13071467623821  au
    0.59872623523132      0.65011426313179     -3.80149889327175  c
   -0.71659904856216     -0.66924421033542      3.74874231734089  c
    3.23000299710333      2.10525580673127      0.09716460799460  c
    2.72268745144979      2.04813871752260     -4.49026857864158  c
   -1.10845391781683     -0.34981707341307     -5.53140502072558  c
    0.07512259689244     -2.87695473414121      4.92082314204401  c
   -2.03154322607847      1.00681889470181      5.27778822215846  c
    4.20348410726867      2.87023664096161     -2.28806389212045  c
    4.48202044233282      2.77851084703111      2.29776116481128  c
    3.13708992690281      2.45528214099640     -7.06572793175831  c
   -0.66737243526007      0.07377741283079     -8.11408704514681  c
    1.35811137335594     -4.63832278626048      3.57670011223664  f
   -0.37815222600540     -3.41882988927020      7.45117379157094  c
   -2.89503321110762      3.20796544338691      4.30115180807541  f
   -2.53981771376108      0.55788634905290      7.81636332344597  c
    6.41720034564287      4.29676285133067     -2.37384986065115  c
    6.69912092796419      4.21051434213157      2.17153667275032  c
    3.74976464294968      2.19976128923031      4.11823180536402  h
    1.44229249607923      1.46609716904747     -8.83810837583867  c
    4.75680648110489      3.52821883234241     -7.72024237859059  h
   -1.93156137526430     -0.66027602497988     -9.55043384018186  h
    0.42703449592958     -5.58078557612365      8.50224673460558  f
   -1.69980138077926     -1.67858172728509      8.90820838277381  c
   -3.82631860014580      2.23090102654304      9.22104198775136  f
    7.17810481489585      4.89127817197027     -4.18282466930657  h
    7.66007621969718      4.96497430864785     -0.15311546187022  c
    7.66636892747417      4.73002671596043      3.90162193929953  h
    1.78301411250239      1.79286630450834    -10.83131468546233  h
   -2.17112422166951     -2.15885596615840     11.34609810673353  f
    9.37937323374851      6.07528636837490     -0.24218901088955  h
   -3.21665343524500     -1.76304172172141     -4.41606337418762  c
   -5.15411022094585     -2.92437163334632     -5.77741564757381  c
   -3.21265486753385     -1.90742331203636     -1.83701494689184  n
   -7.05590358530886     -4.21000603024086     -4.51491592227149  c
   -5.04929941599509     -3.14788597478979     -0.62433979396633  c
   -7.01387359061111     -4.33044100574309     -1.88928726121398  c
   -5.15454791890649     -2.80948257429284     -7.81900967150657  h
   -8.56088859892107     -5.11166512863218     -5.57147260162663  h
   -4.90597650444015     -3.17152648659251      1.41680827039360  h
   -8.46182235915664     -5.31414491854019     -0.83313467538513  h
$end
```

[(C^C^C′)Au(III)CCPh] @ S0; TPSSh/def2-TZVP(P)

```
$coord
   -0.23456655877848      4.75143615458614     11.24517249246243  au
    0.16824044866007      2.88984972788168     14.58703181386553  c
   -0.60393990500308      6.51856996776178      7.92133422018239  c
   -1.56167022663779      8.33817414466007     12.36571771787803  c
    0.92443760441509      1.92209390480167      8.82416676304433  c
    0.40640846989286      1.78225301583283     16.60047751753066  c
   -1.45628200649501      8.98835667953216      7.88696663247793  c
    0.00999420675585      5.21818494698151      5.71631635172791  c
   -1.96599263710866      9.93088185302070     10.36832121825471  n
   -2.18394861894527      9.68809190650249     14.42681362508799  n
    0.87234903144322      2.62257949741394      6.22695595777104  c
    1.71262591397014     -0.49210115926740      9.48622043457254  c
    0.69087812558857      0.47305188854770     18.93642451396547  c
   -1.73926527275160     10.29054080232112      5.62142102712837  c
   -0.26528377709845      6.50357525175330      3.41773744865409  c
   -2.83029417847260     12.24341252967032     11.19445487160446  c
   -2.04229965980517      8.72352111042870     17.00988337890069  c
   -2.96859277486442     12.09300441532677     13.75290581340803  c
    1.61103434256559      0.88105761481840      4.39070697993781  c
    1.75643154992211     -1.03592940797265     11.45991530407663  h
    2.44687558150106     -2.21611390610077      7.62448958365603  c
   -1.29071006139298     -0.99512868716128     19.92620163196832  c
    2.96164799948118      0.61312896564369     20.30965697433231  c
   -2.40330772940454     12.22647015658074      5.54138142405298  h
   -1.12717867751261      8.99638417713136      3.40006884108724  c
    0.18269540856389      5.58987627553940      1.63871142393256  h
   -3.26863254403655     13.77597961073037      9.93343825678999  h
   -3.91353133473863      8.78059805110221     17.87209648343608  h
   -0.73660316298370      9.87942034643582     18.10858132964666  h
   -1.36437580769157      6.78177371435218     16.92405104647107  h
   -3.54949128875697     13.46958528378858     15.13300224333824  h
    1.57525459457167      1.40390720349988      2.40765151448550  h
    2.39591258561116     -1.53166643749859      5.08772118795013  c
    3.05875018344451     -4.09617783325101      8.16642641424958  h
   -3.04541684533180     -1.12441461828090     18.87901571857305  h
   -1.00546583600953     -2.26900895440257     22.20283458282482  c
    3.23224870497924     -0.66660836584130     22.58477296962840  c
    4.50462832574168      1.73059825545817     19.55942423712774  h
   -1.33143310587402      9.96911624285074      1.60904890210353  h
    2.96694506658002     -2.87398793268866      3.64853005108487  h
   -2.55503088575636     -3.39514108453752     22.93162659845119  h
    1.25344622925201     -2.11267988795945     23.54526572943372  c
    5.00077775022691     -0.53794268767740     23.61250400774631  h
    1.47137462651085     -3.11202094246255     25.32013763178303  h
$end
```

[(C^C^C)Au(III)C_6F_5] @ S0; TPSSh/def2-TZVP(P)

```
$coord
   -0.02761828638669     -0.03311010823023      0.06049169143804  au
    0.59242560422807      0.58774109684741     -3.62886155952461  c
   -0.56212348201757     -0.58532738838388      3.98502345893934  c
    3.24795703592532      2.08031372585042      0.25247181779623  c
   -3.11070074819889     -1.94274308810112     -1.63006105856436  c
    2.69105896714117      2.00566699722339     -4.33684076292712  c
   -1.08048148328457     -0.39258904769896     -5.37517940906564  c
    0.32609898513464     -2.70653110836042      5.24424211464214  c
   -1.77955035722819      1.18592116731676      5.48750092993770  c
    4.18987917566430      2.84545460837419     -2.14954463205299  c
    4.55599410508035      2.78848307020924      2.41475122220304  c
   -3.08863566163620     -1.77504613162913     -4.21171826650115  n
   -5.17504310763177     -3.32709399641325     -1.08532977558406  n
    3.07166242913772      2.41976330467322     -6.92459192717645  c
   -0.73024729522586      0.00049665074956     -7.95050224922432  c
    1.51746175633549     -4.55535011837978      3.93455801173275  f
    0.05640709176631     -3.07563420072966      7.83187830166588  c
   -2.73097789565889      3.31083956189997      4.42792759992554  f
   -2.10075950766261      0.90982069191126      8.08086918664027  c
    6.39131191220476      4.28695911273713     -2.29393189580758  c
    6.76116094018698      4.23285136311140      2.24237774786074  c
    3.87007488064860      2.22178976088789      4.25878553005454  h
   -5.11474938531895     -3.04102020681414     -5.24248794677132  c
   -5.96993383616291     -4.00933581094777      1.46543244353475  c
   -6.43304971673724     -4.02216728322780     -3.27288231172633  c
    1.37428856150772      1.42216024183153     -8.67907033000222  c
    4.67262754534986      3.51016688658167     -7.59367501515048  h
   -2.01280574975244     -0.74644203336075     -9.36179493959629  h
    0.94769180940127     -5.16197286124459      8.96511186989649  f
   -1.16868575975694     -1.24379255986793      9.26075693432736  c
   -3.29354109925698      2.67548463190527      9.45494051991721  f
    7.11314121648050      4.87354291308696     -4.12173816231760  h
    7.67436078389482      4.98006171234084     -0.10412968248628  c
    7.75862360270425      4.76987314172323      3.95050717933397  h
   -5.45327844249414     -3.14306467579081     -7.24392902398324  h
   -7.87445505890788     -3.30260677797025      1.81122250803511  h
   -4.65427699565001     -3.14870116583159      2.78747194466404  h
   -5.93713837485258     -6.05866793351724      1.68116065290722  h
   -8.13301430756547     -5.13826476250150     -3.23744315131374  h
    1.69029169266930      1.75653100723887    -10.67491980619493  h
   -1.45588971677277     -1.55547855900252     11.75511252389586  f
    9.38443817269805      6.10101817150349     -0.23396228337769  h
$end
```

[(C^C^N)Au(III)CCPh] @ T1; TPSSh/def2-TZVP(P)

```
$coord
   -4.45241398440573      3.54364420924720     11.35104082250042  au
   -6.88517905965387      2.30790809744323     14.07143973703408  c
   -2.07064983337772      4.79769057961121      8.73565823438572  c
   -4.33868622283190      0.45945928177508      9.07260728675515  c
   -8.32732437500069      1.61995250716379     15.73885032967029  c
   -1.12534313911383      7.21838755864000      9.02019331430442  c
   -1.46407655213778      3.16744487430002      6.73717417860306  c
   -2.69231625395239      0.79318827388890      6.90062438582653  c
   -5.60914408592055     -1.78841199909926      9.38659707386951  c
  -10.00569541730187      0.81756063866677     17.68633878613916  c
    0.62828835426584      8.08878822543718      7.06632655480981  c
    0.29976949369448      4.07616765863119      4.79530202621238  c
   -2.42851057634276     -1.21519521490315      5.14204996010581  c
   -6.83808682835426     -2.04688499012535     11.00232870070168  h
   -5.31052201355043     -3.74630102194232      7.61129846672360  c
  -12.62963368365070      1.15898276839760     17.44981339935662  c
   -9.07648791820712     -0.33352517051528     19.89310521641315  c
    1.44873720465274      9.96280410769636      7.15633819015544  h
    1.26358280350980      6.48728820093846      5.04613187431871  c
    0.82859488813520      2.89049672777063      3.21493565821127  h
```

```
   -1.20520017500979     -0.98536716180736      3.51566352173599  h
   -3.72822545163809     -3.44778886808194      5.50907124517675  c
   -6.32010421531449     -5.50949743105164      7.87698338296360  h
  -13.36475349875086      2.04335930138156     15.75588717855570  h
  -14.25729374175949      0.37651194707407     19.35383397110467  c
  -10.71628244195317     -1.11089002138447     21.78865100428918  c
   -7.05718364920278     -0.60660403300702     20.09256121286134  h
    2.56849324222616      7.19031495084091      3.63068703088074  h
   -3.52747844970705     -4.98192169100081      4.16654100335851  h
  -16.27586694827787      0.65611712519293     19.13650069158926  h
  -13.31244255485294     -0.76082436015334     21.53156735535554  c
   -9.96311386683447     -1.99558008668129     23.47686975527797  h
  -14.58782487837088     -1.36927609236375     23.01466122452392  h
   -1.98783471630880      8.55996797720737     11.19504773199230  c
   -3.66796655211253      7.25238953338644     12.74618552984245  n
   -1.29490136189978     11.04154235964852     11.88618951515638  c
   -4.59354897279489      8.32665579460873     14.83019913307111  c
   -2.26667811652953     12.12625967037098     14.04429064831688  c
   -3.95519986952136     10.75893228115862     15.56677050248308  c
   -5.88462376279446      7.16317680748128     15.91440708241243  h
   -1.72563468077255     14.03300849755184     14.56197354355818  h
   -4.75349784491480     11.55128649877328     17.27272703459940  h
    0.00868910418001     12.07835174719840     10.69800859622949  h
$end
```

[(C^C^N)Au(III)C_6F_5] @ T1; TPSSh/def2-TZVP(P)

```
$coord
   -0.05055931217659      0.01217148349691     -0.11272642595801  au
    0.57935520437894      0.63566049048853     -3.77103732723155  c
   -0.74880297448098     -0.69423925044644      3.76789935200655  c
    3.18464984527575      2.07178034135129      0.14043781095622  c
    2.71462160071976      2.03904945605113     -4.42699051761225  c
   -1.13233113267405     -0.36762480068814     -5.47546448512244  c
    0.05804399248916     -2.89410872395595      4.94337837105876  c
   -2.06653470260467      0.98167114481285      5.29354624025170  c
    4.15560631034747      2.83869228202604     -2.30784925717909  c
    4.47305392330786      2.77173709486902      2.29085674398054  c
    3.20282730494677      2.50147768464936     -7.11988743421530  c
   -0.61282508430969      0.11240835356293     -8.15447891894300  c
    1.35434130362752     -4.64736586226736      3.60292817686138  f
   -0.39284947726184     -3.43248079148347      7.47493818742384  c
   -2.93412242873717      3.17945022754225      4.31227978239976  f
   -2.57198235332205      0.53544943712425      7.83317430080610  c
    6.40362994602118      4.28743012431222     -2.43476893550474  c
    6.70037532317586      4.21289240902076      2.11150039134563  c
    3.77937689309580      2.21737601616279      4.13399827595039  h
    1.51930944861667      1.51752236542244     -8.85929833004467  c
    4.83194056926076      3.57833345722752     -7.72715452957845  h
   -1.86329374092552     -0.61029914049548     -9.60606040101306  h
    0.42526112508302     -5.58691240363389      8.53060646141282  f
   -1.72297590419727     -1.69579494505698      8.92859790636125  c
   -3.86161736464150      2.20781474097422      9.23542645890685  f
    7.13743982234546      4.86358895712013     -4.25785082384304  h
    7.64967204814847      4.95976052492739     -0.24093280713451  c
    7.69195087125408      4.75009817258132      3.82209043131758  h
    1.85011231036547      1.83835751227838    -10.85606853151470  h
   -2.18930028944643     -2.17225041007084     11.36812195433854  f
    9.36850794421427      6.06941186003748     -0.33679239057388  h
   -3.18236151643353     -1.74100995252729     -4.40419249857006  c
   -5.15183733306297     -2.92354329050193     -5.76442728267496  c
   -3.19977730126806     -1.90105376727348     -1.76817341882988  n
   -7.04169921322368     -4.19717030678670     -4.51168704891088  c
   -5.04983815913527     -3.14341413351604     -0.58749925928054  c
   -7.01174316057144     -4.32217812357741     -1.85924892561516  c
   -5.15191647485395     -2.81180790134924     -7.80730038403306  h
   -8.54571300441309     -5.09885203976071     -5.56977591956962  h
   -4.92762913447025     -3.17793391341021      1.45550480444574  h
   -8.46348329773603     -5.30361085705025     -0.80865562283788  h
$end
```

[(C^C^C`)Au(III)CCPh] @ T1; TPSSh/def2-TZVP(P)

```
$coord
   -0.23882987280378      4.75314910242515     11.26115343678432  au
    0.16325352171909      2.89221398880737     14.60567984711790  c
   -0.60419882916281      6.50377595535831      7.96631828448646  c
   -1.56919572083472      8.32723147751887     12.37833353514584  c
    0.91836016005810      1.94794810423984      8.87887976117338  c
    0.40224087550978      1.78294251160571     16.61868058613543  c
   -1.45620517012178      8.96501644910775      7.91105610297493  c
    0.04142064706129      5.14567322171777      5.68360393509223  c
   -1.97596959408188      9.92580231819326     10.38261019877453  n
   -2.19423981485025      9.67405153757113     14.44112826714156  n
    0.86159180924025      2.69677934531996      6.15408110017488  c
    1.71035955065975     -0.45637988426971      9.50258752052194  c
    0.68732565079457      0.47587485071780     18.95565844273000  c
   -1.73803105078976     10.26551934753160      5.64579718294650  c
   -0.25619740252413      6.50411127234257      3.34448162199683  c
   -2.84294409271627     12.23518616318242     11.20986760412896  c
   -2.05360897614841      8.71093354659902     17.02265283710718  c
   -2.98324249061095     12.08381638217310     13.76748310257352  c
    1.64182261531618      0.86687653656767      4.28672502258028  c
    1.75829935710636     -1.01714253527171     11.47200323953967  h
    2.45165857698756     -2.17684865437935      7.63045150859760  c
   -1.31505510801677     -0.93939784006169     19.98090145833064  c
    2.97977703087079      0.56444486606147     20.29745732876261  c
   -2.40369419992548     12.19901745382679      5.55892026283076  h
   -1.10718705228083      8.94595642804084      3.36025691326149  c
    0.19160721965835      5.60231291080416      1.56004322655636  h
   -3.28203638836691     13.76844450794308      9.94979545578760  h
   -3.92544878061271      8.76533838742431     17.88472461847646  h
   -0.75026981149210      9.86818232738706     18.12354654565296  h
   -1.37302479919074      6.76991845298047     16.93907060113344  h
   -3.56649845811537     13.45761971331944     15.14888750373324  h
    1.61240578292475      1.38028170969978      2.30286647693792  h
    2.40482511298606     -1.47612901677279      5.01281569735815  c
    3.06837489209743     -4.05807361914003      8.15601237834342  h
   -3.08737146246284     -1.02884293264819     18.95938066845015  h
   -1.02938241121671     -2.21122570268810     22.25866085123039  c
    3.25130772319565     -0.71276489759992     22.57390721656789  c
    4.53833469388569      1.64234895782649     19.52182604815767  h
   -1.32242477592365      9.94757178711725      1.58672031777212  h
    2.98974195086132     -2.84722616291082      3.60652932845485  h
   -2.59623864403380     -3.29490273515610     23.01461516327211  h
    1.25151755724440     -2.10598331089848     23.56859205552328  c
    5.03687255915163     -0.62352450542026     23.57622539022777  h
    1.46984147318155     -3.10334600837869     25.34459341213902  h
$end
```

[(C^C^C′)Au(III)C_6F_5] @ T1; TPSSh/def2-TZVP(P)

```
$coord
   -0.03733010838541     -0.03749053858144      0.07212167800447  au
    0.57929604267839      0.57850203758140     -3.58526670872528  c
   -0.57776135024559     -0.59470964029143      3.99831950936623  c
    3.20226283275118      2.05063354142151      0.27737084186151  c
   -3.10954005373766     -1.94220957418592     -1.61335297323796  c
    2.76080062982241      2.04950262369395     -4.30986834761745  c
   -1.07572091702356     -0.39272741066964     -5.34068726702941  c
    0.30393873096742     -2.72032480197653      5.25689220052686  c
   -1.79691134152428      1.17344126968010      5.50484206398398  c
    4.18164840713739      2.85076918742203     -2.25482061911133  c
    4.52966551978982      2.76913161504752      2.40333164132958  c
   -3.09244197959788     -1.77856752240208     -4.19818275819318  n
   -5.17438331248707     -3.32623776940994     -1.06579490740160  n
    3.11551094552265      2.44650886150012     -6.97891873394659  c
   -0.72359200018414     -0.00196672826457     -7.91617748102506  c
    1.49700952009798     -4.56954828192008      3.95073312720994  f
    0.02711153279053     -3.09559515880644      7.84307311220843  c
   -2.74428803545947      3.30398527677019      4.45426438281205  f
   -2.12480157041368      0.89079400034977      8.09693045999952  c
    6.46171628218371      4.34619112699597     -2.35989934674919  c
    6.73934599113544      4.21790813811574      2.22068221134357  c
    3.86015442173840      2.20973192575798      4.25611653502293  h
   -5.11786508570276     -3.04468598671046     -5.22650013554943  c
   -5.97049804065626     -4.00789652794429      1.48236014553073  c
   -6.43605149903032     -4.02454009310749     -3.25708810745915  c
    1.43378747305300      1.45378553115557     -8.67445724563825  c
    4.71368277848024      3.53257474202644     -7.65974578212495  h
   -2.00250042216116     -0.74641405725915     -9.33003437526526  h
    0.91422215292572     -5.18594041268653      8.97365858869705  f
   -1.19936726059303     -1.26675508693445      9.27399279343399  c
   -3.31834260407722      2.65531757180372      9.47314858988940  f
    7.18729921968708      4.94152596163639     -4.18153645044638  h
    7.68361334533212      4.99737741033333     -0.19792822066389  c
    7.74934141260916      4.76060076073440      3.91753309609516  h
   -5.45717983644676     -3.14807244038582     -7.22783972943679  h
   -7.87663560145124     -3.30379805997414      1.82715693961399  h
   -4.65821299304849     -3.14564932039503      2.80651467628525  h
   -5.93598184033961     -6.05735124763214      1.70074355699188  h
   -8.13598423488268     -5.14003696001652     -3.21917747634944  h
    1.72198200417073      1.76666476102077    -10.67781676834990  h
   -1.49278438690176     -1.58432003503205     11.76738741395321  f
    9.39578522147667      6.11971127783946     -0.28208012983936  h
$end
```

[(C^C^N)Au(III)CCPh] @ planar TS; TPSSh/def2-TZVP(P)

```
$coord
   -0.65532534446055      0.20889588596982      0.00004569654695  au
    3.17802242798459     -0.20181658250155      0.00000862869704  c
   -4.40452202771155      0.49086328064841      0.00008779356165  c
   -1.00214375953877      4.03521818906355     -0.00004190066488  c
    5.46317774977319     -0.54486187952210     -0.00001834522905  c
   -5.82700914966797     -1.72323064340192      0.00014424217694  c
   -5.47287182234636      2.90257787571127      0.00004465034587  c
   -3.54467462294309      4.90293268929800     -0.00002669090701  c
    0.97699611042395      5.75137933198522     -0.00010418296609  c
    8.13365372594343     -0.88790920450298     -0.00005154153085  c
   -8.47261958620026     -1.51616616964751      0.00023837224725  c
   -8.10634617658120      3.07869787061434      0.00009307662999  c
   -4.01135948324600      7.49718662487222     -0.00008465880876  c
    2.90794290184736      5.07556943815810     -0.00011434225311  h
    0.46726944820148      8.34361908197087     -0.00015469421371  c
    9.76978434486370      1.20602948612828     -0.00009382917261  c
    9.20622743583936     -3.31855152150943      0.00000782623256  c
   -9.67560085921940     -3.17560376151284      0.00035562828314  h
   -9.56790569222162      0.87437992160737      0.00018712104512  c
   -9.04472720887819      4.90164112910279      0.00006326171545  h
   -5.94239702908837      8.18752842032427     -0.00005383220227  h
   -2.01350347213687      9.20958240801942     -0.00016920621941  c
    2.02099931283922      9.68013803466621     -0.00016607054406  h
    8.96686699692884      3.08916475903585     -0.00027618186598  h
   12.37233084744186      0.87453831919423      0.00003857124944  c
   11.81058057482316     -3.63797785683089      0.00015738672720  c
    7.96761080843903     -4.94923503827960     -0.00011937397850  h
  -11.61014865869263      1.03395784748980      0.00020648098087  h
   -2.39769622281244     11.22206516798661     -0.00026528312155  h
   13.60092620369655      2.51468890585917      0.00011956209745  h
   13.40748942223931     -1.54577483252852      0.00011550265212  c
   12.59916527123675     -5.52957318838448      0.00035979174986  h
   15.44025100745627     -1.79897565936812      0.00009762895934  h
   -4.34324847467988     -4.06549522954405     -0.00003240255629  c
   -1.78130712056693     -3.74551610611629     -0.00011509118439  n
   -5.34016681286945     -6.50770632414142     -0.00005518686317  c
   -0.23114863227480     -5.73885210896240     -0.00008265652246  c
   -3.73233722135433     -8.57704487358215     -0.00004993759630  c
   -1.12997039381095     -8.19959082901649     -0.00006991037388  c
    1.76772150913005     -5.29225665154621      0.00000671951357  h
   -4.50466420947478    -10.47408526024330     -0.00003486637510  h
    0.18294676078824     -9.76707760792952     -0.00006979845330  h
   -7.36882329283419     -6.76593587237464     -0.00012795780952  h
$end
```

[(C^C^C′)Au(III)CCPh] @ planar TS; TPSSh/def2-TZVP(P)

```
$coord
   -0.66776963132037     -0.09314107167645     -0.00005286424417  au
    3.18226402238250     -0.07588698738744     -0.00003671586062  c
   -4.44906705002252     -0.00931239768125      0.00007683745411  c
   -1.57736868175407     -3.97420125005879     -0.00009510549744  c
   -1.27660227917319      3.75986337890105     -0.00009872348991  c
    5.49277614880656     -0.04029269901804     -0.00001634528256  c
   -5.76844858569487     -2.26473994219833      0.00014188868434  c
   -5.66860871942990      2.32389308239853      0.00011138061817  c
   -4.12683527612548     -4.41090595125686      0.00001183463095  n
   -0.51186439949856     -6.28179512485879     -0.00013827259945  n
   -3.87660284032091      4.45145867627377     -0.00000588942771  c
    0.54928863842433      5.64448537245646     -0.00019518699179  c
    8.18344815248905      0.07918507395274     -0.00000046456471  c
```

```
-8.39647661472045    -2.29637724021000     0.00018815015750  c
-8.31636698073276     2.32490069959226     0.00019488880965  c
-4.62524842562628    -6.96587273519677    -0.00002391580535  c
 2.21194494301708    -6.72356757907429    -0.00032374481672  c
-2.34736079648351    -8.14833694495446    -0.00002276021785  c
-4.54973893173047     7.00038396425528    -0.00002583277798  c
 2.53040147676069     5.12805409946323    -0.00022699829730  h
-0.15364043899851     8.19038229686240    -0.00023035018738  c
 9.43447115343537     2.42412169529273     0.00002782578679  c
 9.66229154655582    -2.12798049433124     0.00003543505238  c
-9.47483426342133    -4.03773497986303     0.00011938350118  h
-9.63263444024643     0.03926526976070     0.00025493918823  c
-9.36963369903378     4.08305910023605     0.00026920482760  h
-6.51036266887008    -7.72571297609377    -0.00008441361183  h
 2.74035817182538    -7.78620017089637    -1.68578616380787  h
 2.74056444146857    -7.78631878612373     1.68499863706826  h
 3.14565107047927    -4.88902852883206    -0.00032254698280  h
-1.88051341160981   -10.12801434222501     0.00009631608547  h
-6.52904119395244     7.53828707815232     0.00007374427361  h
-2.69352290226035     8.86493683628809    -0.00015055488896  c
 1.29205419192617     9.64406116211231    -0.00033764162570  h
 8.31789898219224     4.13990959847704    -0.00007181840773  h
12.05502041699125     2.54843331906320     0.00015866979186  c
12.28285459996192    -1.99261977366737     0.00021779476685  c
 8.72723682273738    -3.95005765315091    -0.00012988793806  h
-11.68076272243906    0.06661434260859     0.00041050587891  h
-3.23308614149175    10.84177379921220    -0.00020291390484  h
12.98080275455238     4.37670414483894     0.00015237927512  h
13.49392420232472     0.34415036464810     0.00027807391387  c
13.38699122098093    -3.71924124484869     0.00033443256816  h
15.53984480437520     0.44659507045718     0.00042678889573  h
$end
```

S 8 Bibliography

[1] a) P. Espinet, A. M. Echavarren, *Angew. Chem. Int. Ed.* **2004**, *43*, 4704-4734; b) A. F. Renaldo, J. W. Labadie, J. K. Stille, *Org. Synth.* **1989**, *67*, 86-97.

[2] a) M. A. Düfert, K. L. Billingsley, S. L. Buchwald, *J. Am. Chem. Soc.* **2013**, *135*, 12877-12885; b) N. C. Bruno, M. T. Tudge, S. L. Buchwald, *Chem. Sci.* **2013**, *4*, 916-920.

[3] a) R. D. a. B. Rieke, Stephen E., *J. Chem. Soc., Chem. Commun.* **1973**, 879-880; b) T. P. Burns, R. D. Rieke, *J. Org. Chem.* **1987**, *52*, 3674-3680; c) R. D. Rieke, *Science* **1989**, *246*, 1260-1264.

[4] a) K. L. Billingsley, T. E. Barder, S. L. Buchwald, *Angew. Chem. Int. Ed.* **2007**, *46*, 5359-5363; b) M. G. Organ, S. Calimsiz, M. Sayah, K. H. Hoi, A. J. Lough, *Angew. Chem. Int. Ed.* **2009**, *48*, 2383-2387; c) J. Nasielski, N. Hadei, G. Achonduh, E. A. Kantchev, C. J. O'Brien, A. Lough, M. G. Organ, *Chem. Eur. J.* **2010**, *16*, 10844-10853.

[5] A. J. Oelke, F. Antonietti, L. Bertone, P. B. Cranwell, D. J. France, R. J. Goss, T. Hofmann, S. Knauer, S. J. Moss, P. C. Skelton, R. M. Turner, G. Wuitschik, S. V. Ley, *Chem. Eur. J.* **2011**, *17*, 4183-4194.

[6] K. Umezawa, Y. Ikeda, Y. Uchihata, H. Naganawa, S. Kondo, *J. Org. Chem.* **2000**, *65*, 459-463.

[7] a) T. Ishiyama, M. Murata, N. Miyaura, *J. Org. Chem.* **1995**, *60*, 7508-7510; b) M. Murata, T. Oyama, S. Watanabe, Y. Masuda, *J. Org. Chem.* **2000**, *65*, 164-168.

[8] a) Q. Jiang, M. Ryan, P. Zhichkin, *J. Org. Chem.* **2007**, *72*, 6618-6620; b) W. Li, D. P. Nelson, M. S. Jensen, R. S. Hoerrner, D. Cai, R. D. Larsen, P. J. Reider, *J. Org. Chem.* **2002**, *67*, 5394-5397; c) Q. Zhou, B. B. Snider, *J. Org. Chem.* **2010**, *75*, 8224-8233.

[9] a) P. Buck, G. Köbrich, *Tetrahedron Lett.* **1967**, *8*, 1563-1565; b) G. Köbrich, P. Buck, *Chem. Ber.* **1970**, *103*, 1412-1419.

[10] a) X. Huang, K. W. Anderson, D. Zim, L. Jiang, A. Klapars, S. L. Buchwald, *J. Am. Chem. Soc.* **2003**, *125*, 6653-6655; b) T. E. Barder, S. D. Walker, J. R. Martinelli, S. L. Buchwald, *J. Am. Chem. Soc.* **2005**, *127*, 4685-4696.

[11] a) S. D. Ross, I. Kuntz, *J. Am. Chem. Soc.* **1951**, *74*, 1297-1302; b) J. W. Barton, M. A. Cockett, *J. Chem. Soc.* **1962**; c) H. J. Reich, B. Ö. Gudmundsson, D. P. Green, M. J. Bevan, I. L. Reich, *Helv. Chim. Acta* **2002**, *85*, 3748-3772.

[12] a) H. Groß, J. Gloede, *Angew. Chem.* **1963**, *75*, 376-376; b) X. Pang, L. Zhao, D. Zhou, P. Y. He, Z. An, J. X. Ni, R. Yan, *Org. Biomol. Chem.* **2017**, *15*, 6318-6322.

[13] E. V. S. a. V. S. Mokrushin, *Izv. Akad. Nauk, Ser. Khim.* **2006**, *7*, 1208-1213.

[14] A. F. P. a. A. M. S. a. L. M. Sitkina, *Chem. Heterocycl. Compd.* **1969**, 916-922.

[15] H. Schmidbaur, W. Graf, G. Müller, *Angew. Chem. Int. Ed.* **1988**, *27*, 417-419.

[16] a) J. Guenther, S. Mallet-Ladeira, L. Estevez, K. Miqueu, A. Amgoune, D. Bourissou, *J. Am. Chem. Soc.* **2014**, *136*, 1778-1781; b) F. Rekhroukh, R. Brousses, A. Amgoune, D. Bourissou, *Angew. Chem. Int. Ed.* **2015**, *54*, 1266-1269.

[17] M. Livendahl, C. Goehry, F. Maseras, A. M. Echavarren, *Chem. Commun.* **2014**, *50*, 1533-1536.

[18] I. Fernandez, L. P. Wolters, F. M. Bickelhaupt, *J. Comput. Chem.* **2014**, *35*, 2140-2145.

[19] a) J. P. Perdew, K. Burke, M. Ernzerhof, *Physical review letters* **1996**, *77*, 3865; b) J. P. Perdew, K. Burke, M. Ernzerhof, *Physical Review Letters* **1997**, *78*, 1396-1396.

[20] T. Yanai, D. P. Tew, N. C. Handy, *Chemical physics letters* **2004**, *393*, 51-57.

[21] J. Tao, J. P. Perdew, V. N. Staroverov, G. E. Scuseria, *Physical Review Letters* **2003**, *91*, 146401.

[22] F. Weigend, R. Ahlrichs, *Physical Chemistry Chemical Physics* **2005**, *7*, 3297-3305.

[23] D. Andrae, U. Haeussermann, M. Dolg, H. Stoll, H. Preuss, *Theoretica chimica acta* **1990**, *77*, 123-141.

[24] a) F. Weigend, *Physical chemistry chemical physics* **2006**, *8*, 1057-1065; b) A. Hellweg, C. Hättig, S. Höfener, W. Klopper, *Theoretical Chemistry Accounts* **2007**, *117*, 587-597.

[25] S. G. Balasubramani, G. P. Chen, S. Coriani, M. Diedenhofen, M. S. Frank, Y. J. Franzke, F. Furche, R. Grotjahn, M. E. Harding, C. Hättig, *The Journal of chemical physics* **2020**, *152*, 184107.
[26] C. Holzer, W. Klopper, *The Journal of chemical physics* **2019**, *150*, 204116.
[27] D. Figgen, G. Rauhut, M. Dolg, H. Stoll, *Chemical physics* **2005**, *311*, 227-244.
[28] D. F. Shriver, M. A. Drezdzon, *The manipulation of air-sensitive compounds*, Wiley, New York, **1986**.
[29] C. Y. Liu, P. Knochel, *Org. Lett.* **2005**, *7*, 2543-2546.
[30] W. T. Miller, K. K. Sun, *J. Am. Chem. Soc.* **1970**, *92*, 6985-6987.
[31] W. C. Still, M. Kahn, A. Mitra, *J. Org. Chem.* **1978**, *43*, 2923-2925.
[32] G. R. Fulmer, A. J. M. Miller, N. H. Sherden, H. E. Gottlieb, A. Nudelman, B. M. Stoltz, J. E. Bercaw, K. I. Goldberg, *Organometallics* **2010**, *29*, 2176-2179.
[33] H. Friebolin, *Basic one- and two-dimensional NMR spectroscopy*, 5th completely rev. and enlarged ed., WILEY-VCH, Weinheim, **2011**.
[34] TOPSPIN, *Bruker Corporation*, **2016**.
[35] OriginPro 2019b, *OriginLab Corporation*, **2019**.
[36] J. F. Araneda, W. E. Piers, B. Heyne, M. Parvez, R. McDonald, *Angew. Chem. Int. Ed.* **2011**, *50*, 12214-12217.
[37] G. M. Sheldrick, *Acta Crystallogr A Found Adv* **2015**, *71*, 3-8.
[38] G. M. Sheldrick, *Acta Crystallogr C Struct Chem* **2015**, *71*, 3-8.
[39] J. Wang, E. Yao, Z. Chen, Y. Ma, *Macromolecules* **2015**, *48*, 5504-5510.
[40] R. Kumar, A. Linden, C. Nevado, *Angew. Chem. Int. Ed.* **2015**, *54*, 14287-14290.
[41] C. K. Li, R. W. Sun, S. C. Kui, N. Zhu, C. M. Che, *Chem. Eur. J.* **2006**, *12*, 5253-5266.
[42] N. J. T. Turro, V. Ramamurthy, J. C. Scaiano, *Modern Molecular Photochemistry of Organic Molecules, Vol. 10*, University Science Books, Sausalito, CA, **2010**.